The Expedition El'gygytgyn Lake 2003 (Siberian Arctic)

Edited by Martin Melles, Pavel Minyuk, Julie Brigham-Grette and Olaf Juschus with contributions of the participants

Ber. Polarforsch. Meeresforsch. 505 (2005)
ISSN 1618 - 3193

Martin Melles
University of Leipzig
Institute for Geophysics and Geology
Talstrasse 35
D-04103 Leipzig
Germany

Pavel Minyuk
Northeast Interdisciplinary Scientific Research Institute
Russian Academy of Sciences, Far East Branch
Portovaya 16
685 010 Magadan
Russia

Julie Brigham-Grette
University of Massachusetts
Department of Geosciences
Amherst, MA 01003
U.S.A.

Olaf Juschus
University of Leipzig
Institute for Geophysics and Geology
Talstrasse 35
D-04103 Leipzig
Germany

The Expedition El´gygytgyn Lake 2003 (Siberian Arctic)

Edited by M. Melles, P. Minyuk, J. Brigham-Grette and O. Juschus

Content

"El´gygytgyn" - Chukchi word for "White Lake"

1 INTRODUCTION

(M. Melles, P. Minyuk, J. Brigham-Grette)

1.1 Objectives

Environmental changes in the Arctic are known to play a major role in the global climate system. For instance, the waxing and waning of Arctic ice sheets, changes in sea level, sea ice cover, productivity and circulation of the Arctic Ocean, and related variations in permafrost behaviour, snow cover and vegetation in the terrestrial Arctic through feedback processes have strong impacts on the global water and carbon cycles, and on the global heat balance. This is certainly the case for the cooling step at the Pliocene/Pleistocene boundary that led to the intensification of the Northern Hemisphere Glaciation (e.g., Jansen et al., 1990; Maslin et al., 1998) and the Quaternary glacial/interglacial cycles driven by variations in solar radiation (Milankovitch, 1941), but is also likely true for abrupt climate changes, such as the Dansgaard-Oeschger events triggered by changes in fresh-water supply into the North Atlantic during the last glaciation (e.g., Dansgaard et al., 1993; Labeyrie et al., 2003). Many parts of the Arctic are currently experiencing environmental change at rates unprecedented in historical times (e.g., Chapman and Walsh, 1993; Overpeck et al., 1997), making this region a major focus for monitoring and the development of numerical models for predicting future change. Existing climate models, however, partly produce results incompatible with historical data and Holocene reconstructions (e.g., Moore et al., 2001; Polyakov et al., 2002).

In order to validate numerical models, and to achieve a better understanding of relevant feedback mechanisms between the high and low latitudes, past climatic and environmental change must be studied in the Arctic on different spatial and temporal scales. Records covering the past glacial/interglacial cycles have recently become available from the marine environment, from the North Atlantic (Thiede et al., 1998) as well as the North Pacific (Keigwin, 1998) and the Arctic Ocean (Nowaczyk et al., 2001).

The first deep drilling in the Arctic Ocean, conducted in 2004 on the Lomonosov Ridge, gathered a record that even penetrates into the Cretaceous (Kerr, 2004). The longest ice sheet records, in contrast, only cover the last climatic cycle (Johnsen et al., 1995; Andersen et al., 2004) and are restricted to the Greenland ice cap. In the terrestrial Arctic, repeated glaciations and lack of long-lasting sedimentary basins in many areas have excluded the formation of long continuous records of high enough resolution for comparison with the marine archives. In consequence, the Holocene history is reasonably well known, but limited information exists concerning the older history of the terrestrial Arctic, when climate forcings and boundary conditions were different from what they are today.

However, recent findings have shown that there is a unique place in the terrestrial Arctic, where the sediment record continuously covers the entire Quaternary and further extends into the Pliocene: The Lake El'gygytgyn in

central Chukotka, northeastern Siberia (67°30´ N, 172°05´ E). This lake of roughly 12 km diameter and 170 m depth is located in a meteorite impact crater formed about 3.6 Ma ago (Layer, 2000), in a region not inundated by Quaternary ice sheets (Glushkova et al., 1994). The sedimentary record of the crater thus has become a major focus of multi-disciplinary, multi-national paleoclimatic research and is now a potential target for deep drilling within the scope of the International Continental Scientific Drilling Program (ICDP).

First joint Russian-American-German expeditions were carried out on remote Lake El´gygytgyn in spring 1998 and summer 2000, the former concentrating on lake sediment coring and the latter on seismic measurements (for details see Chapter 2). A ca. 13 m long sediment core retrieved from the deepest part of the lake revealed a basal age of approx. 250 kyr BP, confirmed the lack of glacial erosion, and underlined the sensitivity of this lacustrine environment to reflect high resolution climatic change. A single channel seismic survey carried out in 2000 discovered undisturbed and well-stratified sediments to a depth of at least 180 m below the lake floor. These data could not resolve the basal sediments including the sediment/bedrock contact as a result of masking by strong multiples, however, refraction data from sonobuoys indicated the top of the impact breccia near the centre of the lake at about 370 m subbottom.

Based on these results, an ICDP workshop held in 2001 recognised the unique potential of the El´gygytgyn Crater for both paleoclimate and impact-related research and suggested more site survey work to be carried out prior to the submission of an ICDP full proposal. This final pre-site survey expedition, reported here, took place from April to September 2003. The expedition had three major objectives, namely:

(1) to obtain a better understanding of the modern climatic and environmental settings in the crater, and of the natural processes taking place under these circumstances;
(2) to obtain data and samples for a more detailed reconstruction of the Late Quaternary climatic and environmental history of the region; and
(3) to obtain some basic information on the structure of the impact crater and on the Pliocene and Early Quaternary history of the region.

For the purpose of objective (1) seasonal and interannual variations in meteorological and hydrological variables are monitored since 2000 with automated weather stations and thermistor strings. In 2003, sets of rain, river and lake water samples were taken during different times of the spring and summer seasons. Besides, the basement rocks and the vegetation in the catchment were sampled, and a bathymetric survey was carried out on the lake with echosounding profiles. Amongst the modern processes taking place in the crater lake level changes, lake ice dynamics, neotectonic movements, and emission of gases from the lake bottom were investigated. For a better understanding of the allochthonous sediment supply into the lake the motion of permafrost ground in the catchment was measured, and samples were taken from the fluvial and aeolian input. Information concerning the autochthonous biogenic production is expected from diatom, bacteria and biomarker samples.

The settling of particles through water column was studied with sediment traps. To what extent all these processes eventually affect the composition of the sediments at the bottom of Lake El'gygytgyn is investigated on a set of sediment surface samples, which are more or less regularly distributed over the entire lake basin.

To address objective (2) comprehensive field work was carried out in 2003 both on Lake El'gygytgyn and in its surroundings. In the lake catchment, deposits of different origin were localized by Ground Penetrating Radar (GPR) measurements and sampled by permafrost drilling and from natural exposures. The deposits range from fine-grained, organic-bearing sediments with incised ice wedges to very coarse-grained fluvial and beach sediments with low ice contents and restricted amounts of organic remains. Ancient terraces above and below the modern lake level were mapped for areal distribution and altitudes. Their chronology, to be determined by radiocarbon, luminescence and exposure dating techniques, will likely supply a comprehensive understanding of predominantly Late Quaternary lake-level changes. On the lake, the uppermost ca. 40 m of the sediment record, representing ca. 1 Ma lake history, were surveyed in detail with a sediment echosounder (3.5 kHz). Lake sediment coring focused on the recovery of a ca. 16 m long core from about 170 m water depth in the central lake, were the 3.5 kHz data indicate fine-grained, 'hemipelagic' sediments. This core is about 3 m longer than that taken from a different locality in 1998, and probably penetrates about 50 kyr deeper into the history, reaching ca. 300 kyr BP. A comparison of both cores shall show whether the sediment composition in all parts of the central lake is representative for the regional climatic and environmental history. In addition, a transect was cored from the shelf to deep waters perpendicular to the western lake margin. In this part of the lake the permafrost ground in the catchment is particularly widespread and mobile, obviously leading to a high sediment supply and frequent debris flows on the slope. From the investigation of the core transect, with two cores penetrating a subrecent debris flow identified in 3.5 kHz profiles, important information on the processes associated with these mass movement events, on their frequency, and on their impact on the sedimentary record in the central lake is expected.

Contributions to objective (3) mainly come from the geophysical measurements conducted in 2003, which employed extended and partly modified technique compared to the survey in 2000. Some information on the structure of the crater may be derived from impact-related magnetic anomalies, which possibly can be localized by a first magnetic survey conducted on the lake and in the catchment. More details on the locations of the boundaries between bedrock and impact breccia and between breccia and lake sediment are expected from new airgun reflection seismic data, obtained with a 26 cubic inch GI-gun and a 280 m long streamer with 15 channels and 130 m offset. These data also promise to achieve a better understanding of the thickness, bedding, and properties of the entire limnic sediment fill in Lake El'gygytgyn, including the Pliocene and Early Quaternary deposits. First sediment samples reflecting the early lake history may have already been recovered in 2003 on the southern shelf of Lake El'gygytgyn. There, a ca. 2.5 m long core beneath a thin veneer

of coarse-grained relict sediments consists of highly consolidated deposits. These sediments according to their high clay contents were deposited in deeper water during a time of higher lake level, and later became exposed by erosion of the overlaying sediments when the lake level dropped to its present position. Additional information on the Pliocene history of the region comes from geomorphic studies and geological analyses conducted on sediments of respective age exposed along the outflow river Enmyvaam.

1.2 Itinerary

The multidisciplinary expedition to Lake El'gygytgyn in 2003 was separated into two parts: a spring campaign from April to June and a summer campaign from June to Sept. 2003.

1.2.1 Spring Campaign

Most of the field equipment for the expedition, comprising 168 items amounting to 6.5 tons and 33 m^3, were sent by truck from Bremerhaven, Germany, to St. Petersburg, Russia, in the middle of March 2003. In Russian customs, one snowmobile (Ski-Doo) and three outboard engines were delayed due to paperwork. All remaining cargo was transported to Moscow by truck on April 15, 2003. From there, the field equipment and about 2 tons of food and consumables, the latter purchased in Moscow, were sent by cargo plane to Pevek, a small town located on the coast of the East Siberian Sea (69°42′ N, 170°22′ E), on April 16, 2003.

The 5 German participants on the spring campaign of the expedition took commercial flights from Berlin to Moscow on April 28, and continued to Pevek on April 29, arriving on April 30, 2003. In Pevek they were eventually joined by the two Russian colleagues that arrived separately from St. Petersburg via Moscow on April 23, and from Magadan via Keperveem (near Bilibino) on April 30, 2003, respectively.

Further transport to Lake El'gygytgyn, located 260 km to the southeast of Pevek (67°30′ N, 172°05′ E), was by helicopter (Mi-8). The 7 participants on the spring campaign (see Fig. 1a) and about 9 tons of cargo, including 2000 l of gasoline and 4 gas bottles bought in Pevek, were shifted to the lake by 5 helicopter trips from May 5 to 7, 2003. The snowmobile stuck in customs never actually made it to Pevek. Therefore it was necessary to rent a Russian snowmobile (Buran) in Pevek. A sixth helicopter flight on May 26, 2003 became necessary when this snowmobile broke down beyond repair in the field and had to be replaced. This flight to Lake El'gygytgyn included all other equipment remaining in Pevek at this stage.

The field camp for both campaigns was set up at the southern shore of the lake, at a comfortable cabin just east of the outlet stream Enmyvaam River (67° 26,81′ N, 172°10.83′ E). The cabin, rented for the entire expedition, has a kitchen, some sleeping places, a small workshop, and additional space for food

storage and various scientific activities. The owner of the cabin (Yuri Gopkalo) was hired as a care-keeper and cook. He arrived on June 12, via a helicopter trip of the Pevek Gold Mining Company, and remained with the expedition until finished.

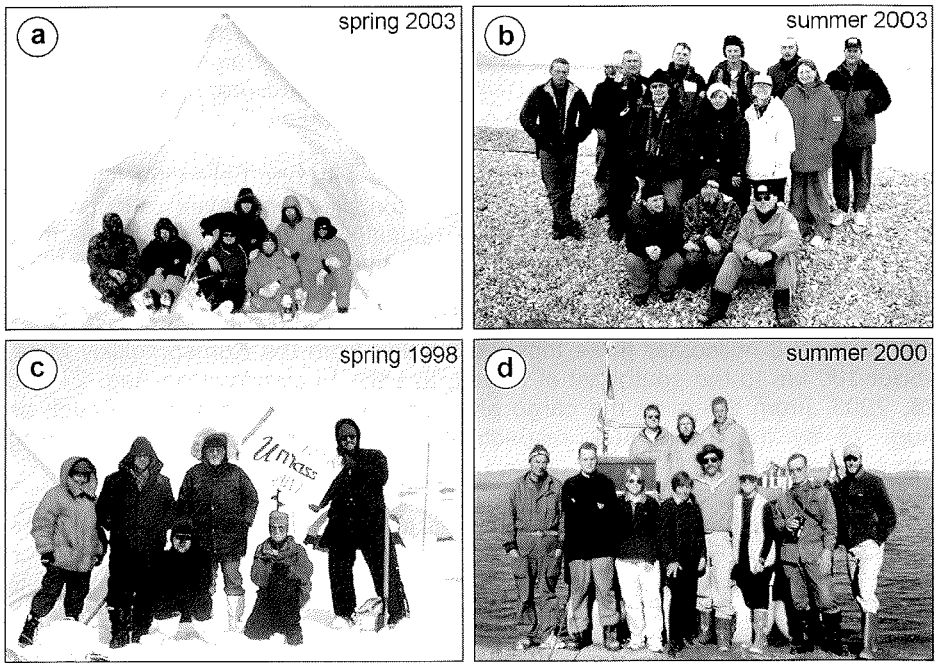

Figure 1: *Participants on the expeditions to Lake El'gygytgyn (a) in spring and (b) in summer 2003 (list of participants see Chapter 8), (c) in spring 1998 (from left: O. Glushkova and P. Minyuk, NEISRI, P.P. Overduin and A. Zielke, AWI, J. Brigham-Grette, UMass, M. Nolan, UAF), and (d) in summer 2000 (from left, in the front: P. Minyuk, NEISRI, G. Federov, AARI, C. Asikainen, UMass, O. Glushkova, NEISRI, M. Molan, University of Alaska, Fairbanks, J. Brigham-Grette, UMass, V. Smirnov, NEISRI, M. Apfelbaum, UMass; in the back: F. Niessen, C. Kopsch and B. Wagner, AWI); for institute abreviations and locations see Chapter 8.*

1.2.2 Summer Campaign

Seven of the fourteen participants on the summer campaign (Fig. 1b) joined in Moscow, carrying some particularly delicate equipment and replacement parts. Three German participants took a plane from Berlin to Moscow on June 21, another two on June 23, 2003. Later that same day the American participant arrived by plane from Boston via Frankfurt, and 1 Russian participant arrived by train from St. Petersburg. Further travel of this group to Pevek was by commercial flight on June 24, arriving on June 25, 2003. In Pevek the group was joined by two Russian colleagues who took commercial flights from Magadan to Keperveem (near the town Bilibino) on June 26, reaching Pevek on June 27, 2003.

The exchange between the spring and summer campaigns was accomplished by one helicopter trip to Lake El'gygytgyn on June 27, 2003. On the flight to the lake the nine new participants were accompanied by their cargo, by the three outbord-engines, whose arrival in Pevek was delayed due to custom problems, and by about 400 kg of fresh food, which had been sent from Moscow to Pevek some 2 weeks before by cargo flight. The flight back to Pevek included two German students who participated only in the spring campaign, and the equipment only needed for the spring activities, such as the Burans, a sledge, and ice drills. This flight also exported the garbage accumulated so far.

Evacuation of the expedition started on Aug. 25 with one helicopter flight from Lake El'gygytgyn to Pevek. With this flight the pilots in Pevek reached their limits of admissible monthly flight hours, excluding further flights before Sept. 1. Because several participants had fixed commercial flights from Pevek on Sept. 3, the only other helicopter in the region, owned by the Pevek Gold Mining Company, was chartered to complete the evacuation of the field camp. With this MI-8 helicopter three trips were made from the Komsomolskiy Mine, about 100 km to the southeast of Pevek, to Lake El'gygytgyn on Aug. 27 and 28, 2003. From the mine the cargo and participants were driven to Pevek on Aug. 28 by truck and bus, respectively, both chartered from the mining company as well.

From Pevek the three NEISRI participants took commercial flights via Keperveem back to Magadan on Aug. 28. The other participants left Pevek on Sept. 3. All but one participant from the AARI took commercial flights to Moscow, from where they proceeded to Berlin, Boston and St. Petersburg by plane and train on Sept. 4. The AARI member joined the flight of a cargo plane that was chartered to deliver all equipment and samples to St. Petersburg. The charter was shared with the AWI Potsdam, which had to evacuate a smaller expedition carried out in the Lena Delta. This required a stop and loading operations in Tiksi, and led to the arrival of the plane in St. Petersburg not before Sept. 4.

Following custom operations and paper work for the extensive sample sets to be exported the equipment and samples were jointly sent by truck from St. Petersburg to Bremerhaven on Sept. 26, arriving Oct. 1, 2003.

2 PAST WORK

2.1 Expedition to Lake El'gygytgyn in 1998

(J. Brigham-Grette)

The first attempt to collect sediment cores from Lake El'gygytgyn was made in May of 1998 based upon the encouraging recommendation of Dr. Olga Glushkova, NEISRI Magadan, who had been to the lake in earlier years to study its geomorphology. An international team consisting of two Russians from Magadan, two Germans from the Alfred Wegener Institute (AWI) and two

Americans from the University of Massachusetts and University of Alaska-Fairbanks (Fig. 1c) successfully collected 23 m of core in liners (several 3 m cores with overlapping sections) and 2 m of sediment sectioned in vials from the deepest part of Lake El'gygytgyn, penetrating nearly 13 m of record in 175 m of water. Over a period of 15 days using the lake ice as a coring platform, the lake sediments were sampled at two sites, 300 m apart, roughly in the middle of the lake (site PG1351 to 13.46 m and site PG1351 to 4.12 m; see Fig. 70, p. 111) with gravity and percussion piston corers from a 4 m tripod with hand winches. For details of the coring technique employed see Melles et al. (1994).

All core material was kept at 4°C, and shipped to the AWI in Potsdam, Germany. The cores were split, described, photographed, and subsampled in 2 cm intervals jointly by Russian, American, and German investigators. The subsamples were freeze-dried and weighed to determine water content, and split into aliquots for a variety of proxies to be measured by different members of the project.

Preliminary results from this series of cores were first reported at the Fall AGU in 1999 and 2000 and published by Shilo et al. (2001) and Minyuk et al. (2003). Nowaczyk et al. (2002) published the first core chronology based upon magnetic susceptibility measurements, optically stimulated luminescence ages, and radiocarbon ages, demonstrating that the 13 m long sediment represented nearly 300 ka of record. As such it represented the longest continuous record from the terrestrial Arctic. Subsequently, ten papers documenting the first results regarding aspects of the sedimentology, geochemistry and paleoecology of this record are now in press, as a dedicated issue of the Journal of Paleolimnology (Brigham-Grette, Melles and Minyuk, editors).

2.2 Expedition to Lake El'gygytgyn in 2000

2.2.1 General Information

(J. Brigham-Grette)

The promising chronology and paleoclimate record found in cores taken in 1998 provided the impetus for the first major summer program to begin studies of the modern lake and its catchment. The shared trilateral nature of the field program, including 11 American, German, and Russian scientists (Fig. 1d), was an intellectual and cultural bonus to the effort that served to strengthen mutual respect and trust. This was especially true given some spine-tingling difficulties with logistics. The accomplishments from this field season focused on 6 shared objectives, including the seismic survey.

Modern Limnology

Limnological studies were aimed at understanding lake systematics in order to make accurate relative assessments of the paleoenvironmental record. Near real-time observations via SAR and satellite imagery from the Internet, allowed monitoring of the seasonal lake ice disintegration before our arrival in August.

Since that time, seasonal changes and the mechanics of breakup have now been recorded and assessed via a time-series of remote sensing images establishing that the modern ice free season lasts from roughly mid-July to mid September (Nolan et al., 2003).

The entire water column to a depth of 170 m was sampled on two different days three weeks apart using a vertically mounted Alpha bottle deployed via steel cable and winch. Water brought to the surface was characterized for pH, temperature, conductivity, and dissolved oxygen using bench-top instruments. A multi-parameter Troll 8000 probe was deployed in shallow water for about two weeks to monitor changes in the water column over the shelves in comparison with the central part of the deep basin. In addition, the Troll was used to take vertical measurements to a depth of 75 m (maximum depth range). The lake itself was instrumented at the deepest point in the lake (170 m, 70 m, 30 m, 8 m, 3 m depths) with a permanent thermistor string and a pressure sensor for retrieval of data 4 times a day (it was successfully retrieved in 2003, see below).

Lake El'gygytgyn is a cold oligotrophic, monomictic system. Our measurements showed that during the open water season, the lake lacks a true thermocline being characterized by a narrow range in temperatures between 2.98°C and 3.30°C throughout the entire water column with conditions trending towards isothermal in early September. Measurements taken in 2000 were the first to suggest that warm water (~4°C) on the shallow shelves likely sinks to warm and oxygenate the bottom combined with the normal wind mixing of most of the water column. The isothermal water column was consistent with relatively uniform pH measurements in the range of 6.4 - 6.9, with a slight rise in pH to 7.7 near the bottom. Conductivity measurements averaged only 10.7 to 12.1 µS/cm (less than distilled water), in concert with a Secchi-depth transparency of 20 m quantifiying the clarity of the surface waters. Dissolved oxygen ranged from 8 to 11 mg/l on the shelf at about 5 m depth for a period during late August concordant with measurements in the range of 10 to 12 mg/l taken in the deep basin. Preliminary cation and anion data from the water samples are consistent with the lack the stratification and complete mixing of the water column (Cremer and Wagner, 2003).

Nolan and Brigham-Grette (in press) have summarized aspects of the lake ice cover and controls on lake circulation where as Cremer and Wagner (2003) provide preliminary data on the modern biota, especially diatoms of the lake system.

Geomorphology and Surficial Stratigraphy

Study of the catchment geomorphology and surficial stratigraphy was carried out to understand the basin's lake level history, landscape evolution, and sediment sourcing. One of the most important outcomes of 2000 was confirmation that the El'gygytgyn basin retains a number of intriguing features indicating a history of higher lake levels. The presence of Pliocene age fluvial deposits, found interbedded with impact ejecta in the highest terraces along the exiting Enmyvaam River valley (Belyi and Raikevich, 1994), first indicated that

the crater has remained an open lacustrine basin since the time of impact. As a part of this earlier research, Glushkova and Smirnov (in press) determined that the lake outlet has been down cut through time, probably giving rise to higher lake levels in the basin. In 2000, wave cut bedrock scarps and shoreline remnants were mapped primarily around the southern and eastern part of the lake at elevations of about 40, 18, 8 - 12 and 6 m above lake level. Along the south-western shore of the lake, erosional bluffs up to 12 m high in the toe of low sloping soliflucted fans were found to contain coarse lacustrine littoral facies dating from some earlier time of higher lake level. The stratigraphy of these bluffs was studied and sampled for pollen and microfossils, however, accurate dating of the lacustrine facies was found difficult and remained a focus in 2003.

Studies of the beach morphology around the 37 km perimeter of the lake provided valuable insights into processes controlling the influx of sediments to the lacustrine environment (Nolan and Brigham-Grette, in press; Asikainen et al., in press). Coarse, gravel barrier bars at least temporarily block many of the 50 streams entering the lake during the open water season causing sediments to be stored in shallow lagoons. Though river discharge was observed trickling through these barrier systems in August, it was hypothesized that most of these streams likely supply sediment directly to the lake during the brief spring freshet in June. Strong winds from the north and south combined with the long fetch provides conditions for active longshore drift, which eventually blocks many of the streams. Compounding this process is the development of large ice-shoved ridges of beach gravels up to 5 m high caused by the momentum of winds from passing storms during breakup (Nolan and Brigham-Grette, in press). These ice-shoved ridges armour the backshore, in places preventing the erosion of fine-grained sediments from the margins of soliflucted alluvial fans.

One of the most striking features about El'gygytgyn crater is the asymmetrical distribution of large alluvial fans formed around the western and northern margins of the basin (see Fig. 50, p. 86). On the western margin, the alluvial aprons stretch for a little over 3 km between the shore and the crater rim. In contrast the steeper eastern and southern margins of the lake are characterized either by relatively short fans (< 600 m wide) or steep rock cliffs with little distance between the shore and crater rim. Equally intriguing were our observation that the steeper eastern and southern shores of the lake possess a wide submerged shelf sloping from 4 to 12 m depths at the steep shelf break. On the other hand, the wide alluvial fans on the western and northern sides meet the lake where the bathymetry drops directly into deep water, without the presence of a wide shelf. Investigations into the origin of this asymmetry continued in 2003.

Sediment Coring

One of the important objectives in 2000 was to collect gravity cores of the sediment/water interface along with as much of the Holocene record as possible from different parts of the basin. The goal was to use these cores to further understand the relationships between the modern lake system and the longer paleodata from existing cores. The same AWI gravity core equipment

was use as first deployed through a hole in the ice in 1998. Using the seismic platform (RV "Helga") as a coring platform, 4 gravity cores were successfully collected from the centre of the basin penetrating between 30 and 43 cm or roughly 6 or 7 ka of record. In addition to the longer cores, nine gravity cores between 11 and 24 cm in length were collected from water depths ranging from 52 to 169 m. These cores were studied for their diatom stratigraphy (Cremer and Wagner, 2003), sedimentology, and clay mineralogy (Apfelbaum et al., unpubl.).

Lake Hydrology and Meteorology

Hydrological and meteorological studies of the basin were launched in 2000 (Nolan and Brigham-Grette, in press; Nolan, unpubl.). Left at the lake were 12 data loggers, including a fully automated meteorological station (nicknamed "YuriMet") instrumented to measure air temperature and relative humidity at two heights, wind speed and direction, solar radiation, barometric pressure, snow depth, precipitation, and soil moisture and temperature at 5 depths. Two small met stations (air temp., soil temp., and precipitation) were deployed at sites on the north and south ends of the lake. Most of this equipment was established to collect data for two to three years. Approximately 2 and 4 weeks of summer data were collected from these instruments by the end of the field season. Vandalism by humans and bears in the fall of 2000 required repairs to the meteorological stations in early September 2001; the large meteorological station functioned until downloaded in 2003 (below). Nolan (unpubl.) gauged most of the 50 inlet streams in 2000, and gauged the outlet stream channel several times to create a rough stage-discharge curve.

Remote Sensing and DEM Development

An important contribution to the science effort at Lake El'gygytgyn includes remote sensing and terrain analyses. Maps at 1:50,000 scale of the crater were obtained by Nolan (unpubl.), the contours digitized, and a Digital Elevation Model (DEM) of the crater region was produced (cp. www.uaf.edu/water/faculty/nolan/lakee). Based upon remote sensing data collected over the past three years (ERS-2, Radarsat-1 and Landsat-7 scenes) Nolan et al. (2003) have developed a comprehensive understanding of the lake ice dynamics at Lake El'gygytgyn over the several recent winters, and speculated on some controls on the lake biogeochemistry and biological production from bubbles in the lake ice.

A rough bathymetric map of the lake was obtained from Russian sources, from which the contours were digitized, merged with the DEM, then used to calculate lake volume and hypsometry. Nolan also created numerous visualizations of these data, now available via the Internet (address above). The 50 or so inlet streams within the crater were analysed for size, slope, etc., and Nolan (unpubl.) has run a hydrological model on a test watershed using the data collected in 2000.

2.2.2 Seismic Investigations in 2000

(F. Niessen, C. Kopsch, B. Wagner)

Introduction

The aim of seismic investigations carried out on the lake in 2000 was to study the geometry and thickness of the sediment fill and to provide a pre-site survey for future drilling proposals according to ODP/IODP and ICDP standards. In order to obtain both high resolution and deep penetration acoustic data, 3.5 kHz echosounding was combined with single-channel airgun seismic profiling.

One of the major problems of using marine equipment on Lake El'gygytgyn is its remote location and lack of naval infrastructure (no ship, no marina) and thus difficult logistics. Standard marine seismic equipment including heavy airgun arrays, powerful compressor units and long streamers cannot be used because:

1. The only reasonable way to bring equipment to the lake is by helicopter (type MI-8)
2. There is no vessel to carry the gear. We brought an aluminium platform (frame size 4 x 3 m) equipped with 4 inflatable tubes and a 25 HP Honda outboard engine to the lake. This vessel (RV "Helga") can only carry a small airgun system combined with small portable electronic units including echosounders.

Methods

Based upon the success of using a very small airgun system on Alpine lakes (Finckh et al., 1984) we have combined a Bolt 600B airgun (5 inch^3, courtesy of Geophysical Institute, University of Munich, Germany) with a diving compressor (Bauer, Germany, model Oceanus, capacity 140 l/min) as acoustic energy source. Shooting intervals were 6 seconds with ca. 110 bar gun pressure. The speed of the vessel was 4 to 5 km/h on average. For data acquisition we used a 20-element single channel hydrophone (Geoacoustics, UK, model CP937) connected via interface box to a digital receiver (Octopus, UK, model 360) to create digitized seismic traces in SEG-Y formate. In addition to the Geoacoustic hydrophone streamer, a single hydrophone (OYO Geospace/Kalamos, Canada, model MP24-L3, 10-500 Hz) was towed some 20 m behind the vessel in about 0.5 m water depth. Analogue seismic data were plotted on chart recorders (Ultra, UK, models 3710 and 120) and stored together with the trigger signals and navigation data on a 4-channel DAT-recorder (Sony, Japan, model PC204Ax). Using these techniques a total of 62.5 km of single-channel vertical reflection data were recorded along 6 profiles (Fig. 2).

In order to record wide angle reflection and refraction data for subbottom velocity analysis, two sonobuoys (construction by AWI-Bremerhaven equipped with on hydrophone, OYO Geospace/Kalamos, Canada, model MP24-L1, 6 - 250 Hz) were deployed during calm weather periods in areas where single channel reflection data indicated horizontal subbottom layering (Fig. 2). Sonobuoys recorded airgun-generated acoustic pulses by a single hydrophone under the buoy. The signals were amplified and transmitted via radio to RV

"Helga" where WINRADIO on PC was used as receiver. The lengths of the sonobuoy profiles were 3.6 and 4.39 km (one way) for profiles 1/2 and 3/4, respectively (Fig. 2). The profiles were shot and recorded in both directions along each line near the centre of the lake. Sonobuoy data were plotted and stored in a similar way as described above.

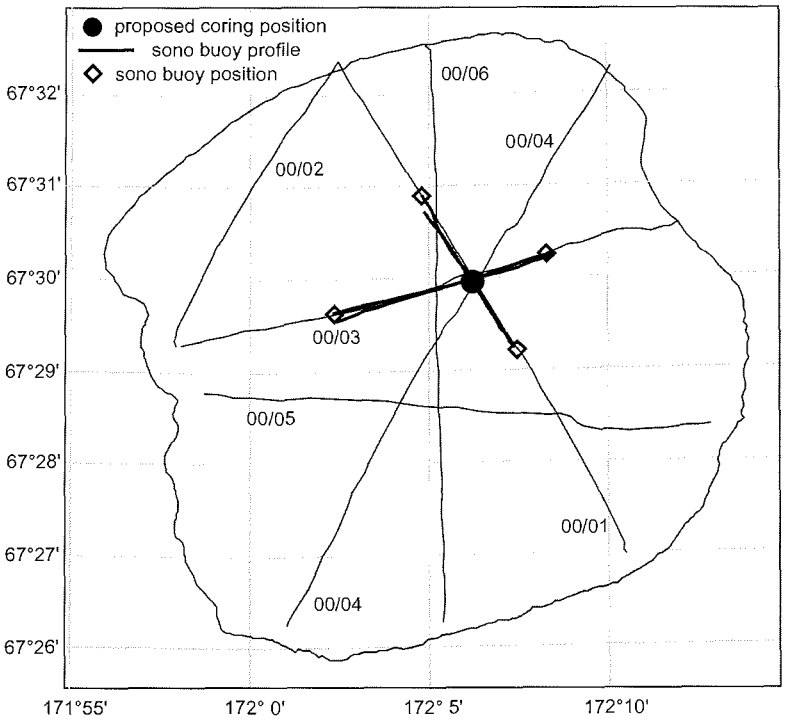

Figure 2: *Map of single-channel airgun track lines recorded in 2000 including four sonobuoy profiles near the centre of the lake and one proposed coring location.*

Based upon the success of the AWI sediment echosounding system in other arctic lakes (Niessen and Melles, 1995; Niessen et al., 1999; Hubberten et al., 1995) a chirp system (GeoAcoustics, UK model Geochirp I) was brought to the lake which, unfortunately, failed and could not be used. As a replacement, an older 3.5 kHz sediment echosounder functioned as high-frequency pulse source (ORE, USA, model 140). Because DAT-tape storage was limited, the 3.5 kHz system could not be run simultaneously with the airgun system. Thus, 3.5 kHz data were obtained on separate track lines mostly along previous airgun lines plus along additional profiles where only 3.5 kHz data were recorded (Fig. 2). In total 69.4 km of sediment echo-sounding data were taped along seven 3.5 kHz profiles. Analogue-data printing and data storage were done in a similar way as described above. 3.5 kHz data were also recorded with the Octopus 360 to create digital formate in SEG-Y. In addition, along all course lines a bathymetric echosounder (Hapelco, Japan) was in operation. Data were stored together with navigational information on a PC in intervals of one second.

Results

The results of the acoustic investigations in 2000 are published in Niessen et al. (2000) and Niessen et al. (in press). In order to avoid duplication, only a short summary is presented in this report. For further details and figures the reader is referred to the above publication and to the new data obtained in 2003 (cp. p. 121).

Refraction seismics using sonobuoys indicate two layers of unconsolidated muds with velocities of 1580 m/s to a depth of 185 m under lake bottom and 1640 m/s to a depth of 371 m under lake bottom, respectively. The second layer is underlain by a refractor characterized by velocities of 3400 to 3900 m/s and is interpreted as brecciated bedrock. This implies a total sediment thickness of about 370 m near the centre of the lake.

Single-channel reflection profiles exhibit well-stratified sediments to a depth of at least 180 m subbottom, locally intercalated with debris flow deposits. The latter are clearly documented in 3.5 kHz profiles and are more common in the western part of the lake and along the slopes. The debris flows are acoustically structureless, have wedge or lenticular-shaped geometries, and can reach several kilometres in length. Proximal thicknesses of the debris flows can be up to ca. 20 m; those in distal areas are still in the range of 5 m or less.

The lower part of the sediment fill appears to be more massive. However, most of the lower sediments including the sediment/bedrock contact, as visible in sonobuoy refraction data, are not documented in vertical analogue reflection profiles because strata is either masked by multiples or not visible due to limited acoustic penetration. Nonetheless, the top of a cone-shaped sediment drape is identified northwest of the centre of the lake at about 180 m sediment depth. This drape may reflect the presence of a breccia centre cone typically observed in impact craters. The drape is completely levelled by overlying sediments and not visible in the modern bathymetry of the lake. However, the drape seems to be associated with a distinct vertical fault visible in both airgun and 3.5 kHz in and above the cone-shaped sediment drape. The vertical displacement of sediments along the fault plane is increasing with sediment depth. According to 3.5 kHz data the displacement is about 1 m in 40 m sediment depth but hardly visible at the sediment surface. This may indicate that tectonic activity related to the impact still does affect the sediments in places up to today. There are not enough profiles yet to state whether the fault plane is an elongated or round feature. Therefore, based upon the data of 2000, it remains open whether the fault is related to the impact or caused by younger regional tectonic activity.

At both the 1998 and newly proposed drill sites (Fig. 2) the sediments appear to be well-stratified and largely unaffected by debris flows and faults. The general pattern suggests undisturbed, continuous sedimentation to at least a sediment depth of 180 m. There is no evidence for erosion and/or deposition from grounded ice in the acoustic data. This suggests that no direct physical imprint affected the sedimentary record of Lake El'gygytgyn possibly during the entire Quaternary glaciations.

In summary, as indicated in both high-resolution and deep-penetration acoustic data, the potential of the Lake El'gygytgyn sedimentary record for paleoenvironmental research is large because the sequences are undisturbed and appear to be complete possibly down to the impact breccia created 3.6 Mio. years ago. A long sediment core from surface to bedrock would provide unique material with reasonably high time resolution to study the transition from warmer Tertiary into Quaternary climates up to today in the Siberian continental Arctic. Sediments draping a subbottom feature in the centre of the lake, possibly related to a centre cone, may be used as further indication for the impact origin of the lake. This and the fact that relatively young faulting is evident in the sediments makes the lake also attractive for additional impact studies. Nonetheless, from the data of 2000 it became evident that additional seismic investigations were essential to better resolve the lower part of the sediment fill and the sediment bedrock interface. To achieve this goal and to overcome the problems of multiples masking the record, a new seismic survey using multi-channel streamer techniques on Lake El'gygytgyn was the clear challenge. Also more high-resolution acoustic profiles were needed to allow three-dimensional mapping of subbottom features such as debris flows and faults. Both of these goals were achieved during the 2003 Expedition.

3 GENERAL GEOLOGY AND GEOGRAPHY

(O. Glushkova, V. Smirnov)

3.1 Geological Position of the El'gygytgyn Crater

Following the results of the geological survey in 1971, the El'gygytgyn Crater is represented by the occurrence of felsic up to basic tuffogenic and effusive rocks creating a huge volcanic cover (Fig.).

The stratigraphy of the cover, its petrographic composition and chemical character was most completely characterised by Belyi and Raikevich (1996). Rhyolites, ignimbrites and tuffs with subordinated development of dacite and daciandesite tuffs and lavas prevail in the series of volcanogenic rocks composing the crater cone. Their thickness amount to ca. 500 m. Medium tuffs and tuffites with subordinate development of dacite and rhyodacite ignimbrites and tuffs are more widely developed within the southern and eastern sector of the crater. Their thickness amount to 350 m. On the top of these series basaltic and andesibasaltic covers were found. They only preserved at small sections, partly as basaltic dikes. Within the tectonic structures of the Anadyr volcanic field (Central-Chukchi sector of the Okhotsk-Chukchi volcanogenic belt), the crater of Lake El'gygytgyn occupies the southeastern part of a tectonic graben formed during the middle Cretaceous.

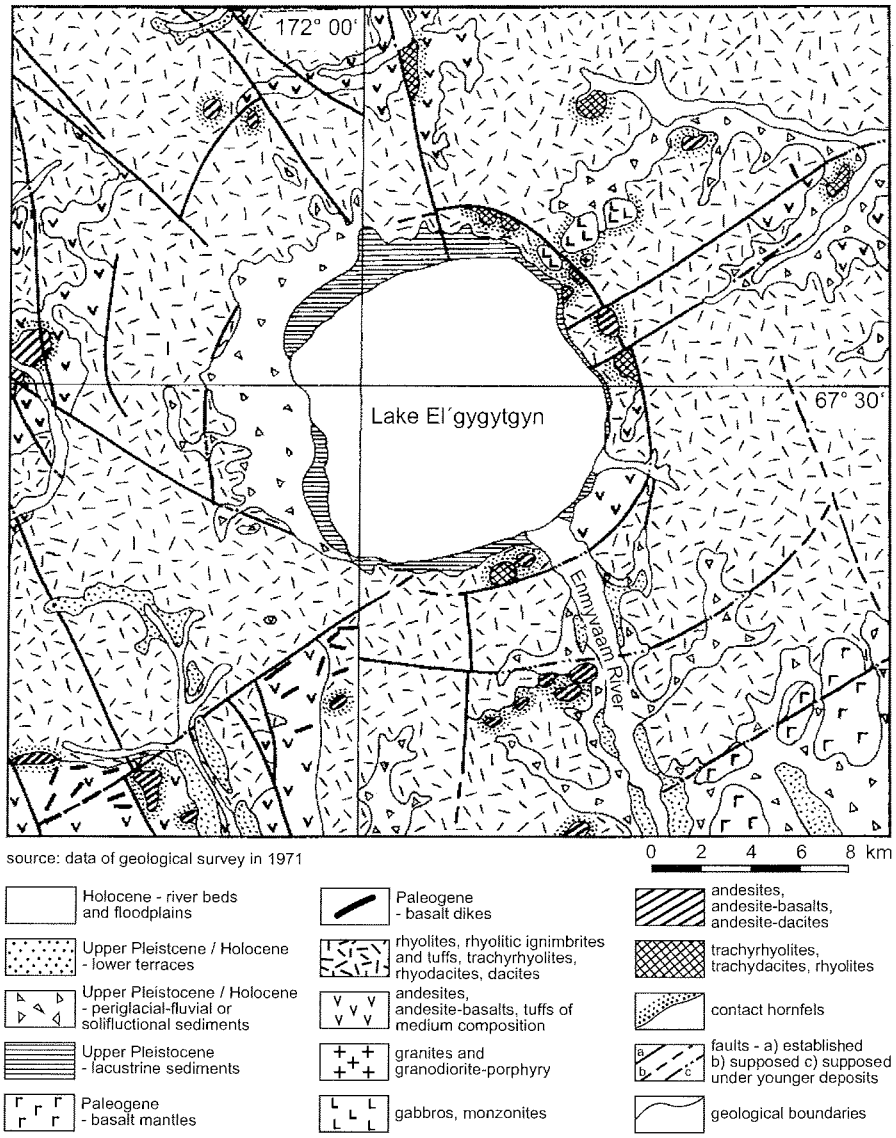

Figure 3: *Simplified geological map of the El'gygytgyn region.*

3.2 Main Orographic Elements

Lake El'gygytgyn is located in the central part of the Anadyr upland. The main mountains in the lake vicinity are:

- The Ridge "Academic Obruchev". It is associate with the course of the Pacific-Arctic drainage divide
- A mountain ridge without a name adjacent to the southeast. It forms the watershed between the Enmyvaam and Yurumkuveem River basins.

Their absolute altitude range between 700 and 800 m. As maximum 941 m was measured. Due to the convergence of the above mentioned ridges, the triple point is the drainage divide between the Ugatkyn River and Malyi Chaun River (tributary to the Arctic Ocean, see Fig. 4) and Yrumkuveem River and Enmyvaam River (tributary to the Pacific Ocean). This situation is complicated by the basin of Lake El'gygytgyn with a water level of 492.4 m.

3.3 Fragments of Planation Plains

In the frame of the Lake El'gygytgyn basin there are tops crowned with fragments of regional planation plains (Glushkova, 1993). The plains form geomorphological stages (levels) with altitudes between 590 and 870 m. As a rule, they are inclined into the lake basin. Their maximal area reaches 300 x 1000 m. In the western part of the lake catchment, in the upper reaches of the Tikhyi and Golcovy Creeks (inlet streams nos. 16 and 14, cf. Fig. 23, p. 50) their heights culminate with altitudes between 830 and 870 m. At the Lishainikovy Creek (inlet stream no. 12) the heights are decreasing down to 780 - 820 m. In the northwestern sector of the lake catchment, at the upper reaches of the Rybnyi Creek (inlet stream no. 21) and Malyi Chaun River the altitudes of the plains further decrease down to 685 - 770 m. In the northern sector the planation surface fragments are poorly preserved. Here the authors distinguish only 6 separated surfaces ranging fom 590 to 840 m. In the eastern and northeastern part the regional surface fragments are most completely preserved. They mainly occur at slopes inclined to the Otvegyrgyn River and Chivirynnet River catchments. Their absolute altitudes range from 590 to 695 m. Within the northeastern part of the Lagerny Creek basin (inlet stream no. 49) the plain surfaces reach up to 750 m. There, the fragments of regional planation surface, as a rule, have isometric forms and occupy large areas. They are overlain by a thin cover of alluvial sediments containing small fractured and sandy debris with variable parts of clay. Periglacial debris is developed at the bedrock with different composition: ignimbrites, rhyolites, tuffs, basalts and other rocks of volcanic origin. Its thickness varies from 30 up to 60 m.

Several samples were collected on the flat tops of the southern and south-western lake catchment. The clay fraction was analysed with SEM (analyses by T.V. Anisimova, NEISRI, Magadan). The clay fraction is polydispersional and represented by large particles of isometric-bend or pseudo-hexagonal shape. It includes hydromica, in small quantity montmorillonite, and in some samples kaolinite. In addition, iron oxides and iron bacteria with the shape of rounded particles with distinct plane margins were found.

The sediments from the planation plains are correlated with sediments forming a chemical weathering crust in basins to the south of Lake El'gygytgyn, at bank outcrops of the Enmyvaam, Mechekrynnetveem, and Chanubenvaam Rivers. This crust was developed in rocks of various composition. It is represented by sandy-clayey sediments, 1 to 6 m in thickness. Depending on the rock structures and composition its colour varies between bright-orange (on ignimbrites) and black (on siltstones). Within the weathering crust non-rounded fragments of impact rocks are common. On the basis of palynological analyses

(by B.V. Belaya, NEISRI, Magadan) of spore-pollen spectra from both under- and overlying sediments it is concluded that crust formation had started in post-Senonian time and became finished during the Early Pliocene. Thus, the planation surfaces are estimated to be of Pliocene age.

3.4 Neotectonic Structure, Geomorphology and Paleogeography

Schemes of the planation surfaces were made to reconstruct the neotectonic structures of the Lake El'gygytgyn region (Glushkova, 1993; Glushkova et al., 2001). They result in the occurence of vertical movements. Two large neotectonic uplifts appeared. The first one occupies the "Akademik Obruchev" Mountains forming a large block that trends to the northeast. The second uplift, to the east of the lake, occupies the Baraniy Mountains and adjacent massifs. Lake El'gygytgyn is situated on the southeastern slope of the former structure.

The neotectonic movements had strong impact on the recent development of both the mountain and the lake basin morphologies. Neotectonic structures are obviously pronounced by the occurrence of an angular fault and drainage system outside the lake catchment. A comparison of the high planation surface with the base of modern valley floors, expressing the level of the most recent erosional level, shows clear and considerable disharmony.

One of the most important points of geomorphological studies was the investigation of the regional glacial history. Geomorphological data have shown that glacial morphosculptures like cirques, trough valleys, moraines, and fluvio-glacial sediments are completely absent in the catchment of Lake El'gygytgyn (Glushkova et al., 2001). Hence, the authors conclude that the lake basin and the framing mountains have never been glaciated. In consequence, limnic sedimentation in Lake El'gygytgyn has never been influenced or interrupted by glacier ice.

Geomorphological analysis of the Anadyr Highland revealed that traces of glacial activity occur only at a distance of 40 km to the west of Lake El'gygytgyn (Fig. 4). Within the valleys and on the slopes of the east-west striking Ilirney Ridge, that reaches altitudes of 1200 - 1500 m, glacial complexes of different ages were observed. The most ancient moraines (supposably of Middle Pleistocene age) fill the bottom of the Malyi Anyui River valley in its upper reaches. Various deposits of the two most recent Pleistocene glaciations, during the Zyrian (approx. Early Weichselian) and Sartan (approx. Late Weichselian), are well preserved in the Pucheveem, Lelyuveem, Malyi Anyui and other river valleys. The paleogeographical reconstruction suggests that only the Zyrian glaciation had a considerable size. Glaciers moving from Ilirney Ridge to the south and north reached maximum lengths of 50 - 60 km. During the Sartan glaciation, in contrast, due to more continental climate with maximal coldness but lower precipitation, the mountain-valley glaciers had filled only the upper reaches. With maximum lengths of 15 - 24 km they did not advance into the basins. Two additional glaciated mountain areas are located to the southeast and southwest of Lake El'gygytgyn, in a distance of about 100 - 140 km.

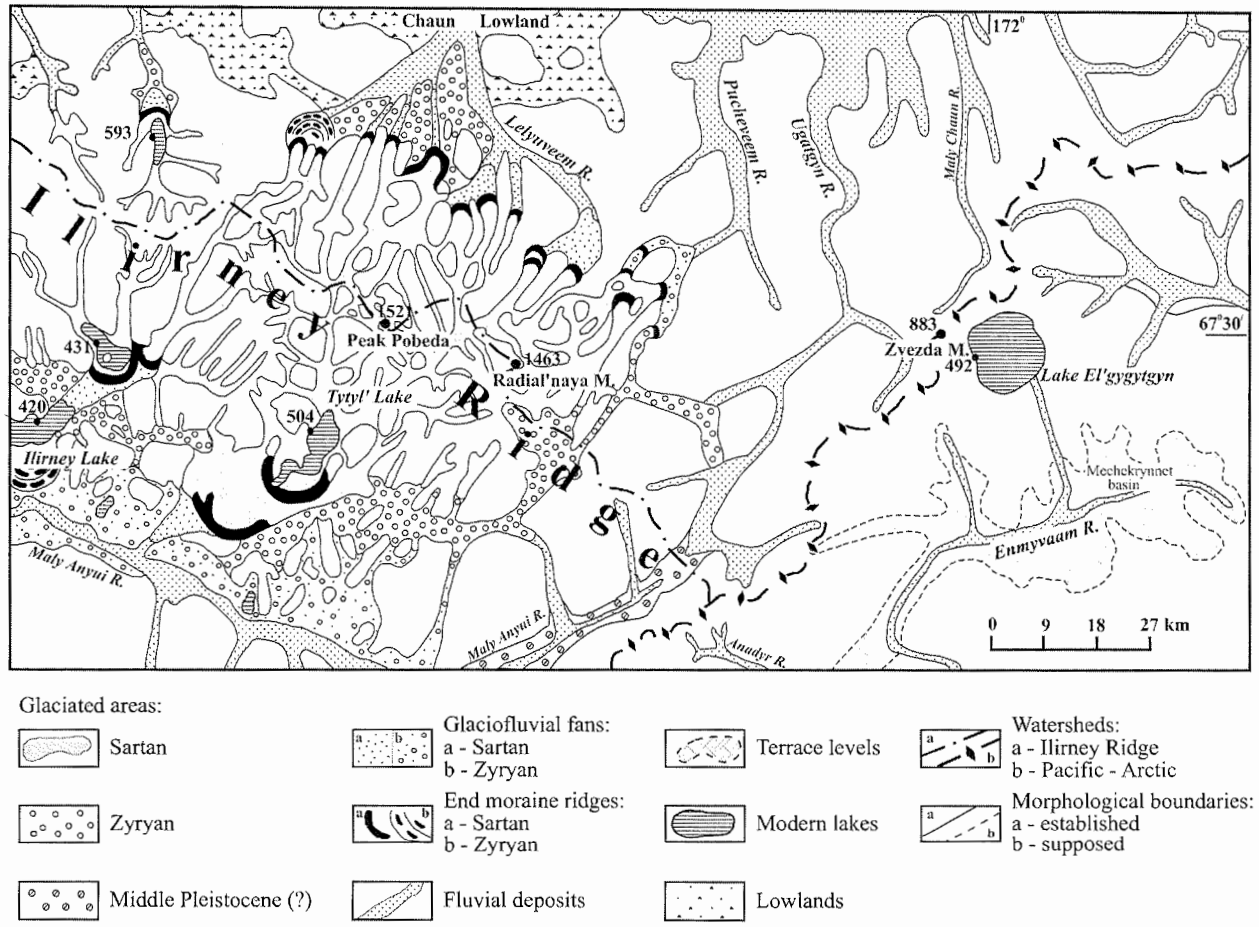

Figure 4: *Geomorphological indications for Pleistocene glaciations to the west of Lake El'gygytgyn.*

4 MODERN ENVIRONMENT AND PROCESSES

4.1 Weather Monitoring

(J. Brigham-Grette, M. Nolan)

The full meteorological station (nicknamed "Yuri Met") erected by Matt Nolan in 2000 and repaired in September, 2001, was downloaded documenting continuous data on all instruments from early September, 2001 to 2 July, 2003; July and August data for 2003 were downloaded by the departing field party (Table 1). The data show that the air temperature sensor at 1 m height was damaged by a bear in March, 2003 but repairs were made by June.

Table 1: *Lake El'gygytgyn climate monitoring stations.*

location	latitude	longitude	logger type	launch date	download date
Micro Met Stations					
Geodetic Peak	67.25.789 N	172.08.158 E	Rain gauge events	30-Jun-03	5-Jul-03
Geodetic Peak	67.25.789 N	172.08.158 E	Air temperature	30-Jun-03	5-Jul-03
North Shore Beach	67.32.516 N	172.02.995 E	Rain gauge events	1-Aug-03	
North Shore Beach	67.32.516 N	172.02.995 E	Air temperature	1-Aug-03	
Yuri Meteorological Station					
100 m SE of Cabin	67.26.808 N	172.10.835 E	Air temperature 1 m	2-Sep-01	2-Jul-03
			Air temperature 3 m		22-Aug-03
			Relative Humidity 1 m		
			Relative Humidity 3 m		
			Net Radiation		
			Wind Speed Average/hr		
			Wind Speed Max		
			Wind Speed Minimum		
			Wind Speed Direction		
			Precipitation Events		
			Snow Depth		
			Barometric Pressure		
			Soil Pit No. 1		
			Soil Moisture 1cm		
			Soil Moisture 5cm		
			Soil Moisture 10 cm		
			Soil Moisture 20 cm		
			Soil Moisture 40 cm		
			Soil Moisture 60 cm		
			Soil temperature 1 cm		
			Soil temperature 5 cm		
			Soil temperature 10 cm		
			Soil temperature 20 cm		
			Soil temperature 40 cm		
			Soil temperature 60 cm		
			Soil Pit No. 2		
			Soil Moisture 3 cm		
			Soil Moisture 8 cm		

The climate data collected from this station have been analysed and assessed for comparison with regional reanalysis data dating back to 1948 (Nolan and Brigham-Grette, in press). These data show that the meteorological station is recording regionally significant weather events and that the site has experienced a dramatic increase in winter temperatures. Specifically, the eight

warmest years and ten warmest winters have occurred since 1989, with the number of days below -30°C dropping from a pre-1989 mean of 35 to zero in recent years. In addition to these analyses, the data will also be used in the future to develop energy balance models of the climatological controls on lake ice cover thickness and persistence (Nolan, unpubl.).

The two small micromet stations deployed at Geodetic Peak and on the North shore of the lake to record air temperatures, ground temperatures and rain events (Table 1) failed to function over the period from September 2001 to 2003. The cause for this malfunction was determined to have been internal to the recording instruments. All of the instruments were field checked, repaired and relaunched to record data continuously for the remainder of the summer. Data from these instruments will be downloaded during a future visit to the lake.

4.2 Vegetation around Lake El'gygytgyn

(P. Minyuk)

Lake El'gygytgyn is located in the zone of hypoarctic tundra (Yurtsev, 1973). The recent vegetation of this area was studied in detail by Kohzevnikov (1993). He identified 249 species and races of vascular plants belonging to 108 genera and 39 families. Rich varieties occur in the families Poaceae (29 species), Cyperaceae (24), Asteraceae (25), Saxifragaceae (20), Caryophyllaceae (19), Brassicaceae (17), and Ranunculaceae (13). In addition, the flora includes approximately 100 rare species. Circumpolar arctalpine species are dominant.

In summer 2003 herbarium samples of typical recent plants occurring close to the lake were sampled. As a rule all plants were collected abloom. This procedure was accomplished in order to establish a standard pollen collection of the local vegetation at Lake El'gygytgyn. Additional recent and subrecent pollen samples were taken from soils, peat bogs, lake sediments as well as lake ice and snow remains that were not completely melted until the beginning of August in some places (Table 28, p. 82). The collection will help to interpret fossil pollen data from the lake sediments. A preliminary determination of some collected plants was made by O.A. Mochalova and M.G. Khoreva from the Institute of Biological Problems of the North in Magadan (Table 2).

Table 2: *Plant species collected around Lake El'gygytgyn in 2003.*

species	species
Acomastilis glacialis (Adam) Khokhrjakov	*Arctophila fulva* (Trin.) Anderss.
A. sp.	*Arenaria tschuktschorum* Regel
Aconitum delphinifolium s.l. (*ssp. anadyrense* Worosch.)?	*Arnica iljinii* (Maguire) Iljin
	A. frigida C.A. Mey
Alectorta sp.	*Artemisia arctica* Less.
Alopecurus alpinus Smith.	*A. borealis* Pall.
Androsace capitata (Willd. ex Roemer et Scultes)	*A. glomerata* Ledeb.
A. septentrionalis L.	*A. sp.*
Anemone narcissiflora s.l.	*Astragalus alpinus* L.
A. richardsonii Hook	*A. sp.*
A. sibirica L.	*Beckwihia chamissonis* (Schlecht.) Tolm.
Antennaria villifera Boriss.	*Betula exilis* (*Betula nana ssp. exilis* [Sukacz.] Hult.)

continuation next page

Table 2: *continuation*

species	species
Calamagrostis aff. purpurascens (*purpurea ssp. langsdorffii* [Link] Tzvel.)	*Nardosmia gmelinii* Turcz.
C. sp.	*N. glacialis* Ledeb.
Caltha arctica R. Br.	*Oxyria digyna* (L.) Hill
Cardamine bellidifolia L.	*Oxytropis aff. chucotica* Jurtz.
C. pratensis (*pratensis ssp. angustifolia* [Hook] O.E.Schulz)	*O. sp.*
Carex sp.	*Pachypleurum alpinum* Ledeb.
C. lugens (Holm.)	Papaver sp.
C. podocarpa (C.B.Clarke)	*Pedicularis capitata* Adams
Cassiope tetragona (L.) D. Don.	*P. lapponica* L.
Cerastium beeringianum (Chamisso et Schlechtendal)	*P. sp.*
C. sp.	*Pinguicula variegata* Turcz.
Cetrarta sp.	*Pyrola minor* L.
Chamaenerion latifolium (Chamaerion latifolium [L.] Holub)	*Poa malacantha* Kom.
Chrysosplenium wrightii Franch. et Sav.	*P. sp.*
Chrysosplenium sp.	*Potentilla nivea* L.
Claytonia acutifolia Pall.,	*Polemonium boreale* Adams
Comarum palustre L.	*Polygonum tripteracarpum* Gray
Crepis nana Richards	*P. viviparum* L.
Delphinium maydellianum (Traut.)	*P. ellipticum* (*P. bistirta ssp. ellipticum* [Willd.] Petrovsky)
D. sp.	*Primula tschuktschorum* Kjellm.
Descurainia sophioides (Fiscer et Hook) Schulz.	*Ranunculus sulphyreus* Soland
Dianthus repens Willd	*Ranunculus pygmaeus*? (Wahlenb)
Diapensia obovata (*Diapensia lapponica ssp. obovata* [F.Schmidt] Hult)	*R. nivalis*? (L.)
Douglasia ochotensis (Willdenow ex Roemer et Schultes) Hulten	*Rhodiola rosea* L.
Draba sp.	*Rhodiola rosea* s.l.
Dryas punctata (*Dryas octopetala ssp. punctata* [Juz.] Hult)	*Rhododendron lapponicum* (*Rhododendron lapponicum ssp. parvifolium* [Adams] Hult.)
Equisetum arvense ssp. arctica (Bong.) Tolm.	*Rumex graminifolius* Lamb.
E. variegatum Schleich.	*R. sp.*
Erigeron sp.	*R. acetosa* L.
Eriophorum polystachyon L.	*Salix reticulata* L.
E. vaginatum L.,	*S. arctica* Pallas
Eritrichium sp,	*S. tschuktschorum* (Skvortz.)
Eritrichtum villosum (Ledeb.) Bunge	*S. polaris* Wahlenb.
Ermania parryoides Cham.	*S. rotundifolia* (?) Traut.
Gastrolychnis apelata	*Salix sp.*
Gentiana algida Pall.	*S. sphenophylla* (*S. sphenophylla ssp. pseudotorulosa* Skvortz.)
G. glauca Pall.	Saussurea sp.
Hedysarum hedysaroides (L.) Shinz.et Thell. *ssp. arcticum* (B. Fedtssch.) P. Ball	*Saussurea tilesii* (Ledeb.) Ledeb.
Hierochloe alpina (Sw.) Roem et Schult.	*Saxifraga nelsoniana* D. Don.
Hippuris vulgaris L.	*S. cernua* L.
Juncus sp.	*S. flagellaris* (*S. flagellaris ssp. setigera* (Pursh) Tolm.
Lagotis minor (*Lagotis glauca* Laertn. *ssp. minor* [Willd.] Hult.)	*S. funstonii* (Small) Fedde
Ledum decumbens (*Ledum palustre ssp. decumbens* [Ait.] Hult.)	*S. hirculus* L.
Leymus mollis (Trinius) Hara	*S. hyperborea* R.Br.
Lemna minor L.	*S. multiflora* Ledeb.
Lloydia serotina (L.) Reichb.	*S. punctata* L.
Luzula sp.	*S. serpyllifolia* Pursh
Minuartia macrocarpa (Pursh) Ostenf.	*Silene acaulis* (L.) Jack
Myosotis suaveolens (*Myosotis suaveolens ssp. asiatica* [Vestergr.] Ju. Kozhevn)	*Stellaria sp.*
	Taraxacum sp.
	Vaccinium minus (Loddiger) Woroshilov
	V. uliginosum L.
	Valeriana capitata Pall
	Veratrum oxysepalum Turcz

4.3 Lake El'gygytgyn Ice Characteristics and Dynamics

4.3.1 Ice Formation, Thickness and Breakup in 2003

(O. Juschus, V. Wennrich, G. Schwamborn, S. Quart)

Introduction

The ice cover of Lake El'gygytgyn is an important feature concerning the formation and properties of the limnic sediments. Changes in lake ice dynamics during the past three climatic cycles have strongly influenced the characteristics of the lake sediments (e.g., Nowaczyk et al., 2002; Melles et al., in press). Knowledge of the modern duration, thickness and stability of the lake ice cover also is important for the preparation of the aspired deep drilling campaign on the lake, since the drilling is planned to be conducted from the ice cover.

First results of investigations of the lake ice dynamics based on remote sensing data were published by Nolan et al. (2003, see Table 3). Usually the formation of a stable lake ice cover starts during the second half of October, the first snow melt occurs during May and the lake became ice free at the end of July and the beginning of August. The ice thickness was modelled by Nolan et al. (2003) to have a maximum of approximately 1.8 m.

Table 3: *Important dates of lake ice dynamics derived from SAR (after Nolan et al., 2003).*

winter	onset of lake ice freezing	onset of lake ice snowmelt	onset of lake ice moat formation	completion of lake ice melt
1997 – 1998	no data	<8 July	<8 July	8 July – 9 Aug.
1998 – 1999	>6 Oct.	17 May – 18 May	24 June – 4 July	28 July – 13 Aug.
1999 – 2000	16 Oct. – 19 Oct.	8 May – 11 May	23 June – 2 July	16 July – 19 July
2000 – 2001	18 Oct. – 20 Oct.	14 May – 17 May	20 June – 23 June	13 July – 17 July

Ice Formation

Some indications for the processes taking place on Lake El'gygytgyn during the formation of the lake ice cover come from ice structures formed during autumn 2002 and winter 2002/03 but observed in spring 2003.

The occurrence of ice floes found incised in younger ice at the southern shore (Fig. 5, upper left) indicates storm events during the formation of the ice cover. Storms, or at least strong winds, probably have led to an almost complete destruction of a closed ice cover in autumn. Only a few floes survived and later became frozen into more recent ice forming the final ice cover.

Storm events likely have also occurred at a later stage of ice formation, leading to a remarkable ice barrier 500 m to the north of the southern shoreline. A younger age of the ice barrier is evidenced by the fact that it cuts some of the ice floes. The storm event obviously at this time was no any longer able to break the ice cover into floes. It was only able to break the cover along one huge crack and to press both ice margins into each other (Fig. 5, lower left).

Smaller ice cracks found cutting both new ice and ice floes (Fig. 5, right) also

are younger than the ice floes, but probably not formed due to storm events. More likely for these remarkable structures we regard a formation due to variations in temperature.

Figure 5: *Lake ice features, formed during autumn and winter 2002/03, photographed in spring 2003; upper left: old ice floes, integrated into the younger lake ice cover (06-17-03); lower left: ice barrier 500 m to the north of the southern shoreline (05-07-03); right: a refrozen ice crack (06-06-03).*

Ice Thickness

Ice thickness measurements were conducted between May and July 2003. The lake ice cover was perforated using two different coring equipments: An engine-based ice drill (Jiffy-Corporation) and a simple hand-operated ice corer (Fig. 6). The boreholes produced by these equipments have diameters of 18 and 12 cm, respectively. The lake ice thickness was measured by tape, usually shortly after the drilling. During the ice breakup in July 2003 the ice thickness was measured on ice floes at the lake shore.

In May 2003 the ice thickness varied predominantly between 1.8 and 2 m (Fig. 7). A significantly higher thickness of 2.37 m was measured at a site, 500 m north of the southern lake shore. This unusual thickness is probably due to some ice movement that has happened during storm events in the previous winter.

During June 2003 a significant variability in ice thickness was noticed. The values ranged from 1.95 to 1.40 m, probably due to local differences in melting processes which had started at that time.

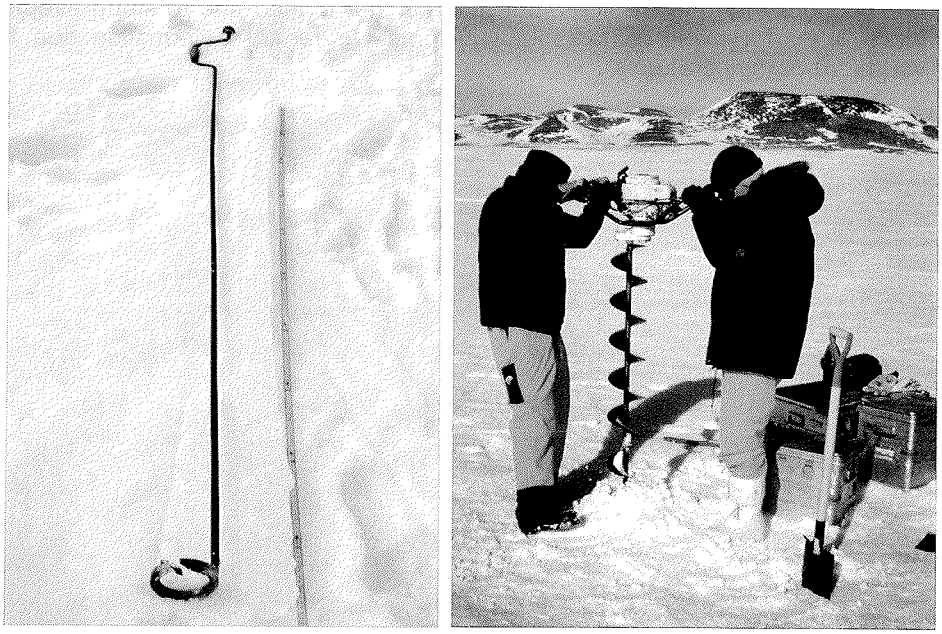

Figure 6: *Hand-operated (left) and engine-based (Jiffy Corp., right) ice coring equipment used during the expedition in 2003.*

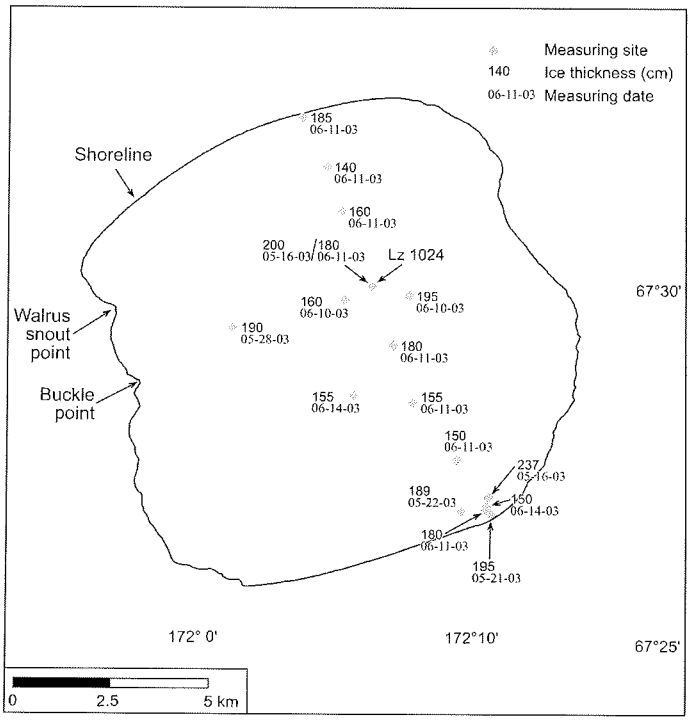

Figure 7: *Measurements of ice thickness on Lake El'gygytgyn in 2003.*

In the middle of June a moat had been formed around the lake shore and it became too dangerous to step on the lake ice. However, some measurements became possible during the start of the lake ice breakup on July 3. At that time most of the ice floes had a thickness of only about 40 - 60 cm. During the following days the lake ice cover became more and more thin and unstable, decreasing to 15 cm on July 12.

Ice Breakup

A first phase of lake-ice breakup started on May 18, 2003, with the onset of melting of the blanketing snow cover (Table 4). The snow melt was completed on June 8, 2004, when the formation of moats started, especially at the lake shore and at an ice ridge 500 m to the north of the southern shore (Fig. 8). At the southern shore the moat breadth between June 7 and June 17 increased from 0 to approximately 10 m. On July 2 about 20 - 30 m were reached. These first moats were primarily formed by ice melt processes. Due to weak winds at this time only some ice floes were disintegrated by wave action. The lake ice cover was still stable against wind pressure.

Table 4: *Summary of lake ice dynamics during spring and summer 2003.*

onset of lake ice snow melt	completion of lake ice snow melt	onset of lake ice moat formation	completion of lake ice melt
May 18	June 8 / 9	June 8	July 19

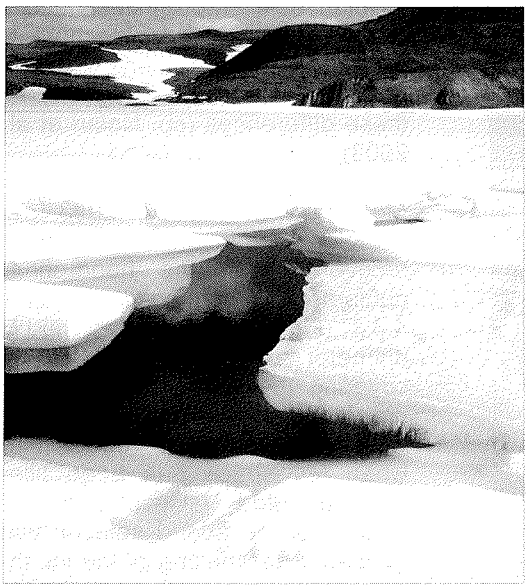

Figure 8: *Large moat formed by ice melt 500 m to the north of the southern shore on June 17, 2003.*

Lake ice breakup tuned into a second phase on July 3, 2003, when a strong storm from the north pushed the ice cover to the southern lake shore. There, the moat got quickly closed and eventually the ice became pushed onshore leading to the formation of an barrier (Fig. 9, left). After melting of the ice barrier several ice pushed ridges with maximum heights of 50 cm became exposed at the shore bar (Fig. 9, right). These features were often noticed around the lake, especially on the peninsulas at the western shore (walrus snout point and buckle point; see Fig. 7). Thus ice pushing seems to be one of the main processes of recent shore line formation.

After July 3 the ice decomposition was strongly influenced by wind and wave action. On July 10 southern wind was reopening the moat at the southern

shore, which reached a width of about 700 m. After that the lake quickly became ice free. On July 16 the lake was covered by one third with thin ice and on July 19 the lake ice disintegration was almost completed. Only small ice floes were left at the northern shore.

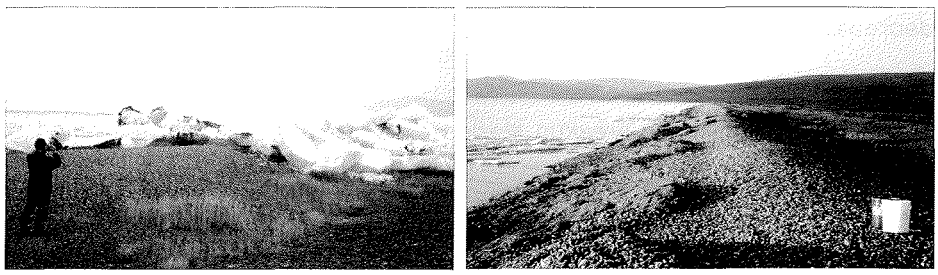

Figure 9: *The ice barrier during its formation on July 3 (left) and ice-pushed ridges at the shore bar after melting of this barrier on July 18, 2003 (right).*

4.3.2 Gas Content of the Lake Ice

(O. Juschus, G. Schwamborn, D. Wagner)

Introduction – The lake ice of Lake El'gygytgyn includes gas bubbles. This fact was mentioned by Glotov & Zuev (1995) and Nolan et al. (2003). According to Glotov and Zuev (1995) the bubbles contain mainly nitrogen and oxygen. Carbon dioxide (less than 0.003 %), methane (less than 0.02 %), and hydrogen (less than 0.0005 %) are only accessories. Nolan et al. (2003) described a remarkable "bull's eye-pattern" in the ice cover (Fig. 10) that is traced back to differences in gas content or bubble characteristics. As yet there are only hypotheses about the reasons for these differences (cp. Nolan et al., 2003).

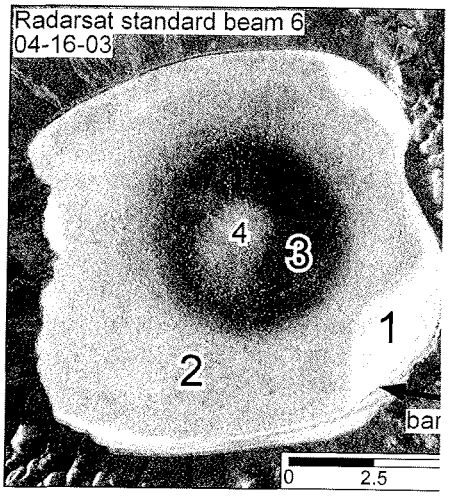

Figure 10: *The "bull's eye"-pattern in th cover of Lake El'gygytgyn during spring with ice bubble regions 1 – 4 after Nolan (2003); Radarsat scene by Nolan (unpubl.). genesis of the ice barrier visible in the sou part of the lake is discussed in Chapter 4.3.1.*

Methods – In spring 2003 gas samples were taken from ice cores recovered with the hand-coring equipment described in Chapter 4.3.1 (Fig. 6). The cores had a diameter of 8.5 cm. After re-covering they were put into leak-proofed steel tubes, whose taps were closed with a rubber plug when left space has been filled with saturated NaCl-solution. The volume of the added solution was noticed. After melting of the ice the gas was excavated through the tab with a syringe and injected into glassy test tubes, which had been filled with saturated NaCl-solution before the expedition. Then the

volume of the water left in the steel tubes was measured and the gas volume calculated. After the expedition the methane content was measured by gas chromatography.

First results – Most significant differences in bubble content and shape were observed between the cores from the southern shore area and those from other parts of the lake. At the southern shore the ice movement and pressure during autumn and winter 2002/2003 (see Chapter 4.3.1) influenced the ice structure. The ice consisted of ice floes, new ice, and especially snow. That's probably why the ice in this area was non-columnar and contained many round-shaped gas bubbles (Fig. 11, left).

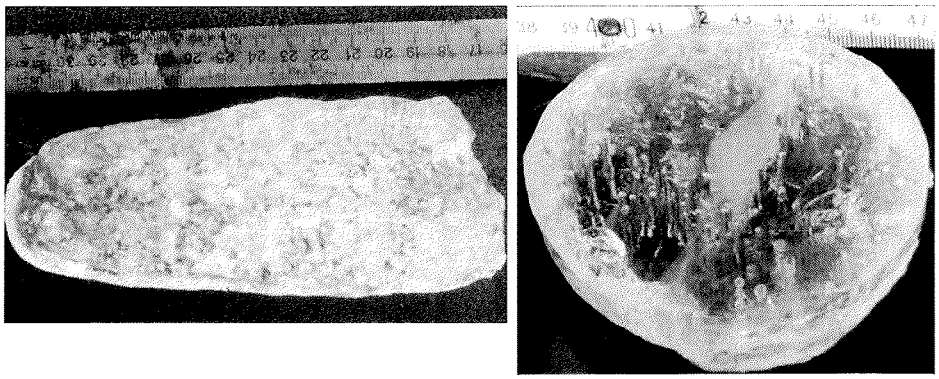

Figure 11: *Gas-rich lake ice from the southern shore area (left). Part of ice core IC-4 with long-shaped gas bubbles (right). Due to the brittle ice with horizontal fissures it was not possible at this position to get core pieces long enough for gas analyses. The long-shaped gas bubbles were not completely recovered. From the upper (at mark 44 cm) to the lower part of the photo a vertical fissure is visible.*

In contrast, the lake ice in the other areas, representing zones 1 - 4 after Nolan et al. (2003) had a columnar ("candle ice") structure. It was brittle and contained many horizontal and vertical fissures (Fig. 11, right). The gas bubbles found within this ice were mostly long-shaped, being up to 10 cm in length and up to 0.3 cm in diameter. Due to the fact that those gas bubbles cut at the walls and at breaks of the ice cores were not accounted for during the gas measurements the real gas content in the lake ice is higher than the measured values. This is particularly the case in the central lake, where the long-shaped bubbles predominate. Hence, this is probably one explanation why the measured gas content at sites IC-6 to IC-8, corresponding with zones 3 and 4 after Nolan et al. (2003), is significantly lower than the gas content at sites IC- 1 to IC-3 at the southern shore (Table 5 and Fig. 12).

With the exception of site IC-7 all gas samples contained more methane than the atmospheric methane content (Table 5). In consideration of the simple sampling equipment some pollution of the gas samples with atmospheric gases likely has happened. The real methane content of the lake ice thus is assumed to be even higher. In any case, the results are strong evidence for methane production within the lake.

Table 5: *Measurements of gas contents in the lake ice of Lake El'gygytgyn and ground ice of Lagerny Creek (station IC-9) during spring 2003.*

station no.	position latitude	position longitude	ice thickness (cm)	date	sample no.	sample depth (cm)	$NaCl_{sat}$ (ml)	liquid vol. (ml)	gas vol. (ml)	ice vol. (ml)	gas vol. (ml)/ 100 ml ice	methane (ppm)
IC-1	67°27.16´ N	172°10.66´ E	237	05-16-03	I	53 - 67.5	700	1270	194	570	34	12.78
					II	117 - 132	625	1220	244	595	41	
					III	195 - 211	650	1215	249	565	44	
IC-2	67°26.92´ N	172°10.76´ E	195	05-21-03	I	29 - 45	600	1340	124	740	17	4.57
					II	85 - 100	600	1350	114	750	15	
					III	141 - 157	670	1285	179	615	29	
IC-3	67°26.97´ N	172°09.69´ E	189	05-22-03	I	54 - 70	680	1400	64	720	8.9	13.78
					II	99 - 115	650	1360	104	710	15	
					III	129 - 145	645	1330	134	685	20	
					IV	23 - 39	970	1375	89	405	22	
IC-4	67°27.22´ N	172°10.32´ E	160	05-20-03		not sampled						
IC-6	67°29.94´ N	172°05.45´ E	160	06-10-03	I	21 - 37	675	1360	104	685	15	3.16
					II	69 - 85	635	1390	74	755	10	
					III	145 - 160	655	1390	74	735	10	
IC-7	67°30.00´ N	172°07.80´ E	195	06-10-03	I	59 - 75	790	1375	89	585	15	0
IC-8	67°28.60´ N	172°05.80´ E	155	06-13-03	I	5 - 20	850	1400	64	550	12	5.63
					II	40 - 60	885	1415	49	530	9.2	
					III	103 - 120	735	no data	no data	no data	-	
IC-9	67°28.20´ N	172°13.46´ E	135	06-13-03	I	40 - 60	600	1375	89	775	11	12.92
					II	75 - 90	790	1395	69	605	11	
					III	115 - 130	660	1355	10	794	1.3	

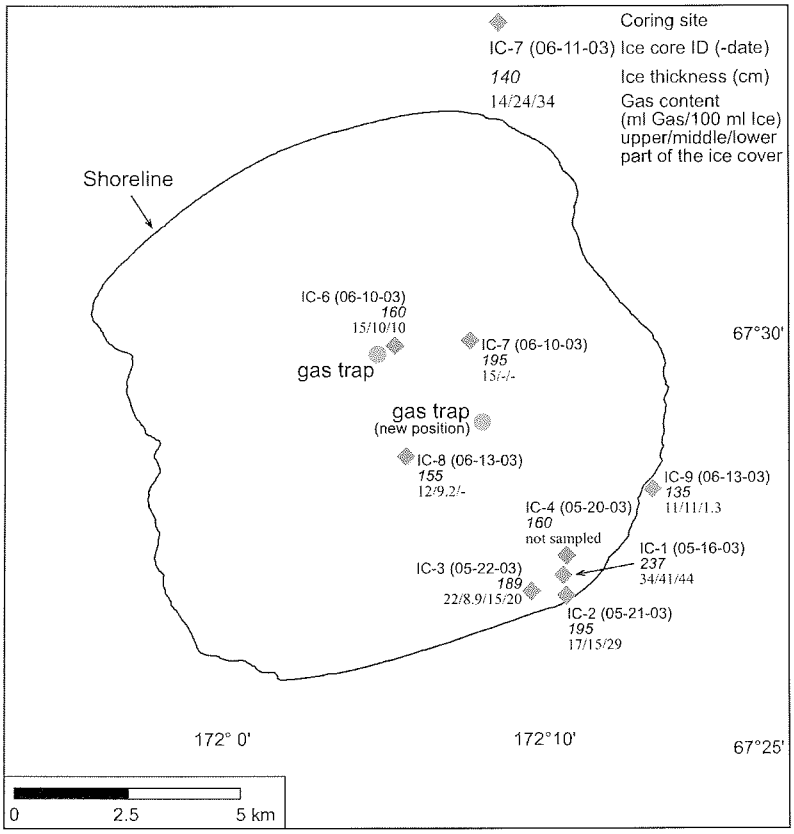

Figure 12: *Positions of ice cores and gas traps sampled at Lake El'gygytgyn and Lagerny Creek during the expedition in 2003.*

4.3.3 Gas Emission from the Lake Bottom

(O. Juschus, D. Wagner)

Introduction – The composition of the gas bubbles within the lake ice does not necessarily reflect the composition of the gases exhausting from the lake sediments, because they can change their chemical composition during the migration through the water column. For instance, methane produced under anoxic conditions will to be oxidised into carbon dioxide. In other cases, the micro and macro organisms living in the lake produce and consume oxygen and carbon dioxide on their way to the lake surface. Hence, the only way to get unchanged gas is to collect it directly above the lake bottom.

Methods and field results – During the preparation for the expedition a gas trap was built by a technician of the Leipzig University (Fig. 13). The trap has a quadratic floorspace with a side length of 50 cm. Its body consist of plastic plates, which can be disassembled for transport. The construction is stabilized by brass sheets, which were fixed and sealed with silicone at the edges.

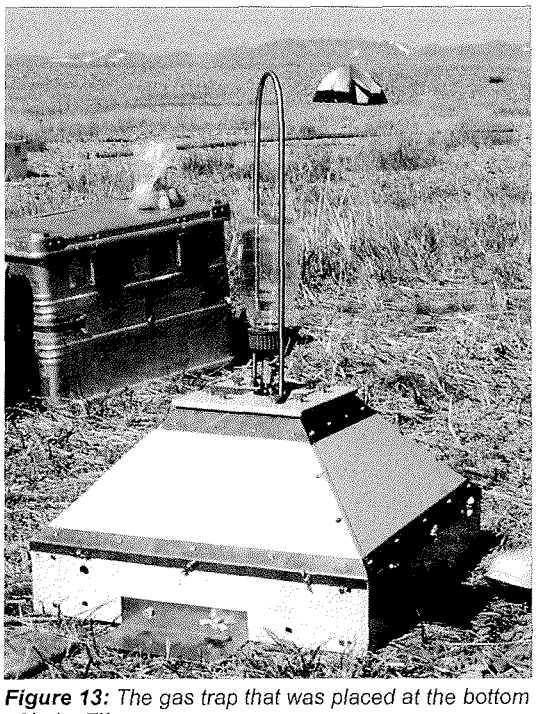

Figure 13: *The gas trap that was placed at the bottom of Lake El'gygytgyn.*

Additional brass sheets were fixed at the bottom plates in order to reduce the ground pressure. At the top of the trap a bottle for gas sampling is fixed.

The gas trap was first deployed at the lake bottom on July 25, 2003, at 67°29.84'N, 172°04.92'E (Fig. 12). At this position, weak sediment fissures were identified in the seismic data obtained in 2000 and interpreted as gas emission channels. After recovering the trap on August 18, 2003, a small bubble (approximately 10 ml) was collected. The trap bottle was changed and the gas trap replaced at the lake bottom on August 19, 2003, at the position 67°29.02'N 172°08.20'E (see Fig. 12).

4.4 Hydrology of Lake El'gygytgyn

4.4.1 Hydrological Field Measurements and Water Sampling

(O. Juschus, J. Brigham-Grette, V. Wennrich, S. Quart, R. Wennrich)

Introduction – Knowledge of the hydrological characteristics of the lake water is important to understand the modern sediment formation, which is strongly influenced by the physical and chemical properties of the water column. This is true for the deposition of both clastic and biogenic sediment components, but also for some early diagenetic processes taking place after the deposition.

Methods – During the field work in spring and summer 2003 hydrological investigations were carried out on water samples from the lake, from inlet streams, and from precipitation (Table 6, Fig. 14).

Table 6: *List of hydrological field measurements done during spring and summer 2003.*

measurement of	lake water	inlet streams	precipitation
temperature	x		
pH	x	x	
conductivity	x	x	x

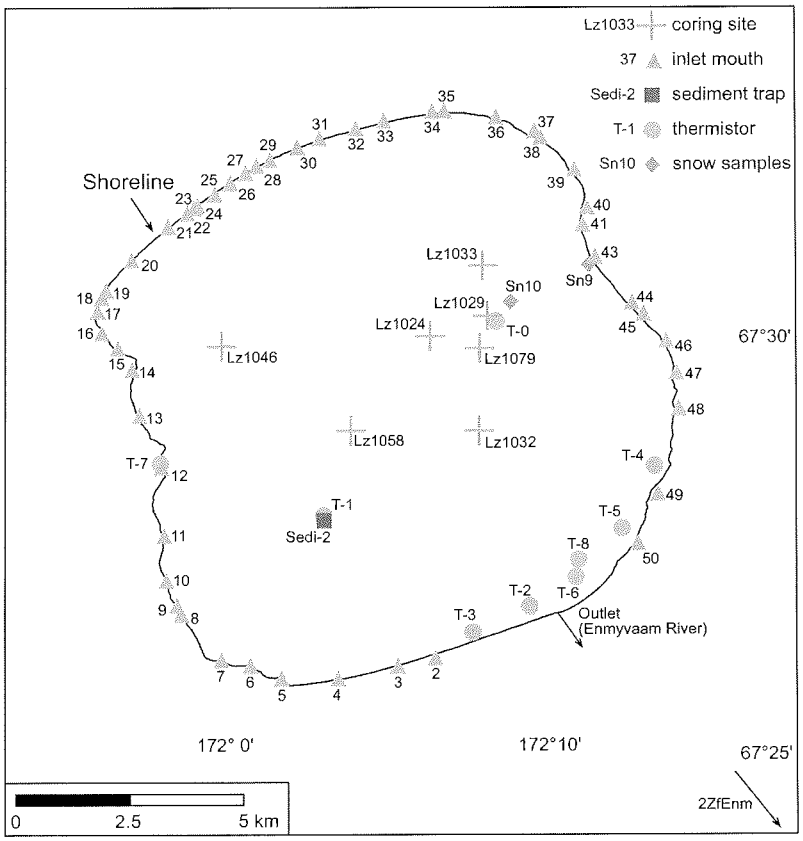

Figure 14: *Sites for hydrological measurements on and around Lake El'gygytgyn in 2003.*

Lake water samples were taken with a 1.5 l UWITEC (Umwelt und Wissenschaftstechnik, Mondsee, Austria) water sampler (Fig. 15). On the samples, the parameters conductivity and pH-value were measured after returning at the cabin with WTW (Wissenschaftlich-Technische Werkstätten GmbH, Weilheim, Germany) instruments, a WTW Cond340i and a WTW 197 N° III, respectively.

Furthermore, samples of 100 ml were taken from lake and precipitation water for analyses of the chemical and isotopical ($\delta^{18}O$, $\delta^{13}C$) composition. The analyses were kindly conducted by R. Wennrich and collaborators at the Department for Analytical Chemistry of the Centre for Environmental Research (UFZ) Leipzig-Halle, using Inductively Coupled Plasma Optical Emission Spectrometry (ICP-OES, Ciros Spectro A.I.), ICP mass spectrometry (ICP-MS, ELAN 5000 Perkin-ELMER) and ion chromatography (DX 500 DIONEX).

Results of temperature measurements - At the beginning of the field campaign, in late May, 2003, the lake was covered by approximately 2 m of ice. From the base of the ice cover to the lake bottom the temperature more or less

constantly increased from 0.2 to 3.0°C (Fig. 16), indicating some stratification of the water column. Exceptions from this trend at 160 and 165 m depth were probably induced by errors in measurements. In August, after the ice melt, the temperature distribution was much more uniform. This indicates that the stratification was destroyed during summer time by mixing, initiated by melt-water supply, wind-induced water movement or density-driven circulation due to temperature rise.

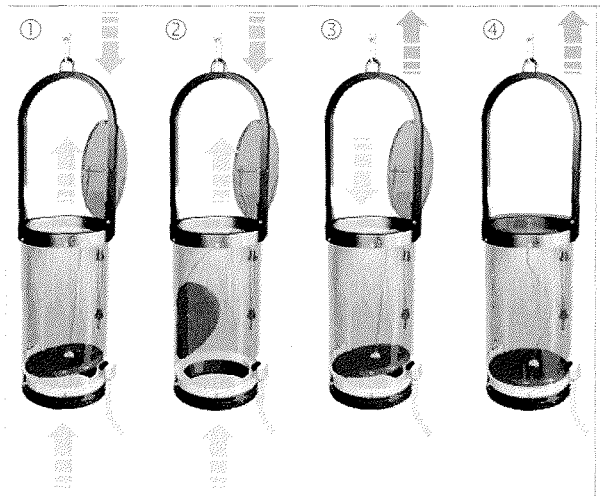

(source www.uwitec.at)

1. *The lid is fixed by a magnet in vertical position.*
2. *The water flow presses the lower flap inside the plastic tube. The water flows freely through the tube.*
3. *The flap moves down once the recovery of the sampler starts.*
4. *The steel string removes the lid from the magnet. The tube is closed.*
5. *The temperature is measured with an internal thermometer.*
6. *At the surface the water is filled into bottles with the tap*

Figure 15: *The UWITEC water sampler.*

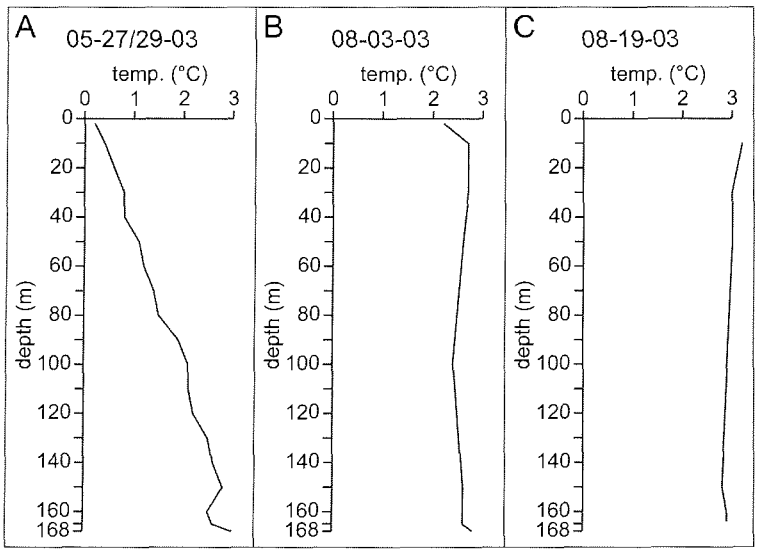

Figure 16: *Seasonal records of temperature in the lake water body; A and B were recorded at the position Lz1024 (67°30.13´N; 172°06.46´E); C was recorded at the position Lz1079 (67°29.91´N; 172°08.01´E).*

Conductivity and pH-value measurements – Almost all conductivity values measured in spring and summer 2003 are between 12 and 15 µS/cm (Table 7). They evidence a low concentration of salts in the lake water. The only exception is a remarkably higher value of 21.4 µS/cm at 2 m depth beneath the lake ice in May. This is probable due to the enrichment of salts in the surface water in consequence of the lake ice formation in winter time, because lake ice consists of almost pure fresh water. The pH values of the lake water on May 27 and August 5, 2003, were very similar and, with the exception of significantly lower values close to the lake bottom, very constant throughout the water column, ranging only between about 6.3 to 6.5. On August 20, in contrast, the pH values were remarkable lower, the reason for which is not clear. In the inlet streams only few conductivity and pH measurements were conducted (Table 8). The results indicate a decrease in conductivity but rather constant pH values in the course of the season.

Table 7: *Seasonal measurements of conductivity and pH-values.*

site	position		depth (m)	cond. (µS/cm)	pH-value	date
	latitude	longitude				
Lz 1024	67°30.13´N	172°06.46´S	2	21,4	6,32	05-27-03
			10	14,7	6,52	
			30	14,4	6,52	
			50	12,9	6,43	
			100	13,3	6,44	
			150	13,9	6,46	
			165	15,5	6,18	
			168	16,8	5,90	
Lz 1024-2	67°30.13´N	172°06.46´S	2	12,3	6,22	08-05-03
			10	12,2	6,45	
			30	11,9	6,46	
			50	11,8	6,35	
			100	11,8	6,33	
			150	11,7	6,43	
			165	12,7	6,21	
			168	12,3	5,87	
Lz 1079	67°29.98´N	172°07.99´S	2	15,1	5,66	08-20-03
			10	14,1	5,76	
			30	12,8	5,74	
			50	13,5	5,78	
			150	14,0	5,77	
			163	13,8	5,86	
			166	14,0	5,87	

Results of chemical analyses – The lake water has very low concentrations of anions and cations (Table 9). On May 27, 2003, the total ion concentration at station Lz1024 ranged between 4 and 5 mg/l (typical mineral waters have 300 - 400 mg/l). Slightly higher values of about 7 mg/l were only measured in the two uppermost samples (2 and 10 m below lake level, 0 and 8 m below ice cover, respectively). This higher ion concentration beneath the lake ice in spring, as the higher conductivity values measured in the same sample (see above), probably is due to the lake ice formation in winter that leads to an enrichment in ions in the underlying the lake water.

Table 8: *Measurements of conductivity and pH-value from inlet streams and snow samples.*

sample-ID	position		date	source	conductivity	pH
	latitude	longitude			(µS/cm)	
Zf2-1	67°26.23´ N	172°06.59´ E	06-07-03	inlet No. 2	22.3	6.37
Zf2-2	67°26.20´ N	172°06.59´ E	06-07-03	inlet No. 2	23.3	6.33
Zf49-1	67°28.20´ N	172°13.46´ E	06-08-03	inlet No. 49 Lagerny	21.4	6.54
Zf50-3	67°27.61´ N	172°12.84´ E	06-15-03	inlet No. 50	15.5	6.12
2ZfEnm	67°24.00´ N	172°15.32´ E	06-22-03	tributary outlet	7.1	5.86
Sn9	67°30.97´ N	172°11.38´ E	05-29-03	snow on lake ice	4.9	-
Sn10	67°30.52´ N	172°08.97´ E	05-29-03	snow on lake ice	4.9	-

Table 9: *Chemical analyses of the lake water at station Lz1024 (67°30.13´N; 172°06.46´S) on May 27, 2003. All data in mg/l; contents of F - (<0.09) B - (<0.3), In (<0.00005), Cs (<0.000035), Pr (<0.00003), Eu (<0.00005), Tb (<0.00003), Ho (<0.00003), Tm (<0.00003), Lu (<0.00003), and Th (<0.00003) are below detection limit; the field ID is according to the sample depth.*

field ID		sample	ICP-OES				Ion chromatography			photometry
LZ1024	date	ID (UfZ)	Na	Mg	S	Ca	chloride	nitrate	sulphate	phosphate
2	05-27-03	A87557	1.04	0.19	0.27	1.05	0.94	0.38	2.63	<0.07
10	05-27-03	A87559	1.24	0.14	0.13	0.88	1.43	0.39	2.58	<0.07
30	05-27-03	A87561	0.61	0.13	0.10	0.83	0.38	0.37	2.56	<0.07
50	05-27-03	A87563	0.53	0.11	0.10	0.72	0.38	0.31	2.67	<0.07
100	05-27-03	A87565	0.53	0.11	0.07	0.71	0.33	0.33	2.52	<0.07
150	05-27-03	A87567	0.55	0.12	0.11	0.76	0.41	0.37	2.55	<0.07
165	05-27-03	A87569	0.54	0.13	0.13	0.83	0.36	0.6	2.44	<0.07
168	05-28-03	A87571	0.54	0.15	0.10	0.94	0.30	1.06	2.72	<0.07
2-2	08-02-03	A87558	0.57	0.11	0.07	0.71	0.32	0.33	2.42	<0.07
2-10	08-02-03	A87560	0.55	0.11	0.05	0.70	0.31	0.36	2.61	<0.07
2-30	08-02-03	A87562	0.53	0.11	0.10	0.70	0.32	0.35	2.59	<0.07
2-50	08-02-03	A87564	0.52	0.11	0.06	0.70	0.33	0.35	2.63	<0.07
2-100	08-02-03	A87566	0.51	0.12	0.08	0.72	0.28	0.31	2.59	<0.07
2-150	08-02-03	A87568	0.49	0.11	0.06	0.69	0.28	0.29	2.56	<0.07
2-165	08-02-03	A87570	0.52	0.11	0.09	0.70	0.31	0.3	2.47	<0.07
2-168	08-02-03	A87572	0.51	0.11	0.08	0.70	0.30	0.38	2.49	<0.07

field ID*	ICP-MS										
LZ1024	Li	Mg	Al	K	Ca	Sc	Ti	V	Cr	Mn	Co
2	< 0.0001	0.23	0.00212	0.19	1.21	<0.0001	<0.0001	0,00010	0.00022	0.00073	<0.00004
10	< 0.0001	0.16	0.00174	0.15	0.94	<0.0001	<0.0001	0,00007	0.00024	0.00054	<0.00004
30	< 0.0001	0.15	<0.001	0.17	0.91	<0.0001	<0.0001	<0.00005	0.00016	0.00026	<0.00004
50	< 0.0001	0.13	0.00227	0.14	0.82	<0.0001	0.00036	<0.00005	0.00014	0.00016	<0.00004
100	< 0.0001	0.13	0.00128	0.15	0.8	<0.0001	<0.0001	<0.00005	0.00014	0.00019	<0.00004
150	< 0.0001	0.13	0.00432	0.15	0.85	<0.0001	0.00025	<0.00005	0.00021	0.00038	<0.00004
165	0.000160	0.14	0.00720	0.14	0.95	0.00024	0.00068	<0.00005	0.00022	0.00048	0.00004
168	0.000124	0.17	0.01540	0.17	1.04	0.00049	0.00107	<0.00005	0.00014	0.00091	<0.00004
2-2	< 0.0001	0.13	0.03610	0.18	0.76	<0.0001	0.00052	<0.00005	0.00012	0.00131	<0.00004
2-10	< 0.0001	0.12	<0.001	0.19	0.76	<0.0001	<0.0001	<0.00005	0.00009	0.00013	<0.00004
2-30	< 0.0001	0.12	0.00327	0.19	0.77	<0.0001	<0.0001	<0.00005	0.00009	0.00010	<0.00004
2-50	< 0.0001	0.12	0.00140	0.19	0.81	<0.0001	0.00018	<0.00005	0.00010	0.00010	<0.00004
2-100	< 0.0001	0.13	0.04300	0.18	0.8	<0.0001	0.00117	<0.00005	0.00015	0.00161	<0.00004
2-150	0.000150	0.12	0.00765	0.22	0.81	<0.0001	0.00038	<0.00005	0.00014	0.00037	<0.00004
2-165	0.000184	0.12	0.01120	0.19	0.81	<0.0001	0.00057	<0.00005	0.00016	0.00040	<0.00004
2-168	0.000123	0.12	0.00189	0.21	0.77	<0.0001	0.00022	<0.00005	0.00010	0.00141	<0.00004

continuation next page

Table 9: continuation

field ID*	ICP-MS cont.									
LZ1024	Ni	Cu	Zn	As	Se	Zn	As	Se	Sr	Rb
2	0.00007	0.00080	0.01480	<0.00035	<0.0005	0.01480	<0.00035	<0.0005	0.00663	0.00019
10	0.00013	0.00087	0.01520	<0.00035	<0.0005	0.01520	<0.00035	<0.0005	0.00549	0.00017
30	<0.00005	0.00051	0.01090	<0.00035	<0.0005	0.01090	<0.00035	<0.0005	0.00529	0.00012
50	0.00006	0.00043	0.00712	<0.00035	0.00060	0.00712	<0.00035	0.00060	0.00466	0.00013
100	0.00007	0.00084	0.01010	<0.00035	<0.0005	0.01010	<0.00035	<0.0005	0.00464	0.00013
150	0.00013	0.00076	0.01040	<0.00035	<0.0005	0.01040	<0.00035	<0.0005	0.00485	0.00014
165	0.00028	0.00106	0.01090	<0.00035	0.00062	0.01090	<0.00035	0.00062	0.00521	0.00018
168	0.00011	0.00065	0.00721	<0.00035	<0.0005	0.00721	<0.00035	<0.0005	0.00620	0.00016
2-2	<0.00005	0.00206	0.00507	0.00041	<0.0005	0.00507	0.00041	<0.0005	0.00455	0.00012
2-10	<0.00005	0.00039	0.00418	0.00038	<0.0005	0.00418	0.00038	<0.0005	0.00456	0.00010
2-30	<0.00005	0.00047	0.00301	0.00038	<0.0005	0.00301	0.00038	<0.0005	0.00447	0.00010
2-50	<0.00005	0.00047	0.00205	0.00048	<0.0005	0.00205	0.00048	<0.0005	0.00450	0.00011
2-100	0.00012	0.00142	0.00373	0.00044	<0.0005	0.00373	0.00044	<0.0005	0.00467	0.00013
2-150	0.00007	0.00073	0.00305	0.00053	<0.0005	0.00305	0.00053	<0.0005	0.00462	0.00013
2-165	0.00010	0.00186	0.00858	0.00072	<0.0005	0.00858	0.00072	<0.0005	0.00456	0.00015
2-168	<0.00005	0.00045	0.00572	0.00070	<0.0005	0.00572	0.00070	<0.0005	0.00454	0.00011

field ID*	ICP-MS cont.									
LZ1024	Y	Zr	Mo	Cd	Ag	Sn	Sb	Ba	La	Ce
2	<0.000035	0.00019	<0.0001	<0.00005	<0.00005	<0.00005	0.00024	0.00125	<0.000035	<0.000035
10	<0.000035	<0.0001	<0.0001	<0.00005	<0.00005	<0.00005	0.00007	0.00106	<0.000035	<0.000035
30	<0.000035	<0.0001	<0.0001	<0.00005	<0.00005	<0.00005	<0.00005	0.00101	<0.000035	<0.000035
50	<0.000035	<0.0001	<0.0001	<0.00005	<0.00005	<0.00005	0.00007	0.00081	<0.000035	<0.000035
100	<0.000035	<0.0001	<0.0001	<0.00005	<0.00005	<0.00005	<0.00005	0.00076	<0.000035	<0.000035
150	<0.000035	<0.0001	<0.0001	0.00006	<0.00005	<0.00005	0.00012	0.00115	<0.000035	<0.000035
165	<0.000035	<0.0001	0.00024	0.00014	0.00005	0.00009	0.00014	0.00142	<0.000035	<0.000035
168	<0.000035	<0.0001	0.00011	0.00018	<0.00005	0.00005	0.00007	0.00235	<0.000035	<0.000035
2-2	<0.000035	<0.0001	<0.0001	<0.00005	<0.00005	<0.00005	0.00010	0.00098	<0.000035	0.000036
2-10	<0.000035	<0.0001	<0.0001	<0.00005	<0.00005	<0.00005	<0.00005	0.00056	<0.000035	<0.000035
2-30	<0.000035	<0.0001	<0.0001	<0.00005	<0.00005	<0.00005	<0.00005	0.00054	<0.000035	<0.000035
2-50	<0.000035	<0.0001	<0.0001	<0.00005	<0.00005	<0.00005	<0.00005	0.00042	<0.000035	<0.000035
2-100	0.00004	<0.0001	<0.0001	<0.00005	<0.00005	<0.00005	0.00009	0.00073	0.00005	0.000083
2-150	<0.000035	<0.0001	<0.0001	<0.00005	<0.00005	<0.00005	0.00005	0.00056	<0.000035	<0.000035
2-165	<0.000035	<0.0001	0.00016	0.00010	<0.00005	0.00006	0.00011	0.00048	0.00004	0.000065
2-168	<0.000035	<0.0001	<0.0001	<0.00005	<0.00005	<0.00005	<0.00005	0.00047	<0.000035	<0.000035

field ID*	ICP-MS cont.									
LZ1024	Nd	Sm	Gd	Dy	Er	Yb	Tl	Pb	Bi	U
2	<0.00003	<0.00003	<0.00005	<0.00003	<0.00003	<0.00003	<0.00003	0.000161	<0.00003	<0.00003
10	<0.00003	<0.00003	<0.00005	<0.00003	<0.00003	<0.00003	<0.00003	0.000155	<0.00003	<0.00003
30	<0.00003	<0.00003	<0.00005	<0.00003	<0.00003	<0.00003	<0.00003	0.000464	<0.00003	<0.00003
50	<0.00003	<0.00003	<0.00005	<0.00003	<0.00003	<0.00003	<0.00003	0.000175	<0.00003	<0.00003
100	<0.00003	<0.00003	<0.00005	<0.00003	<0.00003	<0.00003	<0.00003	0.000075	<0.00003	<0.00003
150	<0.00003	<0.00003	<0.00005	<0.00003	<0.00003	<0.00003	<0.00003	0.000314	<0.00003	<0.00003
165	0.000115	0.00014	0.000121	0.000087	0.000063	0.000093	0.000054	0.000468	0.000048	0.000057
168	0.000077	0.000078	0.000052	0.000054	0.000033	0.000038	<0.00003	0.000149	<0.00003	0.00004
2-2	<0.00003	<0.00003	<0.00005	<0.00003	<0.00003	<0.00003	<0.00003	0.024000	<0.00003	<0.00003
2-10	<0.00003	<0.00003	<0.00005	<0.00003	<0.00003	<0.00003	<0.00003	0.000370	<0.00003	<0.00003
2-30	<0.00003	<0.00003	<0.00005	<0.00003	<0.00003	<0.00003	<0.00003	0.000444	<0.00003	<0.00003
2-50	<0.00003	<0.00003	<0.00005	<0.00003	<0.00003	<0.00003	<0.00003	0.000286	<0.00003	<0.00003
2-100	0.000037	<0.00003	<0.00005	<0.00003	<0.00003	<0.00003	<0.00003	0.013200	<0.00003	<0.00003
2-150	0.000054	0.000048	<0.00005	<0.00003	<0.00003	<0.00003	<0.00003	0.001370	<0.00003	<0.00003
2-165	0.000088	0.000082	0.000093	0.000061	0.00005	0.000059	0.000033	0.000943	0.000036	0.000049
2-168	0.000038	<0.00003	<0.00005	<0.00003	<0.00003	<0.00003	<0.00003	0.000231	<0.00003	<0.00003

4.4.2 Water Sampling for Isotope Geochemistry

(J. Brigham-Grette)

A part of our work on the modern lake system is aimed at testing the broader hypothesis that changes in the biogeochemistry of the sediment/water interface are controlling the preservation of magnetic minerals and other proxies in response to climate change. Specifically we hypothesize that shifts in the mean state of atmospheric circulation influencing Chukotka (as inferred from some matches with the Greenland Ice Core record, e.g., Nowaczyk et al., 2002) persist long enough to impact lake ice cover duration and chemical reactions at the lake floor. An understanding of the lake system then requires an understanding of the modern lake chemistry as well as the source waters to the lake system.

Besides the water samples taken in 2003 for hydrological field measurements and the chemical analyses introduced in Chapter 4.4.1, additional water samples were collected at different times during the summer throughout the lake water column (Table 10, Fig. 14), as well as from incoming streams and the outflow river Enmyvaam (Table 11). These samples will be analysed for the amount and $\delta^{13}C$ of dissolved inorganic carbon (DIC), nitrate, phosphate, cations and anions. In addition to using the pH values to determine the form of DIC (either HCO^{3-} or dissolved CO_2), analysis of the water samples for TOC and TIC will permit an understanding of the carbon systematics and residence times. The entire water column was characterized in the field for pH, temperature, conductivity, and dissolved oxygen bench-top instruments in the field. These data, along with δD and $\delta^{18}O$ will then be used to characterize the isotopic, nutrient, and geochemical input to the lake.

4.4.3 Temperature Monitoring

(J. Brigham-Grette, M. Nolan, C. Kopsch)

Studies of the modern limnology of the lake system require at least baseline data concerning changes in water temperature. In 2000, the lake itself was instrumented at its deepest point (site T-0, Fig. 14) with a permanent thermistor string (170m, 70m, 30m, 8m, 3m depths) for retrieval at all depths of data every hour; also attached to the string at 8 m depth was a pressure sensor for retrieval of lake level data 4 times a day. Measures were recorded using Onset, Inc. Tidbits and sensors (miniature thermistor/data loggers). This thermistor string was replaced with a new string of identical tidbits and relocated (site T-0) on July 23, 2003 (Table 12). A series of Onset Tidbit thermistors were also deployed at several locations across the shallow southern shelf of the lake to test the hypothesis of Nolan et al. (2003) that the warming of shelf water created thermal bars that periodically delivered oxygen rich waters at 4°C to the deepest parts of the lake in summer. Single instruments recording hourly were deployed at sites T-4 through T-7 and another two were deployed on one string at 3 m and 11 m water depth at the very edge of the widest shelf (Fig. 14). The shelf thermistors at sites T-2 and T-3 (manufactured by C. Kopsch, AWI Potsdam) took recordings every 5 minutes limited to the field season.

Table 10: *Lake water samples for isotope geochemistry ($\delta^{18}O$ and δD of water, $\delta^{13}C$ of the DIC) and organic and inorganic geochemistry (total organic carbon, total inorganic carbon, cations, anions, nitrate, phosphate); each sample is 30 ml; isotope samples were stabilized with one drop mercury chloride.*

sample ID	location ID	analyses	water depth (m)	date	position latitude	position longitude
E03BG 23	Sedi-2; 2-J	isotopes	10.0	19-Jul-03	67°27.90´ N	172°03.14´ E
E03BG 24	Sedi-2; 5-J	isotopes	30.0		67°27.90´ N	172°03.14´ E
E03BG 25	Sedi-2; 4-J	isotopes	50.0		67°27.90´ N	172°03.14´ E
E03BG 26	Sedi-2; 3-J	isotopes	90.0		67°27.90´ N	172°03.14´ E
E03BG 27	Sedi-2; 6-J	isotopes	130.0		67°27.90´ N	172°03.14´ E
E03BG 28	Sedi-2; 1-J	isotopes	143.0		67°27.90´ N	172°03.14´ E
E03BG 77	Lz1029-1	isotopes	167.5	25-Jul-03	67°30.37´ N	172°08.24´ E
E03BG 79	Lz1029-2	isotopes	167.5		67°30.37´ N	172°08.24´ E
E03BG 82	Lz1029-3	isotopes	167.5		67°30.37´ N	172°08.24´ E
E03BG 132	Lz1029-5	isotopes	167.5	28-Jul-03	67°30.37´ N	172°08.24´ E
E03BG 133	Lz1029-5	chemistry	167.5		67°30.37´ N	172°08.24´ E
E03BG 153	Lz1032	isotopes	158.7	30-Jul-03	67°29.00´ N	172°07.98´ E
E03BG 154	Lz1032	chemistry	158.2		67°29.00´ N	172°07.98´ E
E03BG 156	Lz1033	isotopes	164.2	30-Jul-03	67°30.98´ N	172°08.09´ E
E03BG 157	Lz1033	chemistry	164.2		67°30.98´ N	172°08.09´ E
E03BG 160	Lz1040-1	isotopes	167.0	31-Jul-03	67°28.99´ N	172°02.05´ E
E03BG 161	Lz1040-1	chemistry	167.0		67°28.99´ N	172°02.05´ E
E03BG 174	Lz1046	isotopes	151.0	2-Aug-03	67°30.01´ N	171°59.98´ E
E03BG 177	Lz1046	chemistry	151.0		67°30.01´ N	171°59.98´ E
E03BG 197	Lz1024 -2m	isotopes	169.5	3-Aug-03	67°30.13´ N	172°06.46´ E
E03BG 198	Lz1024 -2m	chemistry	169.5		67°30.13´ N	172°06.46´ E
E03BG 199	Lz1024 -10m	isotopes	169.5		67°30.13´ N	172°06.46´ E
E03BG 200	Lz1024 -10m	chemistry	169.5		67°30.13´ N	172°06.46´ E
E03BG 201	Lz1024 -30m	isotopes	169.5		67°30.13´ N	172°06.46´ E
E03BG 202	Lz1024 -30m	chemistry	169.5		67°30.13´ N	172°06.46´ E
E03BG 203	Lz1024 -50m	isotopes	169.5		67°30.13´ N	172°06.46´ E
E03BG 204	Lz1024 -50m	chemistry	169.5		67°30.13´ N	172°06.46´ E
E03BG 205	Lz1024 -100m	isotopes	169.5		67°30.13´ N	172°06.46´ E
E03BG 206	Lz1024 -100m	chemistry	169.5		67°30.13´ N	172°06.46´ E
E03BG 207	Lz1024 -150m	isotopes	169.5		67°30.13´ N	172°06.46´ E
E03BG 208	Lz1024 -150m	chemistry	169.5		67°30.13´ N	172°06.46´ E
E03BG 209	Lz1024 -165m	isotopes	169.5		67°30.13´ N	172°06.46´ E
E03BG 210	Lz1024 -165m	chemistry	169.5		67°30.13´ N	172°06.46´ E
E03BG 211	Lz1024 -168m	isotopes	169.5		67°30.13´ N	172°06.46´ E
E03BG 212	Lz1024 -168m	chemistry	169.5		67°30.13´ N	172°06.46´ E
E03BG 254	Lz1058-1	isotopes	166.2	6-Aug-03	67°29.00´ N	172°03.98´ E
E03BG 255	Lz1058-1	chemistry	166.2		67°29.00´ N	172°03.98´ E
E03BG 451	Lz1079 -2m	isotopes	166.0	19-Aug-03	67°29.90´ N	172°08.01´ E
E03BG 452	Lz1079 -2m	chemistry	166.0	19-Aug-03	67°29.90´ N	172°08.01´ E
E03BG 453	Lz1079 -10m	isotopes	166.0		67°29.90´ N	172°08.01´ E
E03BG 454	Lz1079 -10m	chemistry	166.0		67°29.90´ N	172°08.01´ E
E03BG 455	Lz1079 -30m	isotopes	166.0		67°29.90´ N	172°08.01´ E
E03BG 456	Lz1079 -30m	chemistry	166.0		67°29.90´ N	172°08.01´ E
E03BG 457	Lz1079 -50m	isotopes	166.0		67°29.90´ N	172°08.01´ E
E03BG 458	Lz1079 -50m	chemistry	166.0		67°29.90´ N	172°08.01´ E
E03BG 459	Lz1079 -150m	isotopes	166.0		67°29.90´ N	172°08.01´ E
E03BG 460	Lz1079 -150m	chemistry	166.0		67°29.90´ N	172°08.01´ E
E03BG 461	Lz1079 -163m	isotopes	166.0		67°29.90´ N	172°08.01´ E
E03BG 462	Lz1079 -163m	chemistry	166.0		67°29.90´ N	172°08.01´ E
E03BG 463	Lz1079 -166m	isotopes	166.0		67°29.90´ N	172°08.01´ E
E03BG 464	Lz1079 -166m	chemistry	166.0		67°29.90´ N	172°08.01´ E

Table 11: *Stream water samples for isotope geochemistry ($\delta^{18}O$ and δD of water, $\delta^{13}C$ of the DIC) and organic and inorganic geochemistry (total organic carbon, total inorganic carbon, cations, anions, nitrate, phosphate); each sample is 30 ml; isotope samples were stabilized with one drop mercury chloride.*

sample	ID	location ID	analyses	date	position	
					latitude	longitude
E03BG	35	Stream 48	isotopes	21-Jul-03	67°29.22´ N	172°14.13´ E
E03BG	36	Stream 48	chemistry		67°29.22´ N	172°14.13´ E
E03BG	37	Stream 47	isotopes	21-Jul-03	67°29.65´ N	172°14.07´ E
E03BG	38	Stream 47	chemistry		67°29.65´ N	172°14.07´ E
E03BG	39	Stream 46	isotopes	21-Jul-03	67°30.04´ N	172°13.77´ E
E03BG	40	Stream 46	chemistry		67°30.04´ N	172°13.77´ E
E03BG	41	Stream 45	isotopes	21-Jul-03	67°30.35´ N	172°13.05´ E
E03BG	42	Stream 45	chemistry		67°30.35´ N	172°13.05´ E
E03BG	43	Stream 44	isotopes	21-Jul-03	67°30.49´ N	172°12.70´ E
E03BG	44	Stream 44	chemistry		67°30.49´ N	172°12.70´ E
E03BG	45	Stream 43	isotopes	21-Jul-03	67°31.05´ N	172°11.57´ E
E03BG	46	Stream 43	chemistry		67°31.05´ N	172°11.57´ E
E03BG	47	Stream 40	isotopes	21-Jul-03	67°31.64´ N	172°11.32´ E
E03BG	48	Stream 40	chemistry		67°31.64´ N	172°11.32´ E
E03BG	49	Stream 39	isotopes	21-Jul-03	67°32.10´ N	172°10.94´ E
E03BG	50	Stream 39	chemistry		67°32.10´ N	172°10.94´ E
E03BG	51	Stream 38	isotopes	21-Jul-03	67°32.48´ N	172°09.93´ E
E03BG	52	Stream 38	chemistry		67°32.48´ N	172°09.93´ E
E03BG	53	Stream 37	isotopes	21-Jul-03	67°32.53´ N	172°09.74´ E
E03BG	54	Stream 37	chemistry		67°32.53´ N	172°09.74´ E
E03BG	56	Stream 35	isotopes	21-Jul-03	67°32.81´ N	172°06.93´ E
E03BG	57	Stream 35	chemistry		67°32.81´ N	172°06.93´ E
E03BG	58	Stream 34	isotopes	21-Jul-03	67°32.80´ N	172°06.55´ E
E03BG	59	Stream 34	chemistry		67°32.80´ N	172°06.55´ E
E03BG	60	Stream 33	isotopes	21-Jul-03	67°32.69´ N	172°05.02´ E
E03BG	61	Stream 33	chemistry		67°32.69´ N	172°05.02´ E
E03BG	62	Stream 32	isotopes	21-Jul-03	67°32.59´ N	172°04.15´ E
E03BG	63	Stream 32	chemistry		67°32.59´ N	172°04.15´ E
E03BG	64	Stream 31	isotopes	21-Jul-03	67°32.47´ N	172°03.02´ E
E03BG	65	Stream 31	chemistry		67°32.47´ N	172°03.02´ E
E03BG	168	Stream 2	isotopes	2-Aug-03	67°26.23´ N	172°06.59´ E
E03BG	169	Stream 2	chemistry		67°26.23´ N	172°06.59´ E
E03BG	170	Stream 5	isotopes	2-Aug-03	67°25.98´ N	172°01.82´ E
E03BG	171	Stream 5	chemistry		67°25.98´ N	172°01.82´ E
E03BG	172	Stream 6	isotopes	2-Aug-03	67°26.14´ N	172°00.86´ E
E03BG	173	Stream 6	chemistry		67°26.14´ N	172°00.86´ E
E03BG	179	Stream 20	isotopes	2-Aug-03	67°31.02´ N	171°57.19´ E
E03BG	180	Stream 20	chemistry		67°31.02´ N	171°57.19´ E
E03BG	181	Stream 19	isotopes	2-Aug-03	67°30.65´ N	171°56.40´ E
E03BG	182	Stream 19	chemistry		67°30.65´ N	171°56.40´ E
E03BG	183	Stream 18	isotopes	2-Aug-03	67°30.57´ N	171°56.26´ E
E03BG	184	Stream 18	chemistry		67°30.57´ N	171°56.26´ E
E03BG	185	Stream 17	isotopes	2-Aug-03	67°30.40´ N	171°56.14´ E
E03BG	186	Stream 17	chemistry		67°30.40´ N	171°56.14´ E
E03BG	187	Stream 16	isotopes	2-Aug-03	67°30.14´ N	171°56.25´ E
E03BG	188	Stream 16	chemistry		67°30.14´ N	171°56.25´ E
E03BG	189	Stream 15	isotopes	2-Aug-03	67°29.96´ N	171°56.76´ E
E03BG	190	Stream 15	chemistry		67°29.96´ N	171°56.76´ E
E03BG	191	Stream 14	isotopes	2-Aug-03	67°29.70´ N	171°57.21´ E
E03BG	192	Stream 14	chemistry		67°29.70´ N	171°57.21´ E
E03BG	193	Stream 12	isotopes	2-Aug-03	67°28.53´ N	171°58.11´ E
E03BG	194	Stream 12	chemistry		67°28.53´ N	171°58.11´ E

continuation next page

Table 11: *continuation*

sample	ID	location ID	analyses	date	position	
					latitude	longitude
E03BG	195	Stream 10	isotopes	2-Aug-03	67°27.16′ N	171°58.26′ E
E03BG	196	Stream 10	chemistry		67°27.16′ N	171°58.26′ E
E03BG	293	Stream 50	isotopes	9-Aug-03	67°27.61′ N	172°12.84′ E
E03BG	294	Stream 50	chemistry		67°27.61′ N	172°12.84′ E
E03BG	295	Stream 49	isotopes	9-Aug-03	67°28.20′ N	172°13.46′ E
E03BG	296	Stream 49	chemistry		67°28.20′ N	172°13.46′ E
E03BG	299	Enmyvaam	isotopes	9-Aug-03	67°26.72′ N	172°10.63′ E
E03BG	300	Enmyvaam	chemistry		67°26.72′ N	172°10.63′ E
E03BG	426	Stream 30	isotopes	18-Aug-03	67°32.37′ N	172°02.34′ E
E03BG	427	Stream 30	chemistry		67°32.37′ N	172°02.34′ E
E03BG	429	Stream 29a	isotopes	18-Aug-03	67°32.26′ N	172°01.70′ E
E03BG	430	Stream 29a	chemistry		67°32.26′ N	172°01.70′ E
E03BG	431	Stream 28	isotopes	18-Aug-03	67°32.14′ N	172°01.08′ E
E03BG	432	Stream 28	isotopes		67°32.14′ N	172°01.08′ E
E03BG	434	Stream 27	isotopes	18-Aug-03	67°32.06′ N	172°00.74′ E
E03BG	435	Stream 27	chemistry		67°32.06′ N	172°00.74′ E
E03BG	437	Stream 26	isotopes	18-Aug-03	67°31.94′ N	172°00.26′ E
E03BG	438	Stream 26	chemistry		67°31.94′ N	172°00.26′ E
E03BG	440	Stream 25	isotopes	18-Aug-03	67°31.81′ N	171°59.77′ E
E03BG	441	Stream 25	chemistry		67°31.81′ N	171°59.77′ E
E03BG	443	Stream 24	isotopes	18-Aug-03	67°31.66′ N	171°59.24′ E
E03BG	444	Stream 24	chemistry		67°31.66′ N	171°59.24′ E
E03BG	445	Stream 23	isotopes	18-Aug-03	67°31.64′ N	171°59.13′ E
E03BG	446	Stream 23	chemistry		67°31.64′ N	171°59.13′ E
E03BG	447	Stream 22	isotopes	18-Aug-03	67°31.58′ N	171°58.91′ E
E03BG	448	Stream 22	chemistry		67°31.58′ N	171°58.91′ E
E03BG	449	Stream 21	isotopes	18-Aug-03	67°31.42′ N	171°58.32′ E
E03BG	450	Stream 21	chemistry		67°31.42′ N	171°58.32′ E

Table 12: *Thermistors deployed in Lake El′gygytgyn 2003.*

site ID	water depth (m)	position		thermistor		date deployed	date recovered
		latitude	longitude	ID	depth (m)		
T-0	172.0	67°30.27′ N	172°08.52′ E	-	3.0	08-28-00	07-23-03
(T-0 deployed by M. Nolan, University of Alaska,				-	8.0	08-28-00	07-23-03
Fairbanks, in 2000)				-	30.0	08-28-00	07-23-03
				-	70.0	08-28-00	07-23-03
				-	170.0	08-28-00	07-23-03
				SN67	3.0	07-23-03	-
				SN66	8.0	07-23-03	-
				SN65	30.0	07-23-03	-
				SN63	70.0	07-23-03	-
				SN62	170.0	07-23-03	-
T-1	153.0	67°27.91′ N	172°03.12′ E	01	3.0	06-01-03	-
				02	8.0	06-01-03	-
				03	13.0	06-01-03	-
				04	18.0	06-01-03	-
				05	23.0	06-01-03	-
				08	33.0	06-01-03	-
				09	53.0	06-01-03	-
				10	73.0	06-01-03	-
				11	93.0	06-01-03	-
				12	113.0	06-01-03	-
				13	123.0	06-01-03	-

continuation next page

Table 12: continuation

site ID	water depth (m)	position latitude	position longitude	thermistor ID	thermistor depth (m)	date deployed	date recovered
				14	133.0	06-01-03	-
				16	138.0	06-01-03	-
				17	143.0	06-01-03	-
				20	148.0	06-01-03	-
				22	151.0	06-01-03	-
T-2	5.0	67°26.85′ N	172°09.51′ E	-	3.8	07-10-03	08-10-03
T-3	5.3	67°26.54′ N	172°07.75′ E	-	4.1	07-10-03	08-10-03
T-4	5.3	67°28.53′ N	172°13.36′ E	SN 64	4.6	07-10-03	08-10-03
				SN 64	4.6	08-10-03	-
T-5	5.0	67°27.78′ N	172°12.35′ E	SN 69	4.3	07-10-03	08-10-03
				SN 69	4.6	08-10-03	-
T-6	5.0	67°27.20′ N	172°10.92′ E	SN 68	4.3	07-10-03	08-10-03
				SN 68	4.6	08-10-03	-
T-7	0.7	67°28.57′ N	171°58.06′ E	SN 70	0.2	07-20-03	08-18-03
T-8	11.2	67°27.41′ N	172°11.01′ E	SN58	3.0	07-22-03	08-10-03
				SN59	11.0	07-22-03	08-10-03
				SN58	3.0	08-10-03	-
				SN59	11.0	08-10-03	-

4.4.4 Lake Level Changes

(G. Fedorov, A. Kupolov)

Introduction - Seasonal lake level changes play an important role within the hydrological features of Lake El′gygytgyn. For instance, they allow to estimate the residence time of the lake water. Usually the water level has its maximum at the end of the snow melt period and the opening of Enmyvaam River. During autumn (August/September), with the general lowering of the lake level accompanied by northern winds, storms form a levee along the southern shore that impedes the outflow into the Enmyvaam River. In spring time this levee is destroyed by similar storms with the rise of the lake level, leading to the restitution of the river flow.

Methods - During the spring and the summer campaign in 2003 a hydrological measurement picket was established at the southeastern shore of the lake. Reference pickets were installed with the first stripes of ice-free water appearing along the lake shore (June 10 - 15). The measurements ceased with the end of the field season. The lake level changes were monitored from June 14 to August 19 (Fig. 17). Measurement gaps happened during ice plugging in the beginning and strong storms in the end of the field campaign. The ice disappeared finally on July 19 (cp. Table 4, p. 25).

Results - The total amplitude of lake level changes that have appeared during the measurement period was only 26.5 cm (Fig. 14). However, it is obvious that the lake level changes control those of the Enmyvaam River, which amount to almost 90 cm in the measurement period. During summer 2003, before the levee closing the Enmyvaam was removed (i.e. from June 14 to July 3) the level of the lake was steadily rising about 0.8 cm per day. The highest rates (1.2 - 1.8 cm per day) were recorded on June 23 - 26. With the onset of the annual

discharge through the river, the level of the lake went down with an average rate of 0.7 cm per day.

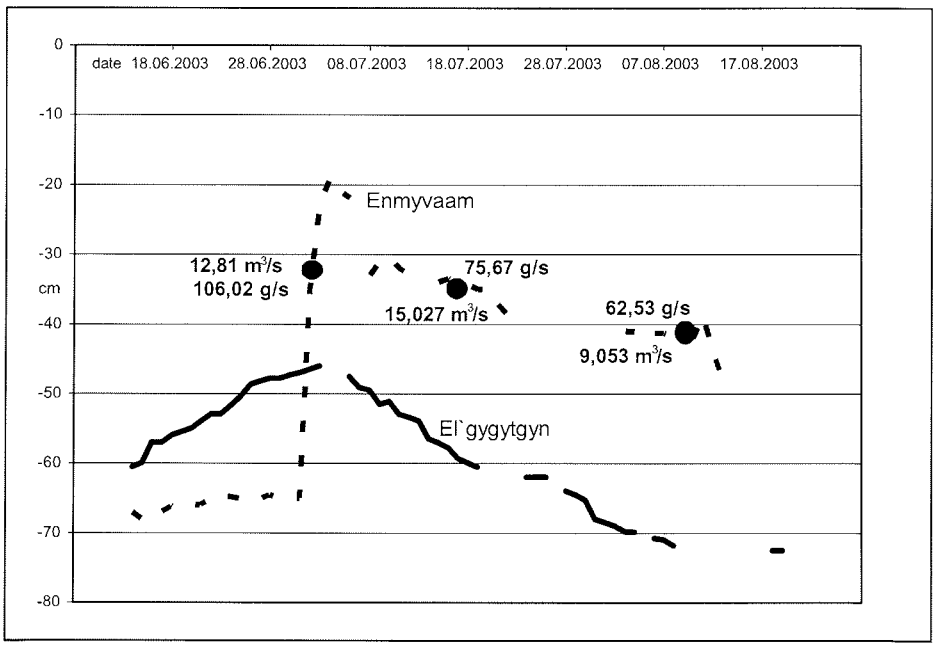

Figure 17: *Water level changes in Lake El'gygytgyn (solid line) and Enmyvaam River (dashed line) during summer 2003; Numbers denote water discharge (m^3/s) and solid material discharge (g/s) in different periods.*

Besides the described long-term trend, the intensity of the surface discharge of water through the bed of the Enmyvaam River on shorter timescales in summer 2003 was also controlled by wind action; it was particularly stimulated by storms from northern directions. In addition to the water discharge through the river bed a considerable sub-bed discharge in the river valley has to be expected due the high porosity of the lacustrine-fluvial sediments. For a full understanding of changes in the level of El'gygytgyn Lake on different time scales, including the changes that took place in the geological past, it is also important to note that the lake has a relatively small catchment area compared to the size of the lake itself, and that there are geomorphologic evidences for several generations of ancient shorelines both above and below the modern lake level (see Chapters 5.2 and 5.3).

The above observations lead us to the following conclusions:

1. If there is low precipitation in winter time and, hence, little rise of the lake level in spring, and if there are no strong northerly winds in spring or summer, there may be no direct outflow from the lake into the Enmyvaam River at all.
2. In general, as evidenced by row of average values per annum, the lake level tends to descend.

4.5 Allochthonous Sediment Supply to Lake El'gygytgyn

4.5.1 Source Rocks

(O. Juschus, J. Brigham-Grette, A. Dehnert)

Introduction – The composition of the source rocks within the El'gygytgyn Crater has an important influence on the properties of the lake sediments. This includes sediment physical properties, such as the grain density or the magnetic susceptibility (cp. Nowaczyk et al., 2002), but via weathering, transport, deposition and diagenesis also the chemistry and the mineralogy of the sediments.

Methods – Altogether 77 bedrock samples were collected in the lake catchment during the expedition in 2003 (Fig. 18, Table 13). Due to the widespread absence of outcrops, the bedrock samples mostly had to be collected from periglacial colluviums. To avoid contaminations with other material, exclusively monomictic colluviums, i.e. those composed of only one kind of rock, were sampled. In case of good outcrop conditions the bedrock samples were taken with directional measurement. Impact rocks had to be collected from periglacial colluviums or from the shore bar (Table 14), because there is no outcrop existing in the catchment of Lake El'gygytgyn.

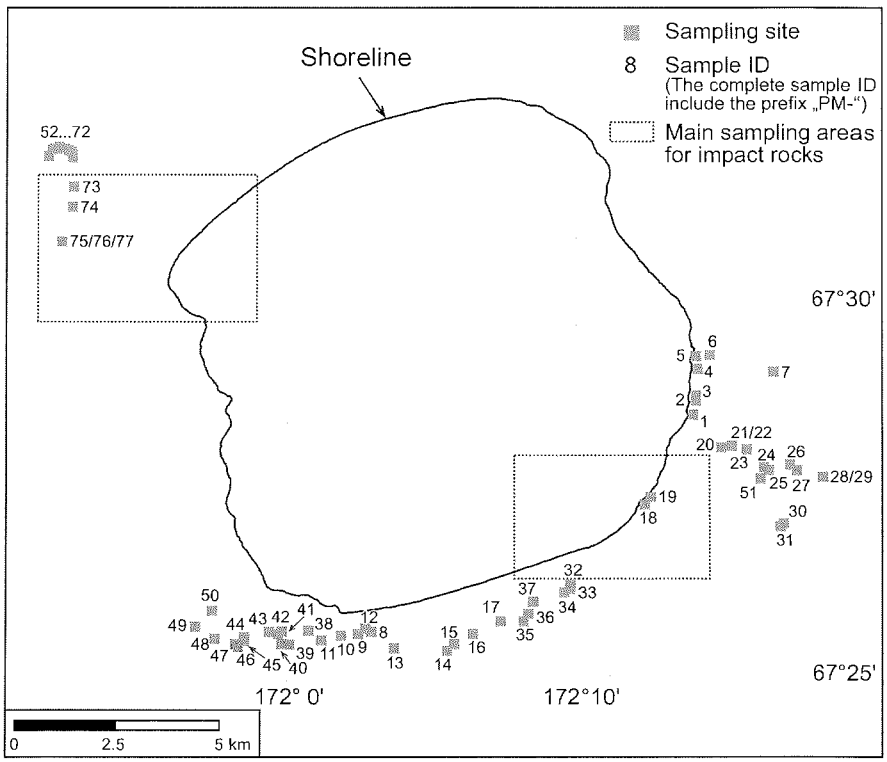

Figure 18: *Locations of bedrock samples collected from the Lake El'gygytgyn surroundings in 2003.*

Table 13: *Bedrock samples collected from the Lake El'gygytgyn catchment in 2003.*

sample ID	source	position		date	dip	
		latitude	longitude		direction	angle
PM-1	bedrock	67°28.55′ N	172°13.94′ E	06-29-03	336°	79°
PM-2	bedrock	67°28.73′ N	172°14.04′ E	06-29-03	232°	59°
PM-3	bedrock	67°28.80′ N	172°14.04′ E	06-29-03	251°	57°
PM-4	bedrock	67°29.16′ N	172°14.10′ E	06-29-03	179°	82°
PM-5	bedrock	67°29.33′ N	172°14.04′ E	06-29-03	7°	68°
PM-6	bedrock	67°29.34′ N	172°14.53′ E	06-29-03	215°	64°
PM-7	colluvium	67°29.11′ N	172°16.72′ E	06-29-03	-	-
PM-8	colluvium	67°25.65′ N	172°02.91′ E	06-30-03	-	-
PM-9	colluvium	67°25.62′ N	172°02.45′ E	06-30-03	-	-
PM-10	colluvium	67°25.60′ N	172°01.85′ E	06-30-03	-	-
PM-11	colluvium	67°25.54′ N	172°01.19′ E	06-30-03	-	-
PM-12	colluvium	67°25.69′ N	172°02.71′ E	06-30-03	-	-
PM-13	colluvium	67°25.43′ N	172°03.69′ E	06-30-03	-	-
PM-14	colluvium	67°25.40′ N	172°05.53′ E	06-30-03	-	-
PM-15	colluvium	67°25.49′ N	172°05.76′ E	06-30-03	-	-
PM-16	colluvium	67°25.62′ N	172°06.42′ E	06-30-03	-	-
PM-17	colluvium	67°25.79′ N	172°07.36′ E	06-30-03	-	-
PM-18	bedrock	67°27.35′ N	172°12.27′ E	07-13-03	-	-
PM-19	bedrock	67°27.45′ N	172°12.48′ E	07-13-03	292°	89°
PM-20	colluvium	67°28.11′ N	172°14.91′ E	07-13-03	-	-
PM-21	colluvium	67°28.13′ N	172°15.26′ E	07-13-03	-	-
PM-22	colluvium	67°28.13′ N	172°15.26′ E	07-13-03	-	-
PM-23	colluvium	67°28.08′ N	172°15.78′ E	07-13-03	-	-
PM-24	colluvium	67°27.84′ N	172°16.36′ E	07-13-03	-	-
PM-25	colluvium	67°27.80′ N	172°16.55′ E	07-13-03	-	-
PM-26	colluvium	67°27.87′ N	172°17.27′ E	07-13-03	-	-
PM-27	colluvium	67°27.79′ N	172°17.51′ E	07-13-03	-	-
PM-28	colluvium	67°27.71′ N	172°18.41′ E	07-13-03	-	-
PM-29	colluvium	67°27.71′ N	172°18.40′ E	07-13-03	-	-
PM-30	colluvium	67°27.09′ N	172°17.04′ E	07-13-03	-	-
PM-31	colluvium	67°27.04′ N	172°16.93′ E	07-13-03	-	-
PM-32	colluvium	67°26.28′ N	172°09.78′ E	07-17-03	-	-
PM-33	colluvium	67°26.22′ N	172°09.77′ E	07-17-03	-	-
PM-34	colluvium	67°26.18′ N	172°09.56′ E	07-17-03	-	-
PM-35	colluvium	67°25.79′ N	172°08.16′ E	07-17-03	-	-
PM-36	colluvium	67°25.89′ N	172°08.32′ E	07-17-03	-	-
PM-37	colluvium	67°26.05′ N	172°08.50′ E	07-17-03	-	-
PM-38	colluvium	67°25.66′ N	172°00.76′ E	08-09-03	-	-
PM-39	colluvium	67°25.48′ N	172°00.11′ E	08-09-03	-	-
PM-40	bedrock	67°25.49′ N	171°59.83′ E	08-09-03	-	-
PM-41	colluvium	67°25.62′ N	171°59.72′ E	08-09-03	-	-
PM-42	colluvium	67°25.63′ N	171°59.73′ E	08-09-03	-	-
PM-43	bedrock	67°25.65′ N	171°59.41′ E	08-09-03	64°	85°
PM-44	colluvium	67°25.58′ N	171°58.58′ E	08-09-03	-	-
PM-45	colluvium	67°25.53′ N	171°58.55′ E	08-09-03	-	-
PM-46	colluvium	67°25.45′ N	171°58.35′ E	08-09-03	-	-
PM-47	colluvium	67°25.49′ N	171°58.27′ E	08-09-03	-	-
PM-48	colluvium	67°25.56′ N	171°57.55′ E	08-09-03	-	-
PM-49	colluvium	67°25.72′ N	171°56.90′ E	08-09-03	-	-
PM-50	colluvium	67°25.93′ N	171°57.47′ E	08-09-03	-	-
PM-51	colluvium	67°27.69′ N	172°16.25′ E	08-14-03	-	-
PM-52	colluvium	67°31.99′ N	171°52.67′ E	08-21-03	-	-
PM-53	colluvium	67°32.00′ N	171°52.67′ E	08-21-03	-	-
PM-54	colluvium	67°32.02′ N	171°52.67′ E	08-21-03	-	-
PM-55	colluvium	67°32.07′ N	171°52.61′ E	08-21-03	-	-

continuation next page

Table 13: continuation

sample ID	source	position latitude	position longitude	date	dip direction	dip angle
PM-56	bedrock	67°32.09´ N	171°52.53´ E	08-21-03	-	-
PM-57	colluvium	67°32.01´ N	171°51.83´ E	08-21-03	-	-
PM-58	colluvium	67°32.01´ N	171°51.83´ E	08-21-03	-	-
PM-59	colluvium	67°32.10´ N	171°51.95´ E	08-21-03	-	-
PM-60	colluvium	67°32.11´ N	171°52.07´ E	08-21-03	-	-
PM-61	colluvium	67°32.13´ N	171°52.19´ E	08-21-03	-	-
PM-62	colluvium	67°32.11´ N	171°52.40´ E	08-21-03	-	-
PM-63	bedrock	67°32.09´ N	171°52.53´ E	08-21-03	-	-
PM-64	bedrock	67°32.09´ N	171°52.53´ E	08-21-03	-	-
PM-65	bedrock	67°32.09´ N	171°52.53´ E	08-21-03	-	-
PM-66	bedrock	67°32.09´ N	171°52.53´ E	08-21-03	-	-
PM-67	bedrock	67°32.09´ N	171°52.53´ E	08-21-03	-	-
PM-68	bedrock	67°32.09´ N	171°52.53´ E	08-21-03	-	-
PM-69	bedrock	67°32.09´ N	171°52.53´ E	08-21-03	-	-
PM-70	bedrock	67°32.09´ N	171°52.53´ E	08-21-03	-	-
PM-71	bedrock	67°32.09´ N	171°52.53´ E	08-21-03	-	-
PM-72	bedrock	67°32.09´ N	171°52.53´ E	08-21-03	-	-
PM-73	colluvium	67°31.60´ N	171°52.72´ E	08-21-03	-	-
PM-74	bedrock	67°31.33´ N	171°52.67´ E	08-21-03	-	-
PM-75	colluvium	67°30.87´ N	171°52.30´ E	08-21-03	-	-
PM-76	colluvium	67°30.87´ N	171°52.30´ E	08-21-03	-	-
PM-77	colluvium	67°30.87´ N	171°52.30´ E	08-21-03	-	-

Table 14: Main sampling areas for impact rocks.

area	no. of samples	position latitude	position longitude
cabin surroundings	67	67°26.81´ N	172°10.86´ E
creek 16 („Tichy") surroundings	72	67°30.14´ N	171°56.25´ E

The following analyses are planned to be carried out on the bedrock samples:

- rock petrological analyses
- rock magnetic measurements
- rock chemistry analysis
- p-wave velocity measurements
- rock dating (fission track)

4.5.2 Fluvial Supply and Export

(G. Schwamborn, O. Juschus, G. Fedorov, A. Kupolov, O. Glushkova, V. Smirnov)

Sedimentological Studies

The permafrost surrounding of the lake is considered in its role as provenance area of the lake sediments. This is expressed and can be studied in mineralogical associations and permafrost related grain properties of the sand fraction. Sample material was collected from permafrost deposits and from fluvial sediments, because particles from both environments are transported into the lake basin, predominantly by the inlet streams, thereby contributing to the lake sediment formation. However, apart from pure fluvial inflow into the

lake, the transport by floating ice (dropstone) and by wind (cp. Chapter 4.5.3) has to be considered as additional driving forces to distribute sediments over the lake.

Mineral compositions from the ephemeral streams compared with the ones from the lake sediments may allow to recognize major source areas of the lake sediments. For this purpose, sediment samples were taken from almost all inlet streams, several small inlets and the Enmyvaam River (Fig. 19, Table 15).

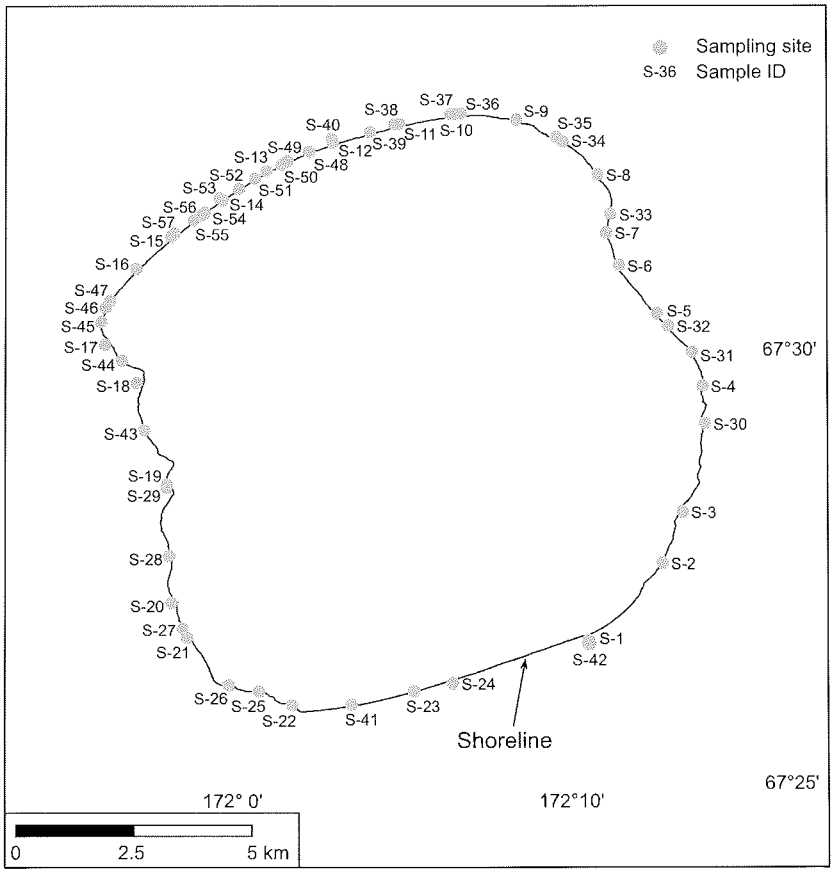

Figure 19: *Map of the Lake El'gygytgyn area showing the location of sediment samples from the tributaries and the outlet stream collected in 2003 predominantly for mineral analyses.*

Besides, the micromorphology of the deposits and their mineral components, mostly quartz grains, to be investigated by optical and scanning electron microscopic (SEM) analysis, supply important information on the permafrost conditions in the catchment. Soils during cryogenesis acquire specific surface microtextures. These are expressed as a stripe and annular microtexture of the sand-silt component (e.g., Konishchev and Rogov, 1993). Because the cryogenically altered grains are transported to the lake basin, the lake sediment

column through time offers an exceptionally good archive to study on- and offset of permafrost conditions in the catchment.

Therefore. sandy sediments of the major inlet streams draining the permafrost soils, and several gravity core sediments from the lake basin grouping around the central part where the deep drilling site is planned, have been sampled (Fig. 20) in order to conduct comparative microscopical studies. The basic preparation and analytical concept is as follows:

1. sieving of fraction (63-125 µm) → **fluvial and permafrost** sediments
   → **lake** sediments
2. separation of **light** and **heavy** minerals using heavy density liquid (2.89 g/cm^3) and centrifuge
3. chemical treatment (HCl, ultrasonic, ethanol, H_2O_2) of light fraction
4. optical microscopy for pre-discrimination of surface types
5. SEM for main identification of typical surface textures
6. polarisation microscopy of the heavy fraction for provenance analysis

A successful use of these microscopical techniques would make the re-construction of permafrost occurrence in the catchment in principal possible, once a lake sediment core that penetrates beyond the northern glaciation cycles during the Pliocene becomes available within the scope of a deep drilling operation.

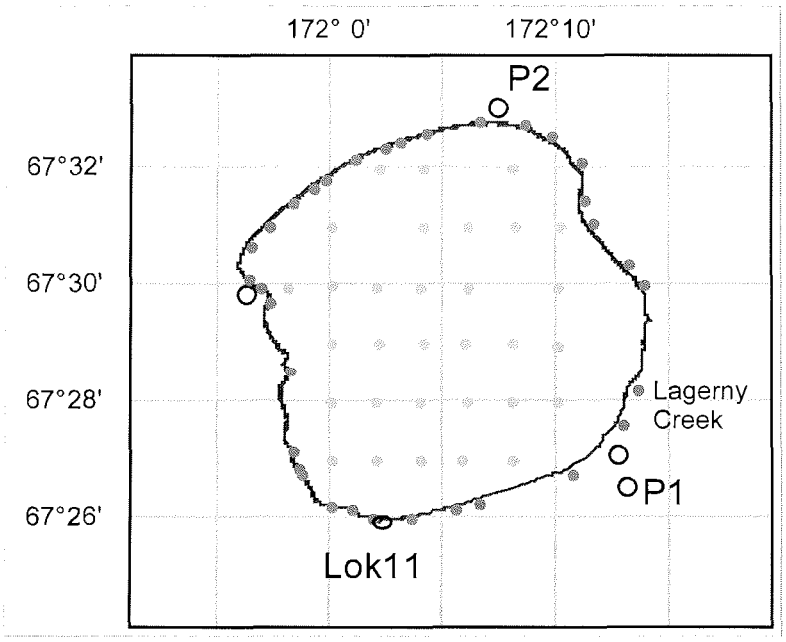

Figure 20: *Map of the Lake El'gygytgyn area showing the sampling sites predominantly for microscopical analyses around and within the lake basin. Circles mark permafrost samples, dark dots fluvial sands, and light dots lake sediment samples.*

Table 15: *Sediment samples collected from the tributaries and outlet stream (Enmyvaam).*

sample ID	field ID	site	source	position		date
				latitude	longitude	
S-1/ S-42	SEnmyvaam	Enmyvaam	stillwater	67°26.72´ N	172°10.63´ E	06-15-03
S-2	ZF50-2SS	creek 50	stillwater	67°27.61´ N	172°12.84´ E	06-15-03
S-3	ZF49-4SS	creek 49	stillwater	67°28.20´ N	172°13.46´ E	06-15-03
S-4	ZF47-2SS	creek 47	stillwater	67°29.65´ N	172°14.07´ E	06-18-03
S-5	ZF44-3SS	creek 44	stillwater	67°30.49´ N	172°12.70´ E	06-18-03
S-6	ZF43-2SS	creek 43	stillwater	67°31.05´ N	172°11.57´ E	06-18-03
S-7	ZF41-2SL	creek 41	stillwater	67°31.43´ N	172°11.19´ E	06-18-03
S-8	ZF39-3SS	creek 39	stillwater	67°32.10´ N	172°10.94´ E	06-18-03
S-9	ZF36-2SS	creek 36	stillwater	67°32.73´ N	172°08.54´ E	06-18-03
S-10	ZF34-2SL	creek 34	lagoon	67°32.80´ N	172°06.55´ E	06-18-03
S-11	ZF33-2SL	creek 33	lagoon	67°32.69´ N	172°05.02´ E	06-18-03
S-12	ZF31-2SL	creek 31	lagoon	67°32.47´ N	172°03.02´ E	06-18-03
S-13	ZF28-2SL	creek 28	lagoon	67°32.14´ N	172°01.08´ E	06-18-03
S-14	ZF25-2SL	creek 25	lagoon	67°31.81´ N	171°59.77´ E	06-18-03
S-15	ZF21-2SL	creek 21	lagoon	67°31.42´ N	171°58.32´ E	06-19-03
S-16	ZF20-2SS	creek 20	stillwater	67°31.02´ N	171°57.19´ E	06-19-03
S-17	ZF16-2SS	creek 16	stillwater	67°30.14´ N	171°56.25´ E	06-19-03
S-18	ZF14-3SL	creek 14	lagoon	67°29.70´ N	171°57.21´ E	06-19-03
S-19	ZF12-2SL	creek 12	lagoon	67°28.53´ N	171°58.11´ E	06-19-03
S-20	ZF10-2SS	creek 10	stillwater	67°27.16´ N	171°58.26´ E	06-19-03
S-21	ZF8-3SS	creek 8	stillwater	67°26.76´ N	171°58.72´ E	06-19-03
S-22	ZF5-2SL	creek 5	lagoon	67°25.98´ N	172°01.82´ E	06-19-03
S-23	ZF3-2SL	creek 3	lagoon	67°26.14´ N	172°05.43´ E	06-19-03
S-24	ZF2-3SS	creek 2	stillwater	67°26.23´ N	172°06.59´ E	06-30-03
S-25	ZF6-2SS	creek 6	stillwater	67°26.14´ N	172°00.86´ E	07-20-03
S-26	ZF7-2SS	creek 7	stillwater	67°26.21´ N	171°59.97´ E	07-20-03
S-27	ZF9-1SS	creek 9	stillwater	67°26.86´ N	171°58.59´ E	07-20-03
S-28	ZF11-2SS	creek 11	stillwater	67°27.70´ N	171°58.19´ E	07-20-03
S-29	ZF12-4SL	creek 12	lagoon	67°28.53´ N	171°58.11´ E	07-20-03
S-30	ZF48-2SS	creek 48	stillwater	67°29.22´ N	172°14.13´ E	07-21-03
S-31	ZF46-1SL	creek 46	lagoon	67°30.04´ N	172°13.77´ E	07-21-03
S-32	ZF45-2SL	creek 45	lagoon	67°30.35´ N	172°13.05´ E	07-21-03
S-33	ZF40-2SS	creek 40	stillwater	67°31.64´ N	172°11.32´ E	07-21-03
S-34	ZF38-2SL	creek 38	lagoon	67°32.48´ N	172°09.93´ E	07-21-03
S-35	ZF37-2SS	creek 37	stillwater	67°32.53´ N	172°09.74´ E	07-21-03
S-36	ZF35-2SL	creek 35	lagoon	67°32.81´ N	172°06.93´ E	07-21-03
S-37	ZF34-4SL	creek 34	lagoon	67°32.80´ N	172°06.55´ E	07-21-03
S-38	ZF33-4SL	creek 33	lagoon	67°32.69´ N	172°04.98´ E	07-21-03
S-39	ZF32-2SL	creek 32	lagoon	67°32.59´ N	172°04.15´ E	07-21-03
S-40	ZF31-4SL	creek 31	lagoon	67°32.52´ N	172°03.00´ E	07-21-03
S-41	ZF4-2SS	creek 4	stillwater	67°25.99´ N	172°03.57´ E	07-21-03
S-43	ZF13-2SS	creek 13	stillwater	67°29.15´ N	171°57.42´ E	08-02-03
S-44	ZF15-2SL	creek 15	lagoon	67°29.96´ N	171°56.76´ E	08-02-03
S-45	ZF17-2SL	creek 17	lagoon	67°30.40´ N	171°56.14´ E	08-02-03
S-46	ZF18-2SL	creek 18	lagoon	67°30.57´ N	171°56.26´ E	08-02-03
S-47	ZF19-2SL	creek 19	lagoon	67°30.65´ N	171°56.40´ E	08-02-03
S-48	ZF30-2SS	creek 30	stillwater	67°32.37´ N	172°02.34´ E	08-18-03
S-49	ZF29a-2SS	creek 29a	stillwater	67°32.26´ N	172°01.70´ E	08-18-03
S-50	ZF29-2SS	creek 29	stillwater	67°32.22´ N	172°01.51´ E	08-18-03
S-51	ZF27-2SL	creek 27	lagoon	67°32.06´ N	172°00.74´ E	08-18-03
S-52	ZF26-2SL	creek 26	lagoon	67°31.94´ N	172°00.26´ E	08-18-03
S-53	ZF25-4SL	creek 25	lagoon	67°31.81´ N	171°59.77´ E	08-18-03
S-54	ZF24-2SL	creek 24	lagoon	67°31.66´ N	171°59.24´ E	08-18-03
S-55	ZF23-2SL	creek 23	lagoon	67°31.64´ N	171°59.13´ E	08-18-03
S-56	ZF22-2SL	creek 22	lagoon	67°31.58´ N	171°58.91´ E	08-18-03
S-57	ZF21-4SL	creek 21	lagoon	67°31.42´ N	171°58.32´ E	08-18-03

Water and Sediment Discharge Measurements

During summer 2003 the water discharge and transparency in the Enmyvaam River was measured twice in order to determine the amount of transported particles. In the results it is interesting that the maximum water discharge from the Enmyvaam River (15.27 m^3/s), documented during the middle of July, did not coincide with the peak of the lake level and that of the river itself (Fig. 17, p. 41). Instead, the maximum discharge occurred during the lake levels lowering. The authors explain this discrepancy with active reworking of the old riverbed during the period of major water discharge into the Enmyvaam River. This interpretation is supported by the data illustrated in Figure 21, showing a general drop of the lake/river level that coincided with a significant deepening of the river bed. A similar explanation is valid for the largest discharge of solid particles (106.02 g/s). This took place in early July (Fig. 17), at a time when the river bed erosion started (Fig. 21).

The water discharge and the water transparency were also measured in several of the inlet streams. Figure 23 illustrates the numbering of the major 50 streams as proposed by O. Glushkova (NEISRI, Magadan). The first measurements were made during the snow melt in spring time (middle of June), the second ones during the middle and the last ones at the end of the field season (middle of August).

The results from selected inlet streams are presented in Figure 22. They show, firstly, that the water discharge and transparency have big differences between individual streams, with changing importance during different times. Secondly, both the water and the sediment discharge into the lake take place predominantly in a short time span during the snow melt, when the input of both water and sediments is one order of magnitude higher than that during summer.

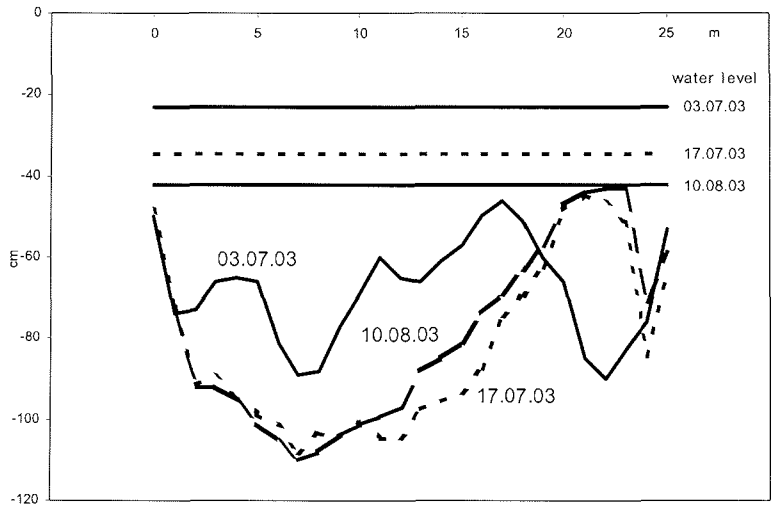

Figure 21: *Depth measurements at the head of Enmyvaam River during the expedition in 2003.*

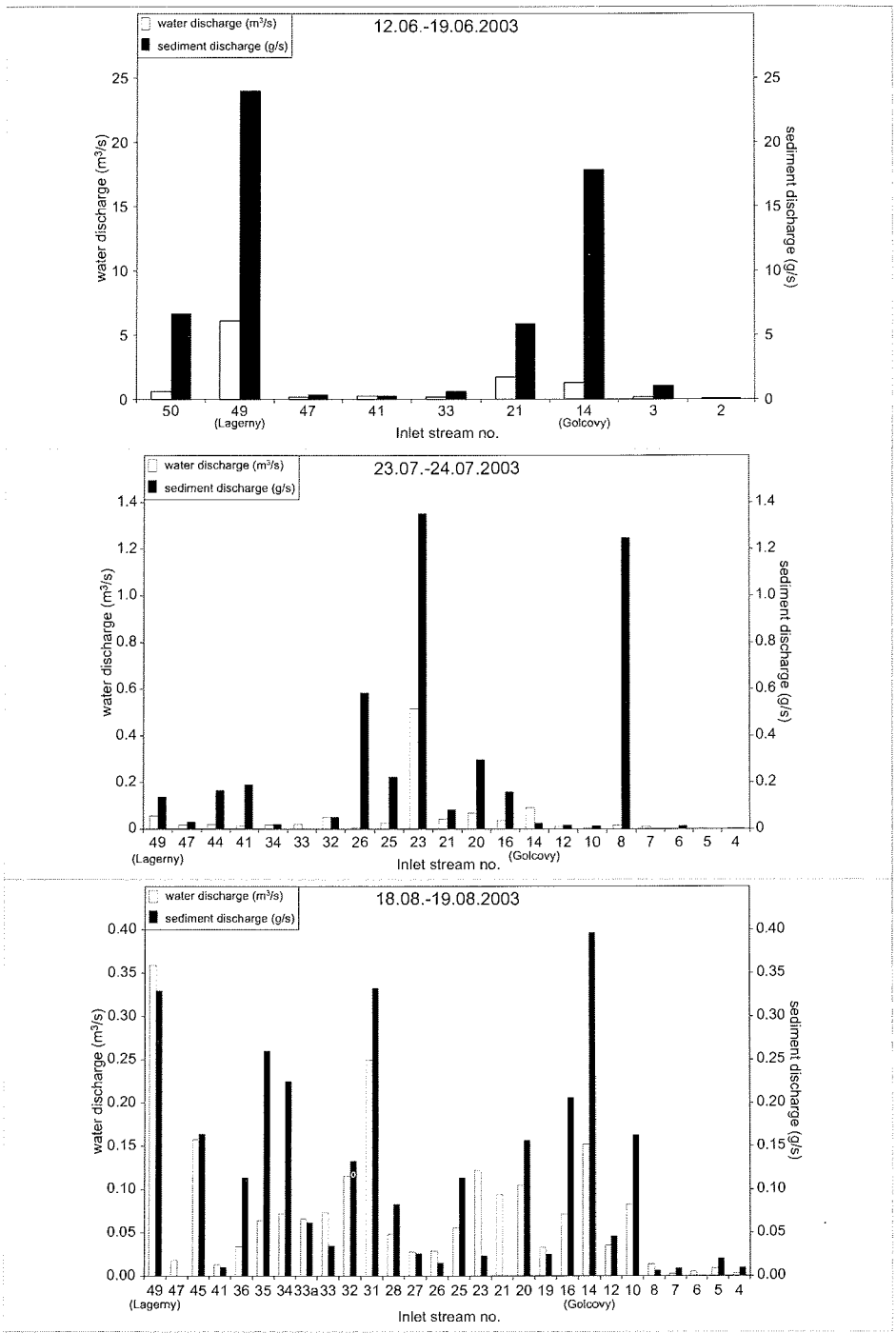

Figure 22: *Water and sediment discharge determined three times in 2003 on selected inlet streams (numbering according to the preposition of O. Glushkova).*

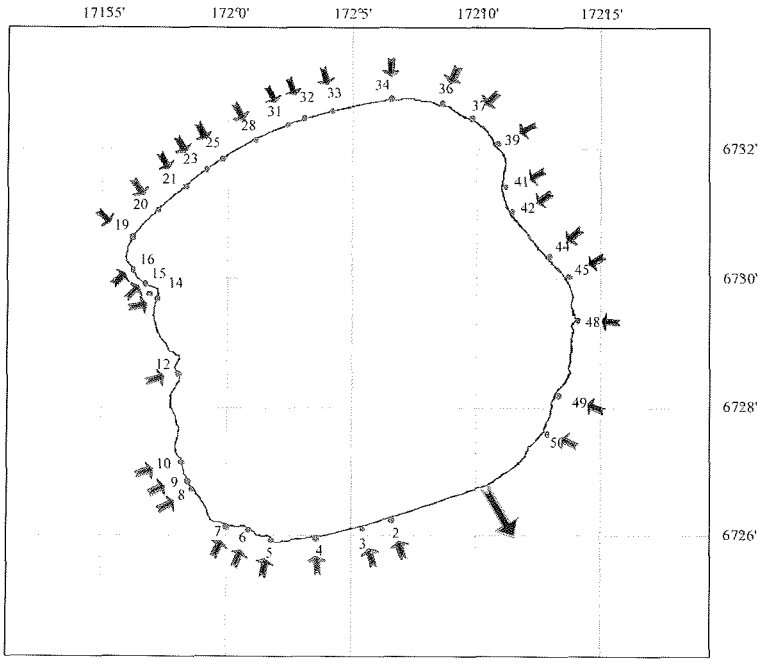

Figure 23: *The inlet streams of Lake El'gygytgyn (small arrows), numbered clockwise starting at the outlet Enmyvaam River (large arrow).*

Heavy Mineral Sampling

In summer 2000 first heavy mineral samples were collected in the El'gygytgyn Crater in order to investigate the traces of meteoritic material within the fluvial sediments. Samples were taken from 19 inlet streams, the upper reaches of the Enmyvaam River, higher terrace levels, from the lake shore terrace, and from outcrops with brecciated bedrocks. Additional samples were taken from a planation surface of an uplifted basement, where impactite rocks were abundant.

The volume of the rock and soil material collected was about 10 l for each sample. The heavy minerals in these samples were concentrated by washing. As a preliminary result of the studies it is worth mentioning that relics of cosmic substance ("cosmic dust") are well preserved within the meteorite impact area, despite the fact that 3.6 Mio years have passed since the impact event in the Pliocene (Layer, 2000). This is probably due to the impact-related glass shells surrounding the melted metallic particles, and to the clay cover of the old weathering crust (Sava et al., 2001).

During the field campaign in 2003 the heavy mineral sampling net existing from the expedition in 2000 was expanded by 48 samples. These samples were taken not only from the river bed sediments close to the mouth areas of the inlet streams but also from alluvial horizons in outcrops, from solifluction terraces, and from lake sediment cores (Fig. 24, Table 16).

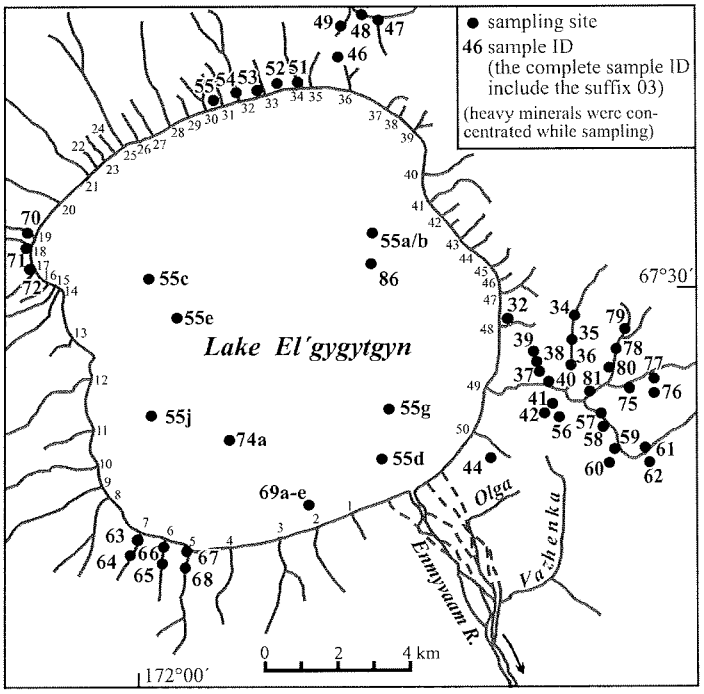

Figure 24: *Locations of heavy mineral samples collected during the expedition in 2003 (for further information see Table 16).*

Table 16: *Heavy mineral samples taken during the expedition in 2003.*

no.	site ID	position		source
		latitude	longitude	
1	2203/II/2	Enmyvaam river, Site GS2203 (Fig. 38, p. 72)		"chaotic horizon"
2	2303/III/1	67°14.426′ N	172°14.362′ E	"chaotic horizon"
3	2703	67°14.537′ N	172°19.428′ E	weathering crust
4	3203	67°29.231′ N	172°14.137′ E	alluvial deposit
5	3403	67°29.140′ N	172°16.844′ E	alluvial deposit
6	3503	67°28.926′ N	172°16.779′ E	periglacial colluvium
7	3503a	67°28.926′ N	172°16.779′ E	alluvial deposit
8	3603	67°28.622′ N	172°16.709′ E	alluvial deposit
9	3703	67°28.620′ N	172°15.294′ E	alluvial deposit
10	3803	67°28.551′ N	172°15.310′ E	alluvial deposit
11	4003	67°28.224′ N	172°15.828′ E	alluvial deposit
12	4103	67°27.938′ N	172°16.142′ E	alluvial deposit
13	4203	67°27.793′ N	172°15.824′ E	alluvial deposit
14	4403	67°27.372′ N	172°13.639′ E	alluvial deposit
15	4603	67°33.564′ N	172°07.838′ E	alluvial deposit
16	4703	67°33.817′ N	172°08.839′ E	alluvial deposit
17	4803	67°33.817′ N	172°08.839′ E	alluvial deposit
18	4903	67°33.817′ N	172°08.839′ E	alluvial deposit
19	5003	67°33.393′ N	172°07.840′ E	alluvial deposit
20	5103	67°32.830′ N	172°06.530′ E	alluvial deposit
21	5203	67°32.802′ N	172°05.672′ E	alluvial deposit
22	5303	67°32.734′ N	172°04.919′ E	alluvial deposit

continuation next page

Table 16: continuation

no.	site ID	position		source
		latitude	longitude	
23	5503a/ Lz1029	67°30.370´ N	172°08.240´ E	lacustrine deposit
24	5503b/ Lz1029	67°30.370´ N	172°08.240´ E	lacustrine deposit
25	5503c/ Lz1046	67°30.010´ N	171°59.980´ E	lacustrine deposit
26	5503d/ Lz1042	67°27.000´ N	172°07.920´ E	lacustrine deposit
27	5503e/ Lz1041	67°29.550´ N	172°01.400´ E	lacustrine deposit
28	5503j/ Lz1044	67°28.000´ N	171°59.990´ E	lacustrine deposit
29	5603	67°27.924´ N	172°16.751´ E	alluvial deposit
30	5703	67°27.718´ N	172°17.808´ E	periglacial colluvium
31	5803	67°27.718´ N	172°17.808´ E	alluvial deposit
32	5903	67°27.433´ N	172°18.342´ E	alluvial deposit
33	6003	67°27.298´ N	172°18.317´ E	alluvial deposit
34	6103	67°27.171´ N	172°19.231´ E	alluvial deposit
35	6203	67°27.171´ N	172°19.231´ E	alluvial deposit
36	6303	67°26.188´ N	171°59.960´ E	alluvial deposit
37	6403	67°25.928´ N	171°59.735´ E	alluvial deposit
38	6503	67°25.795´ N	172°00.769´ E	alluvial deposit
39	6603	67°26.104´ N	172°00.880´ E	alluvial deposit
40	6703	67°25.905´ N	172°01.852´ E	alluvial deposit
41	6803	67°25.714´ N	172°01.793´ E	alluvial deposit
42	6903a/ Lz1065	67°26.500´ N	172°06.150´ E	lacustrine deposit
43	6903b/ Lz1067	67°26.540´ N	172°06.200´ E	lacustrine deposit
44	6903c/ Lz1069	67°26.600´ N	172°06.180´ E	lacustrine deposit
45	6903d/ Lz1064-3	67°26.480´ N	172°06.150´ E	lacustrine deposit
46	6903e/ Lz1068	67°26.570´ N	172°06.210´ E	lacustrine deposit
47	7003	67°30.706´ N	171°56.295´ E	alluvial deposit
48	7103	67°30.623´ N	171°56.106´ E	alluvial deposit
49	7203	67°30.450´ N	171°55.973´ E	alluvial deposit
50	7303a/ Lz1041-2	67°29.550´ N	172°01.400´ E	lacustrine deposit
51	7403a/ Lz1073	67°27.920´ N	172°03.110´ E	lacustrine deposit
52	7503	67°28.158´ N	172°18.750´ E	alluvial deposit
53	7603	67°28.304´ N	172°19.573´ E	alluvial deposit
54	7703	67°28.304´ N	172°19.573´ E	alluvial deposit
55	7803	67°28.842´ N	172°18.595´ E	alluvial deposit
56	7903	67°28.842´ N	172°18.595´ E	alluvial deposit
57	8003	67°28.619´ N	172°18.414´ E	alluvial deposit
58	8103	67°28.109´ N	172°17.404´ E	alluvial deposit
59	8503	67°32.706´ N	172°02.372´ E	alluvial deposit
60	8603/ Lz1079	67°29.980´ N	172°07.990´ E	lacustrine deposit

4.5.3 Aeolian Supply

(O. Juschus, G. Fedorov, V. Wennrich, S. Quart)

Introduction – The lack of a continuous plant cover in the catchment and surroundings of Lake El´gygytgyn supports aeolian processes. Besides fluvial and gravitational transport aeolian sediment transport is believed to be the third main process carrying material into the lake basin. Further on, the long-lasting lake ice cover probably supports transport and distribution of the comparatively coarse-grained material over the entire lake basin.

Methods – Pure aeolian sediments can best be sampled from that part of seasonal snow fields and lake ice which is not contaminated from the underlying sediments. Hence, sampling of aeolian sediments had to be

conducted mainly during the spring campaign, before snow and ice melt was completed. The snow samples (each approx. 10 - 20 kg) were taken with a shovel and a plastic bag at sites both on the lake ice cover and in the lake surroundings. At the most sampling sites also the thickness of the snow cover was measured. A first series of samples was collected by G. Fedorov (St. Petersburg, AARI) during the middle of May (Fig. 25). A second series was accomplished jointly by O. Juschus (Univ. of Leipzig) and G. Fedorov during the end of May and June (Fig. 26, Table 17). Some additional aeolian sediments were obtained from lake ice samples collected during the spring campaign by G. Fedorov.

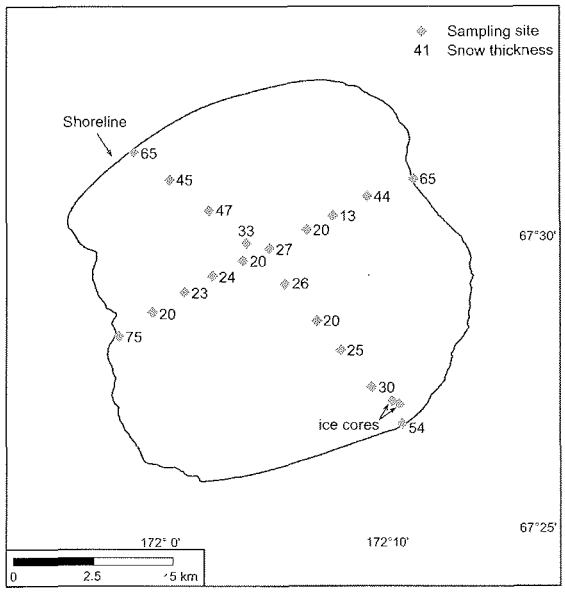

Figure 25: *Locations of aeolian sediment samples collected from snow fields and lake ice cores on Lake El'gygytgyn in the middle of May 2003.*

All samples were melted and divided into three sub-samples. The first ones were filtered with cellulose-acetate filters and the second ones with pre-weighed glass-fibre filters. Both filter types have pore diameters of 0.45 µm. The remaining third sub-samples were decanted and saved for further investigations.

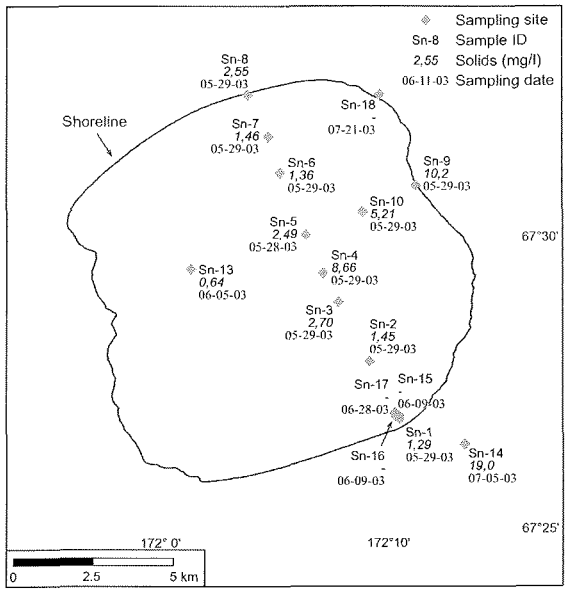

Figure 26: *Locations of aeolian sediment samples collected from snow fields on Lake El'gygytgyn and in its surroundings in late May, June, and July 2003.*

Field results – The first series of snow samples collected had an average solids concentration of about 0.6 mg/l. The values ranged from 0.05 mg/l to 1.32 mg/l. The solid concentration within the lake ice with only 0.012 mg/l was remarkably lower. However, compared with the thick sediment layers deposited on the ice

cover by the inlet streams during spring time, the current aeolian sediment supply probably is of minor relevance. This is valid for today, but must not necessarily have been the case in the geological past.

The solids concentrations in the second series of snow samples ranged between 0.64 and 10.2 mg/l (average: 3.45 mg/l, Table 17). The higher concentrations compared to the first series may be explained by a relative enrichment of the solids due to proceeding degradation of the snow during the season. This may particularly have been the case with sample Sn-14 (solids: 19.0 mg/l), which was taken from a snow field to the south of the lake during summer time (Fig. 26).

Table 17: *Aeolian sediment samples collected on Lake El'gygytgyn and in its surroundings in late May, June, and July 2003; w = wet snow, vw = very wet snow, gf = glass-fibre, ca = cellulose-acetate; except Sn-16 (snow melt water) all samples were collected as snow samples.*

sample ID	position latitude	position longitude	date	snow thickn.	note	decanted (l)	filtered gf (l)	filtered ca (l)	solids mg/l
Sn-1	67°27.03' N	172°10.58' E	05-29-03	50	w	5.6	6.1	5.8	1.29
Sn-2	67°27.96' N	172°09.26' E	05-29-03	12	w	6.5	6.2	6.3	1.45
Sn-3	67°28.98' N	172°07.89' E	05-29-03	8	-	4.6	5.0	4.5	2.70
Sn-4	67°29.48' N	172°07.22' E	05-29-03	5	-	5.5	5.4	4.9	8.66
Sn-5	67°30.13' N	172°06.46' E	05-28-03	10	-	19.0	8.7	-	2.49
Sn-6	67°31.19' N	172°05.34' E	05-29-03	34	-	5.6	5.7	5.5	1.36
Sn-7	67°31.81' N	172°04.81' E	05-29-03	50	-	3.4	3.6	3.8	1.46
Sn-8	67°32.53' N	172°03.91' E	05-29-03	18	-	3.7	2.4	2.4	2.55
Sn-9	67°30.97' N	172°11.38' E	05-29-03	10	vw	3.3	3.1	2.7	10.20
Sn-10	67°30.52' N	172°08.97' E	05-29-03	12	-	3.9	3.6	3.8	5.21
Sn-13	67°29.55' N	172°01.40' E	06-05-03	25	-	6.8	6.8	6.7	0.64
Sn-14	67°26.54' N	172°13.49' E	07-05-03	20	vw	-	0.5	0.5	19.00
Sn-15	67°27.03' N	172°10.58' E	06-09-03	20	vw	-	-	-	
Sn-16	67°27.03' N	172°10.58' E	06-09-03	-	film	-	-	-	
Sn-17	67°27.07' N	172°10.41' E	06-28-03	10	w	-	-	-	
Sn-18	67°32.53' N	172°09.74' E	07-21-03	50	vw	-	-	-	

4.5.4 Solifluction

(G. Schwamborn, G. Fedorov, A. Kupolov)

Ground Penetration Radar (GPR) Survey

The shallow permafrost subsurface was investigated at various sites around Lake El'gygytgyn using ground penetrating radar (GPR) (Fig. 27). Several geomorphologic surfaces in the crater, as shown by satellite imagery, were surveyed to collect structural information on bedding and layering of near surface sediments. To examine frozen-unfrozen and solifluction-bedrock interfaces, GPR profiles were conducted along intersecting transects at each site. Active layer depth measurements were done using a pricking rod. Thaw depths along the transects measured at the time of the summer GPR surveys ranged from about 50 cm to greater than 80 cm during July/August. Coring results are used to support the interpretation of the GPR results (see Chapter 5.2.4 and 5.2.5; p. 92 and p. 96).

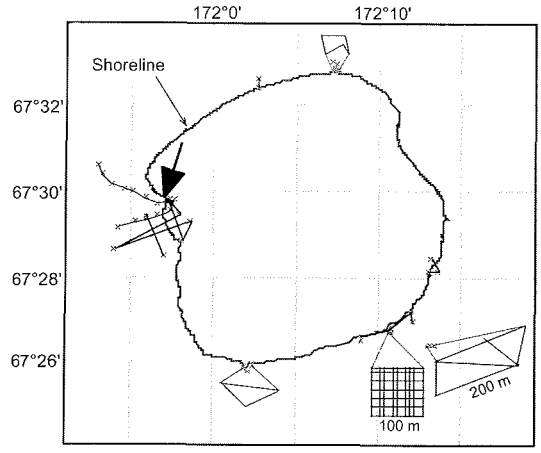

Figure 27: *Overview of GPR measuring sites around Lake El'gygytgyn. The arrow marks the GPR profile described in the text.*

In areas of a prominent solifluction cover (e.g., the western crater area), GPR returns are generally characterized by laterally continuous reflectors and shallow penetration (ca. 5 - 7 m). In contrast, returns from frozen peat and ice rich alluvial and slope sediments were typically chaotic, with little lateral continuity, but greater penetration (ca. 10 - 12 m). Ongoing work involves the application of the processing enhancements modified from seismic techniques, to reduce the distortions produced by diffractions, noise and, weak signals. The commercially available impulse radar equipment used for these observations was a RAMAC/GPR System, which consists of a control unit, a field PC, and 50 and 100 MHz antenna units containing both transmit and receive antennas (Fig. 28). The control unit generates timing signals to key the transmitter on and off and synchronizes this keying with the receiver. Digital commanding and recording in the field was managed on a HUSKY field PC along with the packaged signal processing software. General settings of the software when collecting data have been chosen in the way listed in Table 18.

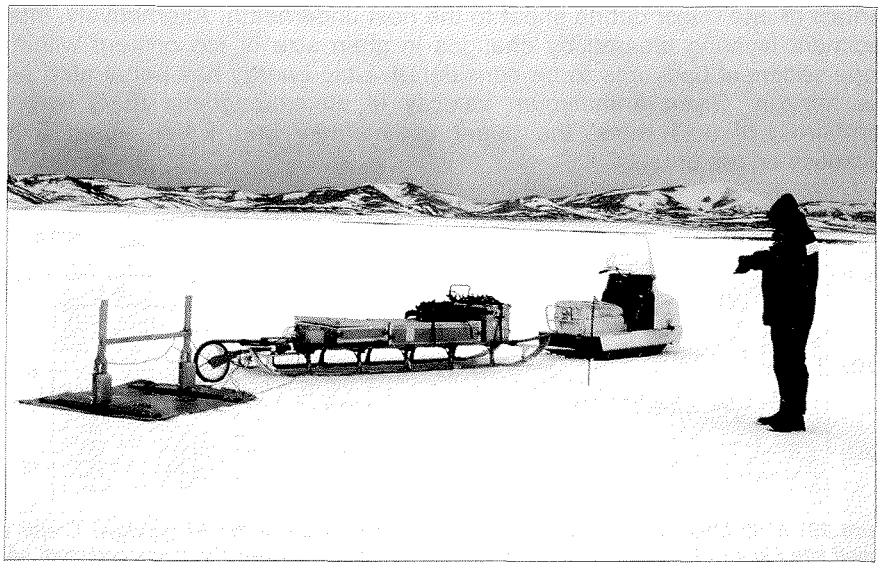

Figure 28: *Set-up of the GPR system during spring season at Lake El'gygytgyn. The antenna sheet and the trigger wheel are fixed to a Nansen sledge and towed by a snowmobile.*

Table 18: *General system settings of the GPR survey conducted in the El'gygytgyn Crater in 2003.*

50 MHz antenna		100 MHz antenna	
samples	536	samples	1024
stacks	64	stacks	32
antenna separation (m)	2	antenna separation (m)	1
trace interval (m)	1	trace interval (m)	1
vertical resolution in permafrost (m)	> 0.6	vertical resolution in permafrost (m)	> 0.3

The penetration depth can be calculated by using the approximated values for ε_r (relative permittivity) and the resulting velocities (m/ns) for media relevant in the crater Lake El'gygytgyn given in Table 19.

Table 19: *Electromagnetic velocities for media relevant in the crater area.*

medium	ε_r	velocity (m/ns)
fresh water	81	0.033
permafrost	4-8	0.106-0.150
granite	5-7	0.113-0.13 4
ice	3-4	0.150-0.173

The profile example (Fig. 29) presents crucial details on lithogenetic elements of the western onshore subsurface. Starting on top, stratified horizons occur below the surface. This is considered to be a loose sediment cover made up of hill debris and slope materials of various grain sizes. It is considered to represent the present and ancient solifluction sheets down the crater slopes. At two-way-travel times (TWT) of about 130 ns an interface produces several continuous to detached reflection returns. These segments may represent the contact of one major debris sheet to the next underneath. Alternatively, internal sediment layering created by changes in grain size or ice content within the slope sediment body has to be considered. Little energy has penetrated below this horizon. Given a minimum velocity of electromagnetic (EM) waves in permafrost of 0.11 m/ns, the upper sedimentary unit 1 has about 5 m in thickness on top of unit 2.

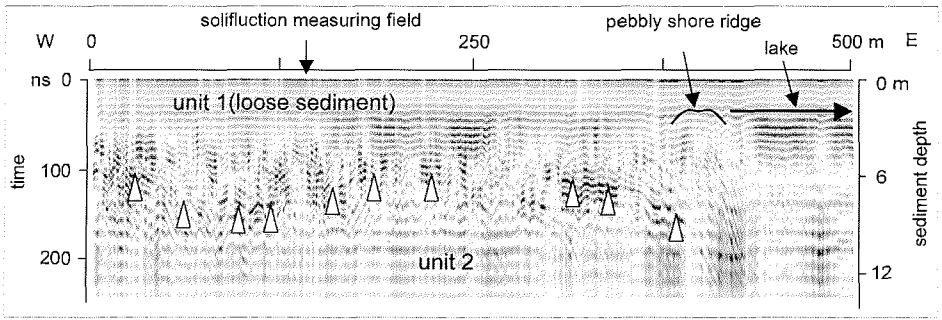

Figure 29: *A 50 MHz GPR-profile of the western slope area of the El'gygytgyn Crater (for location see Figure 27). This profile highlights the boundary between the loose sediment cover and a second unit below (indicated by triangles).*

Solifluction monitoring

To measure the rate of soil slumping two solifluction monitoring profiles were established on slopes within the lake depression. On each profile two piles were driven into the permafrost by at least 30 cm, leaving 25 m between the piles. Within this span, flat stones (coloured orange) were laid each 20 cm. In addition, wooden pegs were pushed into the active soil layer (by 20 cm) each metre (Fig. 30). The profile in the southeastern sector of the lake basin (position: 67°27.09´ N; 172°12.24´ E) has a slope angle of 7°, dipping to the west. The surface coverage of vegetation range around 80 %. The depth of molten ground was 80 cm. In the pit holes, sandy and silty sediments were met with about 20 % of clastic material. Obviously the solifluction type was a slow one. The profile in the north-western sector of the lake depression (67°29.77´ N; 171° 56.84´ E) has a slope angle of 7° as well. The surface is dipping to the east. The vegetation coverage amount to only a total of 30 %. The ground was molten down to a depth between 1.0 and 1.3 m. In the pit holes, wet gravel and pebbly material was found. The solifluction was obviously of a structural type.

Figure 30: *The solifluction monitoring profile in the southeastern sector of the El´gygytgyn Crater.*

4.6 Autochthonous Biogenic Production in Lake El´gygytgyn

4.6.1 Modern Diatom Sampling

(O. Juschus, J. Brigham-Grette, V. Wennrich, S. Quart)

Introduction – Diatoms are probably the most abundant algal group in Lake El´gygytgyn. Further on their concentration and assemblages in the lake sediment record are amongst the most important proxies for reconstructing past environmental settings in the lake water column. This is due to their fossilization potential and environmental sensitivity. In spite of this, there are only a few modern publications on the diatoms of Lake El´gygytgyn. Cherepanova (in Minyuk et al., 2003) described the diatoms occurring in the 12.9 m long core PG1351, recovered in 1998. Additional information on the Holocene diatom flora was published by Cremer and Wagner (2003), based on investigations of short gravity cores collected in 2000.

Methods – Modern diatom samples were taken directly from the lake water (Table 21, Fig. 31), from a sediment trap (Table 20), but also from the inlet streams, from the outlet stream (Enmyvaam River) and from pebble surfaces on the shelf (Table 22, Fig. 31). Sampling of the diatoms occurring in the lake water column was accomplished at different times of the season together with the hydrological sampling and measurements (cp. Chapter 4.4, p. 30). The diatoms were isolated in the field from 500 ml lake water samples using cellulose-acetate filters (Ø 0.45 µm). These filters were also employed to quantitatively isolate the diatoms caught over longer periods with sediment traps which have been deployed in different water depths of Lake El'gygytgyn (cp. Chapter 4.7, p. 63). For this purpose, the content of one of four tubes was washed into a bottle and filtered immediately after recovery. For retrieving samples from the inlet streams or from the shelf, in contrast, pebbles, plants or bio-films were filled into plastic bottles and preserved with iodide solution.

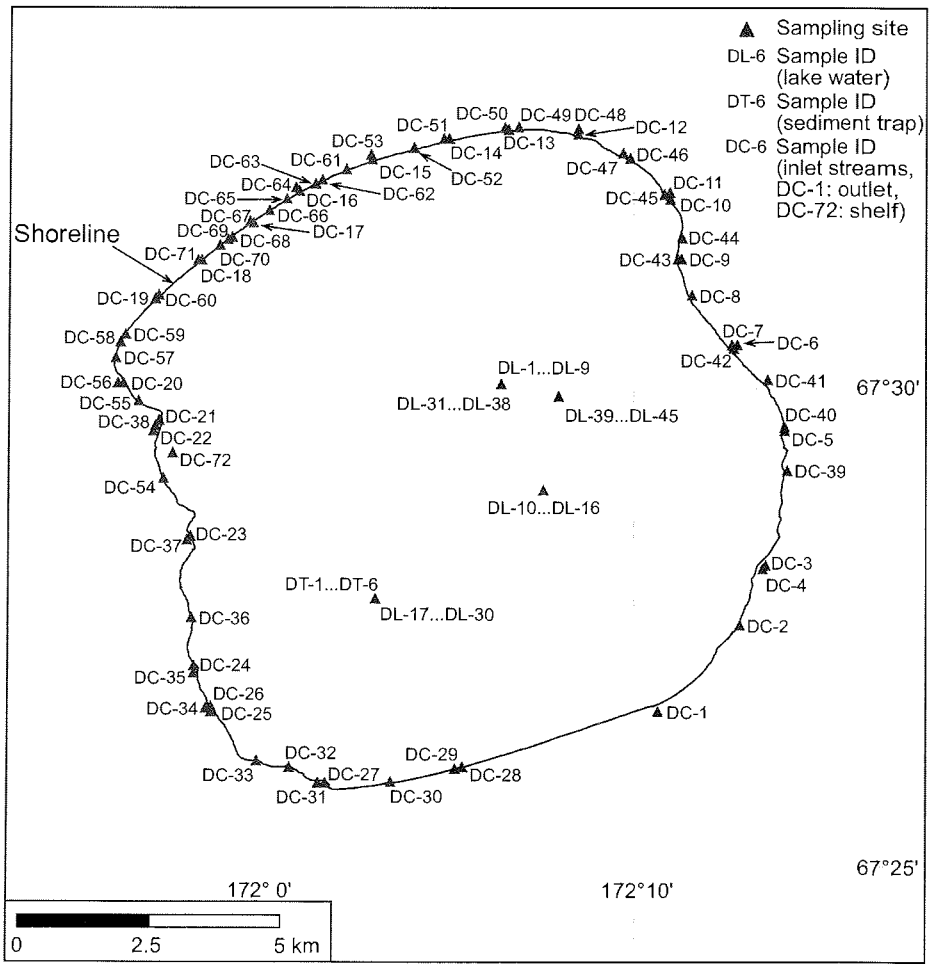

Figure 31: *Samples of modern diatoms collected in 2003 from Lake El'gygytgyn as well as the inlet and outlet streams.*

Table 20: *Diatom samples collected from the sediment trap Sedi-2 (67°27.90´ N, 172°03.14´ E).*

sample ID	water depth (m)	date deployed	date recovered
DT-1	10	05-31-03	07-19-03
DT-2	30	05-31-03	07-19-03
DT-3	50	05-31-03	07-19-03
DT-4	90	05-31-03	07-19-03
DT-5	130	05-31-03	07-19-03
DT-6	143	05-31-03	07-19-03

Table 21: *Diatom samples collected in 2003 from the water column of Lake El´gygytgyn.*

sample ID	field name	position		water depth (m)	sampling date
		latitude	longitude		
DL-1	Lz1024-2	67°30.13´ N	172°06.46´ E	2.0	05-27-03
DL-2	Lz1024-10	67°30.13´ N	172°06.46´ E	10.0	05-27-03
DL-3	Lz1024-30	67°30.13´ N	172°06.46´ E	30.0	05-27-03
DL-4	Lz1024-50	67°30.13´ N	172°06.46´ E	50.0	05-27-03
DL-5	Lz1024-100	67°30.13´ N	172°06.46´ E	100.0	05-27-03
DL-6	Lz1024-150	67°30.13´ N	172°06.46´ E	150.0	05-27-03
DL-7	Lz1024-165	67°30.13´ N	172°06.46´ E	165.0	05-27-03
DL-8	Lz1024-2C	67°30.13´ N	172°06.46´ E	2.0	05-29-03
DL-9	Lz1024-168C	67°30.13´ N	172°06.46´ E	168.0	05-29-03
DL-10	Sedi1-2	67°29.02´ N	172°07.59´ E	2.0	05-31-03
DL-11	Sedi1-10	67°29.02´ N	172°07.59´ E	10.0	05-31-03
DL-12	Sedi1-30	67°29.02´ N	172°07.59´ E	30.0	05-31-03
DL-13	Sedi1-50	67°29.02´ N	172°07.59´ E	50.0	05-31-03
DL-14	Sedi1-100	67°29.02´ N	172°07.59´ E	100.0	05-31-03
DL-15	Sedi1-150	67°29.02´ N	172°07.59´ E	150.0	05-31-03
DL-16	Sedi1-156	67°29.02´ N	172°07.59´ E	156.0	05-31-03
DL-17	Sedi2-2	67°27.90´ N	172°03.14´ E	2.0	06-01-03
DL-18	Sedi2-10	67°27.90´ N	172°03.14´ E	10.0	06-01-03
DL-19	Sedi2-30	67°27.90´ N	172°03.14´ E	30.0	06-01-03
DL-20	Sedi2-50	67°27.90´ N	172°03.14´ E	50.0	06-01-03
DL-21	Sedi2-100	67°27.90´ N	172°03.14´ E	100.0	06-01-03
DL-22	Sedi2-150	67°27.90´ N	172°03.14´ E	150.0	06-01-03
DL-23	Sedi2-152.5	67°27.90´ N	172°03.14´ E	152.5	06-01-03
DL-24	Sedi2-2-2	67°27.90´ N	172°03.14´ E	2.0	07-20-03
DL-25	Sedi2-2-10	67°27.90´ N	172°03.14´ E	10.0	07-20-03
DL-26	Sedi2-2-30	67°27.90´ N	172°03.14´ E	30.0	07-20-03
DL-27	Sedi2-2-50	67°27.90´ N	172°03.14´ E	50.0	07-20-03
DL-28	Sedi2-2-100	67°27.90´ N	172°03.14´ E	100.0	07-20-03
DL-29	Sedi2-2-150	67°27.90´ N	172°03.14´ E	150.0	07-20-03
DL-30	Sedi2-2-152.5	67°27.90´ N	172°03.14´ E	152.5	07-20-03
DL-31	Lz1024-2-2	67°30.13´ N	172°06.46´ E	2.0	08-02-03
DL-32	Lz1024-2-10	67°30.13´ N	172°06.46´ E	10.0	08-02-03
DL-33	Lz1024-2-30	67°30.13´ N	172°06.46´ E	30.0	08-02-03
DL-34	Lz1024-2-50	67°30.13´ N	172°06.46´ E	50.0	08-02-03
DL-35	Lz1024-2-100	67°30.13´ N	172°06.46´ E	100.0	08-02-03
DL-36	Lz1024-2-150	67°30.13´ N	172°06.46´ E	150.0	08-02-03
DL-37	Lz1024-2-165	67°30.13´ N	172°06.46´ E	165.0	08-02-03
DL-38	Lz1024-2-168	67°30.13´ N	172°06.46´ E	168.0	08-02-03
DL-39	Lz1079-2	67°30.00´ N	172°08.01´ E	2.0	08-19-03
DL-40	Lz1079-10	67°30.00´ N	172°08.01´ E	10.0	08-19-03
DL-41	Lz1079-30	67°30.00´ N	172°08.01´ E	30.0	08-19-03
DL-42	Lz1079-50	67°30.00´ N	172°08.01´ E	50.0	08-19-03
DL-43	Lz1079-150	67°30.00´ N	172°08.01´ E	150.0	08-19-03
DL-44	Lz1079-163	67°30.00´ N	172°08.01´ E	163.0	08-19-03
DL-45	Lz1079-166	67°30.00´ N	172°08.01´ E	166.0	08-19-03

Table 22: *Diatom samples collected in 2003 from the Lake El'gygytgyn inlet streams, shelf, and outlet stream.*

sample ID	field name	source	location	position latitude	position longitude	sampling date
DC-1	DEnmyvaam	stillwater	Outlet	67°26.72′ N	172°10.63′ E	06-15-03
DC-2	ZF50-1DS	stone	creek 50	67°27.61′ N	172°12.84′ E	06-15-03
DC-3	ZF49-3DS	stone	creek 49	67°28.20′ N	172°13.46′ E	06-15-03
DC-4	ZF49-5DBf	„scumlayer"	creek 49	67°28.20′ N	172°13.46′ E	06-15-03
DC-5	ZF47-1DS	stone	creek 47	67°29.65′ N	172°14.07′ E	06-18-03
DC-6	ZF44-1DM	moss	creek 44	67°30.49′ N	172°12.70′ E	06-18-03
DC-7	ZF44-2DS	stone	creek 44	67°30.49′ N	172°12.70′ E	06-18-03
DC-8	ZF43-1DS	stone	creek 43	67°31.05′ N	172°11.57′ E	06-18-03
DC-9	ZF41-1DS	stone	creek 41	67°31.43′ N	172°11.19′ E	06-18-03
DC-10	ZF39-1DM	moss	creek 39	67°32.10′ N	172°10.94′ E	06-18-03
DC-11	ZF39-2DS	stone	creek 39	67°32.10′ N	172°10.94′ E	06-18-03
DC-12	ZF36-1DM	moss	creek 36	67°32.73′ N	172°08.54′ E	06-18-03
DC-13	ZF34-1DS	stone	creek 34	67°32.80′ N	172°06.55′ E	06-18-03
DC-14	ZF33-1DM	moss	creek 33	67°32.69′ N	172°05.02′ E	06-18-03
DC-15	ZF31-1DM	moss	creek 31	67°32.47′ N	172°03.02′ E	06-18-03
DC-16	ZF28-1DM	moss	creek 28	67°32.14′ N	172°01.08′ E	06-18-03
DC-17	ZF25-1DM	moss	creek 25	67°31.81′ N	171°59.77′ E	06-18-03
DC-18	ZF21-1DM	moss	creek 21	67°31.42′ N	171°58.32′ E	06-19-03
DC-19	ZF20-1DM	moss	creek 20	67°31.02′ N	171°57.19′ E	06-19-03
DC-20	ZF16-1DM	moss	creek 16	67°30.14′ N	171°56.25′ E	06-19-03
DC-21	ZF14-1DM	moss	creek 14	67°29.70′ N	171°57.21′ E	06-19-03
DC-22	ZF14-2DS	stone	creek 14	67°29.70′ N	171°57.21′ E	06-19-03
DC-23	ZF12-1DM	moss	creek 12	67°28.53′ N	171°58.11′ E	06-19-03
DC-24	ZF10-1DM	moss	creek 10	67°27.16′ N	171°58.26′ E	06-19-03
DC-25	ZF8-1DM	moss	creek 8	67°26.76′ N	171°58.72′ E	06-19-03
DC-26	ZF8-2DBf	„scumlayer"	creek 8	67°26.76′ N	171°58.72′ E	06-19-03
DC-27	ZF5-1DM	moss	creek 5	67°25.98′ N	172°01.82′ E	06-19-03
DC-28	ZF3-1DM	moss	creek 3	67°26.14′ N	172°05.43′ E	06-19-03
DC-29	ZF3-3DM	moss	creek 3	67°26.14′ N	172°05.43′ E	07-20-03
DC-30	ZF4-1DS	stone	creek 4	67°25.99′ N	172°03.56′ E	07-20-03
DC-31	ZF5-3DS	stone	creek 5	67°25.98′ N	172°01.82′ E	07-20-03
DC-32	ZF6-1DM	moss	creek 6	67°26.14′ N	172°00.86′ E	07-20-03
DC-33	ZF7-1DM	moss	creek 7	67°26.21′ N	171°59.97′ E	07-20-03
DC-34	ZF8-4DM	moss	creek 8	67°26.76′ N	171°58.72′ E	07-20-03
DC-35	ZF10-3DS	stone	creek 10	67°27.16′ N	171°58.26′ E	07-20-03
DC-36	ZF11-1DM	moss	creek 11	67°27.70′ N	171°58.19′ E	07-20-03
DC-37	ZF12-3DS	stone	creek 12	67°28.53′ N	171°58.11′ E	07-20-03
DC-38	ZF14-4DM	moss	creek 14	67°29.70′ N	171°57.21′ E	07-20-03
DC-39	ZF48-1DS	stone	creek 48	67°29.22′ N	172°14.13′ E	07-21-03
DC-40	ZF47-3DS	stone	creek 47	67°29.65′ N	172°14.07′ E	07-21-03
DC-41	ZF45-1DS	stone	creek 45	67°30.35′ N	172°14.05′ E	07-21-03
DC-42	ZF44-4DS	stone	creek 44	67°30.49′ N	172°12.70′ E	07-21-03
DC-43	ZF41-3DS	stone	creek 41	67°31.43′ N	172°11.19′ E	07-21-03
DC-44	ZF40-1DM	moss	creek 40	67°31.64′ N	172°11.32′ E	07-21-03
DC-45	ZF39-4DM	moss	creek 39	67°32.09′ N	172°10.95′ E	07-21-03
DC-46	ZF38-1DS	stone	creek 38	67°32.48′ N	172°09.93′ E	07-21-03
DC-47	ZF37-1DS	stone	creek 37	67°32.53′ N	172°09.74′ E	07-21-03
DC-48	ZF36-3DBf	„scumlayer"	creek 36	67°32.73′ N	172°08.54′ E	07-21-03
DC-49	ZF35-1DM	moss	creek 35	67°32.81′ N	172°06.93′ E	07-21-03
DC-50	ZF34-3DM	moss	creek 34	67°32.80′ N	172°06.55′ E	07-21-03
DC-51	ZF33-3DM	moss	creek 33	67°32.69′ N	172°04.98′ E	07-21-03
DC-52	ZF32-1DM	moss	creek 32	67°32.59′ N	172°04.15′ E	07-21-03
DC-53	ZF31-3DM	moss	creek 31	67°32.52′ N	172°03.00′ E	07-21-03
DC-54	ZF13-1DM	moss	creek 13	67°29.15′ N	171°57.42′ E	08-02-03

continuation next page

Table 22: continuation

sample ID	field name	source	location	position latitude	position longitude	sampling date
DC-55	ZF15-1DM	moss	creek 15	67°29.96′ N	171°56.76′ E	08-02-03
DC-56	ZF16-3DS	stone	creek 16	67°30.14′ N	171°56.25′ E	08-02-03
DC-57	ZF17-1DS	stone	creek 17	67°30.40′ N	171°56.14′ E	08-02-03
DC-58	ZF18-1DM	moss	creek 18	67°30.57′ N	171°56.26′ E	08-02-03
DC-59	ZF19-1DS	stone	creek 19	67°30.65′ N	171°56.40′ E	08-02-03
DC-60	ZF20-3DM	stone	creek 20	67°31.04′ N	171°57.23′ E	08-02-03
DC-61	ZF30-1DS	stone	creek 30	67°32.37′ N	172°02.34′ E	08-18-03
DC-62	ZF29a-1DS	stone	creek 29a	67°32.26′ N	172°01.70′ E	08-18-03
DC-63	ZF29-1DS	stone	creek 29	67°32.22′ N	172°01.51′ E	08-18-03
DC-64	ZF28-3DS	stone	creek 28	67°32.14′ N	172°01.08′ E	08-18-03
DC-65	ZF27-1DS	stone	creek 27	67°32.06′ N	172°00.74′ E	08-18-03
DC-66	ZF26-1DS	stone	creek 26	67°31.94′ N	172°00.26′ E	08-18-03
DC-67	ZF25-3DS	stone	creek 25	67°31.81′ N	171°59.77′ E	08-18-03
DC-68	ZF24-1DS	stone	creek 24	67°31.66′ N	171°59.24′ E	08-18-03
DC-69	ZF23-1DS	stone	creek 23	67°31.64′ N	171°59.13′ E	08-18-03
DC-70	ZF22-1DS	stone	creek 22	67°31.58′ N	171°58.91′ E	08-18-03
DC-71	ZF21-3DS	stone	creek 21	67°31.42′ N	171°58.32′ E	08-18-03
DC-72	Lz1074DS	stone	Lz1074	67°29.41′ N	171°57.68′ E	08-18-03

4.6.2 Biomarker Investigations

(J. Brigham-Grette)

One important aspect of our studies of biogenic production is determining the linkage between changes in the lake carbon cycle and paleoclimate proxies. While these linkages have been studied in Antarctic lakes (e.g., Melles et al., 1994, 1997; Doran et al., 1998), Lake El'gygytgyn is unique in some aspects. For example, in our 1998 core record, distinct increases in TOC during glacial modes (colder climate) coincide repeatedly with negative shifts in $\delta^{13}C$ of TOC to values of near -33 ‰, a shift that is opposite to that expected with more persistent ice (Melles et al., in press). In most other lakes, persistent ice cover limits the exchange of CO_2 with the atmosphere such that over time, continuing primary productivity under the ice causes enrichment of the DIC in ^{13}C (i.e., DIC and organic matter become more positive in $\delta^{13}C$ not more negative) as ^{12}C is preferentially consumed during photosynthesis.

To quantify the relative input of terrestrial vs. aquatic organic matter to the lake system, compound-specific biomarkers will be analysed in collaboration with Tim Eglinton, Woods Hole Oceanographic Institution (WHOI). Analyses will be performed on a select subset of samples including lake ice (Table 23), and a small number of lake water samples, stream water samples, along side sediments from a few gravity cores. We will also determine the C/N ratio and the stable isotopic signature of particulate organic matter (POM) derived from selected streams (Table 11, p. 38) and compare these results with the isotopic signature of POM collected in sediment trap waters (Table 10, p. 37) tethered at depth in the lake.

One of the many questions we have of sediment sources to Lake El'gygytgyn is whether the lake system today received significant aeolian deposition and might

that deposition be trapped in lake ice? Moreover, what is the abundance of wind-scoured plant waxes in the ice and surface sediments today and can these be used for ^{14}C dating recent portions of the paleorecord?

Using ice and shallow core sediment samples, we still attempt to test our ideas of aeolian input by analysing the melted ice samples for long-chain (C25 - C33) n-alkanes exhibiting an odd-carbon-number predominance, and n-alcohols and n-alkanoic acids exhibiting an even-carbon-number predominance that are synthesized exclusively by vascular plants as epicuticular leaf waxes (Eglinton and Hamilton, 1967; Kolattukudy, 1976). Eglinton will sample for these lipids in the ice and surface sediments to gauge their successful use for molecular ^{14}C dating.

One additional question we hope to test is whether biogenic silica accurately reflect changes in productivity. Because preservation can commonly be species specific and dissolution can alter this important proxy, we will use samples from collected surface sediments and one of the gravity cores to determine the distribution of algal sterols in the underlying sediments. These data will hopefully provide information on aquatic primary production for comparison with standard measurements of biogenic silica.

Table 23: *Samples for biomarkers collected from the bottom of El'gygytgyn lake ice. Note that ice thickness measured per location is about 30 cm less then the May/end of winter maximum; thickness lost since May was from the top; all samples were kept dark and in cellar until poisoned July 4, 2003.*

sample ID	field ID	position		date	ice thickness (cm)	molten ice filtered (l)
		latitude	longitude			
E03BG011	JBG1	67°30.00´ N	172°07.80´ E	06-11-03	195	0.930
E03BG012	JBG2	67°32.51´ N	172°03.92´ E	06-11-03	185	1.190
E03BG013	JBG3	67°31.81´ N	172°04.81´ E	06-11-03	140	1.205
E03BG014	JBG4	67°31.19´ N	172°05.34´ E	06-11-03	160	1.480
E03BG015	JBG5	67°30.13´ N	172°06.46´ E	06-11-03	180	1.690
E03BG016	JBG6	67°29.30´ N	172°07.23´ E	06-11-03	180	1.235
E03BG017	JBG7	67°28.49´ N	172°07.93´ E	06-11-03	155	1.190
E03BG018	JBG8	67°27.70´ N	172°09.54´ E	06-11-03	150	1.300
E03BG019	JBG9	67°26.98´ N	172°10.59´ E	06-11-03	180	1.670
E03BG020	JBG9/II	67°27.03´ N	172°10.58´ E	06-14-03	150	1.170
E03BG021	JBG10	67°28.60´ N	172°05.80´ E	06-14-03	155	0.845

4.6.3 Bacteria

(J. Brigham-Grette)

The decomposition of organic matter at the sediment water interface and at the redox boundary that occurs in the upper few decimeters of the lake sediments today may well involve various levels of anoxia, sulfate reduction and microbially-induced methanogenesis. The very negative nature of the $\delta^{13}C$ isotopic signature measured in the lake sediment cores from 1998 (Melles et al., in press) hints that chemoautrophy may be involved in iron reduction and perhaps selective magnetite dissolution. Such reactions and the factors that control them are important for understanding just what produces changes in the

magnetic susceptibility from Lake El'gygytgyn. Although the proper collection of indigenous bacteria is difficult at a site as remote as El'gygytgyn, nine samples were taken in 2003 of the sediment water interface "fluff" layer as an experiment to determine if methanogenic bacteria are present (Table 24). The presence of methane in some ice bubble samples suggests this is possible (cp. Chapter 4.3.2, p. 26). This visible evidence will be used along side the isotopic analyses of selected biomarkers to determine the direction of future research in this area at El'gygytgyn. Samples in Table 24 are currently being studied in collaboration with Klaus Nusslein, Microbiology, University of Massachusetts (UMass), a specialist in the microbial ecology of aquatic environments.

Table 24: *Cell capture samples sampled in 2003 from "fluff" layers at the floor and bottom waters of Lake El'gygytgyn. Samples were injected onto Sterivex filters and treated with paraformaldahyde and dilute ethanol. Lz1029 has approximately the same location as PG-1351 from 1998.*

sample ID	core location ID	position		date	water depth (m)
		latitude	longitude		
E03BG76	Lz1029-1	67°30.37' N	172°08.23' E	25-7-03	177
E03BG78	Lz1029-2	67°30.37' N	172°08.23' E	25-7-03	177
E03BG80	Lz1029-2	67°30.37' N	172°08.23' E	25-7-03	177
E03BG81	Lz1029-3	67°30.37' N	172°08.23' E	25-7-03	177
E03BG164	Lz1032-2	67°29.00' N	172°07.37' E	30-7-03	159
E03BG165	Lz1033-2	67°30.99' N	172°08.01' E	30-7-03	164
EO3BG166	Lz1040-1	67°28.98' N	172°02.02' E	31-7-03	167
E03BG167	Lz1040-1	67°28.98' N	172°02.02' E	31-7-03	167
E03BG175	Lz1046	67°30.01' N	171°59.98' E	02-8-03	151

4.7 Modern Sedimentation

4.7.1 Particle Settling Through the Water Column

(O. Juschus, M. Melles, V. Wennrich, S. Quart, A. Dehnert)

Introduction – First investigations of the modern particle settling through the water column of Lake El'gygytgyn were carried out during the expedition in 2000. On that expedition a rope with 3 sediment traps was deployed and retrieved 17 days later. Selected results from this experiment were published by Cremer & Wagner (2003).

Methods – In 2003, two ropes, both with 6 sediment traps, were deployed during the spring campaign in the southwestern and southeastern part of the lake basin (Fig. 32). Each sediment trap consisted of a base plate made of plastic with a steel rod to fix the trap in vertical position at the rope (Fig. 33). At this plate four plastic tubes with a diameter of 46 mm were screwed. The rope was anchored at the lake bottom with a bag filled with pebbles and kept up in the water column by buoys fixed beneath the base of the lake ice.

After lake ice melt only the southwestern rope was found, recovered and deployed again. The northeastern rope was lost by unknown reason. Unfortunately, a similar failure happened to the southwestern rope after its

second deployment. This was the worst wastage during the expedition. In consequence, only 6 samples were retrieved from the sediment traps (Table 25). From the four tubes from each sample two were meant for sedimentology, one for biomarker and the last one for diatom analyses. The samples for sedimentological analyses were filtered with pre-weighed glass-fibre filters and dried for mass determination and further analyses.

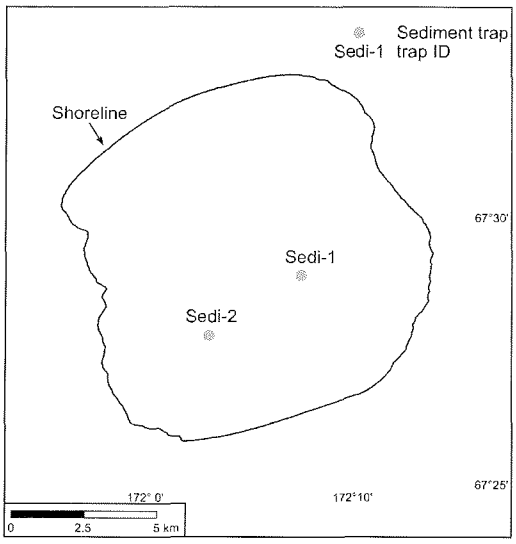

Figure 32: *Location of the sediment traps deployed in Lake El'gygytgyn in 2003.*

First results – As expected, the settling recorded in each sediment trap was very low (Table 26). Relatively small differences in the results between the traps, ranging from 2.20 to 3.77 g/m^3, indicate a simple, vertical settling of the material through the water column, without significant horizontal sediment flux during the lake ice and snow melt. Further analyses on the material will supply important information concerning the modifications of, for instance, the grain-size distributions and the organic versus inorganic contents, in the sediments on their way settling through the water column.

Table 25: *Sediment traps deployed and recovered in Lake El'gygytgyn in spring and summer 2003.*

site ID	water depth (m)	position latitude	position longitude	trap ID	trap depth (m)	date deployed	date recovered
Sedi-1	156.0	67°29.02' N	172°07.59' E	06	10.0	05-31-03	-
				05	30.0	05-31-03	-
				04	50.0	05-31-03	-
				03	90.0	05-31-03	-
				02	130.0	05-31-03	-
				01	146.0	05-31-03	-
Sedi-2	153.0	67°27.90' N	172°03.14' E	02	10.0	05-31-03	07-19-03
				05	30.0	05-31-03	07-19-03
				04	50.0	05-31-03	07-19-03
				03	90.0	05-31-03	07-19-03
				06	130.0	05-31-03	07-19-03
				01	146.0	05-31-03	07-19-03
				02	10.0	07-19-03	-
				05	30.0	07-19-03	-
				04	50.0	07-19-03	-
				03	90.0	07-19-03	-
				06	130.0	07-19-03	-
				01	146.0	07-19-03	-

Figure 33: *Field work with the sediment traps; Left: detailed view of a trap; Right: deployment during the spring campaign on May 31, 2003.*

Table 26: *Sediment settled through the water column at site Sedi-2 between 05-31-2003 and 07-19-2003.*

sample ID	trap ID	water depth (m)	settling (g/m²)
SF-3	trap 2	10	3.77
SF-5	trap 5	30	2.61
SF-4	trap 4	50	3.02
SF-2	trap 3	90	3.36
SF-6	trap 6	130	2.20
SF-1/1	trap 1/I	143	3.18
SF-1/2	trap 1/II	like SF-1/1	
		average:	3.02

4.7.2 Surface Sediments

(A. Dehnert, J. Brigham-Grette, O. Juschus, M. Melles, P. Minyuk)

During the summer campaign 2003 we were able to recover undisturbed surface sediment samples at 54 sites in Lake El'gygytgyn (Fig. 34, Table 27). The sample set is completed by the surface sample Lz1024-1 that was cored in spring 2003 (cp. Chapter 6.1.1, p. 110).

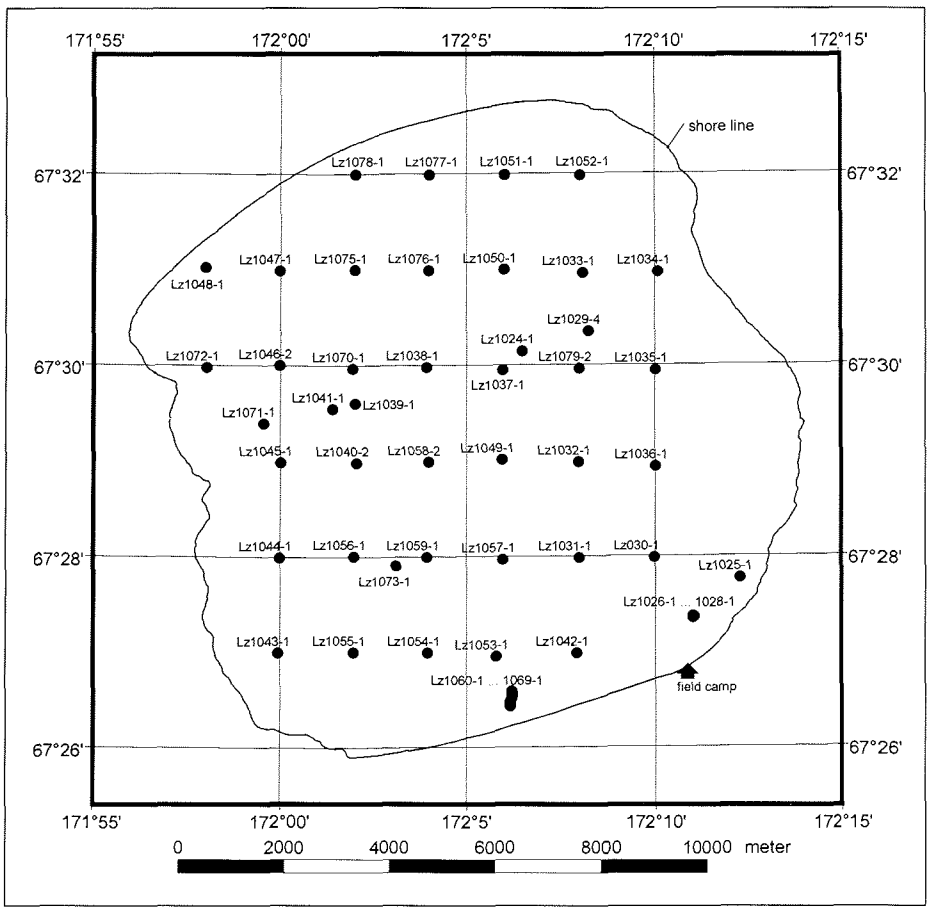

Figure 34: *Positions of sediment surface samples collected from Lake El'gygytgyn in 2003.*

Table 27: *List of surface sediment samples collected from Lake El'gygytgyn in 2003.*

core ID	position		water depth	date
	latitude	longitude	(m)	
Lz1024-1	67°30.162' N	172°06.462' E	169.0	05-16-03
Lz1025-1	67°27.798' N	172°12.255' E	6.3	07-23-03
Lz1026-1	67°27.388' N	172°11.041' E	8.0	07-23-03
Lz1026-1	67°27.388' N	172°11.041' E	8.0	07-23-03
Lz1027-1	67°27.395' N	172°11.007' E	10.5	07-24-03
Lz1028-1	67°27.378' N	172°11.003' E	8.2	07-24-03
Lz1029-4	67°30.372' N	172°08.238' E	167.5	07-25-03
Lz1030-1	67°28.007' N	172°09.991' E	129.1	07-30-03
Lz1031-1	67°28.000' N	172°08.000' E	138.0	07-30-03
Lz1032-1	67°29.002' N	172°07.975' E	158.7	07-30-03
Lz1033-1	67°30.982' N	172°08.092' E	164.2	07-30-03
Lz1034-1	67°30.995' N	172°10.094' E	151.5	07-30-03
Lz1035-1	67°29.971' N	172°10.014' E	157.6	07-30-03
Lz1036-1	67°28.960' N	172°10.010' E	150.5	07-30-03

continuation next page

Table 27: *continuation*

core ID	position		water depth (m)	date
	latitude	longitude		
Lz1037-1	67°29.961′ N	172°05.960′ E	170.0	07-30-03
Lz1038-1	67°29.989′ N	172°03.927′ E	172.0	07-30-03
Lz1039-1	67°29.601′ N	172°02.012′ E	166.0	07-30-03
Lz1040-2	67°28.987′ N	172°02.045′ E	162.0	07-30-03
Lz1041-1	67°29.550′ N	172°01.404′ E	162.0	08-01-03
Lz1042-1	67°27.004′ N	172°07.918′ E	162.0	08-07-03
Lz1043-1	67°27.001′ N	171°59.951′ E	122.0	08-02-03
Lz1044-1	67°27.998′ N	171°59.994′ E	136.0	08-02-03
Lz1045-1	67°28.990′ N	172°00.007′ E	146.0	08-02-03
Lz1046-2	67°30.006′ N	171°59.978′ E	151.0	08-02-03
Lz1047-1	67°30.999′ N	171°59.980′ E	136.5	08-02-03
Lz1048-1	67°31.034′ N	171°58.000′ E	105.0	08-02-03
Lz1049-1	67°29.029′ N	172°05.937′ E	170.5	08-03-03
Lz1050-1	67°31.016′ N	172°05.994′ E	165.3	08-03-03
Lz1052-1	67°32.002′ N	172°08.028′ E	120.0	08-03-03
Lz1052-1	67°32.002′ N	172°08.028′ E	120.0	08-03-03
Lz1051-1	67°32.002′ N	172°06.011′ E	143.0	08-03-03
Lz1053-1	67°26.969′ N	172°05.790′ E	126.6	08-04-03
Lz1054-1	67°26.999′ N	172°03.971′ E	141.3	08-04-03
Lz1055-1	67°27.005′ N	172°01.975′ E	141.0	08-04-03
Lz1056-1	67°28.009′ N	172°01.979′ E	155.2	08-04-03
Lz1057-1	67°27.982′ N	172°05.964′ E	152.0	08-06-03
Lz1058-2	67°28.998′ N	172°03.979′ E	165.6	08-06-03
Lz1059-1	67°27.999′ N	172°03.946′ E	158.6	08-06-03
Lz1060-1	67°26.450′ N	172°06.152′ E	7.8	08-06-03
Lz1061-1	67°26.452′ N	172°06.153′ E	8.7	08-06-03
Lz1062-2	67°26.458′ N	172°06.155′ E	11.5	08-06-03
Lz1062-1	67°26.458′ N	172°06.155′ E	11.5	08-06-03
Lz1063-1	67°26.473′ N	172°06.148′ E	18.8	08-06-03
Lz1064-1	67°26.479′ N	172°06.151′ E	28.2	08-06-03
Lz1064-3	67°26.479′ N	172°06.151′ E	28.2	08-06-03
Lz1065-1	67°26.496′ N	172°06.149′ E	34.6	08-06-03
Lz1066-1	67°26.529′ N	172°06.182′ E	55.2	08-06-03
Lz1067-1	67°26.542′ N	172°06.200′ E	67.0	08-06-03
Lz1068-1	67°26.573′ N	172°06.208′ E	84.4	08-06-03
Lz1069-1	67°26.604′ N	172°06.184′ E	96.8	08-06-03
Lz1070-1	67°29.970′ N	172°01.936′ E	160.9	08-07-03
Lz1071-1	67°29.402′ N	171°59.549′ E	138.0	08-08-03
Lz1072-1	67°29.987′ N	171°58.033′ E	118.5	08-08-03
Lz1073-1	67°27.915′ N	172°03.114′ E	161.0	08-08-03
Lz1075-1	67°31.003′ N	172°02.000′ E	152.2	08-18-03
Lz1076-1	67°31.004′ N	172°03.982′ E	163.4	08-18-03
Lz1077-1	67°32.000′ N	172°04.011′ E	136.4	08-18-03
Lz1078-1	67°32.001′ N	172°02.015′ E	127.4	08-18-03
Lz1079-2	67°29.981′ N	172°07.994′ E	166.0	08-19-03

The scientific goal behind this work is to obtain information about local differences in the physical, sedimentological, chemical, and biological characteristics of the surface sediments of Lake El'gygytgyn in dependence on regional differences in sediment supply from the catchment and lake-internal bioproduction and sediment transport. For this purpose, the bulk densities, grain-size distributions and mineralogies in the bulk sediment and clay fraction will be determined. Geochemical analyses comprise measurements of total inorganic carbon (TIC), total organic carbon (TOC), total nitrogen (TN), and

total sulphur (TS) contents. Biological analyses will focus on the investigation of the diatom and pollen assemblages and concentrations. The understanding of local differences in the surface sediment composition today will provide useful information for the interpretation of longer sediment records from the lake that are used for the reconstruction of long-term climatic and environmental changes in NE Siberia.

The location of most coring sites corresponds with the map grid, using distances of one minute in north-south direction and two minutes in west-east direction. Shallower parts of the lake basin, i.e., the shelf, were not included in this grid, due to difficulties associated with the sampling of the very coarse-grained deposits usually occurring in these regions. Some shelf samples, however, are available from a transect crossing the shelf edge in the southern lake part (Lz1060-1 to Lz1069-1, Fig. 34), and from three sites in the southeastern lake part (Lz1026-1 to Lz1028-1, Fig. 34), where clay patches near the shelf edge have been observed. Coring was carried out from a floating platform (3.6 x 2.8 m, UWITEC Corp.) by a gravity corer (UWITEC Corp.) that is equipped with a PVC liner of 60 cm length and 6 cm diameter, and with a tennis ball as core catcher (Fig. 35 left). The coring device has a total weight of ca. 20 kg. In Lake El'gygytgyn, up to 43 cm long surface sediment cores were recovered using this gear. After recovery, attention was paid that the sediment surface inside the liner was horizontally embedded and that the superstanding water was free of suspension load (Fig. 35 right). Once on bord, the catcher was replaced by a plunger and the liner disconnected from the corer for a better handling. The sediment then was pushed by the plunger slowly towards the liner top, where a 2 cm thick sample from the surface sediment was separated by a sediment cutter. Finally, the samples were stored in pre weighted 50 ml PE vials at dark and cool (±4°C) conditions in order to minimize biological and chemical reactions.

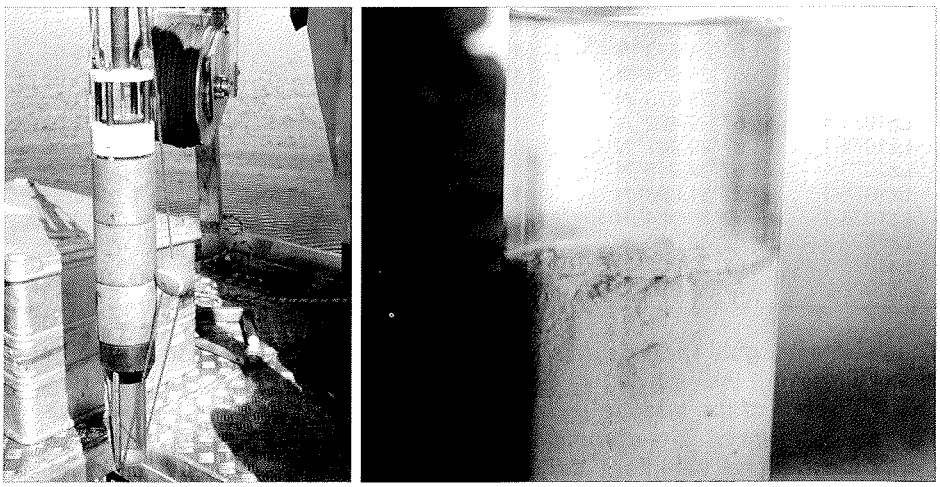

Figure 35: *Left: UWITEC gravity corer with tennis ball catcher and 3 additional weights (each ca. 5 kg). The corer is connected to the winch in the background (300 m x 5 mm steel cable). Right: fluffy sediment surface from core Lz1078-1. Note the horizontal embedding of the surface and the clear superstanding water.*

4.8 Gas Mercury Survey in the El'gygytgyn Crater

(G. Fedorov, A. Kupolov)

4.8.1 Introduction

This survey was aimed at the investigation of the recent fault activity in the lake surroundings (Fig. 36). It is known that mercury anomalies in soil air are accompanying active fault zones and, in this case, do not depend on other environmental factors (Fursov, 1977). The absence of increased concentrations of mercury vapour can only be interpreted with the isolation of these zones. That indicates the current inactivity of faults. This allows to infer fault activity from the measured mercury vapour concentration in the soil air.

4.8.2 Methods and Field Work

The entire lake catchment and its surroundings were too large to be encompassed by the survey in one field season. Hence, the authors had to determine a key location for a detailed survey feasible in the available time. The area chosen is located in the southeastern part of the lake catchment and in the upper reaches of the Enmyvaam River (Fig. 37). The decision for this area is based on the results of the tectonic framework reported by other researchers and our own previous field and airborne observations. In the selected area faults occur along the fault zone bordering the outer and inner parts of the Okhotsk-Chukotka Volcanic Belt (Belyi and Raikevich, 1994). This zone is crossing the lake depression from NE to SW (Fig. 36). The lake depression itself is located within the Malyi-Chaun graben. The faults associated with this graben structure are running NW-SE.

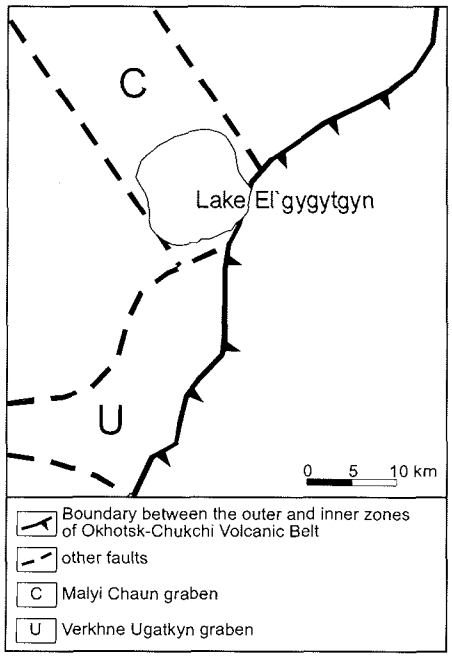

Figure 36: *The location of the El'gygytgyn depression in relation to the local tectonics (after Belyi and Raikevich, 1994).*

The method used at Lake El'gygytgyn was first tried in 1996 for the same purpose in the region of Lake Levinson-Lessing (Taymyr Peninsula) during the field campaign of the Russian-German "Taymyr" project (Antonov, 1997). These data were interpreted to infer the contemporary tectonics of Central Taimyr (Fedorov et al., 2001).

In the present study, we used the portable gas-mercury analyser AGP-01 manufactured 1991 in Yekaterinburg, Russia. It is 12-V-charged by alkali accumulator batteries. This device measures Hg-concentrations in air from 1.0 x 10^{-9} to 9.9999 x 10^{-5} mg/l.

The volume of analysed air may be switched over between 0.5, 1.0, 5.0, and 10.0 l. The error in measurement is equal to ca. 10 %. The limit of systematic error is 30 % of the measured parameter.

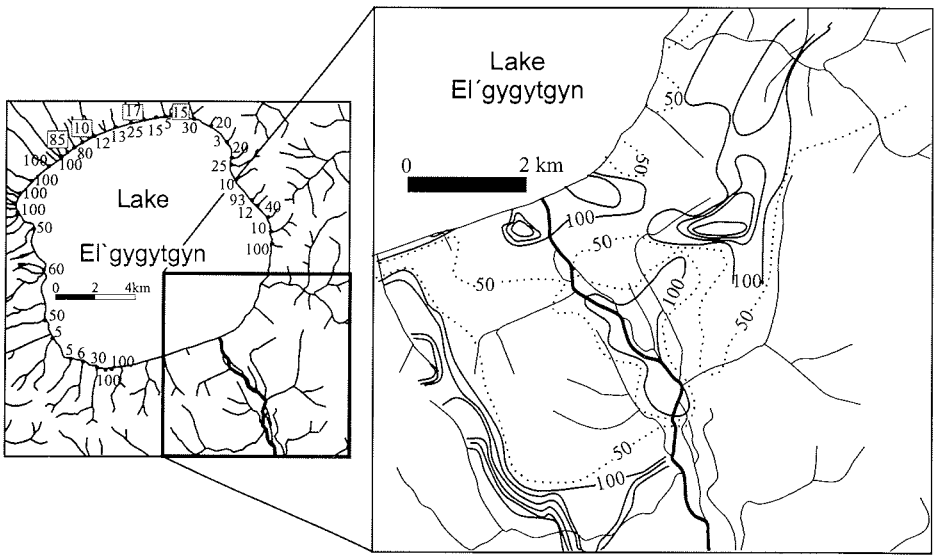

Figure 37: *Mercury concentration in soil air at the mouth areas of the inlet streams and in the southeastern part of the lake depression; main isolines are drawn every 100 ppm, additional ones every 50 ppm.*

4.8.3 Results

The results of the gas-mercury survey indicate ongoing activity of the fault systems mentioned above. As previously concluded from studying the topographic maps and satellite images, there are three principal lineament systems in the area, controlling the local hydrography. These systems are NW-SE-striking (controlling the Enmyvaam valley), NE-SW-striking (following the southern shoreline and the Chivirynnet river valley to the east of the lake) and radially stretching from the lake.

The NW-SE- and NE-SW-striking systems form linear areas, which can be traced along large distances suggesting a regional character of these zones. The hydrographic network largely follows them and implies a recent activation of the two corresponding fault systems.

This activation is documented in the structure of the 10 m lacustrine terraces of Lake El'gygytgyn. Whilst in the eastern part of the lake all terraces are abrasional, those at other shores are accumulative. Alongshore from southeast to southwest the basement of the 10 m terrace level becomes increasingly fractured. Simultaneously, the accumulative cover becomes thicker and more fine-grained. To the northeast of the Lagerny Creek mouth (inlet no. 49, Fig. 23,

p. 50) the 10 m terrace is completely abrasional, but 1.5 km to the south of the mouth fractured basement is overlain by a 4 m thick layer of poorly sorted material. Further to the west, at the opposite side of Enmyvaam Valley, the same terrace level is totally built up of sediments, with the base of the sediment layer being located below the lake level.

The mercury concentration in soil air was measured at 158 points, especially in the southeastern part of the lake depression. The average value of mercury concentration in the study area is 98.2 ppm. Nonetheless, the discrepancy of values is quite high, ranging from 3 up to 600 ppm. The measured concentrations were mapped using isolines (Fig. 37), whose distribution forms notable elongated anomalies stretching NW–SE and NE–SW. These directions coincide, firstly, with the border between the two zones of Okhotsk-Chukotka volcanic belt and, secondly, with the Malyi-Chaun graben faults (Fig. 36).

It is worth mentioning that no notable mercury concentrations have been found along the faults running radially around the lake. This might be due to their "rootless" nature that would, in turn, favour the hypothesis of a meteoritic origin of the lake depression. Similarly, the values measured in the Enmyvaam river valley are very low. This is surprising, because it is clear that this valley is situated inside a large fault zone striking NW–SE. Perhaps this finding can be explained by the large thickness of loose, unconsolidated and porous sediments in the valley, allowing the mercury vapour to escape.

5 GEOMORPHOLOGY, GEOCRYOLOGY AND STRATIGRAPHY

5.1 Enmyvaam River

(O. Glushkova, V. Smirnov, P. Minyuk)

5.1.1 Introduction

Complex geological-geomorphological investigations were carried out in the Mechekrynnetveem Basin, about 20 km to the south of Lake El'gygytgyn. This basin stretches along a distance of 25 km around the mouth of the Mechekrynnetveem River into Enmyvaam River (Fig. 38). The Enmyvaam River on its way to the south crosses the northern and southwestern margin of the basin.

In that part of the Mechekrynnetveem Basin, where the southern course of the Enmyvaam River changes into a more westerly one (Fig. 38), fragments of alluvial terraces were mapped (see also Fig. 4, p. 18). Three natural outcrops, being situated along the left bank of the Enmyvaam River in a distance of about 2 km to each other, were investigated during the expedition in 2003 (points GS-2203, GS-2303 and GS-2403). Their heights were measured, ranging from 18 to 22 m, and the composition and structure of outcropping sediments were studied from the top down to the bottom.

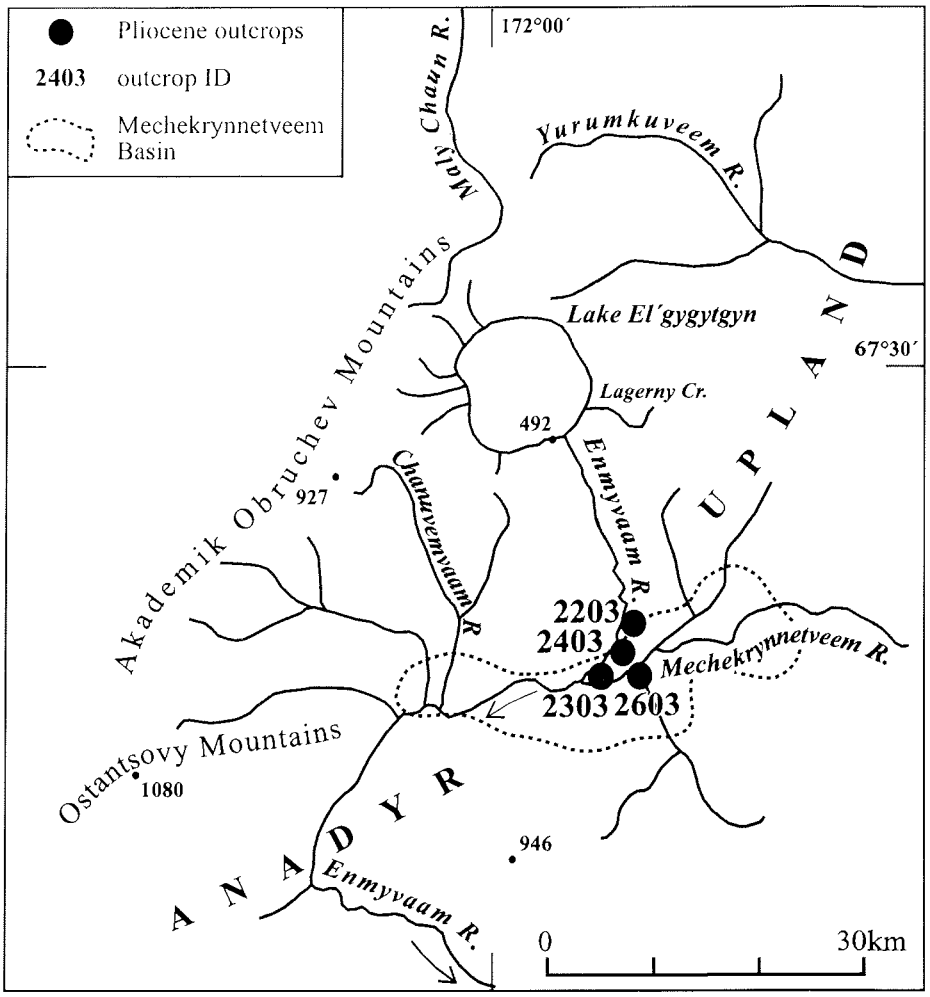

Figure 38: *Locations of outcrops with Pliocene sediments at Enmyvaam River.*

5.1.2 First Results

Summaries of the outcrop descriptions and correlations, along with information on sampling for palynological for lithological, carpological and paleomagnetic investigations, are presented in Figures 39 to 48. Full lists of pollen and radiocarbon samples are provided in Tables 28 and 29, respectively.

At each outcrop major horizons were discovered, which mark sharp changes in the ancient depositional environmental conditions, in particular in the processes of sediment transport into the Mechekrynnetveem Basin. The base of the sediments, mapped in a profile along the Enmyvaam River (e.g., Fig. 43), range

in heights from 1 to 7.2 m above the modern riverbed. Everywhere the bedrock is represented by weathered rocks, with the weathering level ranging from physical fragmentation to structural/chemical weathering crusts.

The outcrops illustrated in Figures 39 to 48 supply a comprehensive understanding of the general lithostratigraphy along the western border of the Mechekrynnetveem Basin (from bottom to top):

1. The bedrock is represented by granodiorite-porphyries, basalts, andesites and mudstones. Despite the occurrence of a weathering crust the primary petrographic structures are still preserved.

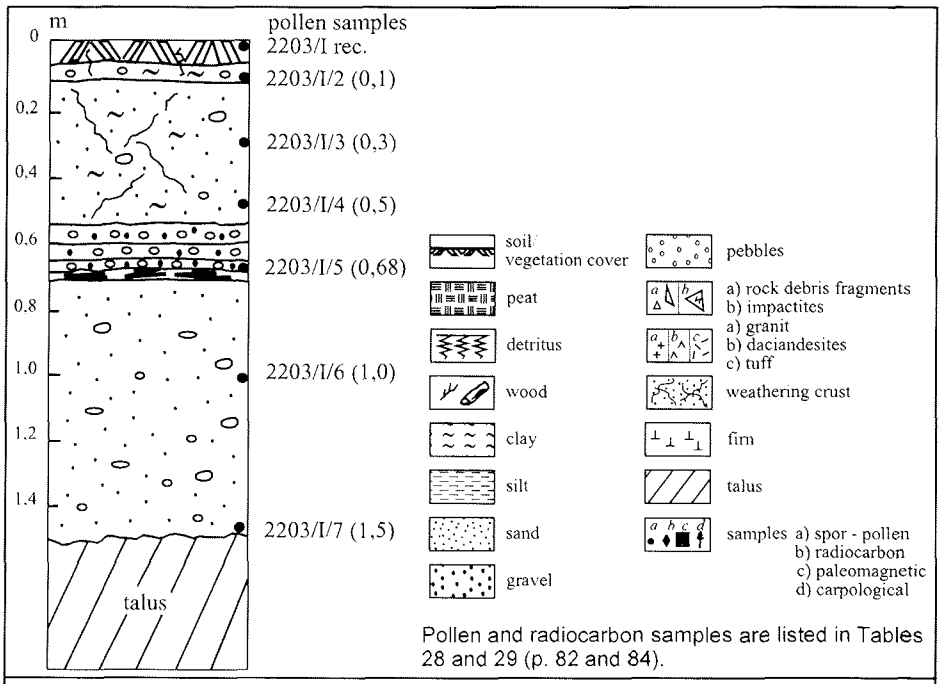

Pollen and radiocarbon samples are listed in Tables 28 and 29 (p. 82 and 84).

section: GS-2203/I
location: left side of Enmyvaam River, ca.5.3 km upstream of the Mechekrynnetveem River mouth
bluff, 20 m high, uppermost part

unit	depth (m)	description
1.	0.00 - 0.05	soil, vegetation cover, sandy gravel, reddish brown, many roots
2.	0.05 - 0.10	pebbles, sandy-loamy matrix, light grey, rare roots, permafrost deformations
3.	0.10 - 0.54	loess-like loam, rare pebbles and gravel, light grey, pellet-like structure, permafrost traces
4.	0.54 - 0.68	small/medium pebbles, sandy gravelly matrix, greyish yellow, gouges on the pebbles
5.	0.68 - 0.70	paleosoil, humus, reddish brown, rare pebbles
6.	0.70 - 1.50	small/medium pebbles, friable, sandy gravelly matrix, brownish grey, gouges on the pebbles
7.	1.50 - 5.80	talus (continuation Fig. 41)

Figure 39: *Sediment section GS-2203/I.*

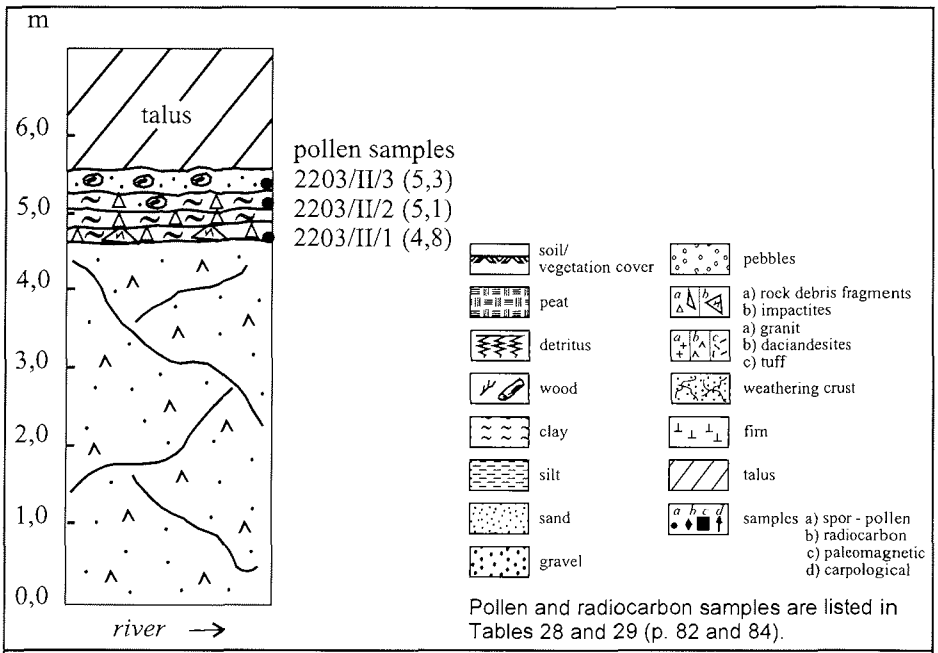

section: GS-2203/II
location: left side of Enmyvaam River, ca.5.3 km upstream of the Mechekrynnetveem River mouth
bluff, 20 m high, lower part

unit	depth (m)	description
1.	7.00 - 5.55	talus
2.	5.55 - 5.25	pebbles, yellowish grey, sandy clayey matrix
3.	5.25 - 5.05	pebbles, yellowish grey, sandy clayey matrix, rock fragments, thin lenses (1 - 2 cm) of fine sand, yellowish, pebbles and fragments are very angular and splintered
4.	5.05 - 4.85	rock fragments and pebbles, dark grey, sandy clayey matrix
5.	4.85 - 4.60	tuff breccia, strongly crushed into fragments with impact pumice and glasses ("chaotic horizon"), sandy clayey matrix, dark grey
6.	4.60 - 0.00	bedrock basement, tuff breccia of andesidacite, strongly crushed

Figure 40: *Sediment section GS-2203/II.*

2. The bedrock is overlain by pebbles, obliquely laminated sands (lenses and beds up to 1 m thick) and/or vegetation detritus. These sediments usually have thicknesses between 1 and 3.5 m.

3. The following "chaotic horizon" contains inclusions of large angular blocks, singular boulders, rock fragments of different petrographic composition, singular pebbles, detritus, sand and gravel without any bedding. The matrix is clayey, usually with a grey, often spotted colour. Impact fragments, like impact glasses, pumice and sintered breccia, sometimes up to 20 cm in diameter, occur within the horizon. The content of impactites at several outcrops reaches about 10 % of all rock fragments.

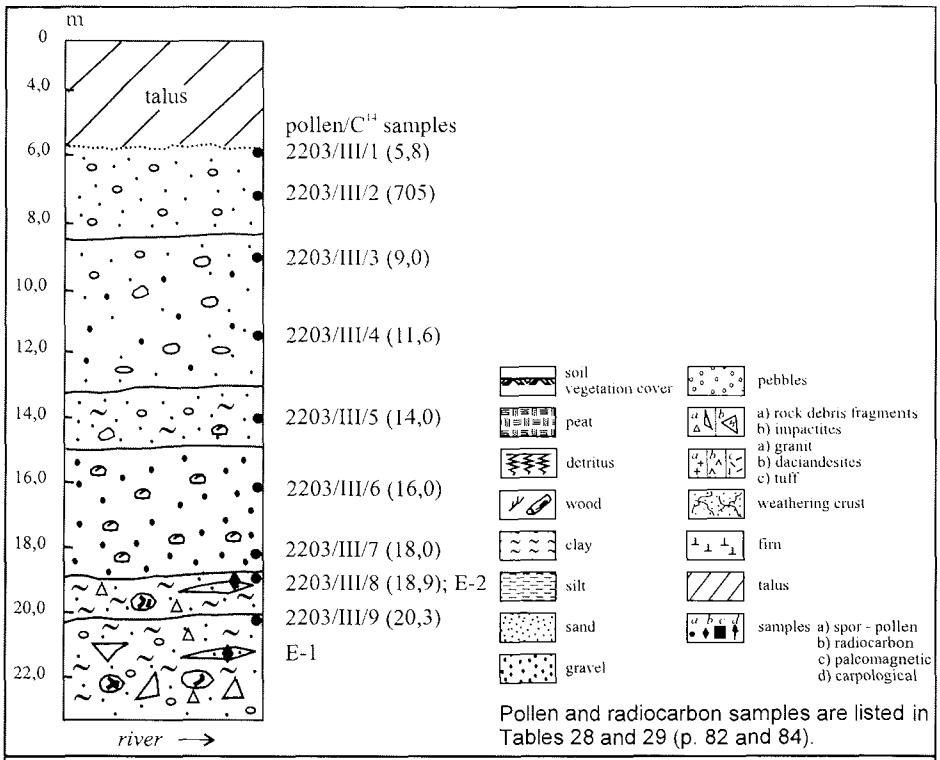

Pollen and radiocarbon samples are listed in Tables 28 and 29 (p. 82 and 84).

section: GS-2203/III
location: left side of Enmyvaam River, ca.5.3 km upstream of the Mechekrynnetveem River mouth
bluff, 20 m high, middle part

unit	depth (m)	description
7.	1.5 - 5.8	talus (cp. Fig. 39)
8.	5.8 - 8.4	small/medium pebbles, friable, sandy gravelly matrix, yellowish brown
9.	8.4 - 13.2	small/medium pebbles, well rounded, coarse sandy, gravelly matrix, dark grey (moist)/ greyish blue (dry)
10.	13.2 - 15.0	like no. 9, additionally gouges on the pebbles
11.	15.0 - 18.3	medium pebbles, gravelly matrix, reddish brown, rare gouges
12.	18.3 - 18.9	transition horizon between pebbles and redeposited weathering crust, pebbles, grey, sandy-loamy and friable matrix, at the bottom sand lenses, yellowish green
13.	18.9 - 20.3	sandy loam, greyish red, rock fragments (various petrographic composition), at the bottom sand lenses
14.	20.3 - 23.0	sandy clayey loam, greyish red, some pebbles, boulders and rock fragments

Figure 41: *Sediment section GS-2203/III.*

4. The "chaotic horizon" is overlain by a more or less thick pebble cover. This cover mostly it is coarse layered within a sandy and gravelly matrix. The majority of pebbles is yellowish grey. In this horizon calcified fragments of large trees were often found. In addition, sand lenses or vegetation detritus occur, but relatively seldom.

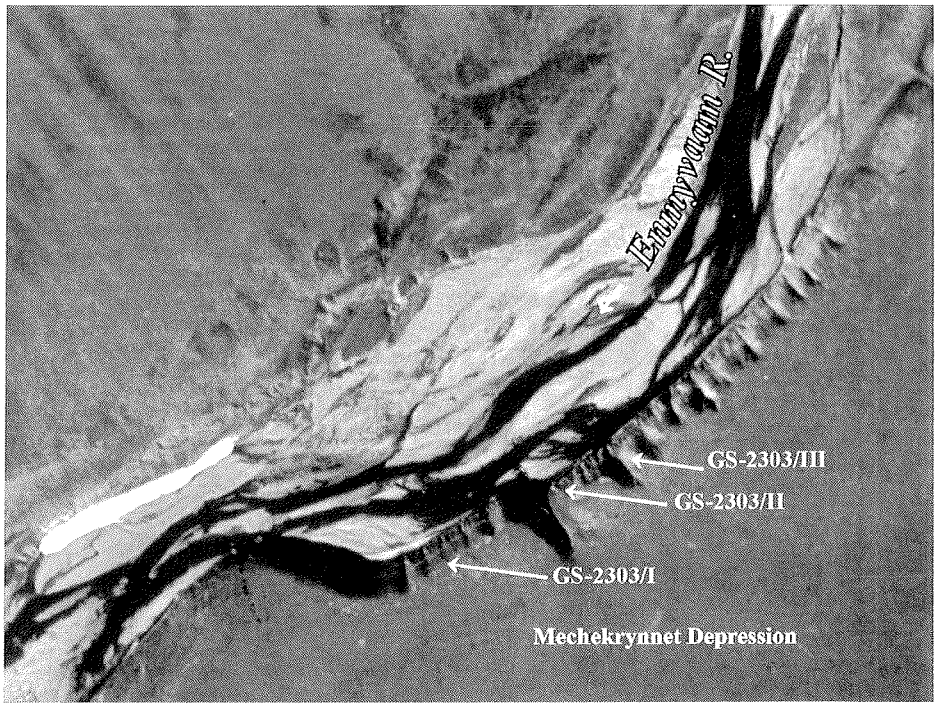

Figure 42: *Aerial view of the outcrop location GS-2303 at the Enmyvaam River.*

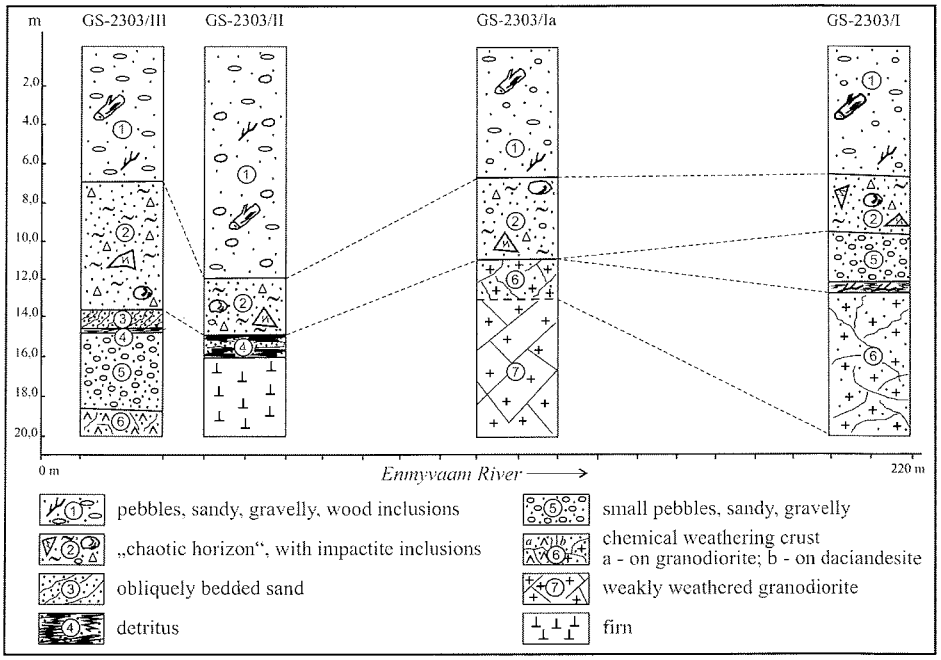

Figure 43: *Correlative scheme of section GS-2303.*

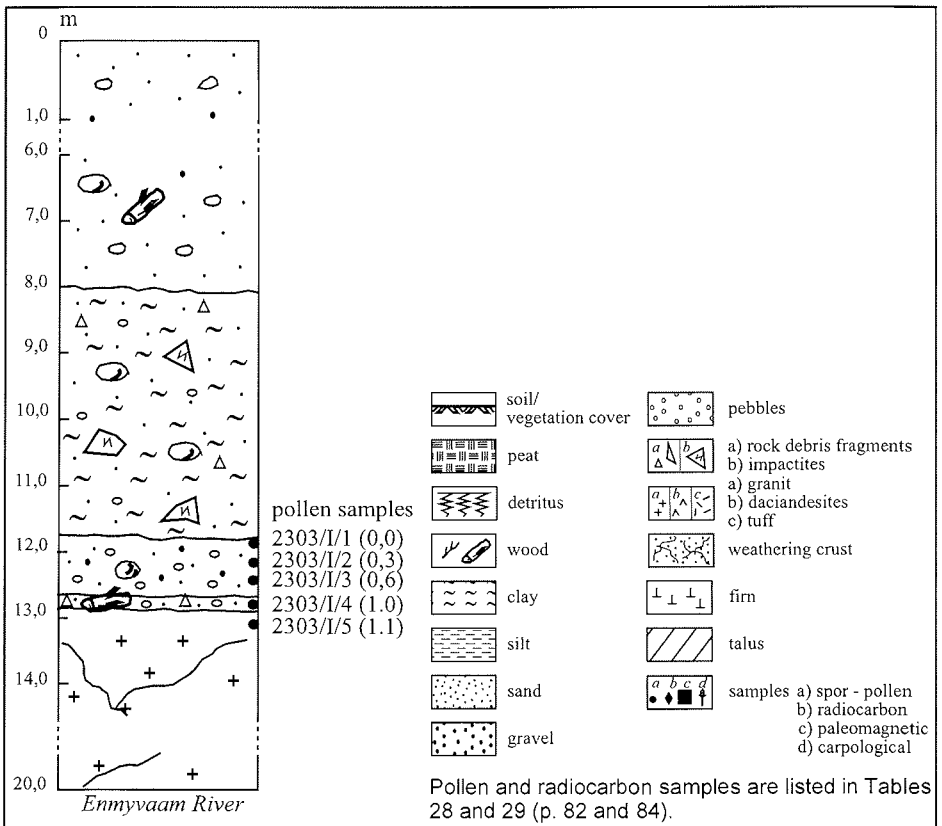

section: GS-2303/I
location: left side of Enmyvaam River, ca.1.8 km upstream of the Mechekrynnetveem River mouth
bluff, 22 m high, complete profile

unit	depth (m)	description
1.	0.0 - 8.0	sandy gravel, greyish yellow, well rounded pebbles, fragments of calcified wood
2.	8.0 - 11.8	"chaotic horizon", loam, spotted, greyish violet - pink, partly weathered rock fragments, pebbles and rock debris, impact pumice and glasses
3.	11.8 - 12.7	sandy gravel, yellowish grey, well rounded pebbles, rare rock fragments
4.	12.7 - 12.8	contact zone, weathering crust - sandy gravel, well rounded pebbles, rare rock fragments, fragments of calcified wood
5.	12.8 - 20.0	"structural" weathering crust (weathering along joints, fissures etc.) within biotite granodiorite/ porphyry

Figure 44: *Sediment section GS-2303/I.*

5. A developed paleosoil evidence rather stable conditions for a considerable time period which have interrupted the sedimentation of the pebble cover. Another soil-like interbed occurs within a loess-like loam, being of light grey colour with orange rust-like spots. The associated soil-vegetation layer has a thickness of about 10 - 15 cm.

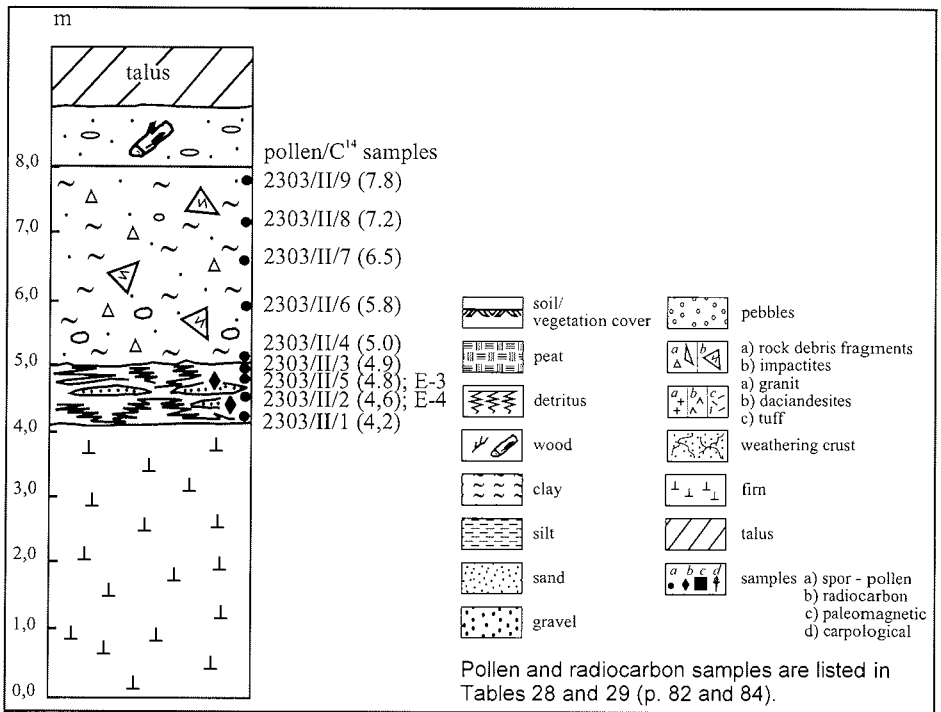

section: GS-2303/II
location: left side of Enmyvaam River, ca.1.8 km upstream of the Mechekrynnetveem River mouth
bluff, 22 m high, lower part

unit	depth (m)	description
1.	10.0 - 8.9	talus, pebbles, sandy gravelly matrix, fragments of calcified wood
2.	8.9 - 7.9	pebbles, sandy gravelly matrix, fragments of calcified wood
3.	7.9 - 5.7	"chaotic horizon", loam, spotted, greyish violet, partly weathered rock fragments (up to 0.5 m), pebbles and rock debris, impact pumice and glasses, often crushed into gravel and sand
4.	5.7 - 5.0	like no. 3, but more pebbles
5.	5.0 - 4.1	plant detritus, horizontal bedded roots and branches, some charred wood, lenses of sandy loam, yellowish grey, weathered minerals, orange
6.	4.1 - 0.0	firn

Figure 45: *Sediment section GS-2303/II.*

6. A mammoth tooth of a cainotypic nature was found at the outcrop GS-2203 (Fig. 49). It was situated in the upper part of the slope, about 15 m above the Enmyvaam River. This is the first finding of a mammoth fragment mentioned for this region. Further geochronological and paleontological studies will supply information on its age and possibly on the mammoth species.

These results from the northern flank of the Mechekrynnetveem Basin represent an essential addition to the results obtained during the past years. The investigations of the "chaotic horizon" testified the preliminary idea that this specific horizon with its unique properties was formed at once after the impact forming the El´gygytgyn Crater.

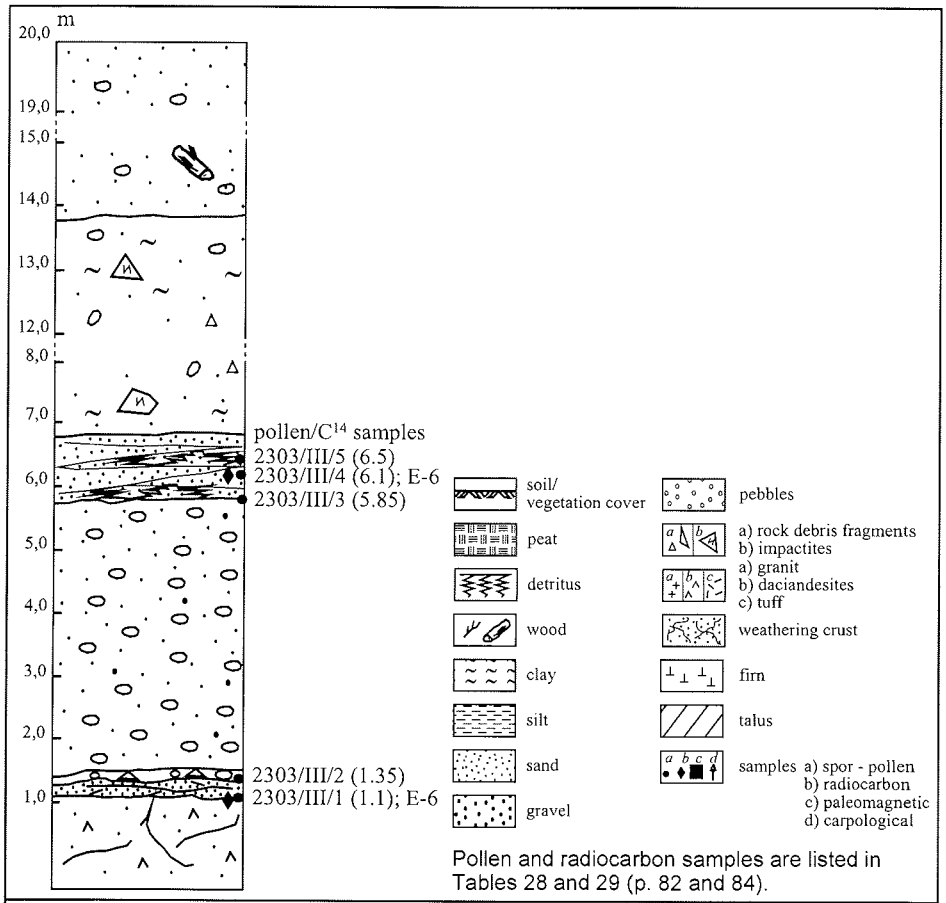

section: GS-2303/III
location: left side of Enmyvaam River, ca.1.8 km upstream of the Mechekrynnetveem River mouth
bluff, 22 m high, lower part

unit	depth (m)	description
1.	20.0 - 13.8	talus, pebbles, sandy gravelly matrix, greyish yellow, large tree fragments
2.	13.8 - 6.9	"chaotic horizon", loam, greyish violet, rock fragments (up to 0.5 m), pebbles and rock debris, impact pumice and glasses
3.	6.90 - 5.85	fine sand, mostly crossbedded, thin "interbed", humus lenses
4.	5.85 - 1.35	pebbles, sandy gravelly matrix, greyish red, coarse layering
5.	1.35 - 1.25	pebbles, sandy gravelly matrix, dark grey, angular rock fragments
6.	1.25 - 1.10	sand, bedded, rare pebbles
7.	1.10 - 0.00	"structural" weathering crust (weathering along joints, fissures etc.) within andesite/ andesidacite

Figure 46: *Sediment section GS-2303/III.*

During the impact, not only impactites but also rock fragments and blocks of various petrographic compositions were probably thrown out of the crater and/or transported during the impact-earthquake. Further on, melted rocks and pumice are present within the horizon.

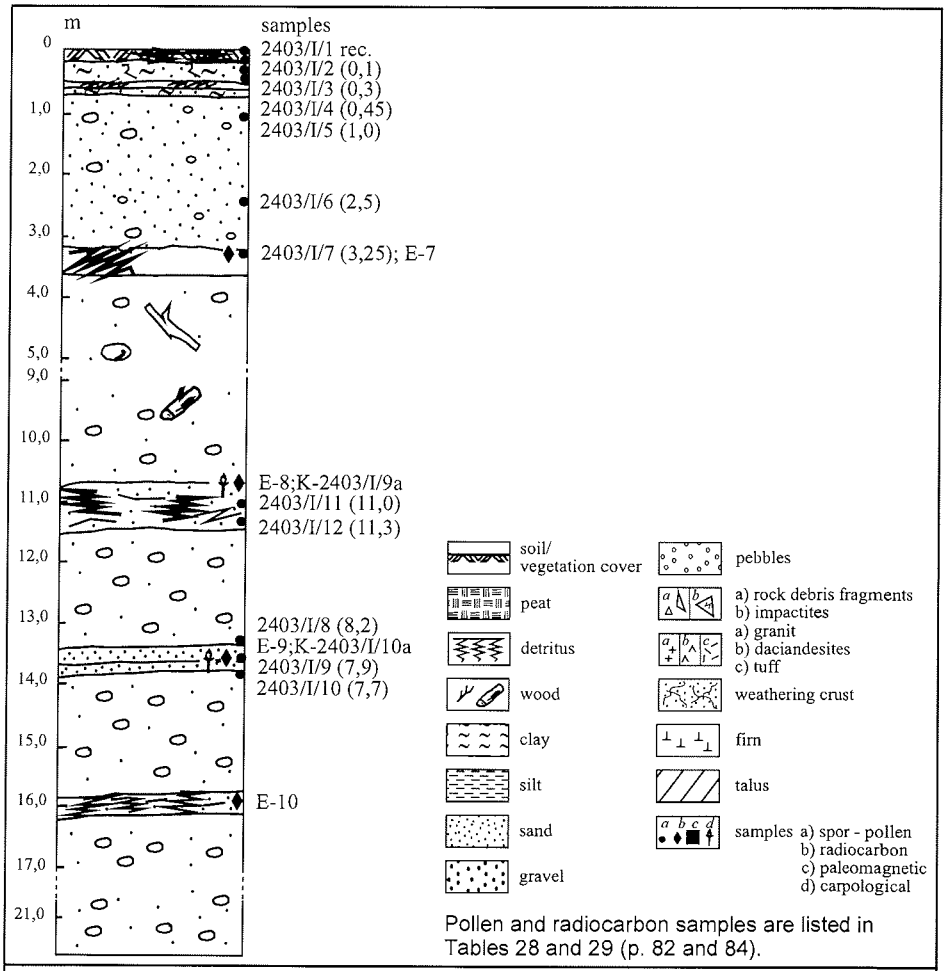

section: GS-2403/I
location: left side of Enmyvaam River, ca.2.3 km upstream of the Mechekrynnetveem River mouth
bluff, 20 - 22 m high, complete profile

unit	depth (m)	description
1.	0.00 - 0.12	soil, vegetation cover
2.	0.12 - 0.44	loess-like loam, pale yellow, modern roots
3.	0.44 - 0.52	paleosoil, humus loam, sandy, reddish brown, rare pebbles
4.	0.52 - 0.65	pebbles, yellowish brown, loamy matrix
5.	0.65 - 3.25	pebbles, sandy gravelly matrix, greyish yellow
6.	3.25 - 3.55	plant detritus, reddish brown
7.	3.55 - 10.7	talus, pebbles, sandy gravelly matrix, greyish yellow, large tree fragments
8.	10.7 - 11.5	plant detritus, sandy matrix
9.	11.5 - 13.4	pebbles, sandy gravelly matrix
10.	13.4 - 13.9	fine sand, some organic remains
11.	13.9 - 15.9	pebbles, sandy gravelly matrix
12.	15-9 - 16.2	plant detritus, sandy matrix
13.	16.2 - 21.5	pebbles, sandy gravelly matrix

Figure 47: *Sediment section GS-2403/I.*

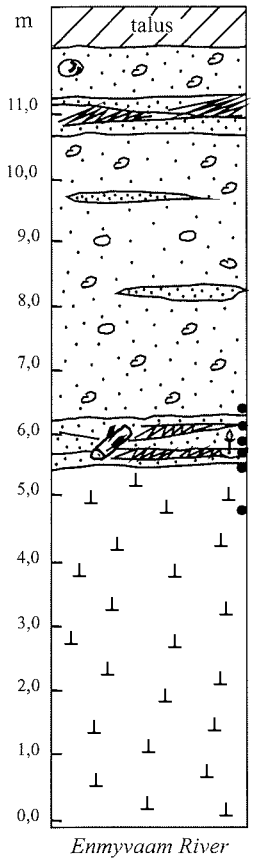

pollen/carpo-logical samples
2403/II/5 (16.0)
2403/II/4 (16,20)
2403/II/2 (16,55); K-3
2403/II/1 (16,80)
2403/1 rec.

soil/ vegetation cover
peat
detritus
wood
clay
silt
sand
gravel
pebbles
a) rock debris fragments
b) impactites
a) granit
b) daciandesites
c) tuff
weathering crust
firn
talus
samples a) spor - pollen
b) radiocarbon
c) paleomagnetic
d) carpological

Pollen and radiocarbon samples are listed in Tables 28 and 29 (p. 82 and 84).

section: GS-2403/II
location: left side of Enmyvaam River, ca.2.3 km upstream of the Mechekrynnetveem River mouth
bluff, 20 - 22 m high, lower part

unit	depth (m)	description
1.	12.5 - 12.0	talus
2.	12.0 - 11.3	talus, pebbles, sandy gravelly matrix, greyish yellow, coarse bedded, large calcified tree fragments
3.	11.3 - 10.7	fine sand, greyish yellow, interbedded with plant detritus, blackish brown, saturated with plant remnants
4.	10.7 - 6.15	pebbles, sandy gravelly matrix, greyish yellow, lenses and small beds of fine sand and plant detritus
5.	6.15 - 5.40	fine sand, greyish yellow, interbedded with plant detritus, blackish brown, horizontal/wavy bedding, tree fragments and branches
6.	5.40 - 0.00	firn (below water level: pebbles, sandy gravelly matrix, grey)

Figure 48: *Sediment section GS-2403/II.*

All this matter was sealed up with the clayey material transported and redeposited from the chemical weathering crust. The lesser but still significant occurrence of lenses and thin interbeds of fluvial sand and pebbles proves the existence of temporal water channels during the time of accumulation.

According to existing palynological data of Belyi and Raikevich (1994) units 2, 3, and 4 were formed during the lower part of the Upper Pliocene. This suggestion is supported by paleomagnetic data, which show predominantly normal polarity, probably related with the Gauss Chron, in the sediments of units 2 and 4.

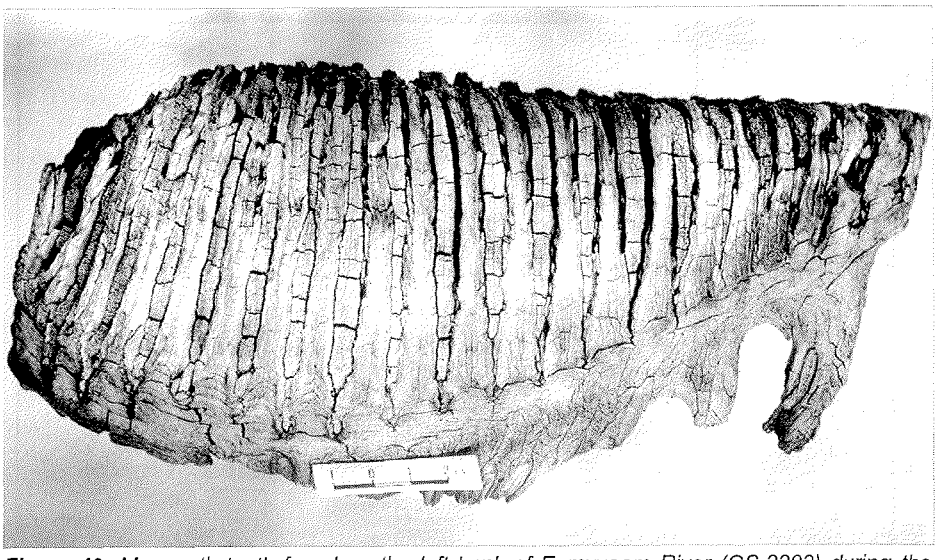

Figure 49: *Mammoth tooth found on the left bank of Enmyvaam River (GS-2203) during the expedition to Lake El'gygytgyn in summer 2003.*

Table 28: *Pollen samples from the Lake El'gygytgyn region taken during the expedition in summer 2003.*

no.	site ID	position		source	depth (m)
		latitude	longitude		
1	1-03	eastern slope of Geodetic peak		soil	surface
2	2-03	(g. Voennych Geodesistov)		soil	surface
3	3-03	same position		soil	surface
4	4-03	same position		soil	surface
5	5-03	same position		soil	surface
6	6-03	same position		soil	surface
7	7-03	same position		alluvial deposit	surface
8	8-03	67°26.896' N	172°13.287' E	soil	surface
9	9-03	67°26.837' N	172°13.291' E	soil	surface
10	10-03	67°28.029' N	172°14.537' E	soil	surface
11	11-03	67°28.029' N	172°14.537' E	soil	surface
12	14-03	67°25.172' N	172°11.615' E	soil	surface
13	15-03	67°23.995' N	172°13.274' E	soil	surface
14	16-03/1	67°26.449' N	172°13.138' E	soil	surface
15	16-03/2	67°26.449' N	172°13.138' E	alluvial deposit	surface
16	18-03	lake ice cover at the southern shore		aeolian deposit	surface
17	22-03/1/1	Enmyvaam river, Site		soil	surface
18	22-03/1/2	GS2203 (see Fig. 38, p. 72)		alluvial deposit	0.10
19	22-03/1/3	same position		alluvial deposit	0.30
20	22-03/1/4	same position		alluvial deposit	0.50

continuation next page

Table 28: *continuation*

no.	site ID	position		source	depth (m)
		latitude	longitude		
21	22-03/1/5	same position		alluvial deposit	0.68
22	22-03/1/6	same position		alluvial deposit	1.00
23	22-03/1/7	same position		alluvial deposit	1.50
24	22-03/2/3	same position		alluvial deposit	5.30
25	22-03/2/2	same position		alluvial deposit	5.10
26	22-03/2/1	same position		alluvial deposit	4.80
27	22-03/3/1	same position		alluvial deposit	5.80
28	22-03/3/2	same position		alluvial deposit	7.05
29	22-03/3/3	same position		alluvial deposit	9.00
30	22-03/3/4	same position		alluvial deposit	11.60
31	22-03/3/5	same position		alluvial deposit	14.00
32	22-03/3/6	same position		alluvial deposit	16.00
33	22-03/3/7	same position		alluvial deposit	18.00
34	22-03/3/8	same position		alluvial deposit	18.90
35	22-03/3/9	same position		alluvial deposit	20.30
36	23-03/1/1	67°14.426´ N	172°14.361´ E	alluvial deposit	0.00
37	23-03/1/2	67°14.426´ N	172°14.361´ E	alluvial deposit	0.30
38	23-03/1/3	67°14.426´ N	172°14.361´ E	alluvial deposit	0.60
39	23-03/1/4	67°14.426´ N	172°14.361´ E	alluvial deposit	1.00
40	23-03/1/5	67°14.426´ N	172°14.361´ E	alluvial deposit	1.10
41	23-03/II/9	67°14.426´ N	172°14.361´ E	alluvial deposit	7.80
42	23-03/II/8	67°14.426´ N	172°14.361´ E	alluvial deposit	7.20
43	23-03/II/7	67°14.426´ N	172°14.361´ E	alluvial deposit	6.50
44	23-03/II/6	67°14.426´ N	172°14.361´ E	alluvial deposit	5.80
45	23-03/II/5	67°14.426´ N	172°14.361´ E	alluvial deposit	5.00
46	23-03/II/4	67°14.426´ N	172°14.361´ E	alluvial deposit	4.90
47	23-03/II/3	67°14.426´ N	172°14.361´ E	alluvial deposit	4.80
48	23-03/II/2	67°14.426´ N	172°14.361´ E	alluvial deposit	4.60
49	23-03/II/1	67°14.426´ N	172°14.361´ E	alluvial deposit	4.20
50	23-03/III/5	67°14.426´ N	172°14.361´ E	alluvial deposit	6.50
51	23-03/III/4	67°14.426´ N	172°14.361´ E	alluvial deposit	6.10
52	23-03/III/3	67°14.426´ N	172°14.361´ E	alluvial deposit	5.85
53	23-03/III/2	67°14.426´ N	172°14.361´ E	alluvial deposit	1.35
54	23-03/III/1	67°14.426´ N	172°14.361´ E	alluvial deposit	1.10
55	24-03/I/1	67°14.854´ N	172°15.534´ E	alluvial deposit	surface
56	24-03/I/2	67°14.854´ N	172°15.534´ E	alluvial deposit	0.10
57	24-03/I/3	67°14.854´ N	172°15.534´ E	alluvial deposit	0.30
58	24-03/I/4	67°14.854´ N	172°15.534´ E	alluvial deposit	0.45
59	24-03/I/5	67°14.854´ N	172°15.534´ E	alluvial deposit	1.00
60	24-03/I/6	67°14.854´ N	172°15.534´ E	alluvial deposit	2.50
61	24-03/I/7	67°14.854´ N	172°15.534´ E	alluvial deposit	3.25
62	24-03/I/11	67°14.854´ N	172°15.534´ E	alluvial deposit	11.00
63	24-03/I/12	67°14.854´ N	172°15.534´ E	alluvial deposit	11.30
64	24-03/I/8	67°14.854´ N	172°15.534´ E	alluvial deposit	8.20
65	24-03/I/9	67°14.854´ N	172°15.534´ E	alluvial deposit	7.90
66	24-03/I/10	67°14.854´ N	172°15.534´ E	alluvial deposit	7.70
67	24-03/II/5	67°14.854´ N	172°15.534´ E	alluvial deposit	16.00
68	24-03/II/4	67°14.854´ N	172°15.534´ E	alluvial deposit	16.20
69	24-03/II/2	67°14.854´ N	172°15.534´ E	alluvial deposit	16.55
70	24-03/II/1	67°14.854´ N	172°15.534´ E	alluvial deposit	16.80
71	24-03/1	67°14.854´ N	172°15.534´ E	alluvial deposit	surface
72	26-03/1	67°14.537´ N	172°19.428´ E	weathering crust	0.20
73	26-03/2	67°14.537´ N	172°19.428´ E	weathering crust	0.30
74	26-03/3	67°14.537´ N	172°19.428´ E	weathering crust	0.50
75	26-03/4	67°14.537´ N	172°19.428´ E	weathering crust	0.75

continuation next page

Table 28: *continuation*

no.	site ID	position		source	depth (m)
		latitude	longitude		
76	28-03	67°18.720′ N	172°18.283′ E	soil	surface
77	29-03	67°19.857′ N	172°17.106′ E	soil	surface
78	30-03	67°21.457′ N	172°15.317′ E	alluvial deposit	surface
79	47-03	67°33.817′ N	172°08.839′ E	alluvial deposit	surface
80	50-03	67°33.393′ N	172°07.840′ E	soil	surface
81	73-03b/ Lz1041-2	67°29.550′ N	172°01.400′ E	lacustrine deposit	0.02
82	73-03c/ Lz1070	67°29.970′ N	172°01.940′ E	lacustrine deposit	0.02
83	74-03b/ Lz1073-1	67°27.920′ N	172°03.110′ E	lacustrine deposit	0.02
84	74-03c/ Lz1071	67°29.400′ N	171°59.550′ E	lacustrine deposit	0.02
85	74-03d/ Lz1072	67°29.990′ N	171°58.030′ E	lacustrine deposit	0.02
86	82-03/7	67°27.647′ N	172°13.470′ E	soil	surface
87	82-03/1	67°27.647′ N	172°13.470′ E	lacustrine deposit	0.10
88	82-03/2	67°27.647′ N	172°13.470′ E	lacustrine deposit	0.30
89	82-03/3	67°27.647′ N	172°13.470′ E	lacustrine deposit	0.40
90	82-03/4	67°27.647′ N	172°13.470′ E	lacustrine deposit	0.60
91	82-03/5	67°27.647′ N	172°13.470′ E	lacustrine deposit	0.80
92	82-03/6	67°27.647′ N	172°13.470′ E	lacustrine deposit	0.70
93	82-03/8	67°27.647′ N	172°13.470′ E	lacustrine deposit	0.85
94	83-03/1	67°27.975′ N	172°13.823′ E	soil	surface
95	83-03/2	67°27.975′ N	172°13.823′ E	lacustrine deposit	0.20
96	83-03/3	67°27.975′ N	172°13.823′ E	lacustrine deposit	0.30
97	83-03/4	67°27.975′ N	172°13.823′ E	lacustrine deposit	0.60
98	83-03/5	67°27.975′ N	172°13.823′ E	lacustrine deposit	0.75
99	83-03/6	67°27.975′ N	172°13.823′ E	lacustrine deposit	0.90
100	83-03/7	67°27.975′ N	172°13.823′ E	lacustrine deposit	1.00
101	83-03/8	67°27.975′ N	172°13.823′ E	lacustrine deposit	1.25
102	84-03/1	67°28.080′ N	172°16.563′ E	soil	surface
103	84-03/2	67°28.080′ N	172°16.563′ E	alluvial deposit	0.20
104	84-03/3	67°28.080′ N	172°16.563′ E	alluvial deposit	0.45
105	84-03/4	67°28.080′ N	172°16.563′ E	alluvial deposit	0.70
106	84-03/5	67°28.080′ N	172°16.563′ E	alluvial deposit	1.00
107	84-03/6	67°28.080′ N	172°16.563′ E	alluvial deposit	1.20
108	84-03/7	67°28.080′ N	172°16.563′ E	alluvial deposit	1.40
109	84-03/8	67°28.080′ N	172°16.563′ E	alluvial deposit	1.50
110	86-03a/ Lz1075	67°31.000′ N	172°02.000′ E	lacustrine deposit	0.02
111	86-03b/ Lz1076	67°31.000′ N	172°03.980′ E	lacustrine deposit	0.02
112	86-03c/ Lz1077	67°32.000′ N	172°04.010′ E	lacustrine deposit	0.02
113	86-03d/ Lz1078	67°32.000′ N	172°02.020′ E	lacustrine deposit	0.02
114	86-03e/ Lz1079	67°29.980′ N	172°07.990′ E	lacustrine deposit	0.02

Table 29: *Samples taken during the expedition in 2003 in the Mechekrynnetveem Basin for radiocarbon dating at NEISRI, Magadan.*

no.	site ID	position		source	depth (m)
		latitude	longitude		
1	GS1603	67°26.449′ N	172°13.138′ E	peat	0.70
2	GS1603	67°26.449′ N	172°13.138′ E	peat	1.00
3	GS1603	67°26.449′ N	172°13.138′ E	peat	1.50
4	GS1603	67°26.449′ N	172°13.138′ E	wood	1.90
5	GS1603	67°26.449′ N	172°13.138′ E	wood	4.20
6	GS8303	67°27.975′ N	172°13.823′ E	peat	0.20
7	GS8303	67°27.975′ N	172°13.823′ E	peat	0.45
8	GS8303	67°27.975′ N	172°13.823′ E	peat	0.60
9	GS8303	67°27.975′ N	172°13.823′ E	peat	0.85

5.2 Lake El´gygytgyn Catchment

5.2.1 Modern Morphosculpture

(O. Glushkova, V. Smirnov)

The level of Lake El´gygytgyn act as a local erosional basis. That´s why it influences the morphology of the outer crater frame and the character of erosional and denudational processes taking place on its slope and within the mountain valleys. The major elements of the modern morphosculpture of the crater are (cp. Fig. 50):

- The shore and the offshore bar, formed by ice-floe pressure, wave- and surf-processes. The ice-floe pressure forms the bars with a height of several meters and with a distance up to ten meters away from the surf line.
- Surfaces and mounds of accumulative and rock terraces of the lake. Three main levels occur: 2.5 - 3.0 m, 9 - 11 m, and 35 - 40 m.
- The lacustrine morphosculpture is dissected by fluvial relief forms. The numerous lake tributaries are represented by riverbeds, floodplains and surfaces of fluvial terraces above the modern floodplains.
- Periglacial landforms are a common feature within the crater. On the native slopes of the basin downfall-talus forms are represented by steep or medium steep slopes covered with coarse colluviums of rock fragments. Partially rock trenches occur. Gently inclined slopes and surfaces with solifluction processes of varying intensity are widespread, especially inside the crater rim.
- Cryogenic forms are widely developed as well. They are represented by nivation cirques, solifluction bars and "terraces", "thermokarst" sinks and trenches, and numerous forms of polygonal micro-relief.

The lake basin consists of three main elements:

- A coastal shelf up to ca. 10 m water depth. This shelf is exceptionally wide (more than 1 km) at the southern and southeastern shores and narrow (only some dozen meters) at the other shore areas.
- Relatively steep slopes with a breadth of about 0.5 km, where the water depth increasing from ca. 10 m down to 70 - 120 m.
- A slightly concave bottom with the maximal depths (ca. 170 m) occurring a little bit towards the northeast of the lake center.

5.2.2 Highest Lake Terraces

(O. Glushkova, V. Smirnov)

Previous search for fragments of high lacustrine terraces, especially the 40 m terrace was continued during the expedition in 2003. In the region of Lagerny Creek (inlet stream no. 49, cp. Fig. 24, p. 51), this terrace has a gently inclined surface and a strict back suture. However, periglacial processes have strongly transformed the terrace sediments. Lacustrine pebbles, originally underlying the terrace sediments, today occur within the solifluction layer (Fig. 51). Disintegrated blocks, small rock fragments, and impact rocks, underlying these deposits, occur at a distance of 15 m from the back suture.

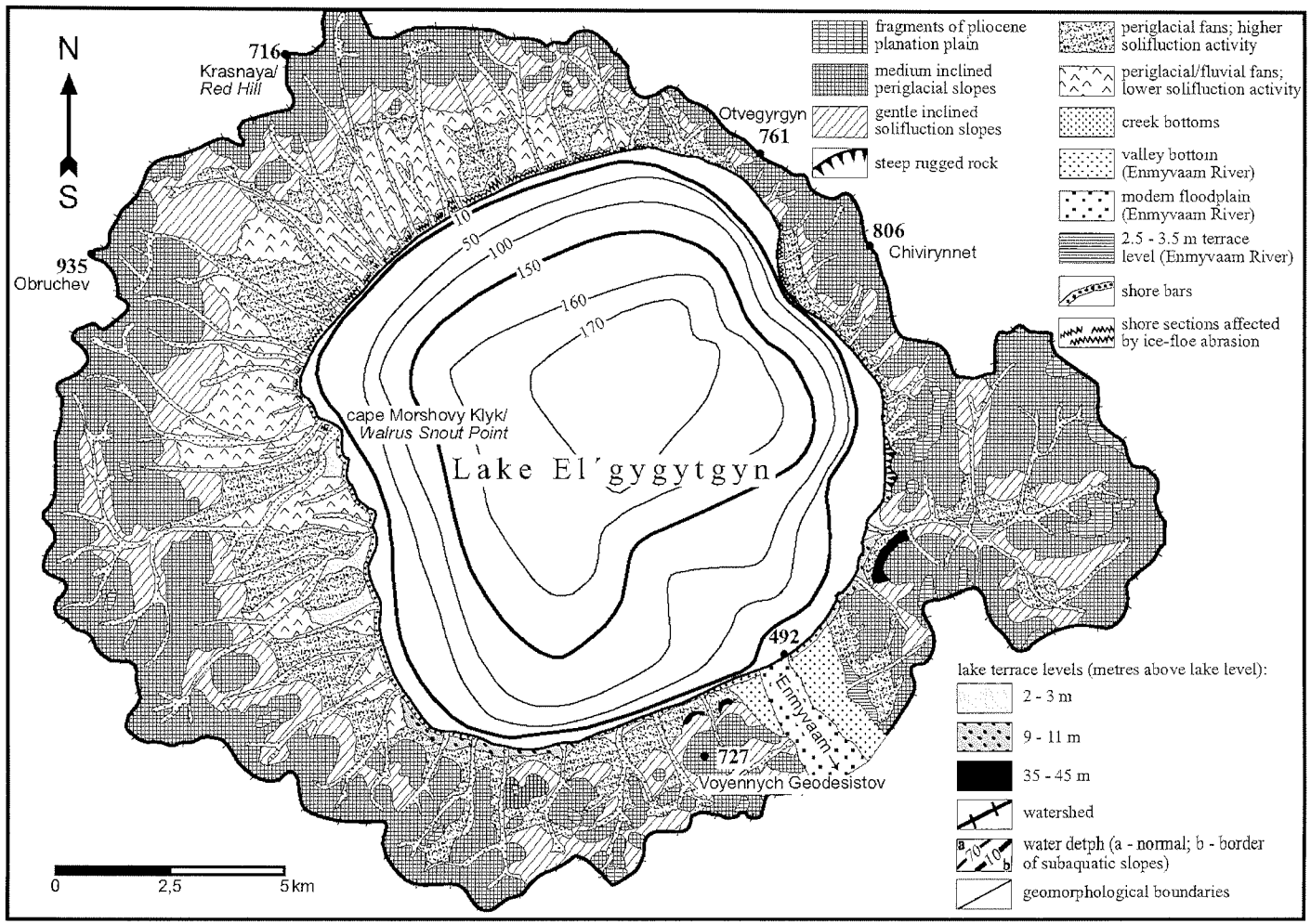

Figure 50: *Geomorphological scheme of the Lake El'gygytgyn catchment (bathymetry simplified after Belyi, 2001).*

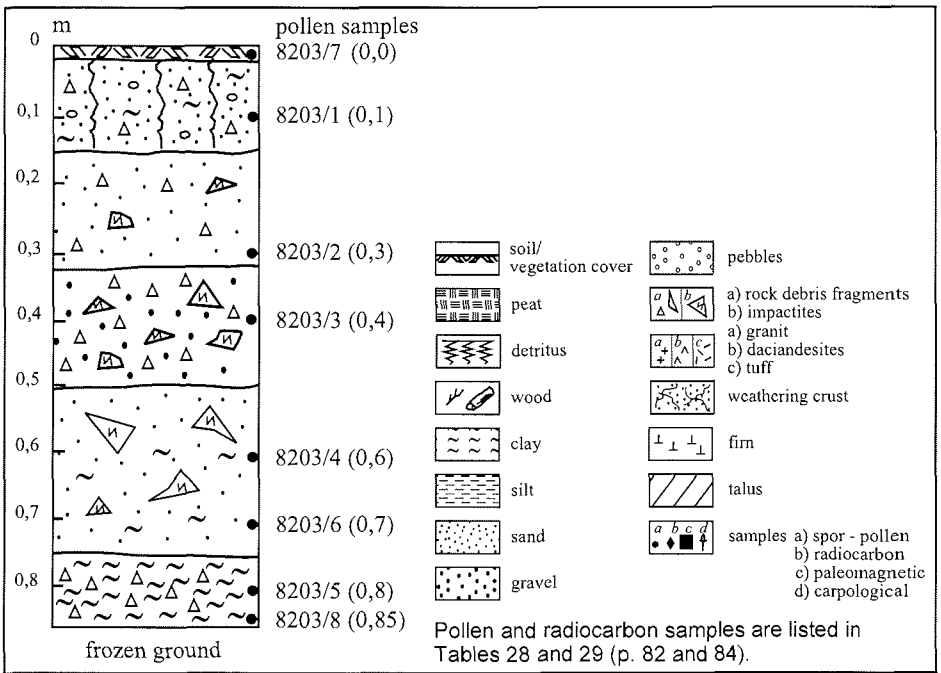

section: GS-8203
location: 0.4 km to the northeast of the mouth of inlet stream no. 50 (cp. Fig. 24, p. 51)
terrace surface, 35 - 40 m above lake level

unit	depth (m)	description
1.	0.00 - 0.03	soil, vegetation cover
2.	0.03 - 0.15	loam, sandy, greyish brown, compact, fragments of non-rounded impactites and rounded pebbles, both 2 - 10 cm in diameter, rock detritus from volcanic rocks or hornfels
3.	0.15 - 0.32	rock detritus, sandy, brownish grey, non-rounded rock fragments (impactites, volcanic rocks)
4.	0.32 - 0.50	like 0.15 - 0.32, but more rock fragments
5.	0.50 - 0.75	rock detritus, sandy, clayey, reddish brown, non-rounded rock fragments (impactites, volcanic rocks)
6.	0.75 - 0.85	clay, reddish black, rock detritus, small rock fragments (impactites, volcanic rocks)
7.	> 0.85	frozen ground

Figure 51: *Sediment section GS-8203.*

New investigations were carried out at the northeastern drainage divide, which separates the El'gygytgyn Lake basin from the Otvegyrgyn River catchment. The watershed height there is ca. 40 m above the lake level, the same height as that of the uppermost terrace level. The investigations have shown that in this area the 40 m terrace is absent. Strongly weathered lacustrine pebbles were only found below the level of the drainage divide.

Well preserved terrace fragments adjacent to the crater rim slopes were found in the southern and southeastern parts of the crater basin at a height of 35 to 40 m above lake level, e.g., on the slope of the "Voyennych Geodesistov"

Mountain ("Geodetic Peak", see Fig. 50) and between the Olga Creek and Vazhenka Creek, the first left tributaries of the Enmyvaam River (cp. Fig. 24, p. 51).

The exact age of this 40 m terrace level is not known. However, it must be rather old, because the terrace has no traces in the modern relief. Taking the ages of the lower terraces (see below), and assuming a gradual lake level lowering, then the higher terrace was formed during the Middle Pleistocene. Traces of a lake level, higher (and older) than the 40 m terrace were not found within the modern relief.

5.2.3 Terrace 10 m above Lake Level

(O. Glushkova, V. Smirnov, G. Schwamborn, G. Fedorov, A. Kupolov)

Introduction

The lacustrine terrace 10 m above lake level is widespread at the southern shore of Lake El'gygytgyn. It represents a continuous deposition in shallow water during a period of higher lake level (Glushkova, 1993; Glushkova et al., 1995). The terrace ranges in width between 20 and 60 m and is mostly composed of matrix-supported coarse layered gravel of dark grey colour. It contains sandy loam and lenses and interbeds of poorly rounded pebbles and coarse sand. Sediment sections from the lower part of the 10 m terrace at the southern shore of the lake were dated to the Karginsky Interstadial, which lasted from 55 to 22 kyr BP, corresponding with the second half of the Middle Weichselian and the beginning of the Late Weichselian (Larsen et al., 1999). In addition, sediments deposited during the Sartan Stage, from 22 to 10 kyr BP, corresponding with most of the Late Weichselian, were found especially in the middle and upper parts of the terrace. These sediments consist of brown-grey loam and poorly rounded pebbles with a loamy matrix.

The shoreline during the deposition of the sediments in the 10 m terrace was generally following the contours of the recent shoreline. This becomes evident when the 500 m line is used for reconstruction. This line is only some dozen of meters landward from the modern shore and only at the western and northern shore it partly expands to up to a kilometre landward. At this time, lacustrine waters no longer filled the Lagerny Creek Basin and the Enmyvaam River tributary valleys. However, the coast at the steep southeastern cliff-section did not change its position. Thus at that time the Enmyvaam River valley attained its modern contours.

Sediment Exposure at the southern Shoreline

A better knowledge of the formation and age of the 10 m terrace is essential for a comprehensive understanding of the Late Quaternary environmental history in the entire crater, because the lake level controls the environment both in the water body and in the catchment of Lake El'gygytgyn. Therefore, a series of samples was collected in 2003 from an exposure at the southern shore, where the complete terrace is exposed ten meters in height (Fig. 52).

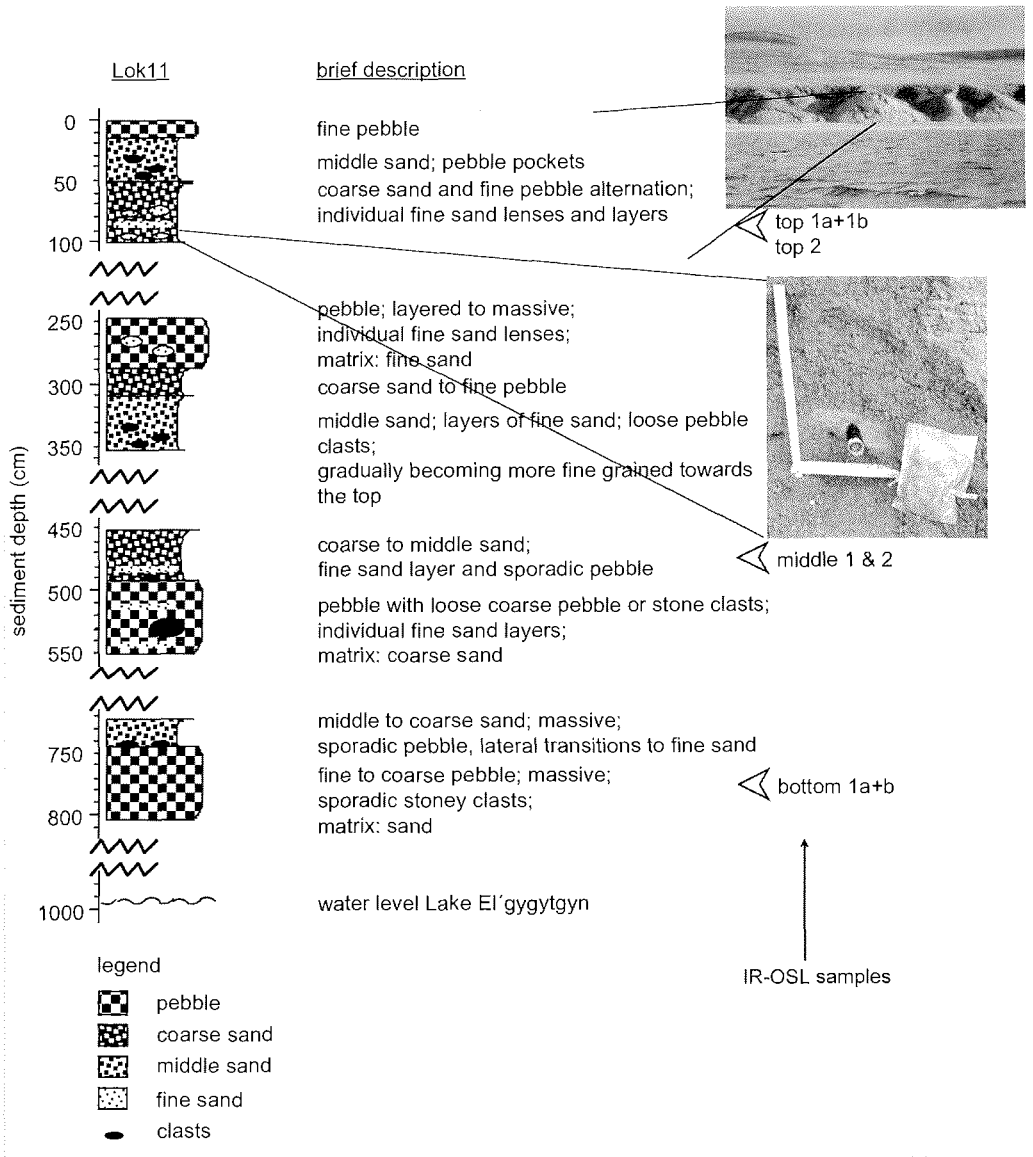

Figure 52: *Sediment log of the 10 m terrace outcropping along the southern shore line of Lake El'gygytgyn. The locality of the log (Lok11) is close to and to the east of inlet stream no. 5 (see also Fig. 20, p. 46). The upper photograph is a view of the section from the lake, the lower photograph displays a typical sand lense, which provides suitable material for the luminescence dating procedure.*

This terrace is expected to represent an ancient lake level highstand. Alternatively, a tectonic movement could have been responsible for the relative uplift of this terrace. In any case, its dating will provide age control on the formation of the terrace deposits. In addition the dating will give the minimum time span for the subsequent formation of the diamictic solifluction cover, which took place posterior to the lake level drop, when the terrace surface became subaerially exposed. The solifluction sheet nowadays covers the fossil beach sequence by about 2 m.

After a ground-penetrating radar (GPR) pre-survey on top of the terrace the outcrop was sampled for fine sandy sediments. The exposure predominantly consists of a coarse-grained, pebbly to sandy sections, interpreted as a massive sequence of littoral sands, but at different heights also contains some discrete layers and lenses of fine sand (Fig. 52). On these fine sands age determination will be conducted by luminescence dating using the potassium feldspar IR-OSL technique. No organic remains can be found in this exposure thereby excluding the use of radiocarbon dating.

5.2.4 "Olga" Creek

(G. Schwamborn, O. Glushkova, V. Smirnov, G. Fedorov, A. Kupolov)

Periglacial environmental changes are thought to trigger sediment export into the lake. In order to amend paleoclimate reconstructions using the lake sediment record, therefore, the properties and histories of the permafrost deposits around the lake, like ground ice (wedge ice), texture ice, and frozen sedimentary sequences, have to be studied.

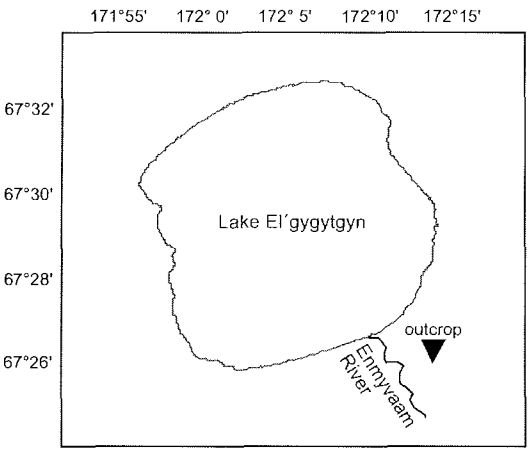

Figure 53: *Position of the outcrop of the 5 m terrace, were an ice wedge incised into the frozen sediment sequence P1 was investigated.*

Parts of these studies were carried out in summer 2003 at "Olga" Creek, a small left tributary to the Enmyvaam River (Fig. 53). At a location about 2 km to the southeast of Lake El'gygytgyn an outcrop of a terrace 5 m above lake level was found. On this outcrop stratigraphic and periglacial evidences were collected to reconstruct the evolution of the terrace during Late Quaternary time. This included the determination of periods favourable for the establishment and growth of ice wedge polygonal networks.

Ice Wedge

As the terrace emerged from the Enmyvaam River valley, climatic conditions allowed the establishment of permafrost conditions in the deposits. In keeping with the cold climate environment, ice wedge networks presumably began to grow, starting from frost fissures on the emergent, ice-rich slope sediment surfaces (Fig. 54). The contact between the underlying ice-rich, diamictic slope sediments (position of "O" profile) to the basal part of the ice wedge (position of "F" profile) can be seen in the lower part of the figure. The climatic and environmental periods are recorded both in the ice wedges and in the frozen sedimentary deposits surrounding them (see below).

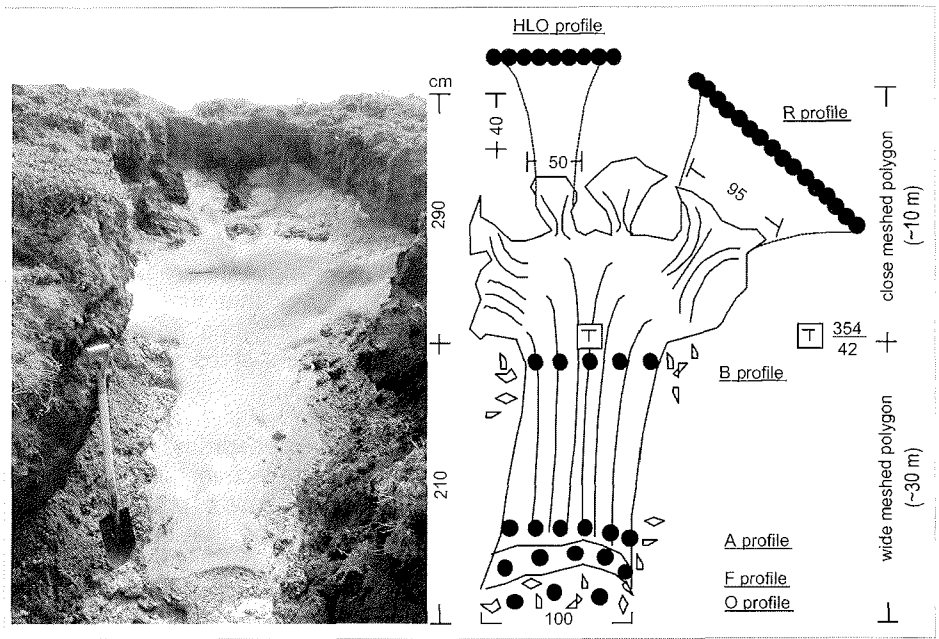

Figure 54: *The ice wedge at "Olga" Creek. The ice wedge (left) and a scetch showing the profile positions (black dots) for oxygen isotope composition and hydrochemistry samples (right). Note the bisection into an upper and lower part associated with different meshed polygons. Strike and dip values for the outcrop position are given in addition.*

Paleoclimate analysis of the ice wedge uses hydrogen and oxygen isotope methods, similar to those in glaciers and ice caps and is supported by hydrochemical measurements (i.e., measurements of major anions and cations). Sampling of wedge ice was directed to cover several times the geological time axis running horizontally through this formation; from the foot area ("F" and "A" profiles) to the uppermost outcrops of the polygonal network (position of "HLO" and "R" profiles). The current climatic phase is a more continental phase of growth, seen by the morphological bisection containing a *wide meshed* (ca. 50 m in diameter) polygon topped by a *close meshed* (ca. 10-15 m in diameter) ice wedge polygon studied herein (Fig. 54).

The individual analyses on the ice wedge and their potentials for paleoenvironmental reconstructions are in brief as follows:

- Field measurements
  - Electrical conductivity (µS/cm) and pH for identification of individual ice bodies, zones, or stripes.
- Laboratory measurements
  - $\delta^{18}O$ for reconstruction of climate or temperature signal, respectively, of winter precipitation.
  - δD for indication of a kinetic fractionation of the isotope signal
  - Major cations (Ca^{2+}; Mg^{2+}; K^{+}; Na^{+}) and major anions (HCO^{3-}; SO_4^{2-}; Cl^{-}) for refining the identification of individual ice bands.

To improve the interpretation of the oxygen isotope composition we sampled modern snowfall, rainfall, and surface water throughout the expedition time. The isotope data from these samples will add to already available data about oxygen isotopic ratios for the Eurasian continent (Meyer, 2003).

Ground Penetrating Radar Survey

Complementary to ice wedge studies we sampled sedimentary permafrost containing hydrochemical texture ice information in close distance to the wedge ice outcrop. Outcropping sediments around the ice wedge site are unfortunately too disturbed to be used for this purpose in the way that they are tilted or collapsed at the rim of the terrace. Moreover, the outcrops do not allow to sample fresh frozen substrate including the texture ice, since the surfaces of the outcrops are melted during the summer months.

Therefore, we run ground penetrating radar (GPR) measurements as a pre-survey to locate a suitable coring position in order to recover an undisturbed frozen sediment sequence. We collected data in various profiles forming triangles, which is the easiest way to cover a subsurface three-dimensionally (Fig. 27, p. 55). Afterwards we narrowed down a locality, where shallow coring could take place. Profiling was completed by common-midpoint (CMP) measurements right above the coring position to determine the wave velocity in the ground and to later convert two-way travel (TWT) times to total depth. In addition, GPR reflections and their amplitudes will be correlated with (cryo-) sedimentary properties (e.g., ice content, grain size, substrate texture etc.). The sediment core is subject to environmental reconstruction of the Late Quaternary permafrost plateau.

One profile example is displayed showing the typical appearance of GPR results in frozen ground containing ice wedge pattern (Fig. 55).

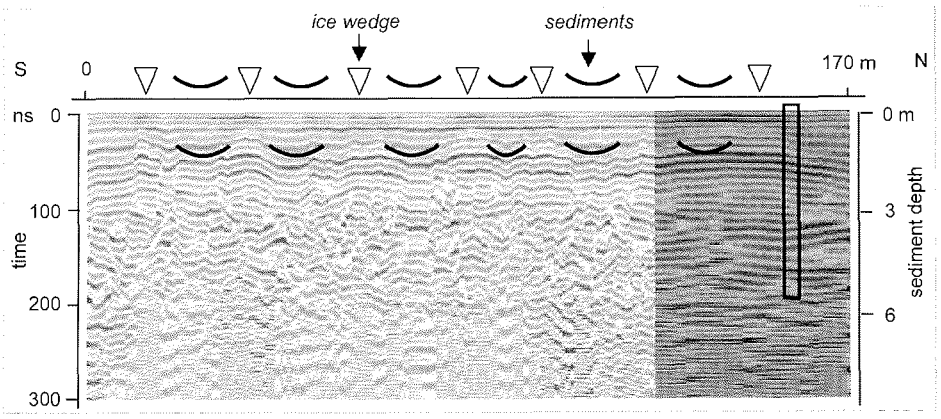

Figure 55: *Example of a GPR profile of the 5 m terrace at "Olga" Creek, indicating alluvial and slope sediments, distorted by cryoturbation. The rectangle marks the position of permafrost core P1.*

Ice wedge growth and cryoturbation is assumed to be the main driving factor turning up sediment layers and cutting them off. Between 100 and 200 m profile

and 0 to 100 ns TWT some horizontal to diagonal layers show up, the same can be observed further right in the profile. These features are believed to represent original horizontal layering derived from slope and/or fluvial processes not affected from ice wedge growth. Energy gets lost and background noise gets up below 150 ns TWT (approximately 8 m sediment depth). We decided to use one of the sites giving strongest horizontal reflection response for permafrost coring and subsequent sedimentary studies.

Ongoing GPR data analysis include:

- the application of processing enhancements to reduce the distortions produced by noise and weak signals and/or energy loss,
- determination of the EM wave velocity using CMP records.
- correlation of GPR reflections and their amplitudes with (cryo-)sedimentary properties (e.g., ice content, grain size, substrate texture, etc.)

Sediment Exposure and Permafrost Core P1

A reconstruction of the Late Quaternary evolution of the sedimentary permafrost, as far as represented by the 5 m terrace, is carried out both on the sediment section exposed at the slope to the creek close to the ice wedge (see above) and on a permafrost core selected after the GPR pre-survey. A scetch and description of the sediment section (GS-1603) is presented in Figure 57.

For shallow permafrost coring of the frozen sediments we used a portable gear (TKB15), powered by a 2.9 kW engine (Fig. 56). The rotary corer has a core diameter of 6 cm. The advantage to take core material rather than outcrop samples is that a core provides a non-disturbed sediment sequence and a complete sediment record including cryosedimentary information.

Figure 56: *Frozen sediment recovering with the portable shallow coring kit.*

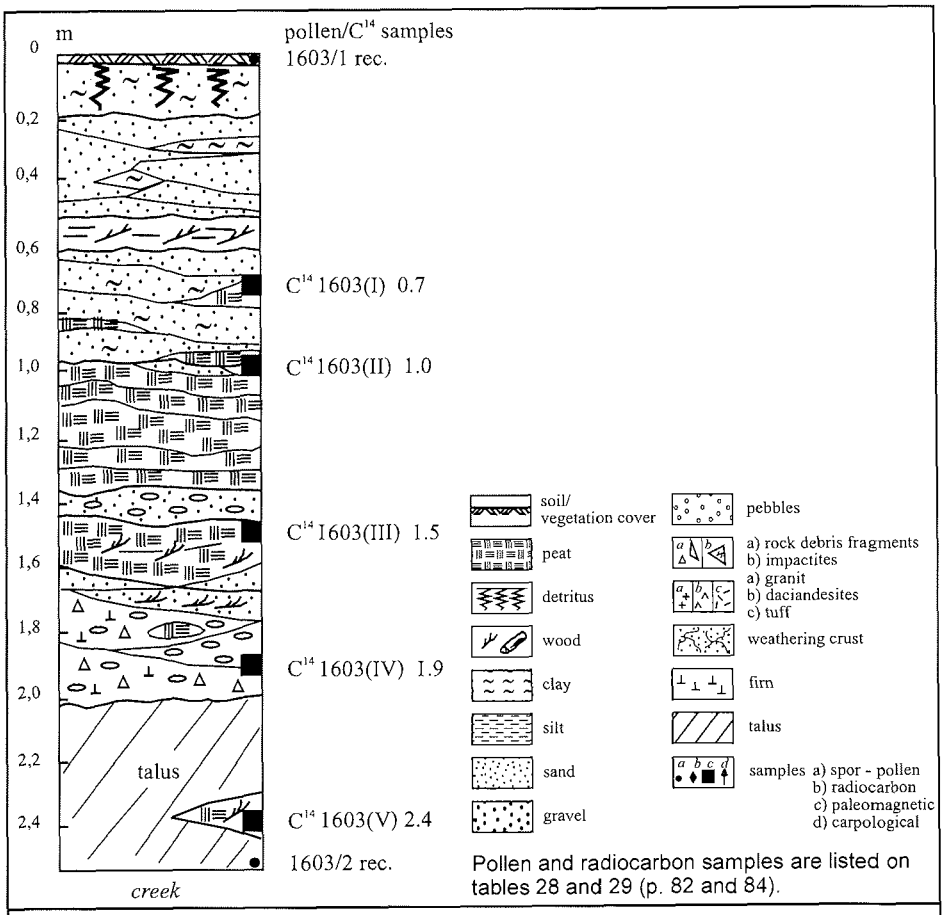

section: GS-1603
location: "Olga" Creek valley, ca.0.4 km upstream its mouth into Enmyvaam River
scarp of Holocene terrace, 2.5 m high

unit	depth (m)	description
1.	0.00 - 0.03	soil, vegetation cover
2.	0.03 - 0.20	loam, pale yellowish grey, roots of grasses and shrubs
3.	0.20 - 0.23	humus, blackish brown, horizontally lying grass stems,
4.	0.23 - 0.50	loam, coloured, small lenses of greyish red clay, ferruginous fine sand
5.	0.50 - 0.59	mud, reddish grey, thin humus interbed, lower boundary is waved
6.	0.59 - 0.65	fine sand, yellowish green
7.	0.65 - 0.75	loam, reddish brown, interbed with horizontally lying grass stems
8.	0.75 - 0.95	like 0.65 - 0.75, but with a peat interbed
9.	0.95 - 1.10	peat, dark brown, shrub roots and branches (2 - 9 cm), leaves from sedges and crowberries
10.	1.10 - 1.35	peat, yellowish brown, fragments of shrubs, lenses of sand and gravel
11.	1.35 - 1.45	gravel, greyish green, loamy matrix, poorly rounded pebbles
12.	1.45 - 1.60	peat, blackish red, fragments of large shrubs, interbeds with fine sand
13.	1.60 - 2.10	pebbles, poorly rounded, greenish grey, gravelly matrix, non-rounded rock fragments
14.	2.10 - 2.50	talus, at 2.4 m ice vein with fragments of large shrubs

Figure 57: *Sediment section GS-1603 ("Olga" Creek).*

The sketch in Figure 58 provides the main macroscopic sedimentary properties of the permafrost core P1. In general, the permafrost stratigraphy is made up by an alternation of diamictic slope sediments, fluvial interlayers, and organic-rich horizons. The portion of breakstones belonging to diamictic slope sediments increases with depth. Ice content and texture vary with layers or within layers. They can contain low volume of interstitial to reticulated ice up to high ice contents made up of lenses or discrete cm-sized ice layers.

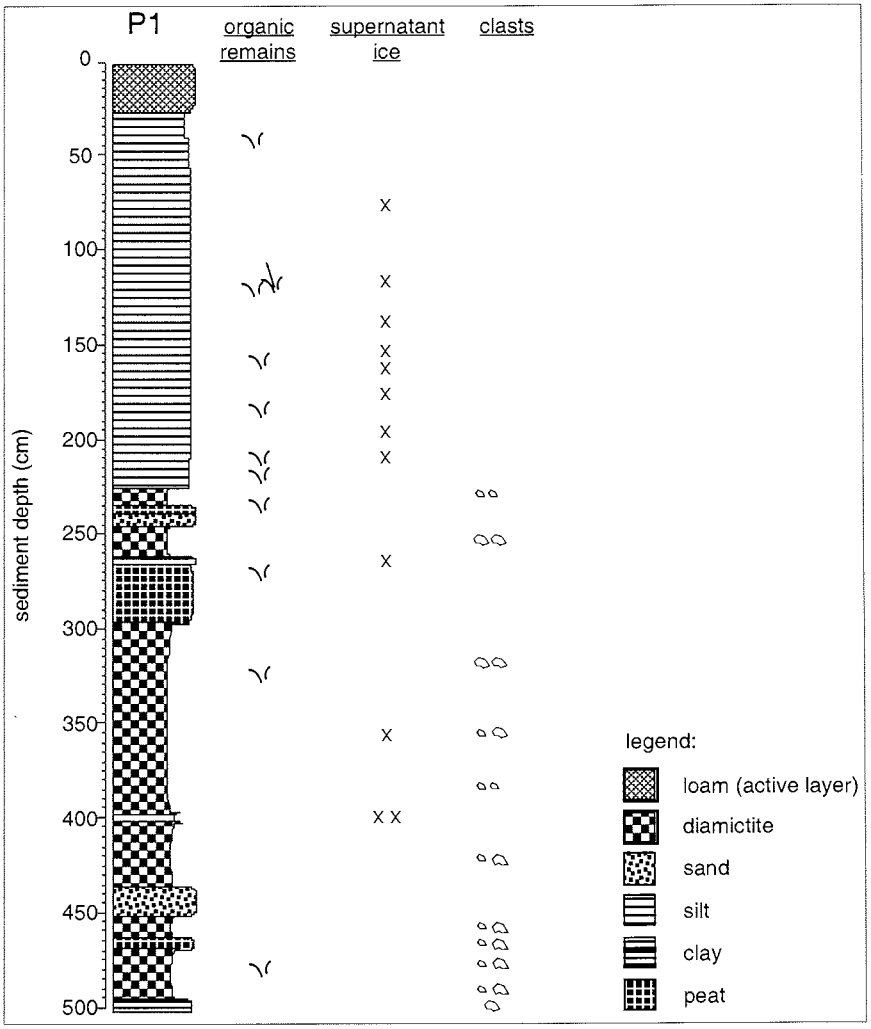

Figure 58: *Sediment log of permafrost core P1 from "Olga" Creek; for location see Figure 20 (p. 46).*

The core sections were sampled already in the field in pieces of ca. 10 cm or smaller in length, dependent on stratigraphic boundaries. Ongoing sediment analysis and interpretation purposes include:

- ice content;

- grain-size characteristics for stratigraphic discrimination and facies analysis;
- mineralogical composition for provenance analysis;
- age determination using plant remains for radiocarbon dating;
- pollen stratigraphy for vegetation reconstruction;
- hydrochemistry of texture ice:
  - electrical conductivity and pH for indication of ice stratigraphy,
  - major cations and major anions for refining the ice identification in order to indicate environmental changes such as erosion, evaporation or sublimation events,
  - $\delta^{18}O$ for reconstruction of climate or hydrology related stratigraphic discontinuities contained in the summer active layer deposits, and
  - δD for indication of a kinetic fractionation of the isotope signal.

5.2.5 Northern Lake Shore

(G. Schwamborn, G. Fedorov, A. Kupolov)

Ground Penetrating Radar Survey

Whereas the southern shore is only about 10 - 20 m in width, the northern part of the lake presents a wide shore line of more than 200 m at maximum. The northern onshore area exhibits a succession of up to three or four gravelly barriers running parallel to the shoreline. This asymmetrical morphology between the southern and the northern shore could either be of tectonic nature, or the result of a lake level drop, or a combination of both (cp. p. 88f). Knowledge about the age of the coastal barriers would crucially advance our understanding of this paleogeographical change. The availability of a sediment sequence from behind the shore barrier is essential to date the barrier itself, assuming that sediments behind the barrier were only deposited after the barrier's formation. A minimum age for the barrier can be expected from the oldest sediments of a sediment sequence at about 3 - 5 m sediment depth, which corresponds to the height of the barrier above the current lake level.

In a comparable manner as being described on page 92 a GPR pre-survey was conducted to locate a suitable coring position for providing a sequence of undisturbed sediments. An example profile from the GPR grid shown in Figure 59, runs across a slope sediment plateau close to the northernmost point of the shoreline (Fig. 27, p. 55). From the GPR imagery it appears that an upper part is separated from a lower part by a broad fringe. We interpret the upper part as of sedimentary nature whereas the lower part represents volcanic basement. The broad fringe 1-2 m in thickness is interpreted to show the lithologic transition from slope sediments to autochthonous but weathered sedimentary material to a weathered hardrock surface. Thus it seems that the sedimentary cover is up to 6-7 m thick. The core position has been set up at a site only 20 m away from the shore barrier.

Ongoing GPR data analysis include:

- the application of processing enhancements to reduce the distortions produced by noise and weak signals and/or energy loss;

- determination of the EM wave velocity using CMP records;
- correlation of GPR reflections and their amplitudes with (cryo-)sedimentary properties (e.g., ice content, grain size, substrate texture, etc.).

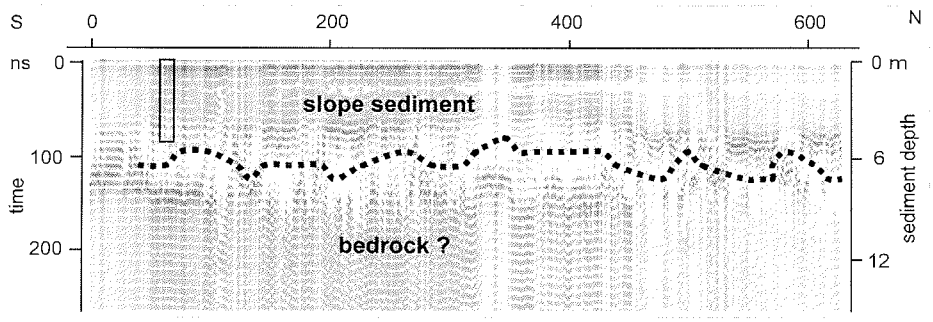

Figure 59: *Example of a GPR profile above a slope sediment plateau close the northern shore of Lake El'gygytgyn. The rectangle marks the approximate position of permafrost core P2.*

Permafrost Core P2

The authors used the portable coring gear already described on page 93 to recover a permafrost sequence of 510 cm in total length. Sediments are used for the reconstruction of the Late Quaternary environment as far as represented by this sequence. In general, most of the permafrost stratigraphy is made up of diamictic slope sediments with few interlayers of peaty or silty horizons. In the upper half of the core the ice content and texture is mostly interstitial. The bottom part of the core is enriched in ice lenses and discrete cm-thick layers of ice. The lowermost occurrence of organic remains is found at 330 cm sediment depth. Below this depth the sedimentary substrate appears fresh in colour and of volcanic origin. We interpret this part as weathered material of the former volcanic surface.

The sketch in Figure 60 provides the main macroscopic sedimentary properties of the permafrost core P2. Core sections were sampled in the field in pieces of ca. 10 cm or smaller in length, dependent on stratigraphic boundaries. Ongoing sediment analysis and interpretation purposes include:

- ice content;
- grain-size characteristics for stratigraphic discrimination and facies identification;
- mineralogical composition for provenance analysis;
- age determination using plant remains for radiocarbon dating;
- pollen stratigraphy for vegetation reconstruction;
- hydrochemistry of texture ice:
  - electrical conductivity and pH for indication of ice stratigraphy,
  - major cations and major anions for refining the ice identification in order to indicate environmental changes such as sublimation, evaporation or erosion events,
  - $\delta^{18}O$ for reconstruction of past climate changes or hydrology related stratigraphic discontinuities contained in the summer active layer deposits.

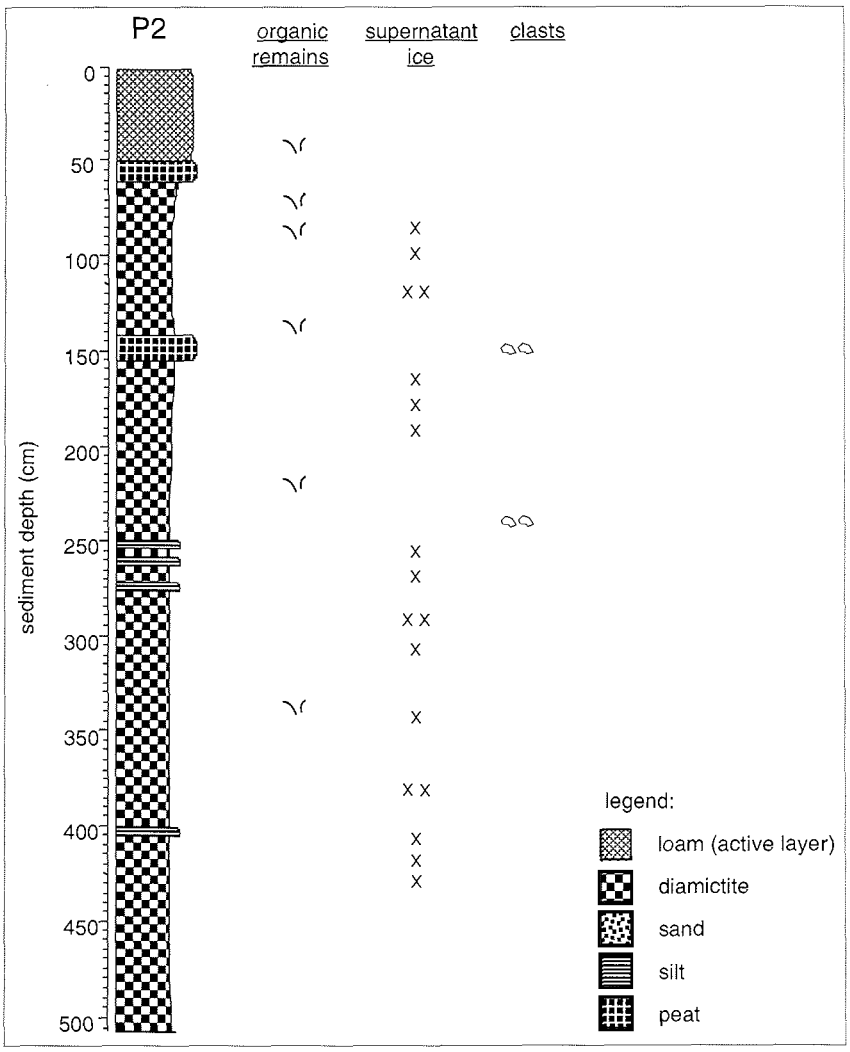

Figure 60: *Sediment log of permafrost core P2 from the northern shore of Lake El'gygytgyn; for location see Figure 20 (p. 46).*

5.2.6 Rock Exposure Ages of Beach Ridges and Fluvial Surfaces
(J. Brigham-Grette)

The lack of materials suitable for the radiocarbon dating of relatively young geomorphic features is a common problem for Quaternary scientists, especially in Arctic settings. Cosmogenic isotope dating, while not a panacea, offers promising potential for deriving meaningful numerical age estimates of features critical to understanding the geomorphic evolution of Lake El'gygytgyn. Large subrounded, bladed-shaped cobbles were collected from two stable sites in summer 2003 from beach surfaces and the outflow fluvial terraces of the

Enmyvaam River in order to learn more concerning recent changes in the lake level history, ages that can not be determined from sediment cores due to the coarse erosive nature of the lake shelf areas.

One of the many intriguing aspects of the Enmyvaam River is the width of its flood plain where it exits Lake El'gygytgyn (Fig. 61). This well-drained cobble surface has less than a meter of relief yet measures ca. 2 km in width; the modern river system is less than 200 m wide. The surface of the entire flood plane is laced with ancient braided channels, however, most are now overgrown with lichen and low tundra vegetation. A few of the lowest lying channels are currently silted in and many hold standing water during the first part of the summer months contributing to the perception of their youthful age.

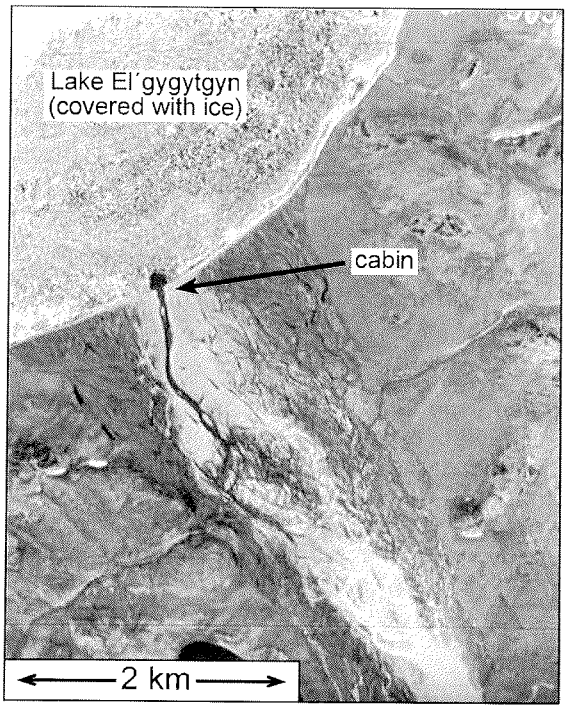

Figure 61: *Braid plain of the Enmyvaam River exiting southward from Lake El'gygytgyn; source: Russian aerial photo (undated).*

Since first visiting this part of the lake in 2000, field parties have pondered the age of this wide braided surface and whether it might have last been active during exceptionally high water years in the early Holocene or whether it is actually much younger. Warmer and wetter regional conditions during the early Holocene could have created slightly higher lake levels than now (Glushkova et al., in press). What is known is that the existing cabin at the lake was built more than 30 years ago and an earlier cabin on the eastern edge of the flood plain was built before that one but not before 1955; neither cabin has ever been flooded. Relatively recent higher lake levels are also indicated by a remarkable series of beach ridges that line the shore at the north end of the lake. These beach ridges lie up to 3-4 meters above the modern shoreline and are continuous for several kilometres. The inlet streams 19 to 35 (see Fig. 14, p. 31) have constructed alluvial fans across sections of these beaches such that its clear that the fans are younger than the beaches (see also geomorphic map of Glushkova, 2001).

Six rock samples were taken from stable locations on both of these surfaces to determine if cosmogenic isotope dating might be successfully employed to test

the lichenometric ages discussed in Chapter 5.3.1 (p. 108). Due to the volcanic nature of the rock types, the samples will likely be dated using the isotopes Chlorine-36 and Aluminium.

Table 30: *Rock samples for Surface Exposure Dating; samples from the north beach terrace were taken within 60 m of the specified point.*

sample ID	surface	position		date
		latitude	longitude	
E03BG02	cabin flood plain	67°26.791′ N	172°11.172′ E	2-July-03
E03BG03	cabin flood plain	67°26.791′ N	172°11.172′ E	2-July-03
E03BG04	cabin flood plain	67°26.791′ N	172°11.172′ E	2-July-03
E03BG05	cabin flood plain	67°26.736′ N	172°12.003′ E	2-July-03
E03BG06	cabin flood plain	67°26.736′ N	172°12.003′ E	2-July-03
E03BG07	cabin flood plain	67°26.736′ N	172°12.003′ E	2-July-03
E03BG68	north beach terrace	67°32.575′ N	172°02.825′ E	21-July-03
E03BG69	north beach terrace	67°32.575′ N	172°02.825′ E	21-July-03
E03BG70	north beach terrace	67°32.575′ N	172°02.825′ E	21-July-03
E03BG71	north beach terrace	67°32.575′ N	172°02.825′ E	21-July-03
E03BG72	north beach terrace	67°32.575′ N	172°02.825′ E	21-July-03
E03BG73	north beach terrace	67°32.575′ N	172°02.825′ E	21-July-03

5.2.7 Lagerny Creek

(G. Schwamborn, G. Fedorov, O. Juschus, V. Wennrich, O. Glushkova, V. Smirnov)

Ground Penetrating Radar Survey

Unlike acoustic systems, GPR can be used for sub-bottom profiling through an ice cover. GPR proved to be well suited to imaging shallow areas of Lake El′gygytgyn. Close to the mouth of the Lagerny Creek, profiling on the lake took place from the ice cover. On land, profiling was completed from the snow cover. EM penetration behaviour above the lake is well and allows bathymetric recognition of the lake floor (Fig. 62). For the hill debris area around the Lagerny Creek mouth area, in contrast, EM penetration is poor.

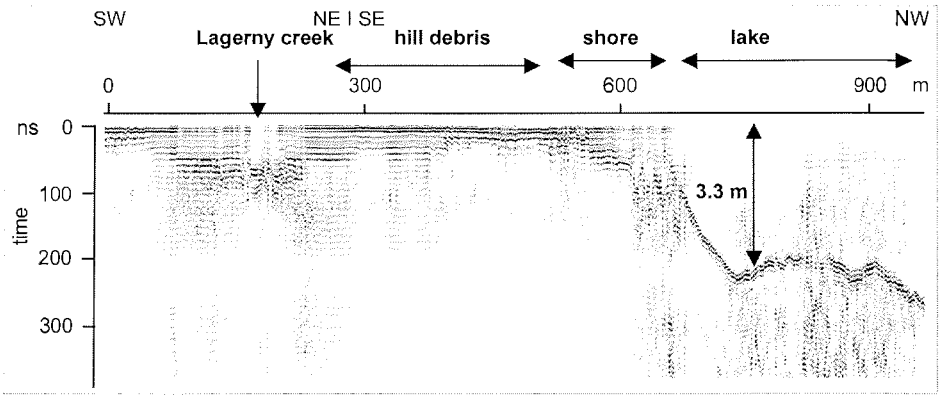

Figure 62: *GPR profile of the Lagerny Creek mouth area with main landscape elements indicated; for location see Fig. 20 (p. 46).*

The rough-textured weathering crust apparently prevents successful penetration and causes hight loss of energy due to scattering effects at the breakstones. Nevertheless, the creek position could be located through the snow cover.

Ground Ice Body at Lagerny Creek Mouth

Introduction – During spring and summer 2003 a ground ice body, underlying fluvial sediments and peat, was observed in the mouth area of Lagerny Creek (inlet no. 49; 67°28.20′N 172°13.46′E, Fig. 63). The ice body covered an area of about 1000 m^2. On June 8, 2003, when the ground ice was first discovered, its sediment cover was destroyed for about 100 m^2. In the course of the following days the area of Lagerny Creek was repeatedly visited by participants of the expedition. They noticed a rapid decomposition of the whole ice body. On June 29 the body had heavily retreated and on July 13, 2003, no ice without sediment cover was visible. Only a few sediment mounds with an ice core remained at that time, but also disappeared in the course of the following days.

Investigations – The ground ice had a columnar "candle" ice structure (Fig. 63). It was quite similar to the lake ice (cp. p. 27) but contained many small long-shaped gas bubbles. The ice thickness reached up to 1.35 m. The ice body was overlying fluvial sediments (coarse pebbles and cobbles). Its cover was also formed by cobbles, in turn overlain by peat. The peat, composed mainly of mosses, at the base was sandy and silty. The measured thickness of the cover reached up to 0.45 m. A radiocarbon sample (Zf49-2) was taken from the base of the peat. The age determination is still in process.

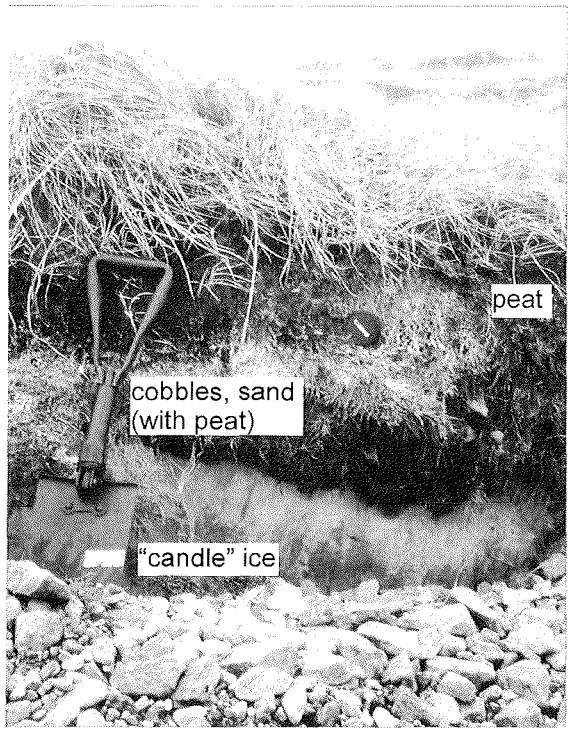

Figure 63: *The ground ice body at Lagerny Creek mouth.*

Conclusions – It is the most probable hypothesis that the ground ice body represents an old lagoon in the mouth area of Lagerny Creek. Lagoons are a common feature around Lake El′gygytgyn. The shore bar often dams the mouth area of the inlet streams. Especially at the northern shore almost every inlet today has a lagoon. The former lagoon at Lagerny Creek probably was completely frozen during a winter and rapidly became covered with fluvial sediments in the subsequent spring. In con-

sequence the ice was protected against melt processes. The comparatively thick peat cover indicates that the ice body was stable for several decades respectively centuries. When the sediment cover became destroyed in spring 2003, probably by melt water, the structure without any protection collapsed within one year.

Holocene and Upper Pleistocene Sediment Exposures

The sediments exposed in the Lagerny Creek area were described and sampled at two sections. Section GS-8303 (Fig. 64) is a natural outcrop located at the mouth of the first left tributary to Lagerny Creek. It is believed to represent parts of the Holocene history. Section GS-8403 (Fig. 65), in contrast, probably is an upper Pleistocene sediment succession that was exposed as a scarp of a 4.5 m high fluvial terrace, 2.5 km upstream Lagerny Creek mouth.

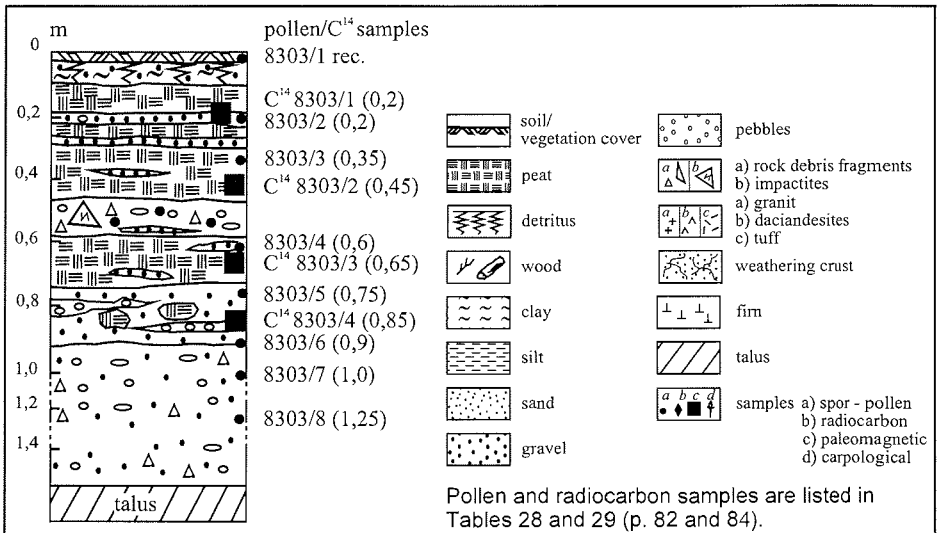

section: GS-8303
location: Lagerny Creek valley, mouth of the first left tributary
natural outcrop

unit	depth (m)	description
1.	0.00 - 0.03	soil, vegetation cover, swampy hummocky tundra
2.	0.03 - 0.10	loess loam, greyish red, modern roots of grasses
3.	0.10 - 0.18	peat, reddish brown, with sandy loam, interbed of plant fragments
4.	0.18 - 0.21	sand, greenish grey, rare small well rounded pebbles
5.	0.21 - 0.27	sedge peat, reddish brown, wavy upper and lower boundary
6.	0.27 - 0.29	loam, sandy, greyish green
7.	0.29 - 0.47	peat, reddish brown, lenses and interbeds of sandy loam, greenish grey
8.	0.47 - 0.56	gravel and pebbles, dark grey, small impactite fragments
9.	0.56 - 0.74	peat, yellowish red, partly disintegrated, lenses and interbeds (3 - 9 cm) of sand including coal particles, yellowish green
10.	0.74 - 0.92	sandy loam, reddish grey, humous, round peat particles, orange-yellow, lenses of small pebbles, dark-grey
11.	0.92 - 1.50	pebbles, greyish brown, non-rounded rock fragments
12.	1.50 - ...	talus

Figure 64: *Sediment section GS-8303.*

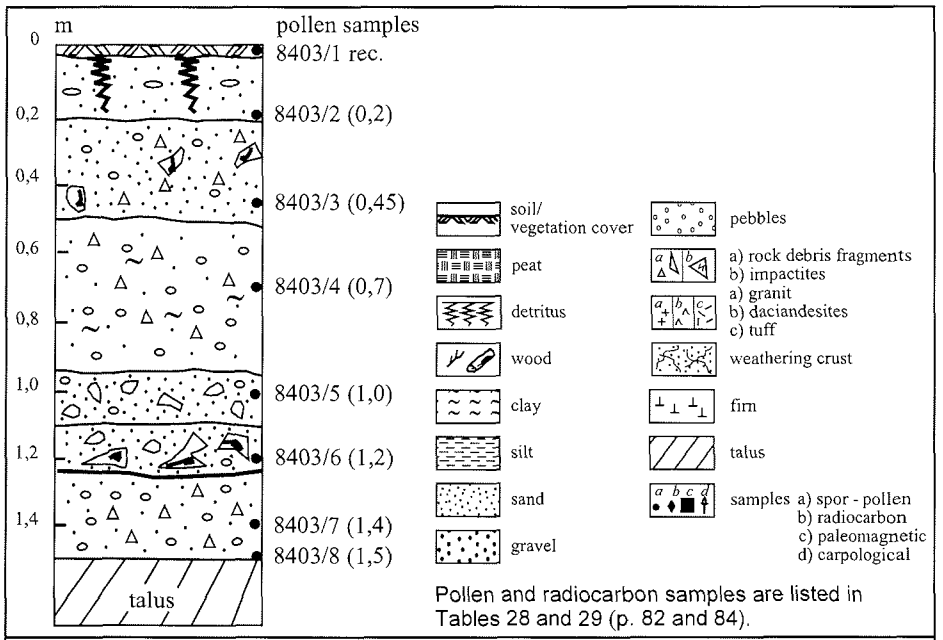

section: GS-8403
location: Lagerny Creek valley, 2.5 km upstream its mouth
scarp of a fluvial terrace, 4.5 m high

unit	depth (m)	description
1.	0.00 - 0.03	soil, vegetation cover
2.	0.03 - 0.20	sandy loam, light-brown, modern roots of grasses
3.	0.20 - 0.50	pebbles, poorly rounded, yellowish red, sandy gravelly matrix
4.	0.50 - 0.95	pebbles, poorly rounded, reddish grey, sandy gravelly matrix, non-rounded rock fragments, clayey inclusions
5.	0.95 - 1.10	gravelly pebbles, reddish brown, non-rounded rock fragments
6.	1.10 - 1.25	like no. 5 but larger rock fragments (up to 8 cm)
7.	1.25 - 1.50	pebbles, yellowish brown, sandy gravelly matrix, common rock fragments, ferruginous membrane around large pebbles and fragments
8.	> 1.50	talus

Figure 65: *Sediment section GS-8403.*

Artefacts

Three new archaeological sites were found during the expedition to Lake El'gygytgyn in 2003: in the Lagerny Creek basin, near the mouth of Lishaynikovy Creek (inlet no. 12, see Fig. 24, p. 51), and on the left bank of the Enmyvaam River about 15 km downstream Lake El'gygytgyn. These sites were described in detail, and rich material was collected.

Some features of the stone tools are similar to the "El'gygytgyn" complex of artefacts found at the lake in 1955, 1991 and 2000. This complex belongs to the North-Chukotskaya Culture dated back to the second half of the second millenium. In the Lagerny Creek basin knife-like plates, incisors, scrapers, arrowheads, and knives were found (Fig. 66). Local rock material (flint, jasper) and material from other places (chalcedony, obsidian) was used for

manufacturing of these artefacts. Only one poorly processed half-finished tool made of local impact glasses was found.

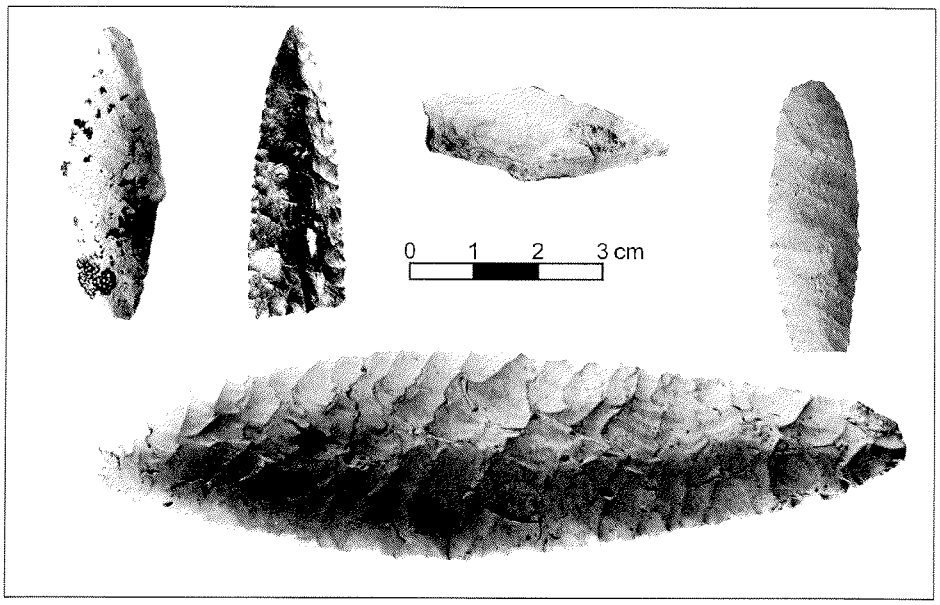

Figure 66: *Artefacts of stone age from Lagerny Creek, found in 2003.*

In the valley of the Mechekrynnetveem River (see Fig. 38, p. 72), on the right bank terrace, 6 m above water level, a new archaeological site was discovered too. This site was probably used for ritual ceremonies and burials. Groups of arranged stones traced the contours of 7 large yarangas. The centre of each circle, 10 - 12 m in diameter, was a bonfire place. Four of them contained large fragments of honey-yellow chalcedonies and bone fragments. This type of settlement was found in this region for the first time and it needs further investigations. The supposed age of the last site visit is the beginning of the last century.

5.3 Lake El´gygytgyn Basin

5.3.1 Coastal Morphology

(O. Glushkova, V. Smirnov)

While terrace fragments of two levels are common in the southern part of the lake basin, they are missing at the western and northern parts. There, instead, a system of ancient shore bars exists. These bars are particularly well preserved between inlet streams nos. 29 - 33 (see Fig. 24, p. 51) and at stream no. 12 (Lishaynikovy). They testify a retreat of the shore line. A detailed description of the morphology and composition of the beach ridges was accomplished in the regions of creek nos. 33 and 31. For the purpose to determine the age, lichenometric measurements were carried out (Fig. 67).

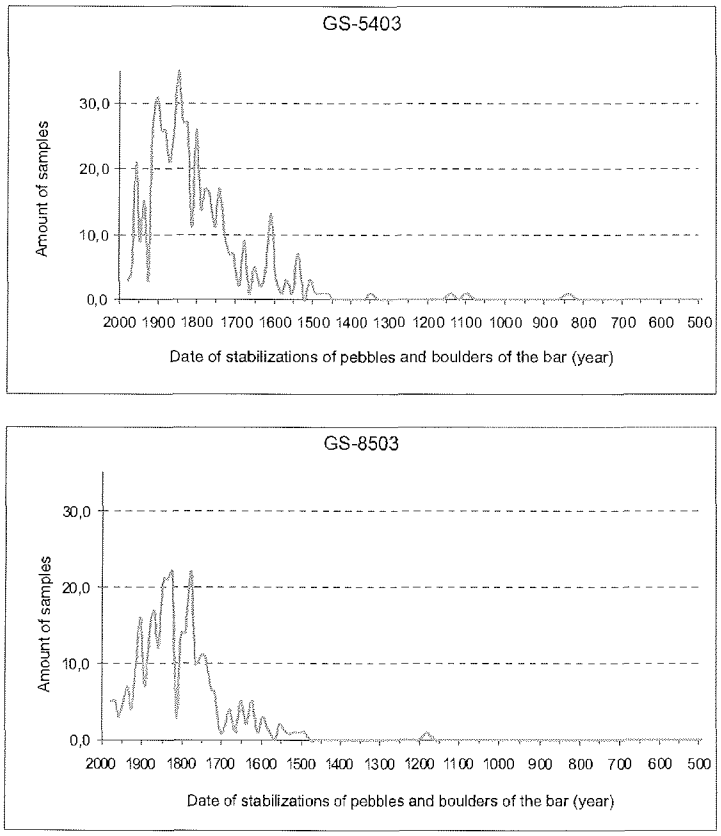

Figure 67: *Lichenometric analyses of beach ridges at the northern shore of Lake El'gygytgyn; for location see Figure 68 and Tables 31 and 32.*

Three generations of shore line retreat features became established, probably during the Late Pleistocene-Holocene. The maximum retreat of the shore line took place in the region of inlet stream no. 34, where it was more than 360 m. These series of ancient coastal bars are clearly visible on air photos (Fig. 68). Their distribution and interrelations with the other relief forms, developed to the north of the coast, was investigated.

The first recent or subrecent bar surface is 3.5 - 4 m high and lacks any permafrost features. On the pebbles, colonies of *rhizocarpon sp.* and *parmelia sp.* lichens were formed. The thalus diameters range between 4 and 65 mm. In the low area between the first and the second bar, small permafrost polygons and small permafrost channels up to 30 cm depth occur. On the surfaces of the second and the third bar systems permafrost features, e.g., polygons and long small channels, are well developed. The lichenometric measurements date the time of bar stabilisation, and allow to correlate the age of the lacustrine terraces. Two profiles, perpendicularly to the shoreline, were mapped in order to investigate the morphological features, the micro-relief and changes in vegetation cover of the beach ridges (Tables 31 and 32).

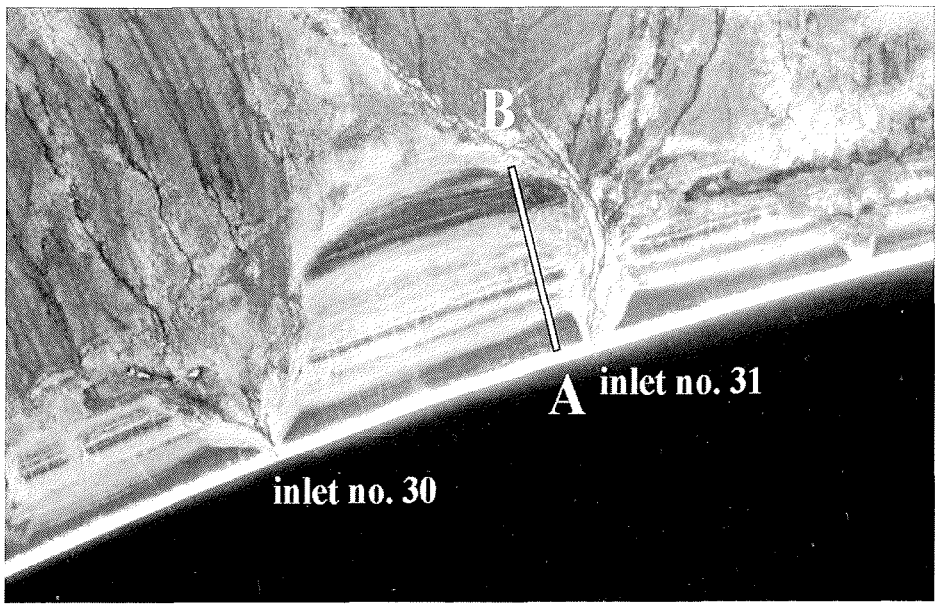

Figure 68: *Aerial photograph showing the beach bar system on the northern coast of Lake El'gygytgyn; the line A-B marks the lichenometric profile GS-8503 (see Fig. 67); source: Russian aerial photo (undated).*

Table 31: *Profile GS-5403 along the northern beach ridges.*

profile:	GS-5403	
location:	67° 32.653′ N; 172° 04.772′ E Lake El'gygytgyn, northern shoreline, beach ridge system 300 m to the west of inlet stream no. 33, from south to north	
unit	distance (m)	description
1.	0.0 - 3.0	modern beach
2.	3.0 - 5.4	bar line, 0.5 m high
3.	5.4 - 14.4	modern wave-cut trenches, four levels, 0.5 - 2.6 m above lake level
4.	14.4 - 30.2	first beach ridge, traces of recent or subrecent coastal activity, three types of lichen covers: • *rhizocarpon sp.*, light green • black elliptic lichens, thallus 1 mm thick and 30 - 50 mm in diameter • *pamelia sp.*, black, dark red leaved, up to 60 mm in diameter
5.	30.2 - 33.8	distal slope of the first beach ridge; rare, poorly developed periglacial polygons
6.	33.8 - 53.6	first moat between beach ridges, depth ~1 m, some periglacial polygons
7.	53.5 - 94.4	second beach ridge, 1.0 - 1.5 m higher than the first one, some periglacial features: • longitudinal and cross channels (depth: 15 - 20 cm) • periglacial polygons
8.	94.4 - 120.4	second moat between beach ridges, surface covered with polygons, in the polygon centres small pebbles and non-rounded rock fragments occur, grass vegetation along the margins of the polygons
9.	120.4 - 129.4	third beach ridge, 0.3 - 0.5 m higher than the second one, surface covered with polygons, in the polygon centres mainly non-rounded rock fragments occur
10.	> 129.4	tussocks tundra, swampy

Table 32: *Profile GS-8503 along the northern beach ridges.*

profile:	GS-8503	
location:	67° 32.470´ N; 172° 03.005´ Lake El´gygytgyn, northern shoreline, beach ridge system 40 m to the west of inlet stream no. 31, from south to north	
unit	distance (m)	description
1.	0.0 - ~10.0	modern beach; pebbles, sandy, gravelly, poorly cemented 4 modern berms formed by storms, uppermost step approx. 1.7 m above lake level,
2.	~10.0 - 12.0	moat between beach and first beach ridge, filled with snow and water
3.	12.0 - 61.0	first beach ridge, 3 m high proximal side: traces of modern formation by storms and waves, yellowish green colour, no lichens, fresh rock surfaces, no permafrost features top and distal side: inactive, blackish green, pebbles covered with *rhizocarpon sp.*, no permafrost features
4.	61.0 - 72.5	first moat between beach ridges, almost no lichens (bright stripe between dark stripes on aerial photo in Fig. 68), indistinct permafrost features (weak crests with larger pebbles, parallel to the shore, rare polygons), some spots with grass vegetation
5.	72.5 - 80.6	proximal slope of second beach ridge, inclination 2 - 3°, some periglacial forms: • longitudinal permafrost channels up to 30 cm depth • crests with larger pebbles mosses within the channels, accumulations of sinter-like *pamelia sp.* on the pebbles
6.	80.6 - 133.6	crest of the second beach ridge, top 19 m to the North of the first moat centre, clearly visible periglacial features: • shallow polygons, some centres with fresh turned pebbles (no lichens), gouges on some pebbles • longitudinal permafrost channels, 30 - 40 cm deep, up to 3 m wide developed vegetation cover: • rare shrubs • small areas with grasses • almost all pebbles partly covered with sinter-like lichens • less common *rhizocarpon sp.* • *pamelia sp.* especially within the polygon margins
7.	133.6 - 159.4	second moat between beach ridges, original surface modified by periglacial features: • polygons, centres with vertically bedded pebbles • longitudinal permafrost channels, up to 10 cm deep, increased number of lichens within the channels • permafrost "nodes"
8.	159.4 - 239.9	third beach ridge, surface modified by periglacial features: • polygons, centres with vertically bedded pebbles • longitudinal and transversal permafrost channels, up to 15 - 25 cm deep, 40 - 60 cm wide • permafrost "nodes" vegetation coverage depends on permafrost features (probably due to different moisture conditions): • shrubs mostly within channels • sinter-like lichens
9.	239.9 - 275.4	distal slope of third beach ridge, periglacial features: • polygons, vertical oriented pebbles, partly fractured • permafrost channels higher vegetation (grasses and shrubs) mostly close to the channels

continuation next page

Table 32: continuation

10.	275.4 - 327.4	low area behind the third beach ridge, numerous periglacial features: • polygons, hexagonal, up to 2.5 m in diameter • small permafrost channels accentuated by vegetation (grasses, shrubs)
11.	327.4 - 347.4	tussocks tundra, swampy, almost completely covered with vegetation

Preliminary conclusions about the age of the described beach ridges can be made based on analyses (300 and 500 measurements) of thalus diameter of *Rhizocarpon sp.* lichens (kindly conducted by Dr. A.A. Galanin, NEISRI Magadan). The results show that the bars were formed during the last 300 years, although their development probably started approx. 500 years ago (Fig. 67). The given variagramms testify the dynamic coastal environment during the ridge formation.

Thus, on the northern coast, the transportation along the coastline led to the observed system of modern and fossil beach ridges. Its relative age correlates with the age of the lacustrine terrace 3 m above lake level. In most areas of the northern coastline, only one, rarely two coastal bars, located one before another, were observed. Only in the region of the inlet no. 31 fragments of 4 coastal bars are established (Fig. 68). More ancient bars can only be found with detailed drilling, because they are currently covered by deluvial-solifluction tails and talus fans of temporal channels.

On the northeastern coast the shoreline was strongly influenced by the youngest tectonic movements and active slope processes. The coastline here on long sections is represented by abrasion scarps and a narrow beach.

Two km to the west and northwest of the modern shoreline, deluvial-solifluction tails containing lacustrine pebbles are still preserved on the surface. They occur especially near the steep mountain slopes and close to the watersheds between the inlet streams. The pebbles are strongly weathered and show little differences compared to the rock debris within the slope sediments. Their lacustrine origin is only evidenced by the heterogeneous petrographic composition. Closer to the lake, at a distance up to 1.5 km from the shoreline, the situation is complicated by periglacial dells, swamps, and areas occupied by placers of angular rock fragments without vegetation. The characteristics of the morphology of the beach ridges on the northern coast show the considerable migration of the shoreline towards the south. The bar series located along the northern coast between the inlets nos. 20 and 35 proves the machinery of shoreline retreat that took place during the entire Quaternary.

5.3.2 Terrace 10 m below Lake Level

(J. Brigham-Grette, M. Melles, O. Juschus)

Careful bathymetric soundings and excellent water clarity permitted the more precise delineation of the shallow submerged shelf around the southern end of Lake El'gygytgyn in summer 2003. The shelf today extends from the shore to a water depth of ca. 12 m at which point slope of the lake floor steepens quickly

toward the deep basin to depths of 100 m or more. The width of the shelf along the southern shore varies from 0.7 to 1.0 km and its surface is predominately composed of rippled sand and large patches of subangular to angular lag gravel and cobbles. Near river inlets, e.g., streams 49 (Lagerny) and 50, the shelf is littered with clumps of detrital peat and turf bank derived from the local catchment during the spring freshet. Also littering the shelf bottom were an impressive number of decaying birds, contributing nutrients to the lake system.

At two locations along the southern shelf edge, in water depths of 11 - 12 m, we discovered a clear morphological bench approximately 1 - 1.5 m in height that we hypothesize may represent a wave cut scarp formed when lake level was lower in the past (Fig. 69). The shelf is relatively flat to a depth of about 11.0 to 11.5 m, marking the top of the observed bench. The scarp at the back of the bench could be traced laterally for about 20 m. It is nearly vertical and broken with a cliff-like character. This morphology suggested to us that the shelf deposits backing the cliff were either very stiff muds or perhaps composed of bedrock. Blocks of material that seemed to make up the cliff typically litter the floor of the bench as seen from the surface. A 2.5 m sediment core (Lz1028) taken of the shelf sediments shoreward of the cliff consists of sandy gravel and extremely stiff mud (while it took "only" 2 hours for us to pound the core barrel completely in, it took just over 5 hours to extract it (Table 33). A 2.2 m sediment core taken offshore the bench, in contrast, is built up of normally consolidated sand and gravel, with incised horizons rich in detrital organics.

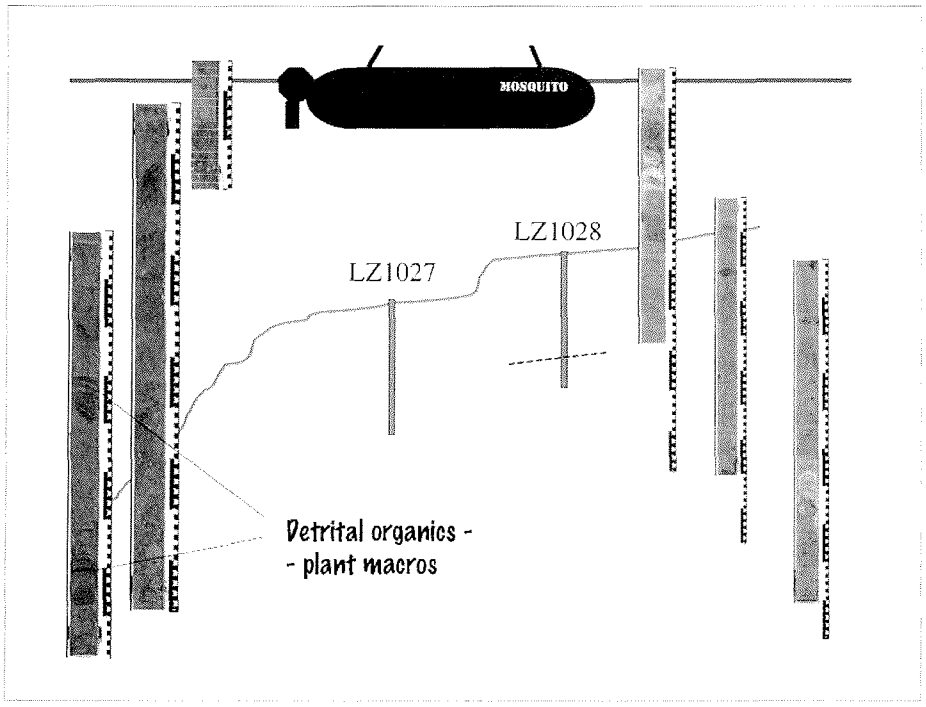

Figure 69: *Relative position of cores taken on and above the bench at the southern shelf of Lake El'gygytgyn.*

Table 33: *Cores taken in summer 2003 from the submerged bench at the southern shelf edge of Lake El'gygytgyn (* = SL - gravity corer; KOL - piston corer).*

core	ID	position latitude	position longitude	water depth (m)	date	gear*	recovery (cm)
Lz1027	-1	67°27.40' N	172°11.01' E	10.5	07-24-03	SL	0 - 2
	-2				07-24-03	KOL	0 - 223
Lz1028	-1	67°27.38' N	172°11.00' E	8.2	07-24-03	SL	0 - 3
	-2				07-24-03	KOL	0 - 253

This submerged cliff could have two origins that we have considered so far. First, we hypothesize that during most of the last full glacial cycle, lake levels were probably well below the level of the modern outlet. Decreased regional precipitation and aridity, in concert with sublimation through the ice cover in glacial winters and from leads during glacial summers, likely allowed lake levels to fall exposing the shallow shelf. This scenario is consistent with the observation that the full glacial portions of the sediment cores from the central lake (e.g., PG1351) are lacking in littoral diatom floras and dominated by planktic floras. A drop in lake level to the edge of the shelf would have significantly reduced available habitat for littoral diatoms. Hence the scarp, perhaps eroded by lake ice, might represent the mean position of lake level during the last glacial cycle. We further speculate that the stiff muds comprising the shelf beneath the surface lag gravel and sand, may have been deposited during an earlier part of the lake's history when water depths may have been as much as 35 - 40 m above present. Work on this shelf core is ongoing.

A second, though less likely interpretation is that the cliff at both locations along the south shore represents the upper headwall of a set of giant slump scars of unknown age. This interpretation is not supported by the seismic stratigraphy and we think it's improbable that a block of this height (over 100 m high) would not have failed entirely and come to rest in the deepest portion of the lake.

6 LAKE SEDIMENT CORING

6.1 Hemipelagic Sediments in the Central Lake

6.1.1 New long Record Lz1024

(O. Juschus, V. Wennrich, S. Quart, P. Minyuk, M. Melles, C. Gebhardt, F. Niessen)

Introduction – Lakes are one of the best natural archives for paleo-environmental investigations, because they function as natural long-term sediment traps on the continents. Therefore, lacustrine sediments contain more continuous information than other terrestrial deposits. Further on, detailed analysis of the lake sediment composition can supply proxies which reflect the regional environmental and climatic histories at least qualitatively, but via transfer functions also quantitatively. Last but not least, lake sediments often are well datable. e.g., by radiocarbon and luminescence techniques, and in

general are formed with a rather high sedimentation rate, allowing a good temporal resolution of the analytical data with good age control.

First sediment coring was conducted on Lake El'gygytgyn during the expedition in 1998 (Chapter 2.1, p. 6). Two cores recovered from the central part of the lake, PG1351 and PG1352 (Fig. 70), penetrated 12.7 m and 4.1 m, respectively. With a basal age of 250 ka (Nowaczyk et al., in press) core PG1351 at that time was the longest continuous sediment record from the entire terrestrial Arctic. One of the objectives of the expedition to Lake El'gygytgyn in 2003 was to take another, if possible even longer record from the central lake. Similarities or differences in the sediment succession of this new core compared to the existing core PG1351 should show how representative sediment successions from the central lake are for the regional climatic and environmental development, and how strong they are affected by local events.

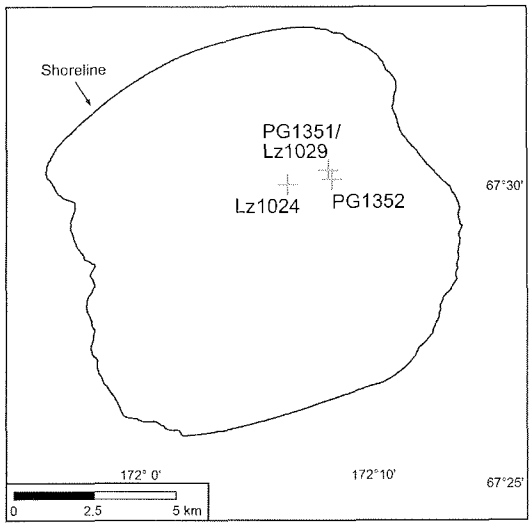

Figure 70: *Long sediment cores available from the central part of Lake El'gygytgyn. Cores PG1351 and PG1352 were sampled in 1998, cores Lz1024 and Lz1029 (the latter at the same position as PG1351) in 2003.*

Methods – The new long core composite, Lz1024, was recovered with coring devices constructed by UWITEC Corp. (Austria). A gravity corer was used for proper sampling of the water-sediment transition. Deeper sediments were collected with a percussion piston corer. The piston corer enables sampling of up to 3 m long sections from defined sediment depths. Thus, much longer composite core sequences can be obtained by coring of several overlapping sections. A more detailed description of the coring equipment was given by Melles et al. (1994).

Coring of Lz1024 (67°30.13´ N; 172°06.46´ E) was performed during the spring campaign, from the frozen lake surface through holes in the lake ice. A tent was built around the tripod to protect the operation against heavy winds. Coring then started on May 16, 2003. The last segment was recovered on May 29, 2003. For the composite core the segments were taken with an overlap of approximately 1 m, based on field measurements at the piston rope and subsequent calculations considering incomplete core segments (Fig. 71). Core Lz1024-7 had to be repeated as Lz1024-8, because an oversight led to a release of the piston in the water column. To avoid sediment disturbances by using one borehole repeatedly, coring was performed through three holes in the lake ice (about 1 m apart), which were used one after another.

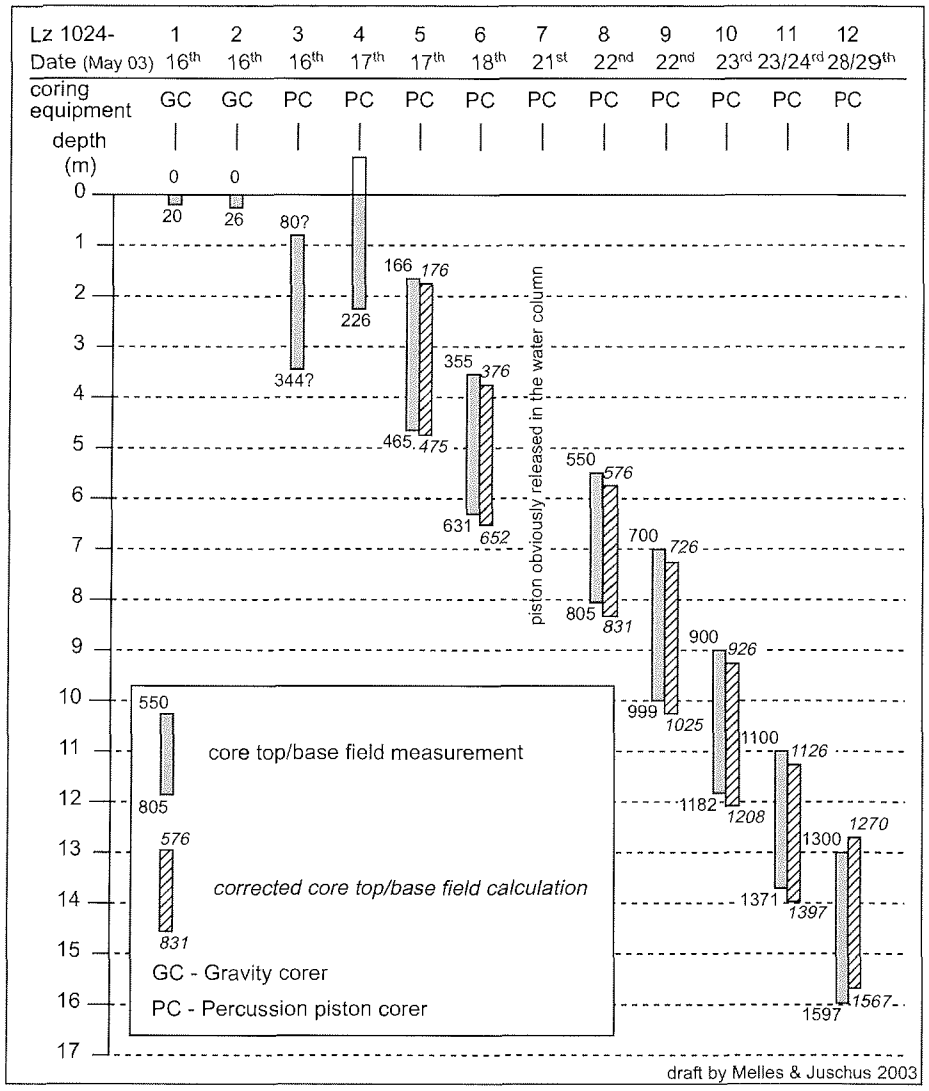

Figure 71: *Coring process scheme of Lz1024 (all values based on field measurements and field corrections).*

In the field, the cores were kept at slightly positive temperatures to protect them against frost damage or too high temperatures. To do so, they were stored in isolated boxes, which were conditioned during spring by adding bottles filled with hot water and during summer by putting them inside the permafrost cellar near the cabin. After the expedition, the cores were stored in cold rooms constantly at +4°C.

Prior to the opening of the lake sediment cores at the University Leipzig, whole-core physical property measurements were perfomed on them at the AWI

Bremerhaven, using a Multi-Sensor-Core-Logging system (MSCL, Geotek, Hazlemere, UK). Besides density and p-wave velocity, the magnetic susceptibility was measured (with a Bartington MS-2 loop sensor). The magnetic susceptibility data were used for the first core correlation.

First results – Two gravity core segments, Lz1024-1 and -2, and nine piston core segments, Lz1024-3 – Lz1024-12 (excl. Lz1024-7), were successfully recovered at site Lz1024 (Fig. 71, Table 34). The magnetic susceptibility data show distinct variations in all core segments (Fig. 72). Horizons of high susceptibilities are believed to reflect warm climates, when a semi-permanent lake ice cover leads to mixing of the water column with good preservation of magnetite in oxic bottom waters (Nowaczyk et al., 2002). Low susceptibilities, in contrast, can probably be traced back to cold climates, leading to a permanent ice cover and a stratified water column with anoxic bottom waters and, consequently, significant magnetite dissolution. The regional causes for the variations in susceptibility justify use of this proxy as a tool for core correlation, which leads to a depth of 16.30 m at the base if the core composite.

Hence, core Lz1024, recovered in 2003, obviously is about 3 m longer that core PG1351 from 1998. Taking the average sedimentation rates determined in core PG1351, core Lz1024 thus could reach about 300 ky BP at its base. Furthermore, the excellent correlation of the variations in magnetic susceptibility in both cores (Fig. 72) indicates that the sediment successions are predominantly controlled by regional rather than local affects.

Table 34: *Core sections sampled during the expedition in 2003 at site Lz1024 (67°30.13´ N, 172°06.46´ E) in the central part of Lake El´gygytgyn (for location see Fig. 70).*

station	core no.	date	gear	measured field depth (cm)	corrected field depth (cm)	correlated depth (cm)
Lz1024-	1	05-16-03	gravity corer	0 - 22	0 - 22	0 - 22
	- 2	05-16-03	gravity corer	0 - 26	0 - 26	0 - 26
	- 3	05-16-03	piston corer	0 - 266	0 - 266	64 - 330
	- 4	05-17-03	piston corer	0 - 226	0 - 226	0 - 226
	- 5	05-17-03	piston corer	166 - 465	176 - 475	174 - 473
	- 6	05-18-03	piston corer	355 - 631	376 - 652	378 - 654
	- 7	05-21-03	piston corer	0 - 297	0 - 297	0 - 297
	- 8	05-22-03	piston corer	550 - 805	576 - 831	591 - 846
	- 9	05-22-03	piston corer	700 - 999	726 - 1025	738 - 1037
	- 10	05-23-03	piston corer	900 - 1182	926 - 1208	938 - 1220
	- 11	05-23/24-03	piston corer	1100 - 1371	1126 - 1397	1160 - 1431
	- 12	05-28/29-03	piston corer	1300 - 1597	1270 - 1567	1340 - 1637

6.1.2 Uppermost Sediments at Coring Site from 1998

(J. Brigham-Grette)

During the first coring campaign on Lake El´gygytgyn in 1998 the uppermost 80 cm of core PG1351 (Fig. 70) were not kept in the core liner for transport. Instead, they were cut into 2 cm slices and filled into vials immediately after the core recovery, in order to avoid disturbance of these soft, water-rich sediments during transport to Germany.

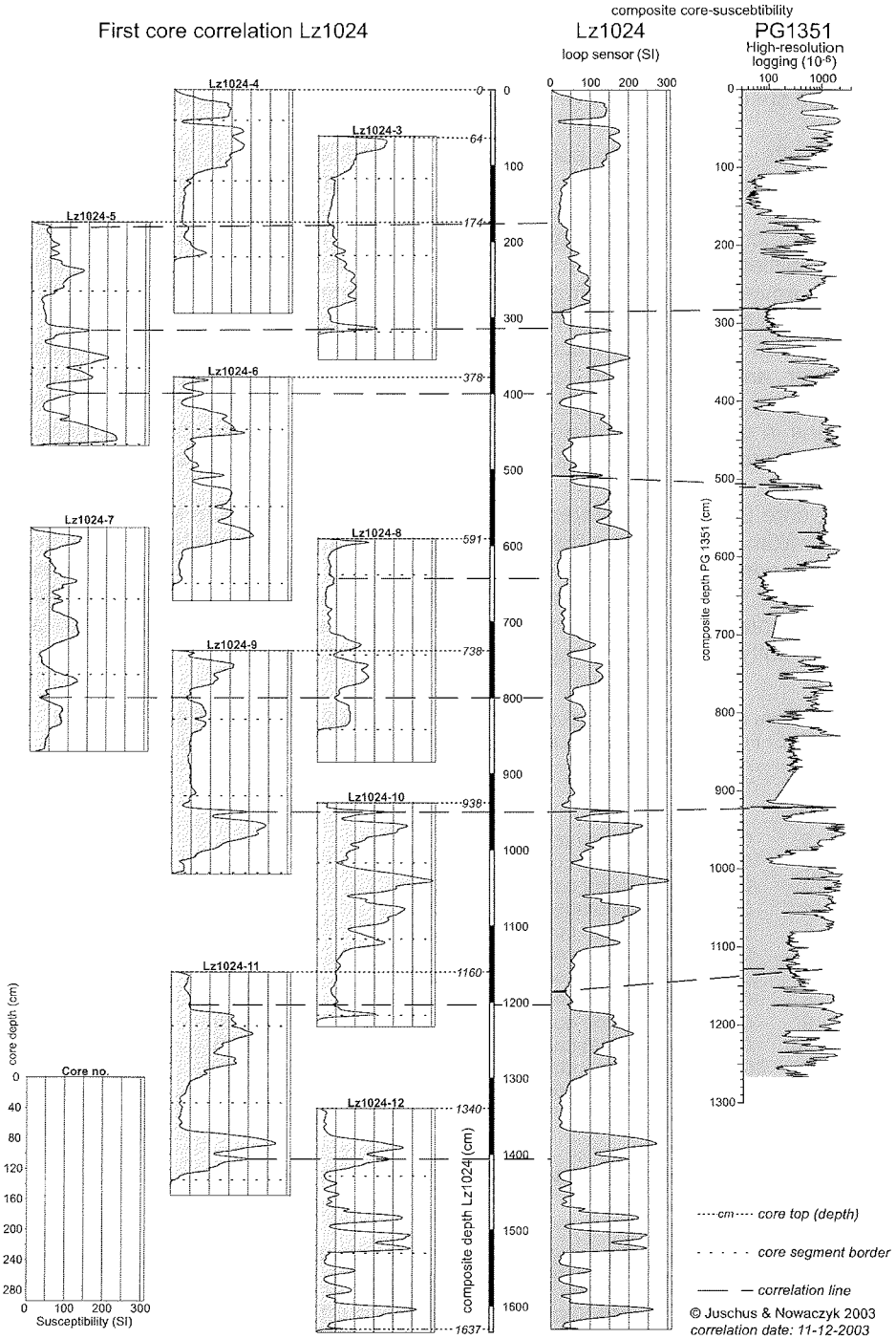

Figure 72: *Correlation of the magnetic susceptibilities in core segments from site Lz1024 to a 16.3 m long composite core, and its comparison the composite core PG1351.*

The disadvantage of this subsampling in the field is that high-resolution data, such as the magnetic susceptibilities measured in 1 mm steps on the remaining core PG1351, are not available from the uppermost 80 cm. In addition, it turned out that the surface sediments in Lake El'gygytgyn consist predominantly of clastic sediment components, making them much more stable than highly biogenic deposits expected to have cored in 1998.

Thus, it was decided to repeat the coring of the uppermost lake sediments at site PG1351 (corresponding with Lz1029; 67°30.37' N; 172°08.24' E), and keep the cores in the liners. The undisturbed sediment sections, firstly, allow to complete the high-resolution datasets from this site and, secondly, supply additional material to conduct new analyses. Coring was carried out in summer 2003 from the floating platform "Mosquito" of the Leipzig University, with the UWITEC gear described in Chapter 6.1.1. Altogether 5 gravity cores and 4 percussion piston cores were recovered (Table 35), meant for the following disciplines (and institutions):

- Lz1029-1 biology of fluff layer (UMass Amherst) and sedimentology (Leipzig University)
- Lz1029-2 pore water chemistry, org. and inorg. geochem. (UMass Amherst)
- Lz1029-3 organic and inorganic geochemistry (UMass Amherst)
- Lz1029-4 surface sediment composition (Leipzig University, Chapter 4.7.2)
- Lz1029-5 physical properties, paleolimnology (Leipzig University)
- Lz1029-6 pore water chemistry, org. and inorg. geochem. (UMass Amherst)
- Lz1029-7 organic and inorganic geochemistry (UMass Amherst)
- Lz1029-8 physical properties, paleolimnology (Leipzig University)
- Lz1029-9 physical properties, paleolimnology (Leipzig University)

Table 35: *Core sections sampled during the expedition in 2003 at site Lz1029 in the central part of Lake El'gygytgyn (same site as PG1351 sampled in 1998; for location see Fig. 70).*

station	core no.	position latitude	position longitude	date	gear	recovery (cm)
Lz1029	- 1	67°30.37' N	172°08.24' E	07-25-03	gravity corer	0 - 22
	- 2			07-25-03	gravity corer	0 - 22
	- 3			07-25-03	gravity corer	0 - 20
	- 4			07-25-03	gravity corer	0 - 2
	- 5			07-28-03	gravity corer	0 - 18
	- 6			07-28-03	piston corer	0 - 234
	- 7			07-28-03	piston corer	0 - 291
	- 8			07-30-03	piston corer	0 - 225
	- 9			07-31-03	piston corer	0 - 129

The core composite Lz1029 is composed of the cores Lz1029-5, Lz1029-8, and Lz1029-9. Correlation of these cores, leading to a composite length of 1.7 m, was performed on the basis of physical property data and sediment descriptions. A first comparison with core PG1351 indicates an excellent correlation but a better quality of core Lz1029.

Because anoxia leads to the dissolution of magnetite and a loss of magnetic susceptibility (Nowaczyk et al., 2002), the origin, flux, and decomposition of organic matter (consuming oxygen) needs to be understood. This is particularly

important if we are to understand how the magnetic susceptibility record and other proxies are linked to regional climate via changes in the water geochemistry of this large lake. One approach to understanding this process is to conduct studies of the conditions controlling the mass balance and phases of iron, its diagenesis and authigenesis, in particular processes at and above the redox boundary driving vivianite diagenesis, haematite/magnetite dissolution, or both. In an attempt to isolate processes leading to diagenesis, porewaters were extracted in the field under ambient conditions from one piston core (Lz1029-6) and altogether three gravity cores (Lz1029-2, Lz1029-6 and Lz1058-1, Fig. 73).

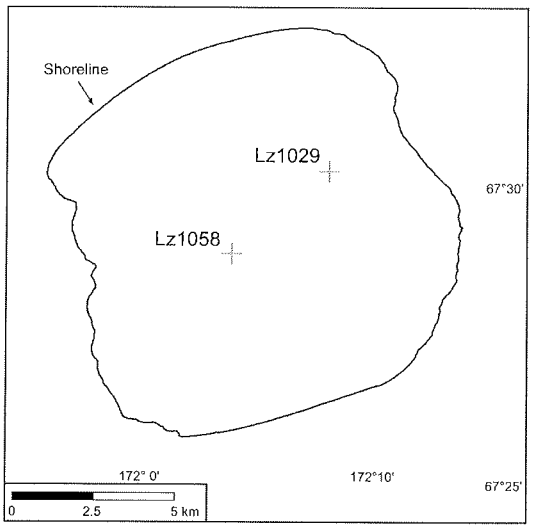

Figure 73: *Coring sites with cores, recovered for porewater analyses.*

The sediments from these cores and sediments from untouched cores (including piston core Lz1029-7 and gravity core Lz1029-3) are now being studied for their organic and inorganic geochemistry. One potential outcome would be the ability to realistically model the time required to sustain levels of anoxia appropriate for explaining seemingly climate related changes in sediment mineralogy.

6.2 Debris Flows on the Western Slope

6.2.1 Shallow Seismic Survey

(C. Gebhardt, F. Niessen, M. Melles, O. Juschus)

Acoustically transparent sediment bodies, first recorded at the slopes of Lake El'gygytgyn in shallow seismic (3.5 kHz) data obtained in summer 2000 (Fig. 74), were interpreted as debris flows or other large-scale sediment deformations (Niessen et al., in press). During the expedition in 2003, a detailed 3.5 kHz profiling was carried out for mapping of the debris flow distribution (Chapter 7.3; Fig. 83, p. 128).

Debris flows do not occur continuously in time, but are enriched within several layers of the upper sedimentary unit, probably linked to paleoclimate changes. The upper sedimentary unit of Lake El'gygytgyn is well stratified and locally – mainly at the lake borders – intercalated with debris flows of up to several meters in thickness. The debris flows are more frequent in the western part of the lake and might have their source in slope instabilities where permafrost soil starts to thaw. Two main types of debris flows were recognised:

- debris flows with a distinct "nose" at their front end, forming a well-defined distal border;
- debris flows that gradually thin out, forming a diffuse distal border, poorly visible in the profiles.

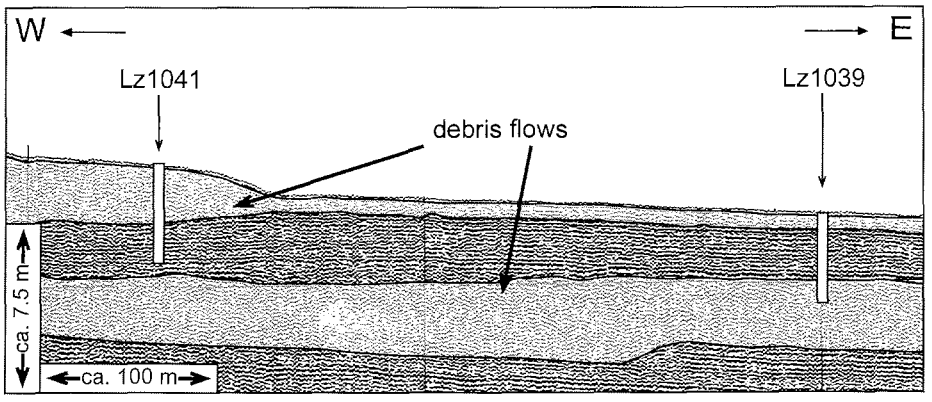

Figure 74: *Shallow seismic profile (3,5 kHz) obtained from the western part of Lake El'gygytgyn in summer 2000. Two debris flows are accentuated with grey colour. The rectangles mark the positions of sediment cores recovered in summer 2003 which penetrate the debris flows; for location see Fig. 77.*

6.2.2 Ground Penetrating Radar Survey
(G. Schwamborn, G. Fedorov)

On the shelves of Lake El'gygytgyn the 3.5 kHz acoustic waves did not penetrate the deposits, probably due to their predominantly coarse-grained nature. In consequence, the shallow seismic survey (see Chapter 6.2.1) did not supply any information on the sediment thickness and layering in these areas, including the western shelf, where a piston core transect crossing a subrecent debris flow starts (Chapter 6.2.3). In order to obtain some basic information on the sediment architecture prior to the coring, therefore, a ground penetrating radar (GPR) survey was carried out close to the western shoreline from the lake ice cover in spring 2003 (Fig. 75).

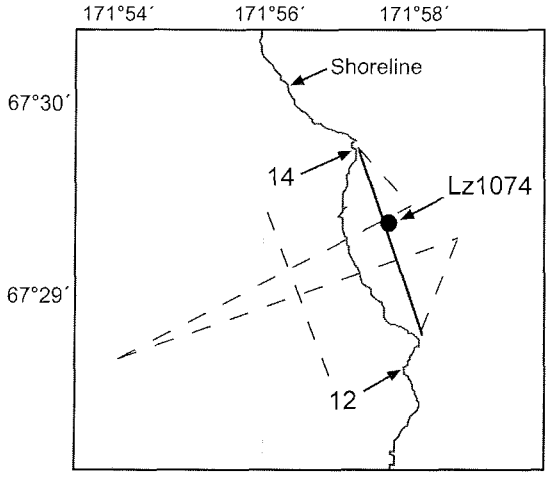

Figure 75: *Position of GPR profiles measured on- and offshore of inlet streams nos. 12 and 14 at the western shore of Lake El'gygytgyn. The solid line marks the profile presented in Fig. 76 and discussed in the text.*

In the GPR profile running between the two small capes created by the inlet streams 12 and 14 (Fig. 75) the lake floor and the uppermost sediment unit including some internal reflectors (Unit 1) are visible beneath a water column of less than 3 m (Fig. 76). A second prominent interface runs distinctly at about 200 ns (top of Unit 2). The thickness of Unit 1 roughly corresponds to 2.7 m. In order to penetrate the physical boundary between Units 1 and 2 for sediment analysis, a piston core (Lz1074, Fig. 76) has been recovered during the summer season from a sediment depth 2.0 m to 3.6 m below lake bottom (Chapter 6.2.3).

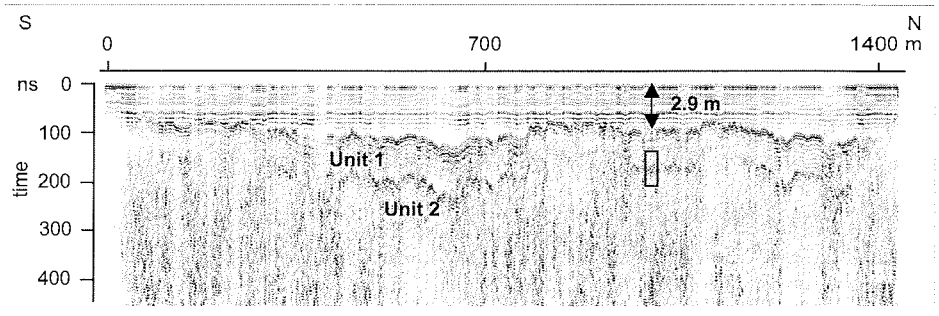

Figure 76: *Cape to cape GPR profile at the western shore of Lake El'gygytgyn, between the mouths of inlet streams 12 and 14 (for location see Fig. 75), showing lateral changes in water depth and sedimentary units 1 and 2. The rectangle indicates the position of core Lz1074.*

6.2.3 Lake Sediment Coring

(O. Juschus, M. Melles)

The acoustically transparent sediment bodies in shallow seismic data (3.5 kHz), interpreted as debris flows (Chapter 6.2.1) are more frequent and increase in thickness towards the shore. This is the case especially in the western lake, where one of them was recognized close to the sediment surface (see Fig. 74).

In order to investigate the genesis of these sediment bodies, and their impacts on the deposition in the central part of Lake El'gygytgyn, it was decided to core a transect in 2003 from the western shelf into the deep basin. Besides cores Lz1024 and Lz1029/PG1351 from the central lake (Chapter 6.1, Fig. 70, p. 111), the transect consists of cores Lz1039 and Lz1041, which penetrated the subrecent sediment body at the western slope, and core Lz1074 from the adjacent shelf (Figs 74 and 77).

Preliminary data from cores Lz1039 and Lz1041 have confirmed that that the acoustically transparent sediment body close to the surface of the western slope represents a debris flow. The lower part of the debris flow is stratified, probably reflecting an initial stage with sediment sliding and limited sediment mixture. Massive sediments above and in front of the stratified deposits indicate a second stage with turbulent transport. The debris flow led to basal erosion of ca. 1 m thick unconsolidated sediments along parts of his flow path. It produced a suspension cloud in the lake water, whose deposition caused the formation of

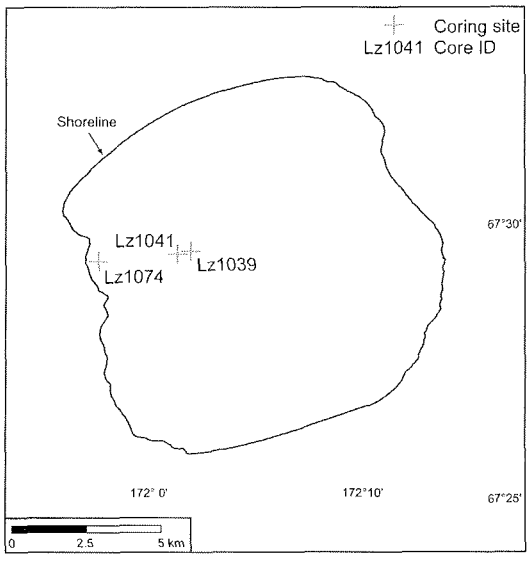

Figure 77: *Coring positions chosen for debris flow investigations.*

a graded subrecent layer in the entire lake, i.e. not only in front but also on top of the debris flow. Hence, this layer was not a product of a density-driven turbidity current, but of 'pelagic rain' following Stokes' Law. In consequence, it was not erosive. According to results from the long core, these conclusions are valid for the majority if not for all of the mass movement events that have taken place in Lake El'gygytgyn during the past 300 kyr. A more detailed discussion of the gravitational sediment transport in the lake, along with statements on the frequency and preferred times of the debris flows is given by Juschus et al. (2004).

Additional sediment coring was carried out on the western shelf of Lake El'gygytgyn, which is assumed to be one of the major source areas of the debris flows. Coring site Lz1074 (67°29.41' N; 171°57.68' E) is located on a GPR profile measured between the two small capes created by the inlet streams nos. 12 and 14 (Figs 75 and 77). One piston core was recovered, from the sediments at 2.0 - 3.6 m below lake bottom. The core Lz1074 consists entirely of coarse-grained sand, gravel and pebbles. At 70 cm core depth (2.7 m below lake bottom) a pebble with a diameter of about 5 cm was found within finer, gravelly sediments. This is the approximate depth in which a distinct reflector occurs in the GPR profile (Fig. 76, Chapter 6.2.2).

6.3 Geochronology of the Lake El'gygytgyn Sediments
(J. Brigham-Grette)

One of the most challenging aspects of determining the geochronology of the sediments from Lake El'gygytgyn has been in understanding the apparent disconnect between the radiocarbon (^{14}C) age of bulk organic carbon and macrofossils vs. the age model based on extrapolation from ages based on optically stimulated luminescence (OSL) dating (Nowaczyk et al., 2002; Forman et al., in press). For example, Apfelbaum et al. (unpubl.) dated several samples from one of the surface cores, PG1463-1 collected in 2000, to resolve the age discrepancy in the upper sediments of PG1351 collected in 1998. AMS ^{14}C ages on the extracted humic acids are slightly older than the IRSL ages from the upper part of core PG1351 (Nowaczyk et al., 2002). While it is well known that bulk humic acid dating can produce ages which are older than all of the other organic fractions (Abbott and Stafford 1996) the offset was not

systematic. Yet we speculated that during glacial intervals, the lake remained perennially ice covered, thereby reducing atmospheric exchange within the organic fraction.

Seven wood macrofossils and four bulk sediment samples were taken at approximately the same stratigraphic horizons and ^{14}C ages were converted to calendar scale with the CALIB program (Stuiver et al., 1998). In general, ages from humic acids are older than the wood samples (Table 36). The dates from all samples fall within the 5,600 - 8,800 calendar year range, however the wood sample ages are extremely variable and exhibit no clear linear trend. The best explanation for this is that terrestrial carbon is likely stored on the landscape around the lake basin for thousands of years, prior to deposition.

Table 36: *AMS ^{14}C ages of samples from core PG1463-1 (Apfelbaum et al., unpubl.). Ages from the upper part of core PG1351 are also shown for comparison (Nowaczyk et al., 2002).*

core PG1463-1: AMS ^{14}C on wood macrofossil samples			
sample ID	depth (cm)	cal. age (a)	error (a)
AA45090	22.4	6691.5	±137
AA45091	23.1	7846	±220
AA45092	24.4	6765	±260
AA45093	25.9	8081.5	±229
AA45094	26.9	6459	±358
AA45095	29	5666	±166
AA45096	33.7	6871.5	±313
AA45097	34.3	8722	±176
core PG1463-1: AMS ^{14}C on humic acids			
Sample ID	Depth	cal. age	error
BETA-168865	22.2	7260	±40
BETA-168866	24.3	7570	±40
BETA-168867	33.6	7500	±50
BETA-168868	34.2	7520	±40
core PG1351: AMS ^{14}C on humic acids			
Sample ID	Depth	cal. age	error
NSRL-11027	21-23	7635	±60
NSRL-11028	64-66	14230	±284

In an attempt to further understand the carbon reservoir and sources at the lake, it was decided to measure a ^{14}C age of the water column to determine if the lake contained a significant hard water effect. For this purpose, four 500 ml borosilicate glass bottles obtained clean from the Woods Hole Oceanographic National Oceanographic Sciences Accelerator Mass Spectrometry Facility, were filled with water from 25 m depth from the centre of the lake (Table 37).

Table 37: *Radiocarbon dating samples of lake waters from site Lz1024, central Lake El'gygytgyn (water depth at the site of collection was 170 m).*

sample ID	position		volume	water depth	date
	latitude	longitude		(m)	
E03BG 213 A	67°30.126' N	172°06.462' E	500 ml	25	08-03-03
E03BG 213 B	67°30.126' N	172°06.462' E	500 ml	25	08-03-03
E03BG 213 C	67°30.126' N	172°06.462' E	500 ml	25	08-03-03
E03BG 213 D	67°30.126' N	172°06.462' E	500 ml	25	08-03-03

7 GEOPHYSICAL SURVEY

7.1 Introduction

(F. Niessen, C. Gebhardt, C. Kopsch)

The main objective of the second seismic campaign on Lake El'gygytgyn 2003 was to improve the preliminary data of 2000 for both quality and density. One important aim was to create a three-dimensional seismic data set including airgun and sediment echo sounding results of high quality to be included in a planned deep drilling proposal. What we learned from the first seismic study of Lake El'gygytgyn in 2000 (Niessen et al., 2000) were two important points:

1. Refraction data suggests the lake basin contains a total sediment thickness of 371 m overlying the impact breccia. Because the recent lake is only 171 m deep, the single-channel vertical reflection profiles of 2000 were strongly affected by multiples masking the lower 170 m of the sediment fill, including the sediment breccia interface. As a result of the strong reflection coefficients in the upper, well-stratified 180 m of the sediment fill, the multiples have high amplitudes and could not be eliminated using post processing techniques. Consequently, the improvements introduced to the 2003 field campaign were a multi-channel streamer and a more powerful airgun.
2. The time window to work on the lake with a small open vessel equipped with highly sophisticated but sensitive electronic systems is small. The lake becomes ice free around middle of July. Usually the regional weather starts to deteriorate around the middle of August, such that snow storms become frequent during the short arctic autumn. Strong winds up to gale force are a common feature at Lake El'gygytgyn all year round so that the days with good working conditions during the short arctic summer are usually in the order of 10. Consequently, another improvement for this year compared to the 2000 campaign was the simultaneous use of several systems, such as single- and multi-channel airgun techniques combined with sediment echo sounding, bathymetry, and magnetic investigations.

Although the expedition in 2003 required more helicopter capacity to transport gear from Pevek to Lake El'gygytgyn, the seismic investigations still depended on the use of a small open platform carried by four inflatable tubes. This vessel is too small to pull commercially available multi-channel streamers. To successfully update our system for the 2003 seismic campaign on the lake, in particular the multi-channel streamer needed to be developed. Once equipped the platform needed a safe harbour to be protected against stormy weather. We parked the vessel in the outlet stream of Lake El'gygytgyn, the Enmyvaam River, which is open only during the summer.

7.2 Methods

(F. Niessen, C. Gebhardt, C. Kopsch)

A Mini-GI-Gun (Sodera, France; courtesy of the University of Hamburg) was used as the acoustic source for both single-channel and multi-channel data acquisition. The gun was operated in airgun mode with a total chamber volume

of 26 cubic inches (for comparison: we used only 5 cubic inches in 2000). To power the gun, two air pressure sources were linked. We pre-compressed air up to 330 bar into 6 steel bottles placed on the platform, which have a total real volume of 198 litres (or 59,400 litres of compressed air). Two light-weight diving compressors (Bauer, Germany, model Oceanus) were used simultaneously for pre-compression and during profiling. Each compressor produced 140 litres of compressed air per minute in addition to the bottle reservoir. The gun pressure was adjusted by a reduction valve to 110 bars. Under normal conditions the air pressure reservoir and capacity lasted for about 8 to 10 hours or 3 profiles across the lake at a constant speed of 6 km/h. For profiles 1 to 6 the gun was shot in intervals of 10 seconds. After one compressor failed late in the campaign, we increased the trigger interval to 14 seconds for profiles 7 to 10. On profile 10 the gun pressure was set to 130 bars. For comparison, during the 2000 campaign, only one Bauer Oceanus compressor combined with one pressure bottle with 5 litres of real volume were used.

Two single-channel hydrophones were pulled along all profiles: a 20 element streamer (Geoacoustics Model CP937, UK), having an active length of 8 m, and a single hydrophone (ARS-Tech, Germany) were placed about 40 m and 30 m behind the vessel, respectively. In comparison with our efforts in 2000, the single-channel results this year were improved significantly for several reasons:

1. The gun was more powerful.
2. The old Geoacoustic streamer was replaced by a new one with better signal to noise ratio.
3. We amplified and filtered (100 to 1000 Hz) the 20 element streamer data with an analogue receiver (Geoacoustic model 5210, UK) prior to signal digitising using a digital receiver (Octopus model 360, UK). In 2000, the latter was directly linked via interface box to the 20-element hydrophone, which produced relatively noisy data of limited quality.

Single-channel data was stored together with trigger and GPS signals on a four-channel DAT-Recorder (Sony Model PC204Ax, Japan) at a sampling frequency of 24 kHz. On the Octopus digital receiver, single hydrophone or 20-element streamer, data were converted to SEG-Y format and stored on a DAT-tape recorder. All 20-element single channel streamer data were plotted in analogue mode on a chart recorder (Dowty, Model 3710, UK).

A 280 m long multi-channel streamer had to be constructed for the expedition in 2003 to Lake El'gygytgyn. The streamer consisted of 15 wide-band single hydrophones (10 to 10,000 Hz sensitivity, ARS-Tech, Germany). Each hydrophone had a pre-amplifier and its own cable connection to the vessel to provide the power supply for amplification and signal transmission. The advantage of this scheme is that the 15 hydrophones were individually transportable to fill only four portable aluminium transport boxes. In the field the hydrophones and cables were placed at full length on the beach of the lake to assemble them into a streamer. One important prerequisite for pulling this long streamer with the small vessel was the full self-floatation of the entire streamer. For floatation we used foam tubes commercially available in 2-m lengths as water pipe insulation (Tubulit, Switzerland). Starting at the rear end of the

280 m long lay of cables, hydrophone cables were then packed and sealed into the tubes successively, increasing the tube diameter from 15 mm internal and 44 mm external diameter for one cable to 37 mm internal and 75 mm external diameter for 15 cables, respectively. Each hydrophone was placed at a loose cable-end of 5 m length hanging out of the streamer tubes. During profiling at a speed of 6 km/h, buoyancy due to motion kept the hydrophones in a water depth of 1 m under the streamer. Each hydrophone formed one channel and the offset between the vessel and channel 1 had a length of 130 m. Distances between the hydrophones were 10 m. The basic principle of the streamer is illustrated in Figure 78. Since channel no. 15 was not functioning for electrical reasons, the streamer had a true active length of 140 m. On the vessel the signals were amplified according to cable lengths. This provided the same order of maximum amplitude for all 14 channels prior to data storage. The traces of all active channels were constantly monitored on a PC using the software PC-Scan. The signals were stored together with trigger and GPS data on a 16-channel DAT-Recorder (Sony Model PC216Ax) using a sampling frequency of 4 kHz. After profiling the streamer was towed on the beach at full length and finally dismantled.

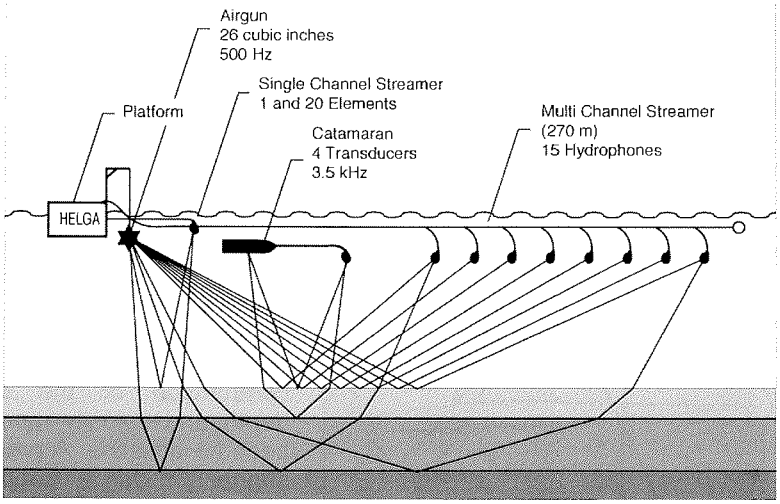

Figure 78: *Basic principle of seismic and sediment echosounding systems used during the expedition in 2003.*

A 3.5 kHz sediment echosounder (ORE, Model 140, USA) was in operation on all profiling tracks. We used a catamaran array with 4 transducers (Massa, USA) for signal transceiving and receiving, which was towed 30 m behind the vessel. The pulse length was 0.5 ms at 10 kW transmission power. Analogue data was printed on a chart recorder (Ultra, Model 120, UK) and stored on one channel of the Sony DAT-Recorder (Model PC204Ax, mentioned above). The system was triggered at 1 or 2 seconds. The trigger is synchronized with the airgun trigger using GPS time. No interference between the airgun and 3.5 kHz systems was observed during profiling. In 2003 we used the same 3.5 kHz system as in 2000 to ensure full compatibility of the data sets from both expeditions.

Navigation was performed along all track lines using a Russian GPS system (courtesy of AARI St. Petersburg) linked to a PC for data acquisition and storage. The same system was used during the expedition in 2000, which also included the circumnavigation of the lake close to the shoreline to provide digitised data of the lake periphery. During circumnavigation of the lake a constant lateral offset of a few hundred metres to the southwest was observed in the GPS positions. This offset is responsible for the fact that some track data of both the 2000 and 2003 expeditions cut across the shore line. Electronic equipment was installed on the same aluminium platform (RV "Helga"), which was used during the expedition in 2000. The platform has a frame size of 4 x 3 m and is equipped with 4 inflatable tubes and a 25 HP Honda outboard engine.

7.3 First Results

(F. Niessen, C. Gebhardt, C. Kopsch)

In total 10 airgun profiles were recorded in 2003 with a total length of 106 km (Fig. 79). Profiles 1 and 2 were recorded without the multi-channel streamer. For all other profiles, both single-channel and multi-channel data are now available (86.56 km). Together with the airgun data of the 2000 expedition we have increased the coverage of our profiles significantly to a total of ca. 185 km. Also, the multi-channel profiles EA03/03 and EA03/04 of 2003 are exactly on, or very close to sonobuoy refraction profiles of 2000 so that a good comparison of the different depth and velocity models will become possible. A preliminary suggestion for a deep-drilling location was crossed along 6 airgun profiles including 3 multi-channel profiles. In this area, a 16.5 m long sediment core was retrieved in 2003 for comparison with previous cores from 1998 (cp. Chapter 6.1.1; p. 110).

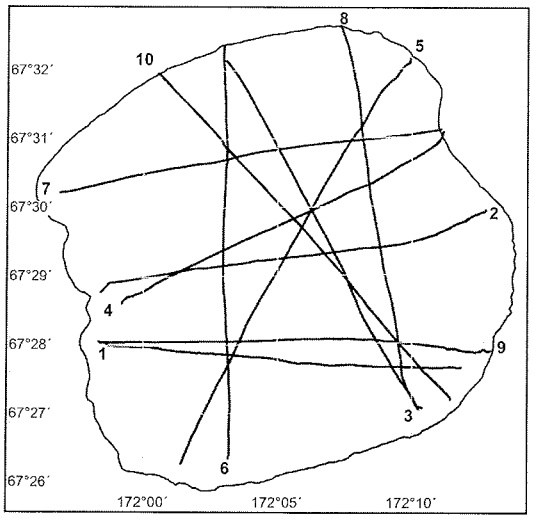

Figure 79: *Map of airgun profiles recorded during the 2003 expedition. The numbers refer to profile numbers (EA03/number) and are placed at the starting location of the profiles. Profiles 1 and 2 were recorded single channel only.*

The quality of the single-channel data, for example, profile EA03/05 crossing the lake from NE to SW direction, can be seen in Figure 80. Multiples are clearly visible below 500 ms two-way travel time in the centre of the lake. However, interpretation line "1" marks (Fig. 80) marks the depth where strong reflectors, indicative of well-stratified sediments, become weaker.

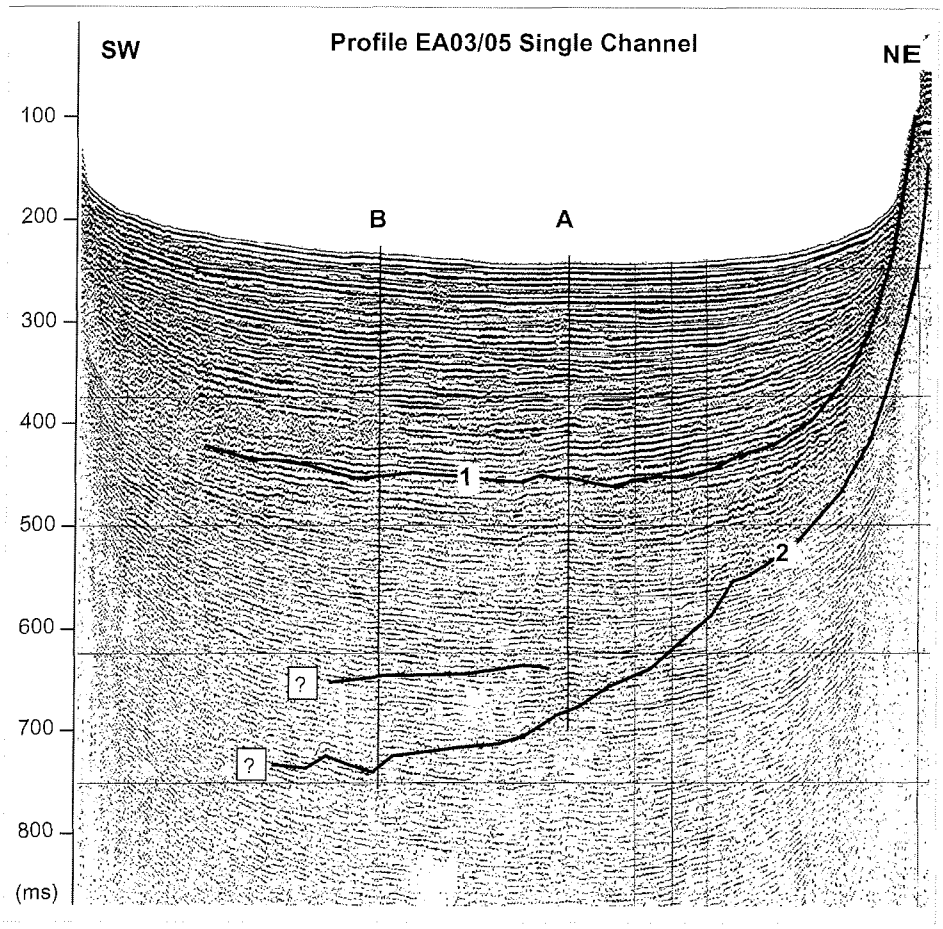

Figure 80: *Profile EA03/05 single channel analogue data. Lines "1" and "2" mark the transitions between the upper and lower sediment layer and brecciated bedrock, respectively; vertical lines "A" and "B" mark positions where total sediment thickness has been calculated (see text).*

This is consistent with the preliminary interpretation of the airgun data of 2000, suggesting that the seismic character of the sediment fill has two layers, an upper well-stratified layer and a lower more massive layer. Within the pattern of multiples between 500 ms and about 650 ms, a steeply dipping reflector is notable (just above interpretation line "2" in Fig. 80) in the northeastern part of the profile. As a first cautionary interpretation we suggest that this reflector is derived from the top of the impact breccia. Profile EA03/05 crossed a previously recorded sonobuoy profile (at line "A" in Fig. 80), which revealed refraction data including velocities and refractor depths (Niessen et al., 2000). Velocities of 1580 ms^{-1} and 1640 ms^{-1} were determined for the upper and lower sediment fill, respectively. The sediment/breccia interface was placed in a depth of 371 m subbottom. Using the above velocities a depth of 365 m subbottom was calculated for the dipping reflector at line "A" in Profile EA03/05 (interpretation line "2"). Considering the resolution in the refraction data this

estimate is in good agreement with the data from 2000 suggesting that, in places, the top of the impact breccia is possibly even visible in single channel data of 2003 despite the presence of multiples. If this is to be true, then a total sediment thickness of 418 m is calculated along Profile EA03/05 at line "B".

In the field we were not able to fully digitise and process the multi-channel data. However, to present an example of the quality of the data, multi-channel number 1 (135 m behind the vessel) recorded in SEG-Y format by the Octopus 360 digital receiver is compared with single-channel analogue vertical reflection data along Profile EA03/10 (Figs 81 and 82). Traces of channel 1 exhibit the same structures like those visible in the single-channel profile. Channel-1-data exhibit a good signal to noise ratio even at travel times of 800 ms, well below the expected surface of the impact breccia. We are confident that, once available, a CDP-stack of all 14 channels will significantly improve the seismic stratigraphy of Lake El'gygytgyn. It is also likely that Profiles EA03/10 were placed well across the impact centre uplift. Although, it is still difficult because of multiples to see the cone at the sediment/breccia interface (interpretation line "1" in Profile EA03/10, Fig. 82), a faulted anticline structure is clearly visible in the upper sediment layer above 250 ms of two-way travel time (question mark in Profile EA03/10, Fig. 82).

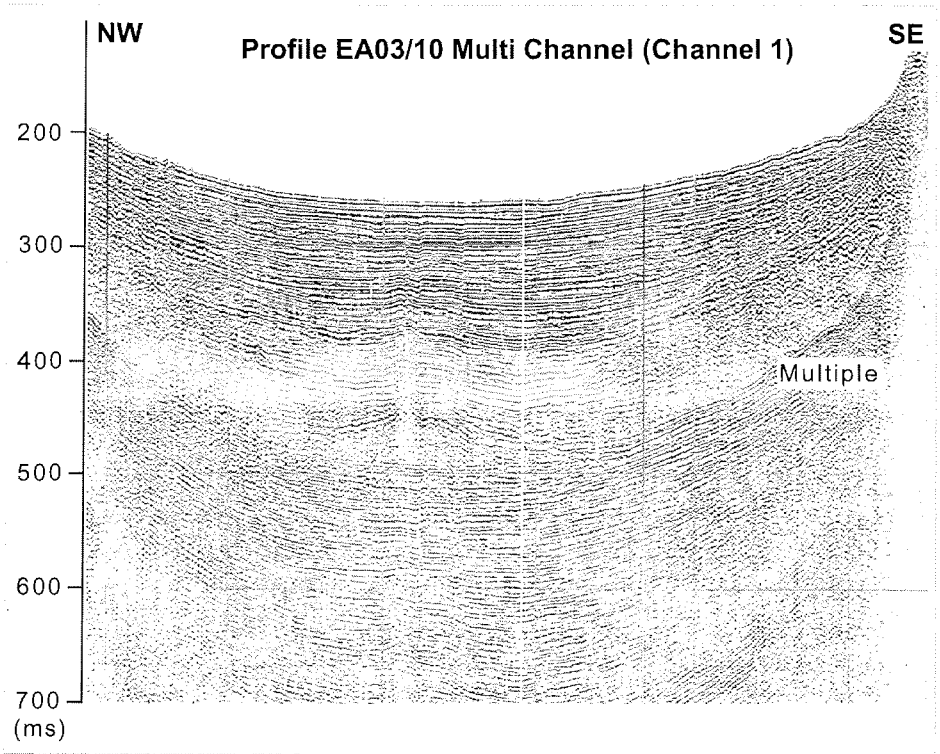

Figure 81: *Profile EA03/10 multi-channel streamer data (unprocessed digital data of channel 1 only). Horizontal grid-line spacing is 100 ms (see Fig. 82 for comparison).*

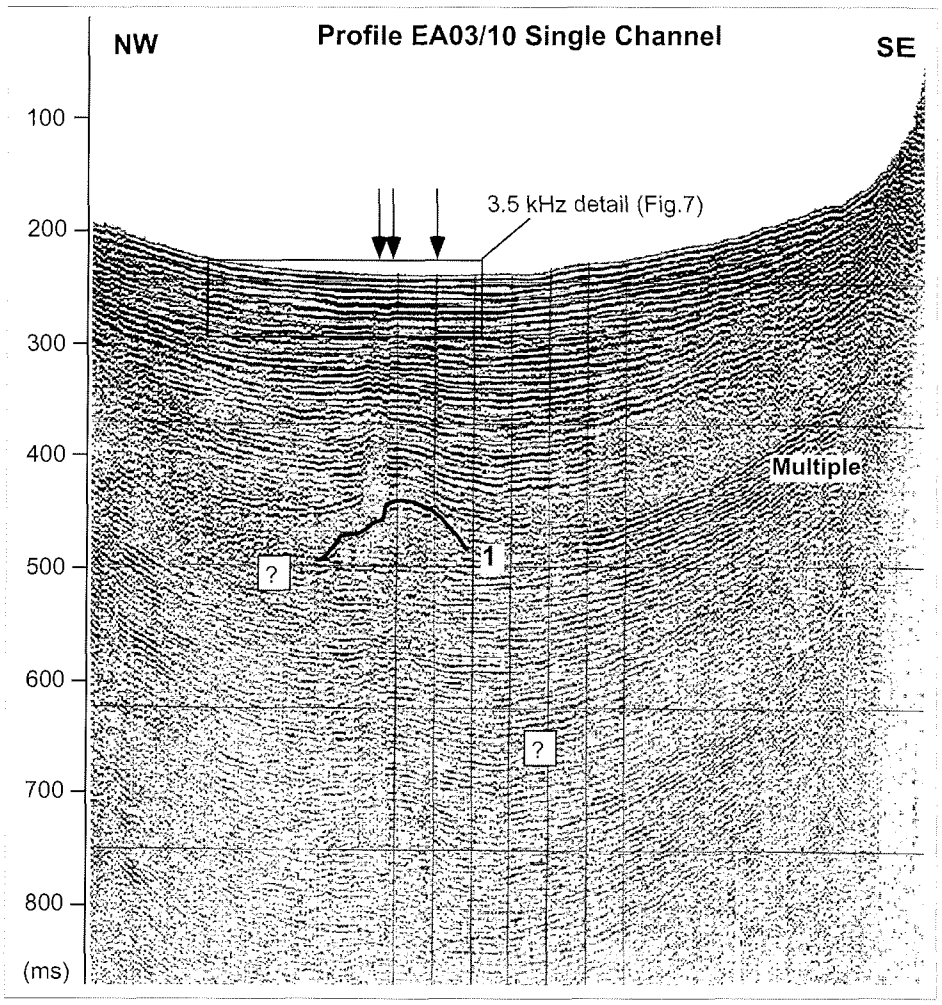

Figure 82: *Profile EA03/10 single-channel analogue data; horizontal grid-line spacing is 125 ms. Line "1" marks an anticline structure visible above the first lake floor multiple. Arrows indicate vertical faults visible in the upper sediment layer (see text for details and Fig. 84 for 3.5 kHz high-resolution profile).*

Consistent with the interpretation of the data of 2000 (Niessen et al., in press), the faults associated with the anticlinal structure displace sediments almost to the present lake floor. This suggests that tectonic movements originally caused by the impact some 3.6 million years ago (Layer et al., 2000) are still active in relatively recent times. This seems to be only true for the expected location of the cone. The suggested drilling sites for paleoclimate investigations are not affected by faults and also largely free of debris flows commonly observed near the slopes of Lake El'gygytgyn (Niessen et al., in press).

One of the major outcomes of our work in 2003 is that we have increased the coverage of 3.5 kHz profiles significantly. During the 2003 expedition a total of

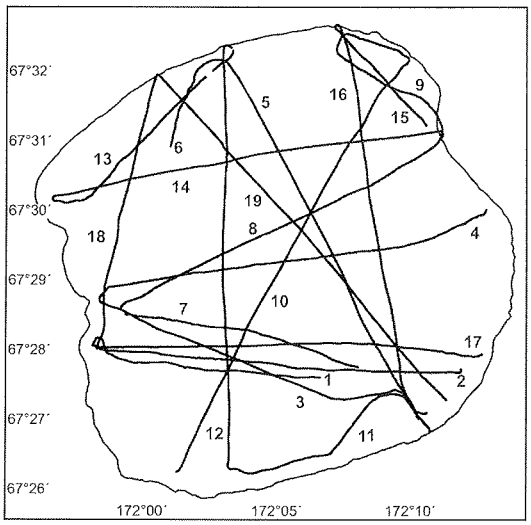

Figure 83: *Map of 3.5 kHz sediment-echosounding profiles recorded on Lake El'gygytgyn during the 2003 expedition. The numbers refer to profile numbers (ES03/number). Note that most profiles were recorded along the same lines as airgun profiles (Fig. 79, p. 124).*

19 profiles were recorded with a total length of 156.1 km (Fig. 83). Together with the previous data of 2000 a total length of 216.5 km of 3.5 kHz high-resolution sediment echo-sounding profiles is available for Lake El'gygytgyn, which should be sufficient to map distinct reflectors and debris flows in space and time. During the expedition in 2003, it turned out to be a great advantage to record the sediment echo-sounding data simultaneously with the airgun data so that comparisons were possible between deep penetration and high-resolution data along the same line. For example, in Figure 84 we present a detail of a 3.5 kHz profile across the anticline structure associated with the central impact cone. The vertical, almost graben-like displacement of relatively young sediments is visible, including a thick debris-flow deposit. This small-scale graben structure is also exhibited in airgun profile EA03/10 to a greater depth (Fig. 82).

In general, the asymmetrical infill structure of Lake El'gygytgyn basin has been confirmed in nearly all profiles. It is obvious that the sediment input and associated deposition on the lacustrine slopes is more prominent along the northwestern to southwestern shoreline of the lake. These slope deposits are often intercalated with debris flows. The acoustic character of these deposits cause strong reflection or defraction patterns and give rise to limited sound penetration combined with strong multiples of near-surface sediments. The asymmetrical sediment fill may also be responsible for partially masking the centre cone anticline structure northwest of the centre of the lake, which is almost in the centre of the crater where one might expect (see also Niessen et al., in press).

During the summer period the party spent at Lake El'gygytgyn in 2003, it turned out that the time window allowing for good seismic working conditions on the lake was rather small. The lake became ice-free on July 18, 2003. On July 19 of we carried out some instrument tests on the lake, and made a few necessary modifications. After a few days of weather deterioration the first profiles were shot on July 24. The last day of seismic data acquisition was on Aug. 7, 2003. An arctic storm system originally derived from a tropical typhoon created strong northerly winds for about 7 days after Aug. 8, which finally lead to the cut off of the Enmyvaam River from the lake. Our platform lost its safe harbour and could

not be brought back to operation on the lake. Comparing the situation of 2000 to 2003, the entire time window to work was only 4 days longer in 2003 than in 2000. Altogether the success of the 2003 seismic work was determined by the careful preparation of the expedition, in particular the significant improvement of the seismic system compared to the level we had available in 2000.

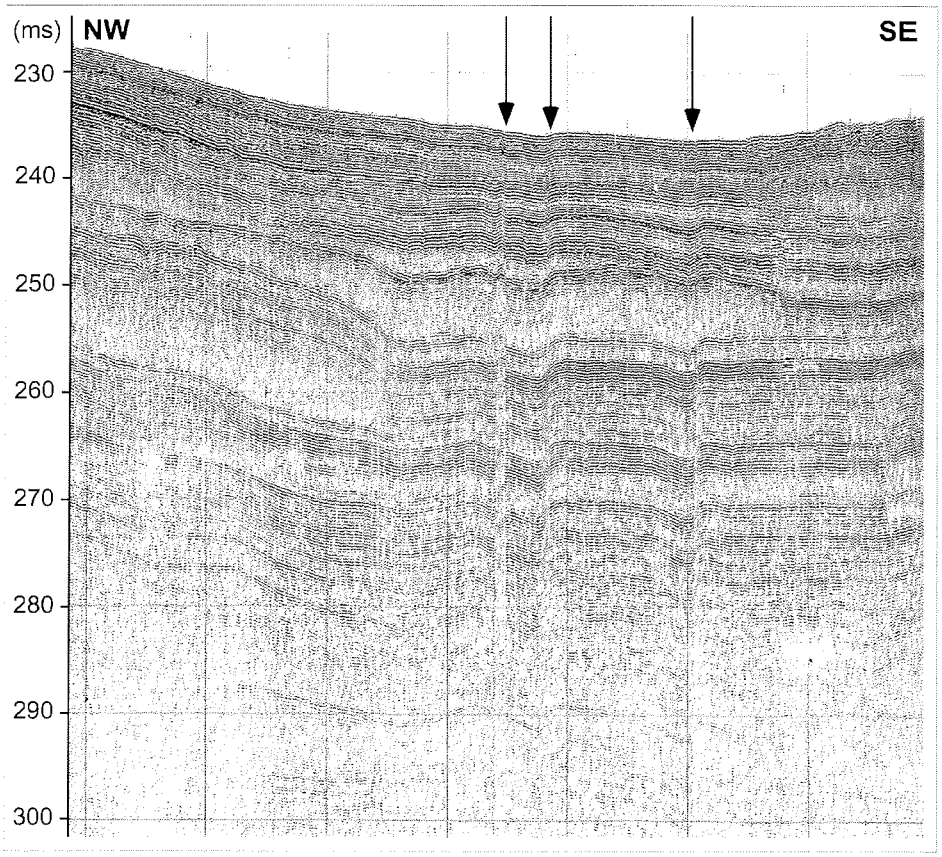

Figure 84: *Selected section of 3.5 kHz sediment echosounding profile ES03/19. This section was recorded above the anticline structure seen in Profile EA03/10 (Fig. 82). Note vertical displacement of sediments along faults (marked by arrows), which are also visible in the deeper part of the sediment fill as shown in Profile EA03/10 (Fig. 82), and a thick debris flow (acoustically transparent sediment body) at about 250 ms two-way travel time.*

7.4 Bathymetric Measurements

(C. Kopsch)

During the expedition to Lake El'gygytgyn in 2003 bathymetric data have been recorded simultaneously with the seismic profiling, using an echosounder FishFinder 240 (Garmin). For navigation the data of the Russian GPS system (courtesy of AARI St. Petersburg) were added to the echosounder data. Both systems were linked to a PC for data acquisition and storage. Data sets were

stored every 5 s, corresponding with a point distance of 7 - 10 m. Processing included validation and editing of navigation data and depth measurements. The complete data set will be made available through the PANGEA database (http://www.pangea.de) for further use to any scientific community interested.

The technical features of the instrument used are as follows:

- Display options: auto ranging, 2x and 4x auto and manual zoom, 3 FishSymbol™ sizes, adjustment bar.
- Alarms: deep water alarm, shallow water alarm, 3 size fish alarm.
- Transducer auto-sense: automatically displays speed and temperature data without menus.
- See-Thru™ Technology: shows weak and strong returns simultaneously.
- Depth Control Gain (DCGTM): automatically adjusts fishfinder sensitivity according to depth.
- Sonar power output: 400 watts (RMS); 3200 watts (peak to peak).
- Frequency: 200 kHz (20° or 8°).
- Depth: 0.5 m to 360 m.
- Power input: 10 to 15 volts DC with high voltage protection.
- Power usage: 10 watts maximum.
- Power nominal: 12 volts DC at 0.8 amps.

A total of more than 200 km of bathymetric profiles have been collected (Fig. 85). The lake's shoreline we determined using a panchromatic "Corona KH-4B" satellite image (from Sept. 19, 1980) offering a spatial resolution of about 6 m. After georeferencing, the lake contour now serves as a map usable to everybody participating in the ongoing scientific projects. A preliminary map and a 3D-model are shown in Figures 86 and 87.

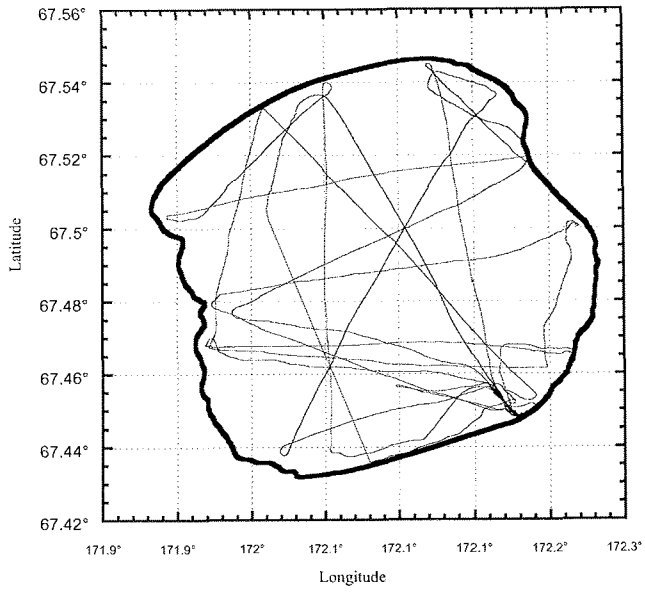

Figure 85: *Bathymetric profiles recorded on Lake El'gygytgyn during the expedition in 2003.*

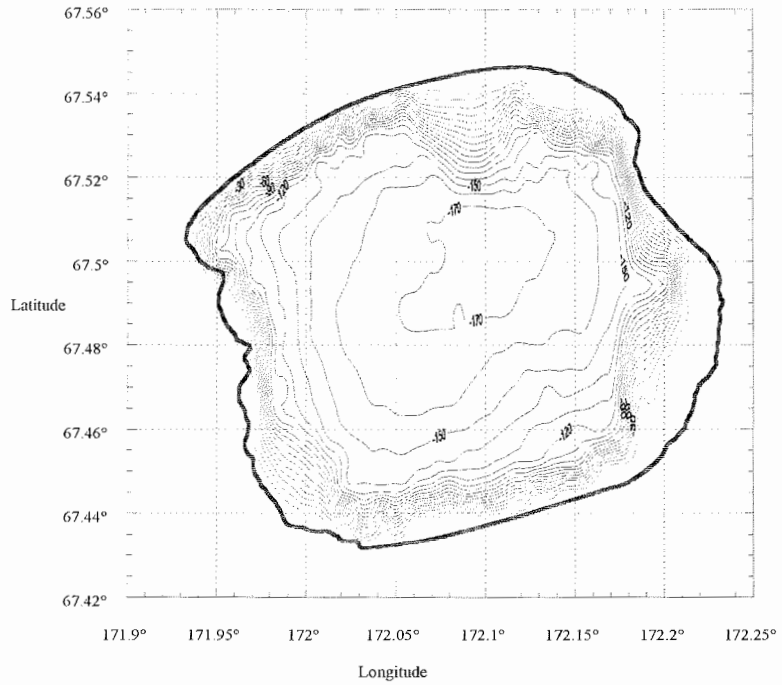

Figure 86: *Preliminary bathymetric map of Lake El´gygytgyn, as based on the bathymetric profiles measured in 2003 (for location of profiles cp. Fig. 85).*

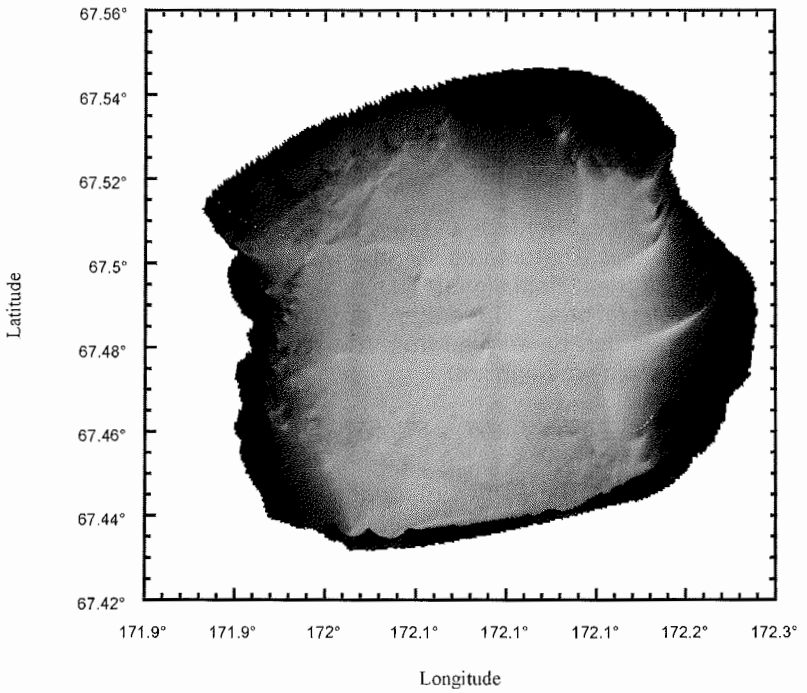

Figure 87: *Preliminary 3D-model of Lake El´gygytgyn´s bathymetry, as based on the bathymetric profiles measured in 2003 (for location of profiles cp. Fig. 85).*

7.5 Geomagnetic Survey

(C. Kopsch)

During the expedition in 2003 magnetometer measurements were accomplished on and around Lake El´gygytgyn. Additional profiles outside the crater were planned but had to be cancelled due to the lack of measuring time. However, from the existing data we expect an improved interpretation of the crater´s structure, because impact structures are known to be connected with distinct magnetic anomalies. Hence, the interpretations of the geomagnetic data will aid to select coring sites for future drilling activities.

The following instruments have been used for magnetic field measurements (courtesy of GeoForschungsZentrum Potsdam):

1. Proton Magnetometer (self construction):
   - sensitivity 0.1 nT
   - resolution 0.1 nT
   - absolute Accuracy 1.0 nT
   - dynamic Range 40,000 to 56,000 nT
   - sampling Rate 1 s

2. Proton Precession Magnetometer GSM-19T:
   - sensitivity <0.10 nT
   - resolution 0.01 nT
   - absolute Accuracy 1.00 nT
   - dynamic Range 10,000 to 120,000 nT
   - sampling Rate 3 - 60 s
   - operating temperature -40 - +60°C

Due to a technical failure of the first magnetometer, all field measurements had to be conducted with the GSM-19T exclusively.

A comparison and adjustment of the measured field data with the aim to emphasise the geological structures is only possible after removing external influences on the magnetic field signal. This is a procedure of various correction and reduction calculations. Thereafter geological interpretations on the subsurface structures can be derived from the anomaly ΔT. In order to extract ΔT the following formula was applied:

$$\Delta T = T - \delta T_v - \delta T_0 - \delta T_{Ni} - \delta T_{TOP}$$

δT_v current variation of the earth´s magnetic field
δT_0 normal (main) magnetic field
δT_{Ni} influence of station´s height
δT_{TOP} influence of field topography

The normal field and its variations exert major influences on field data. Compared with this the instrument's noise is negligible. The influence of regular or continuous variations of the earth´s magnetic field can be eliminated using

recordings of variation series either from a regional magnetic observatory or from a base station nearby (see Fig. 88 as an example). For our purposes we used both possibilities.

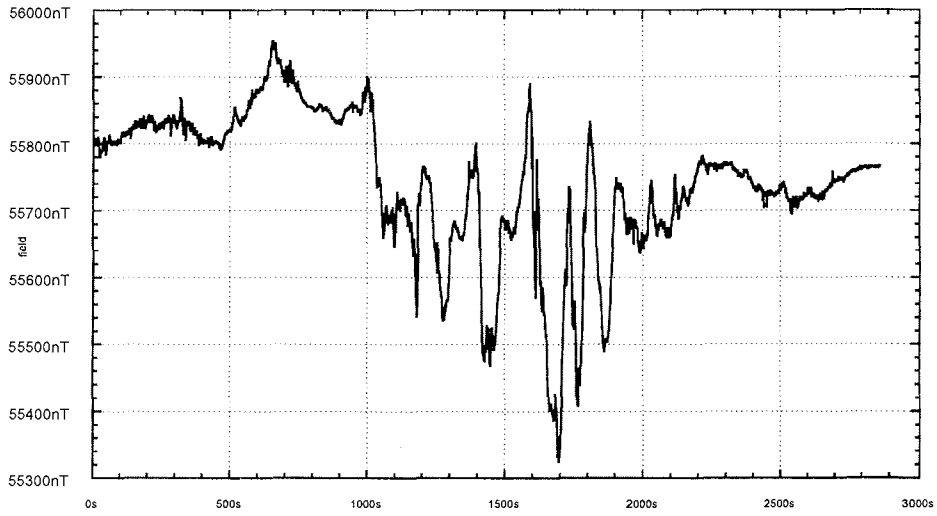

Figure 88: *Daily variation line of the magnetic field at the base station in the Enmyvaam River valley about 200 m to the south of the shore of Lake El'gygytgyn; date: Aug 22, 2003*

The base station (67°26.723′ N, 172°10.797′ E) was constructed about 150 m to the south of the in the Enmyvaam River valley camp (cp. Fig. 34, p. 66) to measure the total magnetic field and its daily variation. The above mentioned GSM-19T magnetometer was used with a recording interval of 30 s, giving a data line for the entire summer campaign in 2003. Further on, the data from the Pevek Magnetic Observatory will be used for data improvement. This station is located approximately 200 km to the north of Lake El'gygytgyn:

- Location: Valkarkay, Pevek, Russia
- Location ID: PBK
- Latitude: 70°50′ N
- Longitude: 170°54′ E
- Elevation: 2 m a.s.l.
- Equipment: fluxgate magnetometer (DMI), proton magnetometer
- Orientation: HDZ
- Owner: AARI St. Petersburg

For field measurements the sensor was installed on an iron-free rubber dinghy and towed either 60 m behind the platform "Helga" (Fig. 78, p. 123) or behind another rubber dinghy equipped with an outboard engine. No noise due to ferruginous equipment was recorded. Additionally to the profiles accomplished together with the seismic profiling, 8 profiles were measured only with the magnetometer in order to expand the geomagnetic network (Fig. 89). The profiles measured together with the seismic data have a record interval of about 16 m, while the single magnetic profiles have about 27 m.

For the additional geomagnetic profiles two reference points (i.e. buoys) were established on the lake:

- buoy at 10 m water depth; position: 67°27.110´ N; 172°09.839´ E
- buoy at 95 m water depth; position: 67°27.314´ N; 172°09.839´ E

These points were passed before and after profiling, thus allowing a quick verification of the results shortly after the measurements.

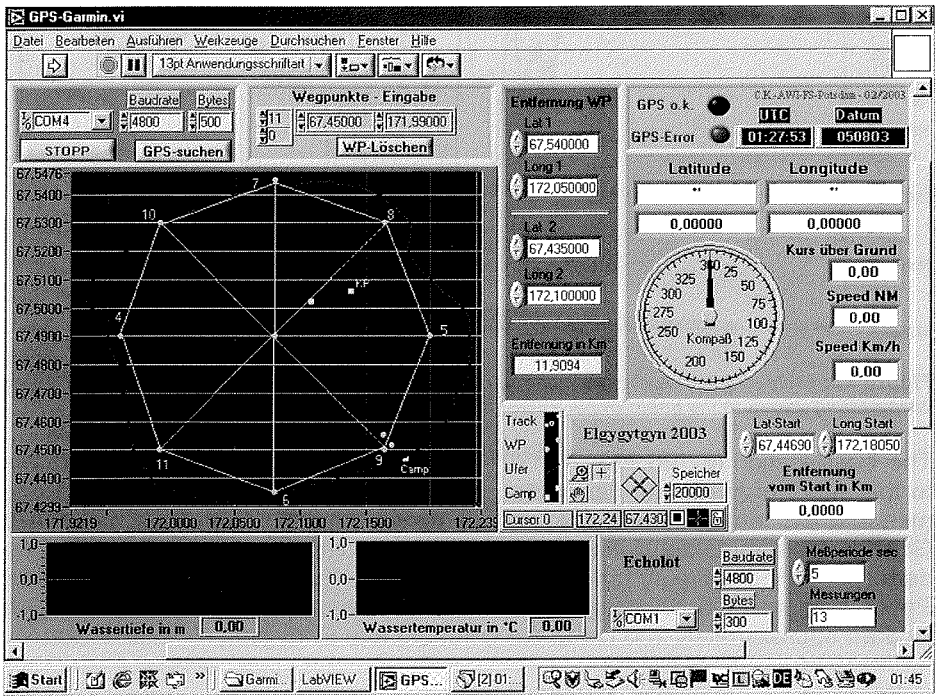

Figure 89: *Example for the geomagnetic network measured at Lake El'gygytgyn in summer 2003.*

Regular measurements at the reference points were additionally used for corrections if there are no other data available. Especially long period variations are linearly adjustable. The error in measurement for time intervals of about two hours is approximately 10 - 20 nT because variations with a period below 2 h are not recordable with this method. In combination with the observatory data from Pevek the error can probably be minimised down to less than 5 nT.

8 PARTICIPATING SCIENTISTS AND INSTITUTIONS

The following scientists and affiliated institutions participated in the expedition to Lake El'gygytgyn in spring and summer 2003 (cp. Fig. 1a and b, p. 5):

Brigham-Grette, Julie	UMass	summer campaign
Dehnert, Andreas	UniL	summer campaign
Fedorov, Grigory B.	AARI	spring and summer campaigns
Gebhardt, A. Catalina	AWI-B	summer campaign
Glushkova, Olga Yu.	NEISRI	summer campaign
Haker, Mario A.	AWI-B	spring and summer campaigns
Juschus, Olaf	UniL	spring and summer campaigns
Kopsch, Conny	AWI-P	summer campaign
Kupolov, Andrej	AARI	summer campaign
Melles, Martin	UniL	summer campaign
Minyuk, Pavel S.	NEISRI	spring and summer campaigns
Niessen, Frank	AWI-B	summer campaign
Quart, Sebastian	UniL	spring campaign
Schwamborn, Georg	AWI-P	spring and summer campaigns
Smirnov, Volodya N.	NEISRI	summer campaign
Wennrich, Volker	UniL	spring campaign

AARI	Arctic and Antarctic Research Institute Korablestroitelei Street 26-111 199 155 St. Petersburg Russia
AWI-B	Alfred Wegener Institute for Polar and Marine Research Columbusstrasse P.O. Box 12 01 61 D-27515 Bremerhaven Germany
AWI-P	Alfred Wegener Institute for Polar and Marine Research Research Unit Potsdam Telegraphenberg A43 D-14473 Potsdam Germany
NEISRI	Northeast Interdisciplinary Scientific Research Institute Russian Academy of Sciences, Far East Branch Portovaya 16 685 010 Magadan Russia

UMass University of Massachusetts
Department of Geosciences
Amherst, MA 01003
U.S.A.

UniL University of Leipzig
Institute for Geophysics and Geology
Talstrasse 35
D-04103 Leipzig
Germany

9 ACKNOWLEDGEMENTS

First of all we are grateful to all those who are responsible for the political and administrative decisions that made the expedition to Lake El'gygytgyn in 2003 possible. Most of the financial support for the expedition was provided by the German Federal Ministry for Education and Research (BMBF; grant no. 03G0586A, B). Additional funding was made available by the Russian Ministry of Education and Science and the U.S. National Science Foundation (OPP Award 00-75122 to Matt Nolan; Atmospheric Sciences Award 99-05813 and OPP Award 02-42324 to Julie Brigham-Grette). We also wish to acknowledge the cooperation of the Pevek Airport. Special thanks are due to Yuri Gapkailo for his good spirit, resourcefulness and fine cooking.

10 REFERENCES

Abbott, M.B. & Stafford, T.W. (1996): Radiocarbon Geochemistry of Ancient and Modern Arctic Lakes, Baffin Island. - *Quaternary Research* 45: 300-311

Andersen, K.K.; Azuma, N.; Barnola, J.M. & 46 co-authors (2004): High-resolution record of Northern Hemisphere climate extending into the last interglacial period. - *Nature* 431: 147-151.

Antonov, O.M. (1997): A Gas-Mercury Survey in Levinson-Lessing Lake Area. - In: M. Melles, B. Hagedorn & D.Yu. Bolshiyanov (eds.): The Expedition Taymyr/ Severnaya Semlya 1996. *Reports on Polar Research* 237: 107-110.

Asikainen, C.A.; Francus, P. & Brigham-Grette, J. (in press): Sediment fabric, clay mineralogy, and grain-size as indicators of climate change since 65 ka from El 'gygytgyn Crater Lake, northeastern Siberia. - *J. Paleolimnol.*

Belyi, V.F. (2001): Structure and formation of the El'gygytgyn Basin (Anadyr Mountains) [in Russian]. - *Geomorphologia* 1: 31-41.

Belyi, V.F. & Raikevich, M.I. (1994): The El'gygytgyn Lake depression [in Russian]. - In: SBKNII DVO RAN, Magadan, 27 pp.

Belyi, V.F. & Raikevich, M.I. (1996): The geology of impact rocks from the El'gygytgyn Lake depression [in Russian]. - *Bull. MOIP* 1: 56-72.

Chapman, W.L. & Walsh, J.E (1993): Recent variations of sea ice and air temperature in high latitudes. - *Bull. Am. Met. Soc.* 74: 33-47.

Cremer, H. & Wagner, B. (2003): The diatom flora from the ultra-oligotrophic Lake El'gygytgyn, Chukotka. - *Polar Biology* 26, 105-114.
Dansgaard, W.; Johnsen, S.J.; Clausen, H.B.; Dahl-Jensen, D.; Gundestrup, N.S.; Hammer, C.U.; Hvidberg, C.S.; Steffensen, J.P.; Sveinbjørnsdottir, A.E.; Jouzel J. & Bond G. (1993): Evidence for general instability of past climate from a 250-kyr ice-core record. - *Nature* 364: 218-220.
Eglinton, G. & Hamilton, R.J. (1967): Leaf epicuticular waxes. - *Science* 156: 1322-1335.
Fedorov, G.B., Antonov, O.M. & Bolshiyanov, D.Yu. (2001): The character of modern tectonic movements in central Taimyr [in Russian]. - *Izvestia RGO* 133/ 1: 76-81.
Finckh, P.G.; Kelts, K. & Lambert, A. (1984): Seismic stratigraphy and bedrock forms in perialpine lakes. - *Bull. Geol. Soc. Amer.* 95: 1118-1128.
Forman, S.L.; Pierson, J.; Gomez, J.; Brigham-Grette, J.; Nowaczyk, N.R. & Melles, M. (in press): Luminescence geochronology for sediments from Lake El'gygytgyn, northeast Siberia, Russia: constraining the timing of paleoenvironmental events for the past 200 ka. - *J. Paleolimnol.*
Fursov, V.Z. (1977): Mercury as an Indicator for Geochemical Reconnaissance of Ore Deposits [in Russian]. - Nedra, Moscow, 1977, 143 pp.
Glotov, V.Ye. & Zuev, S.A. (1995): Hydrological characteristics of Lake El'gygytgyn [in Russian]. - *Kolyma* 3-4: 18-23
Glushkova, O.Yu. (1993): Geomorphology and history of relief development in the El'gygytgyn Lake region [in Russian]. - In: V.F. Bely & I.A. Chereshnev (eds.): The Nature of the El'gygytgyn Lake Hollow. Magadan, 26-48.
Glushkova, O.Yu.; Lozhkin, A.V. & Solomatkina, T.B. (1994): Holocene stratigraphy and paleogeography of El'gygytgyn Lake, northwestern Chukotka. - Proc. Intern. Conf. Arctic Margins, Sept. 6-10, 1994 , Magadan, *NEISRI FEB RAS*, 75-80.
Glushkova, O.Yu.; Lozhkin, A.V. & Solomatkina, T.B. (1995): Stratigraphy and paleo-geography of the El'gygytgyn Lake in the Holocene (North-eastern Chukotka). - *Pacific Geol.* 14/4: 23-30.
Glushkova, O.Yu.; Smirnov, V.N.; Minyuk, P.S. & Sharpton, B. (2001): New data on the morphostructure of the El'gygytgyn meteoritic crater [in Russian]. - In: Problems of Geology and Metallurgy in the North-eastern Part of Asia at the Boundary of Millennium. Quaternary Geology, Geomorphology, Placers. Magadan, *NEISRI FEB RAS* 3, 20-22.
Glushkova, O. Yu. & Smirnov, V.N. (in press): Paleogeography of El'gygytgyn Lake from the Pliocene to the Holocene. - *J. Paleolimnol.*
Hubberten, H.-W.; Grobe, H.; Jokat, W.; Melles, M.; Niessen, F. & Stein, R. (1995): Glacial history of East Greenland explored. - *Eos Trans. AGU* 76(36): 353-356.
Jansen, E.; Sjoholm, J.; Bleil, U. & Erichson, J.A. (1990): Neogene and Pleistocene glaciations in the Northern Hemisphere and late Miocene - Pliocene global ice volume fluctuations: evidence from the Norwegian Sea. - In: U. Bleil & J. Thiede (eds.): Geological History of the Polar Oceans: Arctic versus Antarctic, Kluwer Academic Publishers, Doordrecht, 677-705.
Johnsen, S.J.; Clausen, H.B.; Dansgaard, W.; Gundestrup, N.S.; Hammer, C.U. & Tauber, H. (1995): The Eemian stable isotope record along the GRIP Ice Core and its interpretation. - *Quat. Res.* 43: 117-124.
Juschus, O.; Melles, M.; Brigham-Grette, J.; Dehnert, A.; Gebhardt, C.; Niessen, F.; Minyuk, P.S. & Wennrich, V. (2004): The significance of Late Quaternary mass movement events for the paleoenvironmental interpretation of sediment records from Lake El'gygytgyn, NE Siberia. - *Eos Trans. AGU,* 85(47), Fall Meet. Suppl., Abstract PP21B-1387.
Keigwin, L.D. (1998): Glacial-age hydrography of the far northwest Pacific Ocean. - *Paleoceanography* 13: 323-339.
Kerr, R. (2004): Signs of a warm, ice-free Arctic. - *Science* 305: 1693.

Kolattukudy, P.E. (1976): Chemistry and Biochemistry of Natural Waxes. Elsevier, Amsterdam, 459 pp.

Konishchev, V.N. & Rogov, V.V. (1993): Investigations of cryogenic weathering in Europe and northern Asia. - *Permafrost and Periglacial Processes* 4, 49-64.

Kohzevnikov, Yu.P. (1993): Vascular plants in the vicinities of the El'gygytgyn Lake [in Russian]. - In: V.F. Bely & I.A. Chereshnev (eds.): The Nature of the El'gygytgyn Lake Hollow. Magadan. 62-82.

Labeyrie, L.; Cole, J.; Alverson, K. & Stocker, T. (2003): The history of climate dynamics in the Late Quaternary. - In: K.D. Alverson, R.S. Bradley & T. F. Pedersen (eds.): Paleoclimate, Global Change and the Future. Springer, Heidelberg, 33-61.

Larsen, E.; Funder, S. & Thiede, J. (1999): Late Quaternary history of northern Russia and adjacent shelves – a synopsis. – *Boreas* 28: 6-11.

Layer, P.W. (2000): Argon-40/Argon-39 age of the El'gygytgyn impact event, Chukotka, Russia. - *Meteoritics & Planetary Science* 35, 591.

Maslin, M.A.; Loutre, M.-F. & Berger, A. (1998): The contribution of orbital forcing to the progressive intensification of Northern Hemisphere Glaciation. - *Quat. Sci. Rev.* 17: 411-426.

Melles, M.; Kulbe, T.; Overduin, P.P. & Verkulich, S. (1994): The Expedition Bunger Oasis 1993/1994 of the AWI Research Unit Potsdam. - In: M. Melles (ed.): The Expeditions Norilsk/Taymyr 1993 and Bunger Oasis 1993/94 of the AWI Research Unit Potsdam. *Reports on Polar Research* 148: 27-80.

Melles, M.; Brigham-Grette, J.; Glushkova, O.Yu.; Minyuk, P.; Nowaczyk, N.R. & Hubberten H.W. (in press): Organic and isotope geochemistry of core PG1351 from El'gygytgyn Lake - a sensitive record of climate variability in the East Siberian Arctic during the past 250 kyr. - *J. Paleolimnol.*

Meyer, H. (2003): Late Quaternary climate history of northern Siberia - evidence from ground ice. - *Reports on Polar and Marine Research* 461, 111 pp.

Milankovitch, M. (1941): Kanon der Erdbestrahlung und seine Anwendung auf das Eiszeitenproblem. - Königl. Serb. Akad., Belgrad, 633 pp.

Minyuk, P.S.; Nowaczyk, N.R.; Glushkova, O.Yu.; Smirnov, V.N.; Brigham-Grette, J.; Melles, M.; Cherepanova, M.; Loshkin, A.V.; Anderson, P.; Matrosova, T.V.; Hubberten, H.; Belaya, B.V.; Borkhodoyev, B.Ya.; Forman, S.L.; Asikainen, C.; Layer, P.; Nolan, M.; Prokein, P.; Liston, G.; Nantsinger, R.; Sharpton, W. & Niessen, F. (2003): Paleoclimatological potential of Lake El'gygytgyn, northeastern Russia (multi-disciplinary investigations) [in Russian]. - In: M.I. Malakhov (ed.): The Process of Post-depositional Magnetization and Characteristic Changes of the Earth's Magnetic Field and Climate in the Past. *NEISRI FEB RAS*, Magadan, 91-135.

Moore, J.J.; Hughen, K.A.; Miller, G.H. & Overpeck, J.T. (2001): Little Ice Age recorded in summer temperature reconstruction from varved sediments of Donard Lake, Baffin Island, Canada. - *J. Paleolimn.* 25: 503-517.

Niessen, F. & Melles, M. (1995): Lacustrine sediment echosounding and physical properties. - In: H.W. Hubberten (ed.): The Expedition ARKTIS-X/2 of RV "Polarstern" in 1994. *Reports on Polar Research* 174: 69-75

Niessen, F.; Ebel, T.; Kopsch, C. & Fedorov, G.B. (1999): High-resolution seismic stratigraphy of lake sediments on the Taymyr Peninsula, Central Siberia. - In: H. Kassens, H.A. Bauch, I. Dmitrenko, H. Eicken, H.W. Hubberten, M. Melles, J. Thiede & L. Timokhov (eds.): Land-Ocean Systems in the Siberian Arctic: Dynamics and History. Springer-Verlag, Berlin, 437-456.

Niessen, F.; Kopsch, C.; Wagner, B.; Nolan, M. & Brigham-Grette, J. (2000): The Impact Project: seismic investigation of Lake El'gygytygyn, NE Russia - implication for sediment thickness and depositional environment. - *Eos Trans. AGU.* 81 (48), Fall Meet. Suppl., 230.

Niessen, F.; Gebhardt, C.; Kopsch, C. & Wagner, B. (in press): Seismic investigation of the El'gygytgyn impact crater lake (Central Chukotka, NE Siberia): preliminary results. - *J. Paleolimnol.*

Nowaczyk, N.R.; Frederichs, T.W.; Kassens, H.; Nørgaard-Pedersen, N.; Spielhagen, R.F.; Stein, R. & Weiel, D. (2001): Sedimentation rates in the Makarov Basin, central Arctic Ocean: a paleomagnetic and rock magnetic approach. - *Paleoceanography* 16: 368-389.

Nowaczyk, N.R.; Minyuk, P.; Melles, M.; Brigham-Grette, J.; Glushkova, O.; Nolan, M.; Lozhkin, A.V.; Stetsenko, T.V.; Andersen P.M. & Forman, S.L. (2002): Magnetostratigraphic results from impact crater Lake El'gygytgyn, northeastern Siberia: a 300 kyr long high-resolution terrestrial palaeoclimatic record from the Arctic. - *Geophys. J. Int.* 150: 109–126.

Nowaczyk, N.R.; Melles, M. & Minyuk, P. (in press): A revised age model for core PG1351 from Lake El'gygytgyn, Chukotka, based on magnetic susceptibility variations tuned to northern hemisphere insolation variations. - *J. Paleolimnol.*

Nolan, M. & Brigham-Grette, J. (in press): Basic hydrology, limnology, and meterology of modern Lake El'gygytgyn, Siberia. - *J. Paleolimnol.*

Nolan, M.; Liston, G.; Prokein, P.; Brigham-Grette, J.; Sharpton, V. L. & Huntzinger, R. (2003): Analysis of lake ice dynamics and morphology on Lake El'gygytgyn, NE Siberia, using Synthetic Aperture Radar (SAR) and Landsat. - *J. Geophys. Res.* 108 (D2): 8162.

Overpeck, J.T.; Hughen, K.; Hardy, D.; Bradley, R.; Case, R.; Douglas, M.; Finney, B.; Gajewski, K.; Jacoby, G.; Jennings, A.; Lamoureux, S.; Lasca, A.; MacDonald, G.; Moore, J.; Retelle, M.; Smith, S.; Wolfe, A. & Zielinski, G. (1997): Arctic environmental change in the last four centuries. - *Science* 278: 1251-1256.

Polyakov, I.V.; Alekseev, G.V.; Bekryaev, R.V.; Bhatt, U.; Colony, R.L.; Johnson, M.A.; Karklin, V.P.; Makshtas, A.P.; Walsh, D. & Yulin, A.V. (2002): Observationally based assessment of polar amplification of global warming. - *Geoph. Res. Letters* 29: 10.1029/ 2001GL011111.

Sava, N.E.; Smirnov, V.N.; Glushkova, O.Yu.; Minyuk, P.S. & Sharpton, B. (2001): Spherules from the El'gygytgyn meteorite crater [in Russian]. - In: Problems of Geology and Metallurgy in the North-eastern part of Asia at the Boundary of Millennium. Quaternary Geology, Geomorphology, Placers. Magadan: *NEISRI FEB RAS* 3. 20-22.

Stuiver, M.; Reimer, P.J.; Bard, E.; Beck, W.; Burr, G.S.; Hughen, K.A.; Kromer, B.; McCormac, G.; van der Plicht, J. & Spurk, M. (1998): INCAL98 Radiocarbon age calibration, 24,000-0 cal BP. - *Radiocarbon* 40: 1041-1083.

Thiede, J.; Winkler, A.; Wolf-Welling, T.; Eldholm, O.; Myhre, A.M.; Baumann, K.-H.; Henrich, R. & Stein, R. (1998): Late Cenozoic history of the Polar North Atlantic: results from ocean drilling. - *Quat. Sci. Rev.* 17: 185-208.

Yurtsev B.A. (1973): Botanic-geographical zonation and floristic zoning of the tundra in Chukotka [in Russian]. - *Botanic Journal* 58/7: 812-821.